DOT/FAA/TC-18/8

Federal Aviation Administration
William J. Hughes Technical Center
Aviation Research Division
Atlantic City International Airport
New Jersey 08405

Boeing 737-800 Final Surface Roughness Study Data Collection

February 2017

Final Report

U.S. Department of Transportation
Federal Aviation Administration

NOTICE

Technical Report Documentation Page

1. Report No.	2. Government Accession No.	3. Recipient's Catalog No.
DOT/FAA/TC-18/8		

4. Title and Subtitle	5. Report Date
BOEING 737-800 FINAL SURFACE ROUGHNESS STUDY DATA COLLECTION	February 2017
	6. Performing Organization Code

7. Author(s)	8. Performing Organization Report No.
Skip Hudspeth; David Stapleton; Jeard Ballew; and John Sparkman, PMP	

9. Performing Organization Name and Address	10. Work Unit No. (TRAIS)
Cherokee CRC, LLC 10838 E Marshall St., Ste. 220 Tulsa, OK 74116	
	11. Contract or Grant No.

12. Sponsoring Agency Name and Address	13. Type of Report and Period Covered
U.S. Department of Transportation Federal Aviation Administration William J. Hughes Technical Center Airport Technology Research & Development Branch Airport Pavement Section Atlantic City International Airport, NJ 08405	Final Report
	14. Sponsoring Agency Code ANG-E262

15. Supplementary Notes

The Federal Aviation Administration Airport Pavement Section COR Nicole Sauiskie.

16. Abstract

Airport surface roughness is controlled very closely during construction, and contractors are held to high standards, including maximum variances along the longitudinal and transverse axes of new runway and taxiway construction. However, once construction is complete, the Federal Aviation Administration (FAA) does not have a reliable method to determine when airport pavement deteriorates to the point of becoming too rough for use. To develop a method for evaluating in-service pavement roughness, a rating scale for pilots' subjective response to vertical cockpit vibrations excited by longitudinal pavement surface elevation disturbances was created.

Cherokee CRC began work on the Airport Pavement Surface Roughness Study with the FAA in September 2008 using the FAA's Boeing 737-800 full flight simulator in Oklahoma City, Oklahoma. The Boeing 737-800 simulator's roughness model was modified to allow the use of real-world airport surface roughness profiles and to increase the fidelity of the ground model response to roughness. A methodology was developed for presenting surface roughness profiles and obtaining pilot roughness evaluations. Test scenarios, roughness rating forms, and pre-brief and post-flight sessions were developed and refined during a series of pilot studies in 2010 and 2011. The National Cooperative Highway Research Program highway rideability studies were reviewed and used as models for developing the airport pavement rideability studies.

17. Key Words	18. Distribution Statement
Roughness, Runway surface profiles, Simulation, Boeing 737-800, Subjective rating questionnaire	This document is available to the U.S. public through the National Technical Information Service (NTIS), Springfield, Virginia 22161. This document is also available from the Federal Aviation Administration William J. Hughes Technical Center at actlibrary.tc.faa.gov.

19. Security Classif. (of this report)	20. Security Classif. (of this page)	21. No. of Pages	22. Price
Unclassified	Unclassified	210	

ACKNOWLEDGEMENTS

The work described in this report was supported by the Federal Aviation Administration (FAA) Airport Technology Research and Development Branch, ANG-E260, Dr. Michel Hovan, Manager. Dr. Gordon Hayhoe provided assistance with the simulator roughness model development and accelerometer signal processing. CAE, Inc., the Boeing 737-800 flight simulator manufacturer, provided engineering support for the flight simulator ground model and motion system updates for this project. Boeing provided some of the airport surface test profiles used in the study.

TABLE OF CONTENTS

LIST OF FIGURES

LIST OF TABLES

LIST OF SYMBOLS AND ACRONYMS

$a_W(t)$	Weighted acceleration
$(W_{k)}$	ISO Weighting
D_K	Spinal response acceleration dose
DKup	Spinal dose indicator for estimation of spinal discomfort
fps	Feet per second
G	G-force
Hz	Hertz
m/s^2	Meters per second squared
R^2	R squared (coefficient of determination)
rad/s^2	Radians per second squared
ASTM	American Society for Testing and Materials
CCRC	Cherokee CRC, LLC
CG	Center of gravity
FAA	Federal Aviation Administration
GCP	Cockpit vertical accelerations
IRI	International Roughness Index
ISO	International Organization for Standardization
MATLAB®	Matrix Laboratory
MMAC	Mike Monroney Aeronautical Center
MTVV	Maximum transient vibration value from a running RMS computation
NCHRP	National Cooperative Highway Research Program
RMS	Root-mean-square
VDV	Fourth-power vibration dose value

EXECUTIVE SUMMARY

In a continuation of the Federal Aviation Administration's (FAA) research to determine acceptable limits for airport pavement roughness, the Boeing (B)737-800 Final Surface Roughness Study was conducted on June 4-6 and June 11-13, 2013, using the FAA B737-800 full flight simulator at the Mike Monroney Aeronautical Center in Oklahoma City, Oklahoma. Thirty-six pilots participated in the study over twelve test sessions. Subjective pilot ratings of pavement roughness and objective measures of cockpit accelerations were collected for all sessions. A data analysis was performed to correlate the pilot ratings with cockpit accelerations.

1. INTRODUCTION.

In a continuation of the Federal Aviation Administration's (FAA) research to determine acceptable limits for airport pavement roughness, a surface roughness study was conducted on June 4-6 and June 11-13, 2013, using the FAA CAE Boeing 737-800 full flight simulator (herein after referred to as B737-800 simulator) at the Mike Monroney Aeronautical Center (MMAC) in Oklahoma City, Oklahoma. Thirty-six pilots participated in the study over twelve test sessions. Subjective pilot ratings of pavement roughness and objective measures of cockpit accelerations were collected for all sessions. A data analysis was performed to correlate the pilot ratings with cockpit accelerations.

1.1 BACKGROUND.

Airport surface roughness is controlled very closely during construction, and contractors are held to high standards [1]. These standards include maximum variances along the longitudinal and transverse axes of new runway and taxiway construction [2]. However, once construction is complete, the FAA does not have a reliable method to determine when airport pavement deteriorates enough to be considered too rough for use [3]. To develop a method for evaluating in-service pavement surface roughness, a rating scale was developed to measure pilots' subjective response to vertical cockpit vibrations excited by longitudinal pavement surface elevation disturbances.

Cherokee CRC, LLC (CCRC) began work on the Airport Pavement Surface Roughness Study with the FAA in September 2008 using the FAA B737-800 simulator in Oklahoma City, Oklahoma. The B737-800 simulator's roughness model was modified to use real-world airport surface roughness profiles and to increase the fidelity of the ground model response to roughness. A methodology was developed for presenting surface roughness profiles and obtaining pilot roughness evaluations. Test scenarios, roughness rating forms, and pre- and post-briefing sessions were developed and refined during a series of pilot studies in 2010 and 2011. National Cooperative Highway Research Program (NCHRP) highway rideability studies [4] were reviewed and used as models for developing the airport pavement rideability studies.

A preliminary surface roughness study [5] was conducted on November 8-10, 2011, using the B737-800 simulator located at the MMAC in Oklahoma City, Oklahoma. The study consisted of four pavement rideability rating sessions with three pilots per session, for a total of 12 subject pilots. Subject pilots were presented with a series of 80 taxiway and runway pavement roughness test scenarios. Subjective pilot ratings and objective measures of cockpit accelerations were collected for all sessions. A data analysis was performed to correlate the pilot ratings with cockpit accelerations.

1.2 SURFACE ROUGHNESS STUDY OBJECTIVES.

The following objectives were established for this study.

(1) Evaluate the response of the simulator model(s) when the simulator standard roughness models are replaced by measured runway and taxiway profiles and determine if the

simulator models accurately reproduce the roughness of the surfaces during test scenarios.

(2) Develop a rating scale for pilot subjective response to vertical cockpit vibrations excited by longitudinal pavement surface elevation disturbances. The scale will range from unacceptably rough to very smooth.

(3) Use the rating scale to obtain pilot ratings of simulated surface roughness.

(4) Use statistical correlation techniques to relate the subjective ratings to objective measures of the cockpit vertical vibrations or objective measures of the properties of the pavement longitudinal elevation profiles.

(5) Identify the rating scale limits for cockpit vibration, resulting in unacceptable, or unsafe, ride quality conditions.

2. SURFACE ROUGHNESS STUDY DEVELOPMENT.

The following tasks were accomplished in preparation for the preliminary and final surface roughness studies.

(1) Enhanced the B737-800 simulator software to provide realistic cockpit accelerations in response to real-world airport surface roughness profiles.

(2) Developed simulator test scenarios for obtaining pilot subjective ratings of surface roughness and objective measures of cockpit acceleration and other simulator parameters.

(3) Selected and formatted real-world taxiway and runway surface elevation profiles for the test scenarios.

(4) Created samples of simulator generic (random) roughness for inclusion in the test scenarios.

(5) Developed routines for capturing time histories of objective test data, such as cockpit accelerometer output, profile elevation, and flight model parameters.

(6) Developed roughness rating forms and rating panel briefings.

2.1 ENHANCEMENTS TO THE B737-800 SIMULATOR SOFTWARE.

The B737-800 simulator software was modified to allow integration of real-world airport surface profiles into the simulator ground model and to enhance the existing simulator generic roughness

model. The integration of real-world surface profiles into the flight simulator consisted of the following tasks:

- Integration of real-world profiles into the simulator ground model.
- Alignment of taxiway and runway profiles with simulator visual scenes.
- Initial testing of cockpit acceleration response to real-world roughness profiles.
- Development of aircraft fuselage flex models to provide realistic cockpit accelerations.
- Integration of ground model rigid-body accelerations and flexible mode accelerations into the simulator motion model.
- Tuning the flexible mode and motion models.
- Testing and validation of the simulator roughness simulation enhancements.

This report references two units of measurement for acceleration: (1) G-force (G), used for the simulator cockpit accelerometer output and the ProFAA-simulated cockpit acceleration depicted in figures 1 and 2, and (2) meters per second squared (m/s^2), used for references to acceleration International Organization for Standardization (ISO) indices.

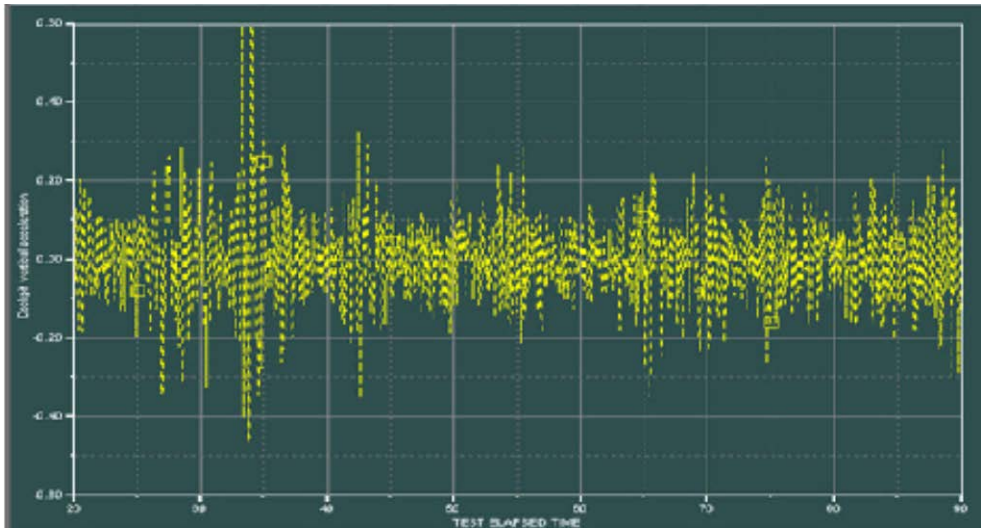

Figure 1. The FAA B737-800 Simulator—Cockpit Accelerometer (G) vs Time (sec)

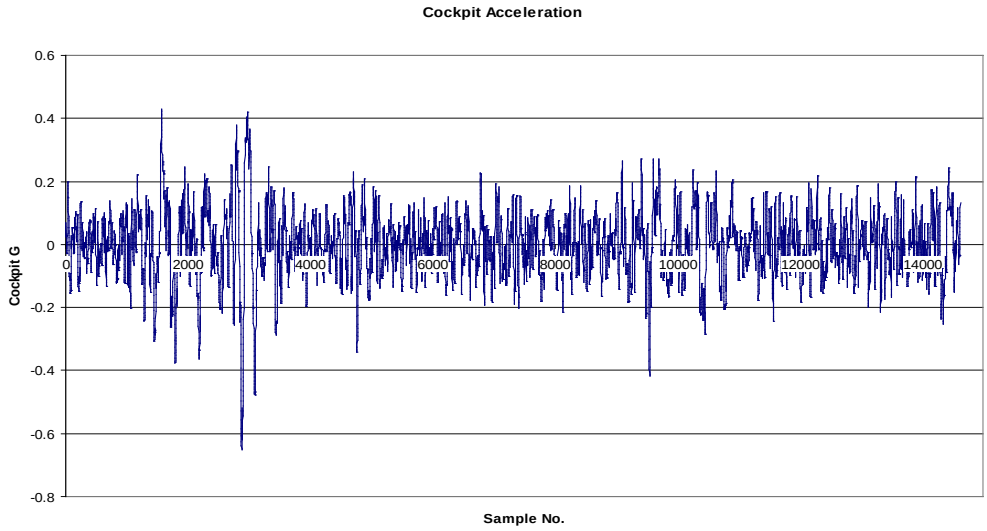

Figure 2. The ProFAA B727 Simulation—Cockpit Vertical Acceleration (G) vs Time (sec)

2.1.1 Overview of B737-800 Simulator Flight and Motion Systems.

The B737-800 simulator is an FAA-certified Level D flight training device, providing a six-degree-of-freedom motion system, high-resolution visual display, and sound systems.

The B737-800 simulator runs at an iteration rate of 60 Hertz (Hz) and provides a simulation of the aircraft equations of motion and interaction with the ground and air. The B737-800 simulator assumes a rigid aircraft and implements buffets due to airframe flexing only in specific instances as needed for realism. The B737-800 simulator sends aircraft linear and rotational velocities and accelerations to the simulator visual and motion systems.

The motion system provides motion cues for aircraft maneuvers. Because the motion system actuators provide limited travel, sustained low-frequency accelerations are not possible. The motion software is optimized using a complex set of filters to provide cueing for the most critical aircraft training maneuvers, such as takeoffs, aborted takeoffs, and landings.

2.1.2 Integration of Real-World Surface Elevation Profiles.

The real-world profiles consist of airport surface elevation changes along the longitudinal axis of the airport runway or taxiway. The elevation profiles are two-dimensional; height varies only with respect to x-distance along the runway.

The B737-800 simulator runs at a rate of 60 times per second. The highest ground speed for a B737-800 is approximately 150 knots or 253 feet per second (fps). At this speed, the B737-800 simulator responds to a change in surface elevation every 4.22 feet (253fps/60 sec) along the surface profile. A surface profile sample spacing of 4 feet was initially chosen to match the sample spacing with the simulator response rate at the highest anticipated ground speed.

During the preliminary and final surface roughness studies' development, ground speeds of 20 and 100 knots were chosen for the taxiway and runway scenarios, respectively. Testing showed that providing a profile resolution higher than the simulator sample rate resulted in increased cockpit accelerations.

For taxiway scenario movement at 20 knots (34 fps), the profile height is sampled by the roughness model software every 0.56 feet (34 feet/60 Hz) along the profile. Runway scenarios at 100 knots (168 fps) provide profile height sampling every 2.8 feet (168 feet/60 Hz).

To improve the cockpit acceleration response, the profile sample spacing was changed to 0.4 feet for taxiway profiles and 2.0 feet for runway profiles.

These simulator profile sample spacings were chosen to provide height data at a higher resolution than the simulator's sample interval while keeping the profile data file size within simulator input limits.

2.1.3 Integration of Surface Profiles Into the B737-800 Simulator Flight Model.

The B737-800 simulator software was modified to allow selection and input of surface profiles into the simulator run-time software. A simulator instructor station control page was created to facilitate profile selection and control. Linear interpolation was used to calculate profile elevation values between data points. Routines were created for aligning the surface elevation profiles with the flight simulator reposition runway and a parallel taxiway. The surface profile elevation data were integrated into the flight model with individual gear height modeled as a function of the gear's position along the elevation profile. When the simulated aircraft moves along the profile, the aircraft tire and landing gear strut models react to changes in surface height and generate strut forces. The strut forces are input into the flight model equations of motion, generating linear and rotational velocities and accelerations at the aircraft center of gravity (CG).

2.1.4 Initial Evaluation of the B737-800 Simulator Response to Roughness Profiles.

The B737-800 simulator response to surface roughness was evaluated both objectively and subjectively. Test scenarios were created to move the aircraft along the surface profile at a fixed speed and record test parameters. An accelerometer (appendix G) mounted below the pilot's seat provided vertical acceleration data. Subjective assessments of the B737-800 simulator response were made by several engineers and two industry pilots. The B737-800 simulator cockpit vertical accelerations were compared with the predicted accelerations generated by the ProFAA airport pavement simulation program [6].

Initial testing showed the B737-800 simulator motion and visual both responded to the surface roughness profiles; however, the cockpit accelerations were lower in intensity than those predicted by the ProFAA program. Subjectively, the cockpit accelerations felt somewhat soft and lacked the higher-frequency vibrations associated with travel on a rough airport surface. Because the B737-800 simulator only calculated rigid-body accelerations, the higher-frequency vibrations resulting from body and wing flexing were missing from the simulated cockpit accelerations.

2.1.5 Additional Enhancements to the B737-800 Roughness Model.

2.1.5.1 Addition of Aircraft Body and Wing Flexing Model.

To provide realistic cockpit vibrations in response to surface roughness, a flexible mode simulation was developed to simulate the cockpit vibrations caused by aircraft fuselage flexing due to surface roughness. The FAA-provided flexible mode model used strut force as input to excite the bending mode accelerations. The model outputs linear bending mode positions, velocities, and accelerations at five modal positions: Nose Gear, Left Main Gear, Right Main Gear, CG, and Cockpit.

The flexible mode model was implemented in the B737-800 simulator software. Modeling of up to four bending modes was provided, with the number of active bending modes selectable from the instructor station. Cockpit vertical accelerations (GCP) were calculated using the following formula:

GCP = (VWGD - VQD * VXXM(1) + ModePosZAccel(5)) / 32.2

VWGD	=	Z-body acceleration (ft/s^2)
VQD	=	Pitch acceleration body axis (rad/s^2)
VXXM(1)	=	X-body distance of nose gear from CG (ft)
ModePosZAccel(5)	=	Flex mode vertical acceleration at cockpit (ft/s^2)

The B737-800 simulator model transfers only the CG (not cockpit) accelerations to the motion system. The motion software transforms the CG accelerations into cockpit accelerations. To send the cockpit flexible mode data to the motion system, the cockpit vertical accelerations were first translated into pitch accelerations at the CG, and then added to the flight model rigid-body pitch velocity and acceleration outputs. An accelerometer mounted beneath the B737-800 simulator cockpit provided measures of actual cockpit acceleration for this study. The addition of the flexible mode simulation provided realistic levels of cockpit acceleration intensity and frequency compared with the B727 cockpit accelerations predicted by the FAA ProFAA simulation, as shown in figures 1 and 2. Simulator cockpit acceleration graphs are provided in appendix D.

2.1.5.2 Motion Filter Tuning.

The motion system filters the flight model accelerations to optimize the motion response within its limited motion range. The filters are tuned to enhance the realism of maneuvers critical for flight training, such as takeoff rotation, aborted takeoffs, and deceleration after touchdown. High-pass filters are used to limit low-frequency motions and maintain the motion actuators near their mid-range. The cockpit vertical response to surface roughness was enhanced by adjusting the vertical high-pass filter. The normal settings for the vertical high-pass filter are a breakpoint of 2.5 rad/sec (0.4 Hz) with a gain of 0.7. The breakpoint frequency was decreased to 0.1 rad/sec and the gain increased to 1.0.

2.1.5.3 Existing Generic Roughness Model.

The B737-800 simulator contains a generic surface roughness model providing five levels of random surface roughness. The generic roughness provides simulation of a random series of surface spalls and mats. The higher-order cockpit vibrations associated with the generic roughness are modeled on a spectral analysis of real-world aircraft vibrations associated with taxiing at 30 knots on a rough runway. The amplitude of the simulated vibrations is modulated with respect to the simulated aircraft ground speed. Figure 3 shows an example of the surface height variations generated by the generic roughness model.

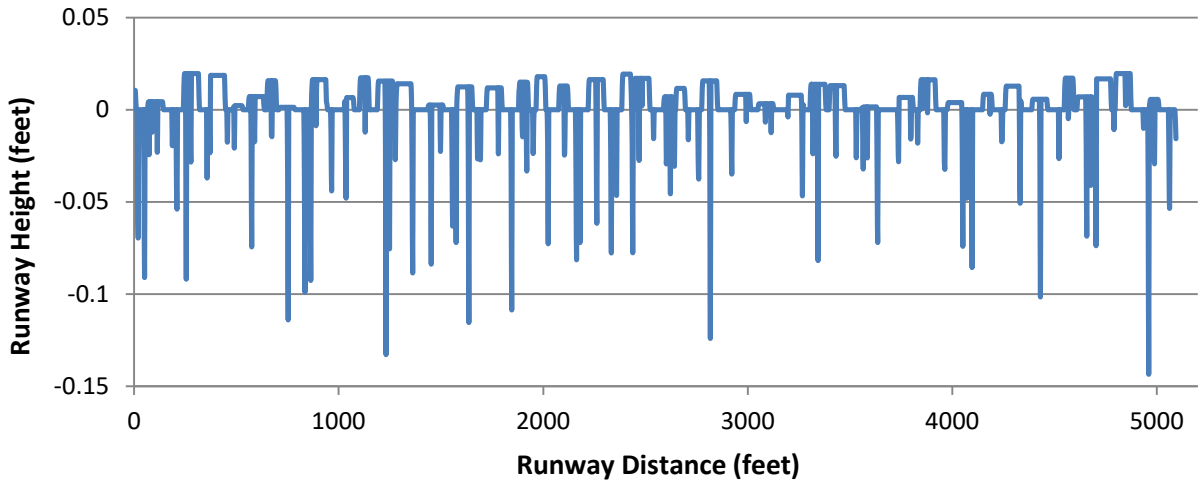

Figure 3. Example of B737-800 Simulator Generic Roughness Surface Height Variations

Some differences between the B737-800 simulator generic and real-world roughness simulations are listed below:

- The real-world roughness profiles provide a range of surface roughness types (such as localized surface deterioration and crests due to crossing runways/taxiways) and provide examples of isolated discrete jolts. The generic profiles are limited to simulation of spalls and mats with a uniform general intensity of roughness along the length of the profile.

- Because the real-world profile roughness is uniform across the transverse width of the surface, no lateral cockpit accelerations are produced. However, the generic roughness simulation models the random roughness separately for the left and right main landing gear and produces lateral cockpit accelerations.

- The real-world roughness simulation models the cockpit accelerations due to aircraft body flexing in response to gear forces from moving along real-world roughness profiles. The generic roughness simulates aircraft body flexing effects by adding motion buffets, with buffet intensity based on aircraft speed, but does not simulate vibrations from isolated jolts.

2.2 REAL-WORLD ROUGHNESS PROFILES.

Real-world airport taxiway and runway profile data were obtained from taxiway and runway surface profiles provided by the FAA, Boeing, and Airbus. Appendix B provides a list of profiles used for the Boeing 737-800 roughness study. Figure 4 shows the FAA surface profiling equipment used to capture the airport surface profiles. The following sensors were used in the profiling devices:

- Vehicle Elevation, Allied Signal QA700 Q-flex® Accelerometer
- Vehicle-to-Pavement Distance, Selcom 2207 Optocator™ Laser Sensor
- Traveled Distance, Datron DLS-2 Optical Speed and Distance Sensor

Figure 4. The FAA Surface Profiling Equipment

The essential element of an inertial profiling device, which makes the technique feasible, is a high-quality accelerometer. The accelerometer is the hardware for a single-axis inertial navigation system and is used to measure the absolute vertical position of a point on the test vehicle (the vertical position relative to an inertial reference). The accelerometer is mounted on the test vehicle with its sensitive axis aligned in the vertical direction. The vertical position is computed by double integrating the accelerometer output signal. Long-term drift errors are removed by high-pass filtering or by other means of compensation. The distance from the accelerometer mounting point to the surface of the pavement is measured with a displacement measurement sensor. The combination of the two measurements then gives the absolute elevation of the pavement surface. Distance traveled by the test vehicle along the pavement is measured with a speed sensor, or a direct-reading, distance-traveled sensor. A continuous longitudinal elevation profile is, therefore, measured relative to an inertial reference (with a slowly moving datum, if the accelerometer signal has been high-pass filtered).

An FAA-designed and -manufactured control box was used to integrate the signals from the three sensors affixed to the data collection vehicle. A standard laptop (notebook) computer was used to collect the raw data from the sensors, to compute the profile from the raw data, and to compute the indices used for the evaluation of pavement condition using FAA software.

For this study, a set of profiles (see appendix B) was chosen to provide a wide range of roughness levels as well as examples of both uniform roughness (consistent roughness intensity along the profile) and non-uniform roughness (variations in roughness intensity along the profile).

The real-world profiles were formatted for integration with the B737-800 simulator ground model as follows.

- A subsection of each profile was selected with proper length for simulator scenarios.
  - Taxiway scenarios: 1000-foot profile length for 30-second duration at 20 knots
  - Runway scenarios: 5100-foot profile length for 3-second duration at 100 knots
- The profiles were filtered to remove low-frequency variations in height using a 1000-foot cutoff high-pass filter.
- The profile height units were changed from inches to feet to match the simulator flight model units.
- The profile height sample spacing was changed to align with the flight simulator's sample rate.
  - Taxiway profiles: 0.4-foot sample spacing
  - Runway profiles: 2.0-foot sample spacing
- Add a 3-second smooth lead-in to each simulator profile.

Figure 5 shows an example of flight simulator surface height variations generated by a real-world roughness profile.

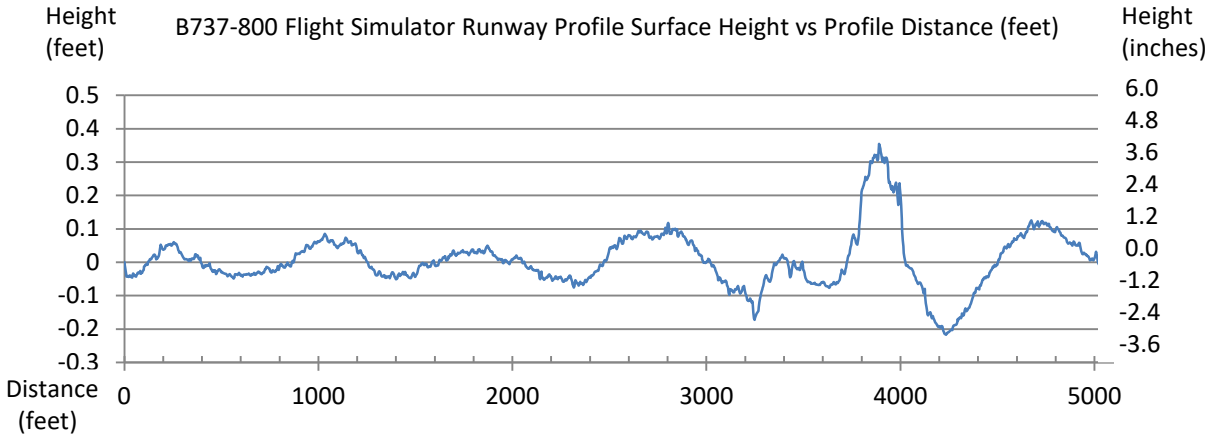

Figure 5. Example of Flight Simulator Surface Height Variations for a Real-World Runway Surface Profile
(Profile height is shown in both simulator units (feet) and original units (inches).)

Additional details for real-world profile formatting are provided in appendix C.

2.3 GENERIC PROFILES.

Twenty generic surface roughness taxiway and twenty generic surface roughness runway profiles were included in the preliminary surface roughness study test scenarios for comparison with the real-world roughness model [5]. The intensity levels of the standard simulator generic surface roughness were not high enough to obtain unacceptable ratings from pilots; therefore, rougher generic roughness profiles were created by increasing the intensity of the generic roughness.

In keeping with the roughness study objectives, the final surface roughness study focused on pilot ratings of real-world surface roughness profiles. For the final roughness study, the number of generic profiles was reduced to three taxiways and three runways, which increased the number of real-world profiles to 37 each for taxiways and runways.

2.4 TEST SCENARIOS.

A methodology was developed to present surface roughness profiles for evaluation and to obtain pilot roughness ratings and objective simulator data. Test scenarios, roughness rating forms, and pilot briefings were developed with input from human factors specialists, and refined during a series of pilot studies in 2010 and 2011 [5]. Early scenario designs explored the following variations:

- Length of test scenarios
- Speed of aircraft movement
- On-ground movement only versus takeoff and landing movement
- Pilot controlled versus automated scenarios

NCHRP highway rideability studies [1] were reviewed, leading to the following scenario design for the preliminary and final roughness airport pavement studies.

Pilots were presented with a set of 40 taxiway and 40 runway scenarios, providing a range of surface roughness.

Scenarios were designed to provide automated movement along the taxiway or runway for 30 seconds. The takeoff and landing scenarios were rejected because of the length of time required (approximately 2 minutes for each takeoff scenario and 3 minutes for each landing scenario).

The pilots assumed the role of a non-flying pilot or observer during the scenarios with no input to the flight controls, allowing the pilots to focus their full attention on assessing the ride quality. Using pilots in a non-flying role allowed placement of a third subject in the cockpit (seated in the observer's seat just behind the pilots), as shown in figure 6, allowing collection of ride-quality ratings from three subjects simultaneously.

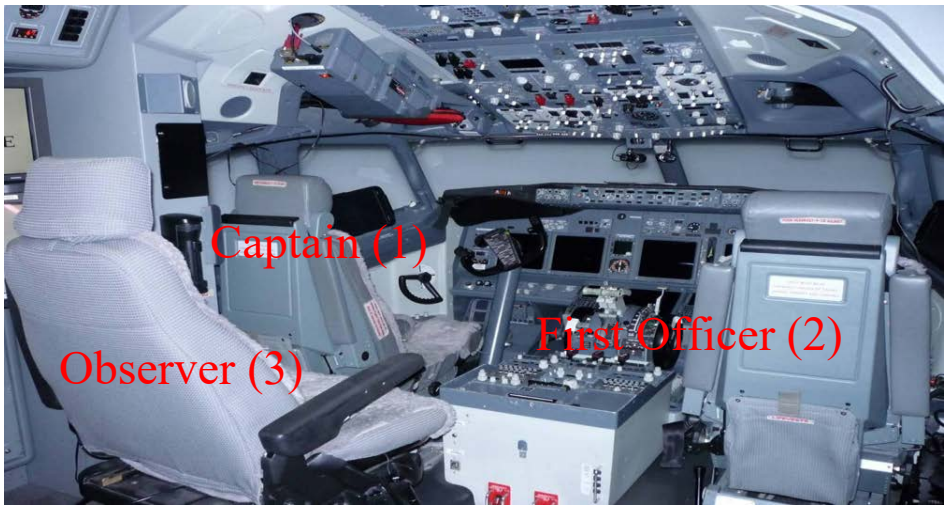

Figure 6. The FAA B737-800 Simulator Cockpit Seating Positions

A statistical analysis of the preliminary surface roughness study [5] ratings showed no significant differences with regards to seat position. The matrices of correlation coefficients for the pilots' average numerical ratings of taxiways and runways were computed from the pilots' responses, as shown in tables 1 and 2, respectively. A correlation coefficient near 1.0 (100%) indicates high correlation, with 1.0 indicating perfect correlation.

Table 1. Pilot Taxiway Correlation Coefficients

Taxiway Correlation	Captain	First Officer	Observer
Captain	1.000	0.989	0.991
First Officer	0.989	1.000	0.990
Observer	0.991	0.990	1.000

Table 2. Pilot Runway Correlation Coefficients

Runway Correlation	Captain	First Officer	Observer
Captain	1.000	0.985	0.990
First Officer	0.985	1.000	0.987
Observer	0.990	0.987	1.000

Since the average numerical ratings from pilots in different seats were about 99% correlated, it was concluded that each pilot received a similar experience regardless of seat location (see figure 6).

Subject pilots were presented with taxiway and runway profiles that provided a range of roughness from very smooth to very rough, as well as examples of both uniform and non-uniform pavement roughness. A standardized roughness rating form was used for capturing pilot

ratings of rideability. For the preliminary surface roughness study [5], a total of 80 scenarios were provided in the following categories:

- 20 real-world taxiway scenarios at 20 knots
- 20 real-world runway scenarios at 100 knots
- 20 generic taxiway scenarios at 20 knots
- 20 generic runway scenarios at 100 knots

For the final surface roughness study, the number of real-world scenarios was increased to present a wider range of real-world roughness. Additional real-world profiles were selected to provide examples of specific types of non-uniform roughness, such as crests occurring at intersecting runways and taxiways. A total of 80 final study scenarios were provided in the following categories:

- 37 real-world taxiway scenarios at 20 knots
- 37 real-world runway scenarios at 100 knots
- 3 generic taxiway scenarios at 20 knots
- 3 generic runway scenarios at 100 knots

2.5 RATING FORM DEVELOPMENT.

The roughness rating form was developed to obtain pilot subjective ratings of airport surface rideability as well as evaluating the need for improvement. The roughness rating form was modeled after the American Society for Testing and Materials (ASTM) rating form [7] and provides the following inputs:

- Rideability Level: Numeric value from 0 to 10 indicating the ride roughness with 10 = perfectly smooth and 0 = impassable

- Need-for-Improvement: Checkbox selection indicating the need for surface improvement

The preliminary roughness study [5] rating form, shown in figure 7, provided the following Need-for-Improvement selections:

- Acceptable: Ride Quality Does Not Need Improvement
- Uncomfortable: Recommend Ride Quality Improvement
- Unacceptable: Ride Quality Must Be Improved

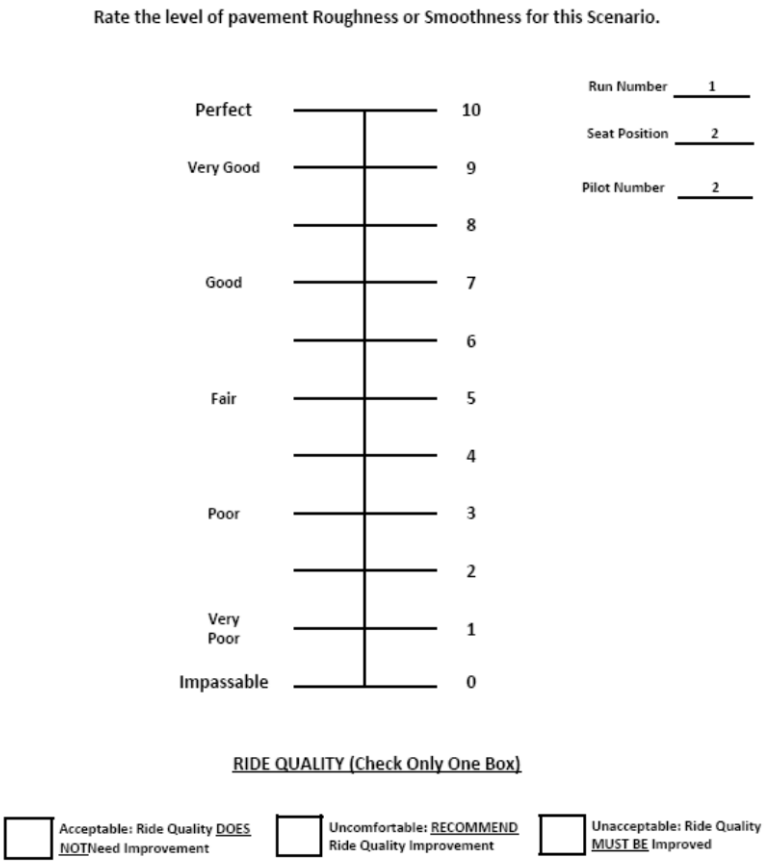

Figure 7. Preliminary Surface Roughness Study [5] Rideability Rating Form

Analysis of the preliminary roughness study data showed that the subjective pilot ratings of profile roughness as compared to their corresponding selection of Need-for-Improvement (acceptable, uncomfortable, and unacceptable) were not consistent. There was a wide range of ride-quality ratings within each of the Need-for-Improvement categories and, therefore, overlapping ranges between categories.

For the final surface roughness study, the pilot rating form was modified to simplify the Need-for Improvement ratings and to align more closely with the ASTM rating form [7]. The number of Need-for-Improvement checkboxes was changed from three (acceptable, uncomfortable, unacceptable) to two (acceptable, unacceptable). Additionally, the Need-for-Improvement section label was changed from Ride Quality to Need-for-Improvement for clarity. The updated final surface roughness study pilot rating form is shown in figure 8 and appendix K.

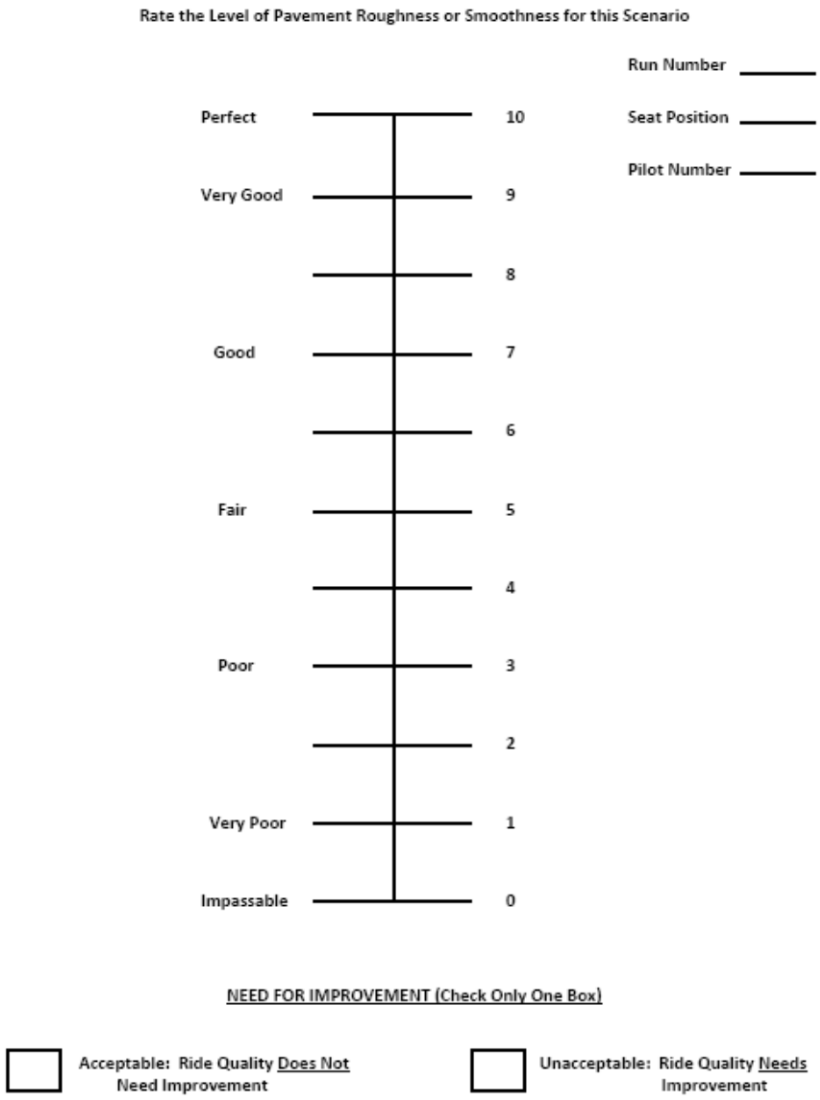

Figure 8. Final Roughness Study Rideability Rating Form

2.6 PILOT BRIEFINGS.

The final roughness study included pre-brief and post-flight sessions. The Microsoft® PowerPoint® presentations for the sessions are shown in appendices I and J. The pre-brief session provided background information about the study, explained the simulator testing process, and defined the rating scale limits. The pre-briefing information provided study background information and an explanation of the study test sessions. The roughness rating form instructions were read from a script to each group of pilots to ensure that the same instructions were provided to each group. A post-flight session was conducted immediately following each test session to capture pilot feedback on the fidelity of the roughness simulation, recommendations on methods for improving the study, and perceptions of airport surface roughness in the real world.

2.7 PILOT RATING PANEL SELECTION.

Thirty-six pilots were recruited to participate in the final surface roughness study. The original plan was to use commercial airline pilots with current experience in B737-800 aircraft and no previous experience in the FAA's pavement roughness studies. However, due to the limited availability of commercial B737 pilots, it was necessary to include some pilots with prior study experience and also some military KC-135 pilots. The KC-135 military pilots were selected because the KC-135 and B737-800 are both Boeing aircraft with similarly sized fuselages.

As part of the pilot data collection, CCRC also collected the following information about each participant: current airline, current type ratings, hours of operation for each aircraft type, rank, and previous military experience.

3. FINAL SURFACE ROUGHNESS STUDY.

3.1 ROUGHNESS RATING SESSIONS.

For the final surface roughness study, 12 roughness rating sessions were conducted. The first rating session was used for final tuning of the roughness profile intensities. The profile intensities were decreased slightly after session 1 to provide a more even distribution of roughness. A gain factor was adjusted to decrease the input profile height for each scenario. Appendix B provides a list of the surface profile gain factors. After adjustment, the profile intensities remained consistent for sessions 2 through 12. For each test session, three pilots provided roughness rideability and Need-for-Improvement ratings for the 80 taxiway and runway profiles. Prior to rating the profiles, two practice scenarios were presented to acquaint the pilots with the scenario format and rating process. Each test scenario presented aircraft movement along a taxiway or runway profile for 30 seconds at a fixed speed of 20 knots for taxiway profiles and 100 knots for runway profiles. Pilots were requested to limit conversations during scenarios and to evaluate each scenario with no discussion.

3.2 COLLECTED SIMULATOR PARAMETERS.

Flight simulator parameters were collected to obtain objective measures of the aircraft response to the roughness profiles. Data was collected during each test scenario at a 60-Hz rate and stored in a comma-delimited text file. The following parameters provided the primary data used for analysis:

- Elapsed time
- Aircraft distance along roughness profile
- Profile height at aircraft
- Cockpit vertical acceleration

An accelerometer mounted under the cockpit floor[1] provided vertical acceleration levels during the test scenarios. The accelerometer output was captured and processed to provide a numeric

[1] The International Organization for Standardization (ISO) specifies that the accelerometer be mounted in pilot's seat [8], but this was not feasible in the flight simulator.

average of the cockpit acceleration for correlation with subjective pilot ratings of roughness. Appendix E provides a detailed list of the collected data parameters.

3.3 INITIAL DATA EVALUATION.

3.3.1 Evaluation of Accelerometer Data for Consistency.

The collected accelerometer data was reviewed for validity and for the consistency of accelerations provided for the 11 test sessions. Figures 9 and 10 show the recorded accelerations for the 37 taxiway and runway scenarios with data for each test session plotted in a different color (sessions 2 through 12). As the close alignment of the plots show, consistent accelerations were provided for the 11 test sessions.

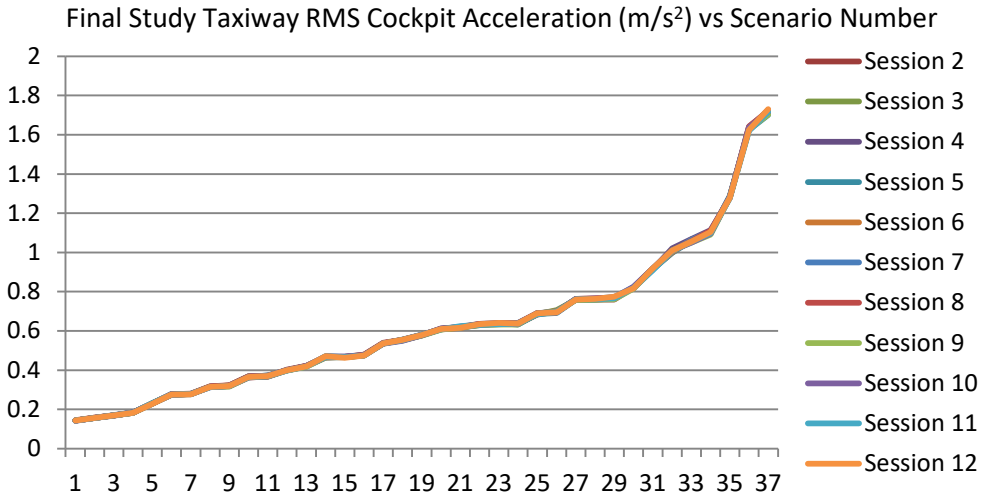

Figure 9. Overlay of Taxiway RMS Cockpit Acceleration for Sessions 2 Through 12

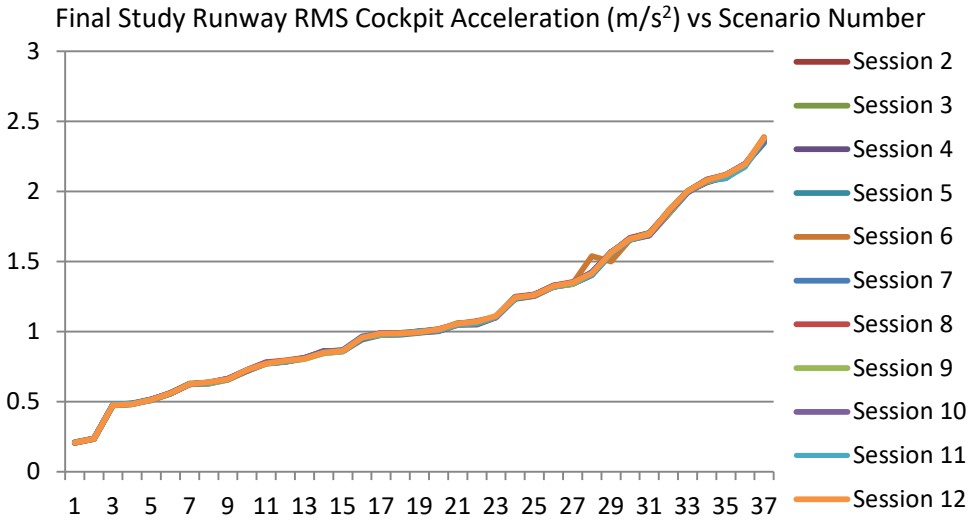

Figure 10. Overlay of Runway RMS Cockpit Acceleration for Sessions 2 Through 12

3.3.2 ISO Processing of Accelerometer Data.

The requirements of ISO 2631 [8] were followed to the extent possible in the collection, processing, and evaluation of the measured cockpit accelerations. The basic evaluation method contained within the standard is in terms of a weighted root-mean-square (RMS) acceleration, as defined in subclause 6.1 by the equation:

$$a_W = \left[\frac{1}{T} \int_0^T a_{\mathrm{W}}^2(t)\, dt \right]^{\frac{1}{2}}$$

where:

$a_W(t)$ is the weighted acceleration (translational or rotational) as a function of time (time history), in m/s^2 or radians per second squared (rad/s^2), respectively.

T is the duration of the measurement, in seconds.

The weighted acceleration ($a_{\mathrm{W}}(t)$) is computed from the measured acceleration by applying a set of transfer functions completely defined in the standard. The transformations have two purposes: (1) lower and upper frequency band limitation and (2) normalization of the acceleration amplitude to mimic relative human response over the frequency range of interest. The transfer functions for ISO Weighting (W_k) were applied to the measured accelerations in the time domain by the method described in appendix F. Amplitude ratio versus frequency plots are shown in figure 11 for the ISO-specified transfer functions (computed directly) and the filtering routines used in this study (computed from the ratio of output to input sine wave amplitudes). In figure 11, the frequency response (absolute value of the transfer function) of the weighting procedure is compared with the ISO-specified frequency response [8] on a linear scale and then in decibels (ten times the logarithm of the response). Calculation of the transfer function is detailed in appendix F.

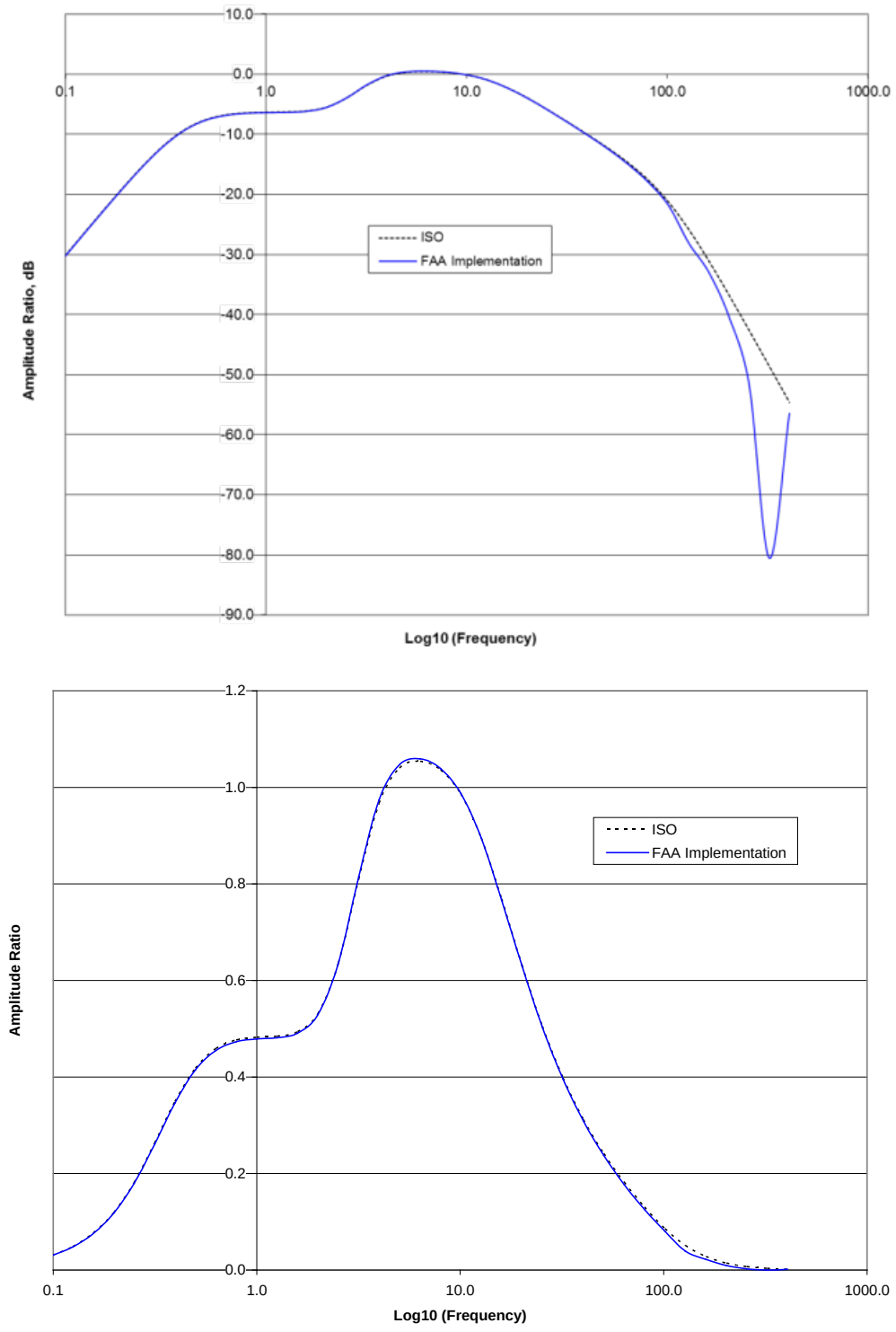

Figure 11. Frequency Response of the Weighting Procedure Compared With the ISO-Specified Frequency Transfer Function for Weighting W_k
(Amplitude ratio plotted on a linear scale (top) and a logarithmic scale (bottom).)

Note that the measured cockpit acceleration's sample rate was 60 Hz and the bandwidth of the measured accelerations, necessarily, was limited to 30 Hz. For this, and other reasons, the sample rate of the measured accelerations was increased to 1280 Hz by cubic spline interpolation before applying the weighting functions.

After applying the weighting functions, the sample rate of the weighted accelerations was decreased by low-pass filtering appropriately, cubic spline fitting, and sub-sampling to 160 Hz. For the results to be compatible, these sample rate transformations should be applied if the weighting and RMS calculations are applied to accelerations from other sources, such as an independent aircraft simulation or an operating aircraft with data rates running at higher than 60 Hz.

3.3.3 Additional Indices.

Compared to almost all other public transportation travel ways, airport pavements, and particularly runways provide very short exposure times to the vibration environment. Also, within these short exposure times, there tends to be a larger than normal number of short-length changes of pavement characteristics in the form of crossing pavements and patching. Additionally, there is a wide variation of speed that occurs during takeoff and landing, meaning that a stationary vibration environment existing within an aircraft cannot be assumed, particularly on runways. The ISO standard provides for these kinds of conditions by providing two alternative indices that can be computed and reported when the weighted RMS method is suspected to be underestimating the true environment due to shocks in the acceleration record [8].

The ISO standard [3] suggests using crest factor, a measure that shows the ratio of peak values to the average value in waveforms, to determine if the alternative indices should be used. General guidance in the ISO standard is that, in addition to the weighted RMS, one of the alternative indices should be reported when the crest factor of the acceleration record is approximately 9.0 or greater. A third alternative is specified in ISO 2631 Part 5: "Method for evaluation of vibration containing multiple shocks" [8]. The three alternative indices are:

- Maximum transient vibration value from a running RMS computation (MTVV).
- Fourth-power vibration dose value (VDV).
- Spinal response acceleration dose (D_K).

Together with crest factor, all three alternative indices are reported for each cockpit acceleration record analyzed. There is no recommended ISO index because the choice of ISO index or indices may depend upon the particular application. However, the following generalities can be made.

- Weighted RMS is the most popular index to indicate the average roughness of a ride in literature and has the most mentions in the ISO standard [8].

- Weighted VDV is sometimes preferred to weighted RMS, particularly when a ride is not uniform because occasional shocks contribute more to calculating its value (because it better estimates discomfort due to occasional shocks).

- Weighted MTVV is the maximum weighted RMS value calculated over a short time period (1 second was used, as recommended by ISO 2631-1 [8]) for estimation of maximum short-term discomfort.

- DKup is a spinal dose indicator for estimation of spinal discomfort.

Complete definitions and the methods used for computing the alternative indices are given in appendix F.

4. DATA ANALYSIS.

Analysis was performed using the subjective pilot ratings (section 2.5) and objective ISO index values (sections 3.3.2 and 3.3.3) for vertical vibrations of the simulated B737-800 real-world taxiway and runway rides compiled from the preliminary and final surface roughness studies. The following were used:

- 37 real-world taxiway and 37 real-world runway simulations with ISO index ratings and ratings by 33 pilots from final roughness testing

- 20 real-world taxiway and 20 real-world runway simulations with ISO index ratings and ratings by 12 pilots from preliminary roughness testing

Also, three pilots who participated in the fine-tuning process for the final roughness tests received 37 slightly different taxiway and runway experiences than the other 33 pilots; therefore, their responses are not included in the pilot average taxiway and runway ratings but are included in the pilot individual response analysis. Since the analysis of the preliminary surface roughness study data was published [5], this report focuses on evaluation of the real-world final surface roughness study data and, where possible, upon analysis of the combined real-world final and preliminary roughness study data.

The ISO index ratings were generated from accelerometer data for each simulated taxiway and runway. An accelerometer mounted under the cockpit floor provided vertical acceleration levels during the test scenarios. The accelerometer output was captured at a 60-Hz rate, and the data was processed to provide a numeric average of the cockpit acceleration for correlation with subjective pilot ratings of roughness. For each taxiway and runway ride, the acceleration indices[2] of section 3.3 were calculated:

- weighted RMS value (m/s^2)
- weighted MTVV (m/s^2)

[2] In preliminary roughness study tests other ISO indices, called weighted VDM and *DKdown*, were also considered, but were dropped as superfluous for the final roughness study test analysis.

- weighted VDV ($m/s^{1.75}$)
- DKup (spinal response acceleration dose, or acceleration dose value) (m/s^2)

The ISO weighted crest factor index was also computed to determine the instances in which one of the last three indices might be appropriate instead of weighted RMS.

The implementation of real-world profiles on the flight simulator may result in the loss of short-duration jolts due to the simulator's 60-Hz iteration rate and the larger profile sample spacing. For this reason, the crest factor index may be less effective for identifying profiles with a high percentage of peak waveforms in the flight simulator roughness implementation compared to the real world. Except in the case of the Acceleration Dose Value Index, the cockpit acceleration signals were processed with a set of weighting (filter) functions before calculating the index values. The intent of the weighting is to normalize the frequency content of the accelerometer signal to account for the variation of the sensitivity of human responses over the frequency range of interest. The Acceleration Dose Value Index was computed using the raw accelerometer signal. See reference 8 and appendix F for more details.

The pilot data consisted of a numerical rating from 0 to 10 (section 2.5), with fractional responses permitted, and an acceptable or unacceptable rating from each pilot for each taxiway and runway in the final surface roughness study. Taxiway and runway data used from the preliminary surface roughness study consisted of a numerical rating 0 to 10 from each pilot[3] for each taxiway and runway.

4.1 ANALYSIS OVERVIEW.

Evaluation of the data was based upon:

- Consideration of the average pilot numerical ratings of 37 taxiways and runways from the final roughness testing as a function of the first four ISO indices.

- Evaluation of the percentage of pilots rating the 37 taxiways and runways in the final roughness testing "unacceptable" as a function of the first four ISO indices.

- Discussion of crest factor as an indicator of large shocks.

- Computations using the combined real-world numerical ratings of all pilots from both studies on taxiways or runways (33 pilots × 37 taxiways and runways in regular final roughness testing, 12 pilots × 20 taxiways and runways in preliminary roughness testing, and 3 pilots × 37 different taxiways and runways in final roughness testing for a total of 1572 taxiway and runway numerical ratings) to evaluate probabilities of individual numerical pilot responses to taxiways or runways, and to verify consistency between the preliminary and final surface roughness study tests.

[3] Pilots in the preliminary surface roughness study also gave a rating of acceptable, uncomfortable, or unacceptable to each ride, but their responses could not be combined with the acceptable, unacceptable data of the final roughness study.

4.2 PILOT NUMERICAL RATINGS AS A FUNCTION OF FOUR ISO ROUGHNESS FACTORS.

The average pilot numerical ratings (0 to 10) of the 37 real-world taxiways and real-world runways of the final roughness study data set were computed and compared with the ISO roughness values: weighted RMS, weighted MTVV, weighted VDV, and DKup. (The pilot average ratings from the preliminary roughness study data were not included because they were based on averages from a different number of pilots.) Correlation coefficients were evaluated relating pilot numerical ratings and the calculated ISO index values for taxiways and runways, as shown in table 3.

Table 3. Correlation Coefficients Relating Subjective Pilot Average Ratings to Objective ISO Roughness Indices

Pilot Subjective Rating	Weighted RMS (m/s^2)	Weighted MTVV (m/s^2)	Weighted VDV ($m/s^{1.75}$)	DKup (m/s^2)
Taxiway average rating (0-10)	-0.960	-0.942	-0.972	-0.951
Runway average rating (0-10)	-0.973	-0.962	-0.983	-0.972

Correlation coefficients are negative because pilot ratings go down as each ISO index rises. These compare favorably with the correlation coefficient used in reference 1 for highway pavement study, in which the subjective rating Mean Panel Rating[4] (MPR) for highway travel was correlated with the objective measure Profile Index (PI) (used to calculate ride number) with a correlation coefficient of 0.93.

The high correlation between pilot ratings and ISO indices for taxiways and runways (with correlation coefficient -1.0 indicating perfect correlation between rising ISO index and falling pilot rating) indicates a strong linear trend between pilot ratings and ISO ratings of taxiways and runways. Therefore, the subjective pilot average numerical rating can reasonably be estimated as a function of each objective ISO index.

Curve fits of average pilot rating were therefore made as a function of each ISO index and showed that taxiways and runways had distinct trends as a function of any index. Figure 12 shows the weighted RMS trends computed by quadratic least squares fits.

[4] Mean panel rating is the average rating over a number of panels in which individual panel ratings have been made using a 0to 5 numerical scale.

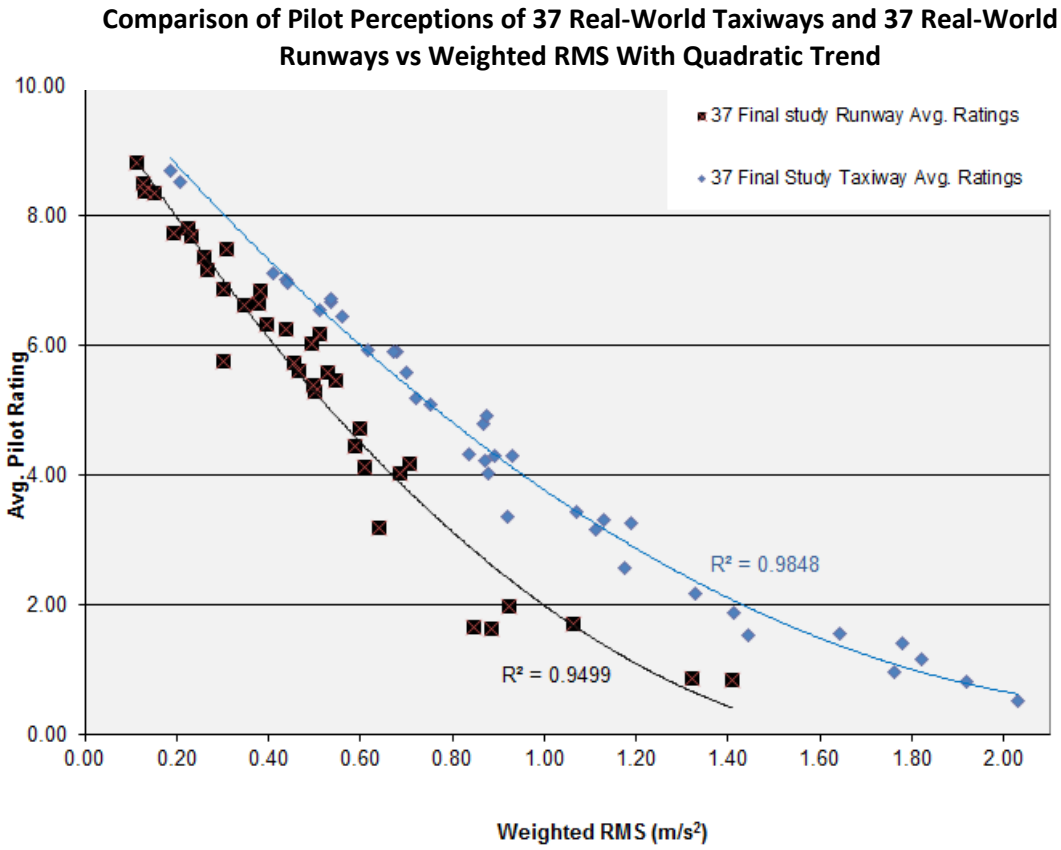

Figure 12. The Distinct Taxiway and Runway Trends for Final Surface Roughness Study Real-World Pilot Average Numerical Ratings vs Weighted RMS

In many applications, a simple least squares fit of a line (also called a linear regression) can be applied to data. However, the data trends shown in figure 12 (and in other plots to come) show substantial curvature, which demands that at least a quadratic fit is required. A quadratic is the simplest function that can be fit to data that shows curvature and fit the data within the data range. However, the quadratic graph is an arch shape (parabola), so when data are noisy, the fit can trend upward on the right before reaching the x axis (see figure 13). Hence, the quadratic fits should not be extrapolated outside the input data range.

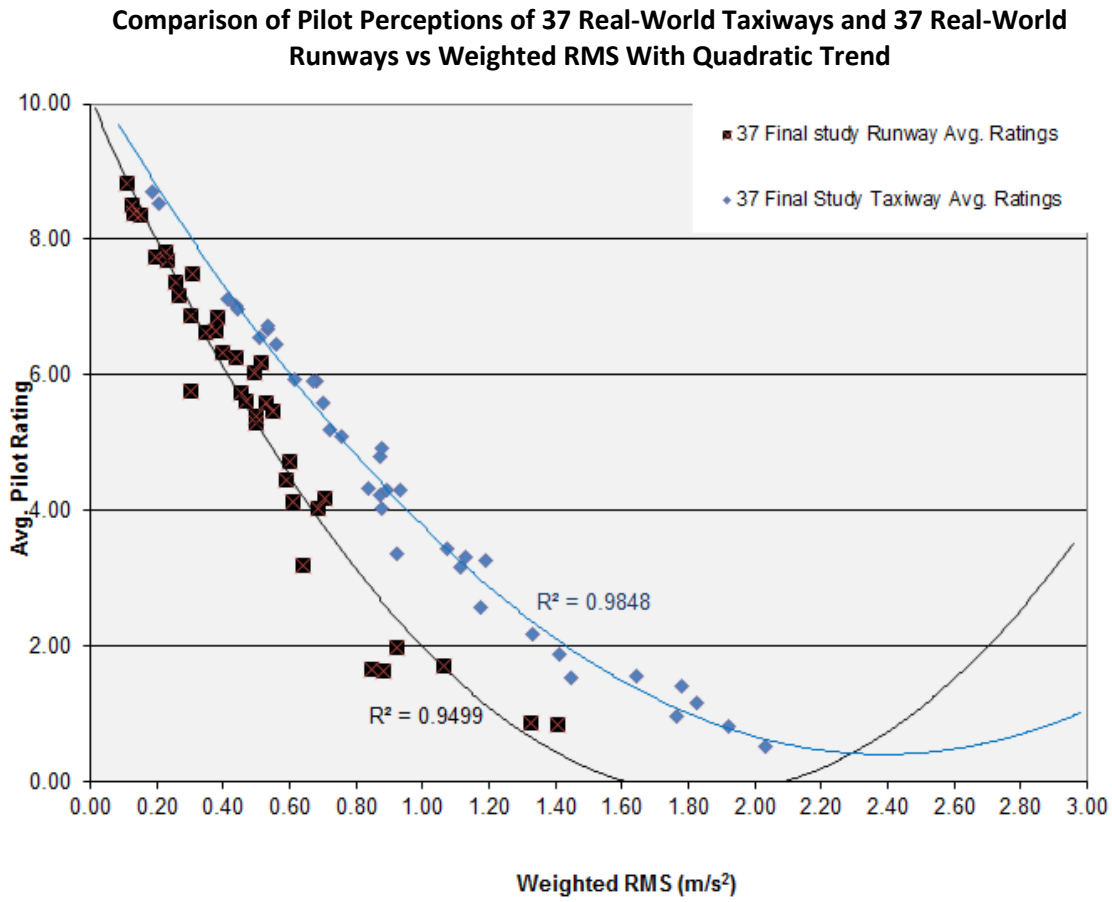

Figure 13. Extrapolating a Quadratic Fit Outside the Data Range

Various types of curve fits were attempted by the least squares method to the average runway ratings y versus each ISO index x, of the final data set:

- linear ($y = ax + b$)
- quadratic ($y = ax^2 + bx + c$)
- exponential ($y = ae^{bx}$)
- exponential through (0,10) ($y = 10e^{bx}$)
- logarithmic ($y = a \ln(x) + b$)
- shifted logarithmic ($y = a \ln(x+c) + b$)

The linear fit is motivated for classical comparison purposes and because its analysis is simple and standard. The quadratic fit is provided as the simplest fit that has curvature. The exponential and logarithmic fits are motivated by previous roughness human vibration models, such as in reference 9. The exponential fit through (0,10) provides an exponential fit in which pilots are modeled to give exactly a 10 rating when (and only when) there is no vibration. The logarithmic fit is the Fechner (or Weber-Fechner) law for general human response to external stimulus, which has been experimentally verified as a reasonable approximation for certain

ranges of human perception of brightness of light and loudness of sound[5]. The fitted functions are mathematically simplistic to avoid accidental insertion of complicated behavior without motivation and so that additional statistical analysis, such as confidence intervals and predictive intervals, can be performed. Figure 14 shows the linear, quadratic, exponential, exponential through (0 to 10), and logarithmic fits for the pilot average numerical taxiway ratings of the 37 runways in the final surface roughness study data set as a function of each ISO index. Figure 15 shows the corresponding average runway ratings.

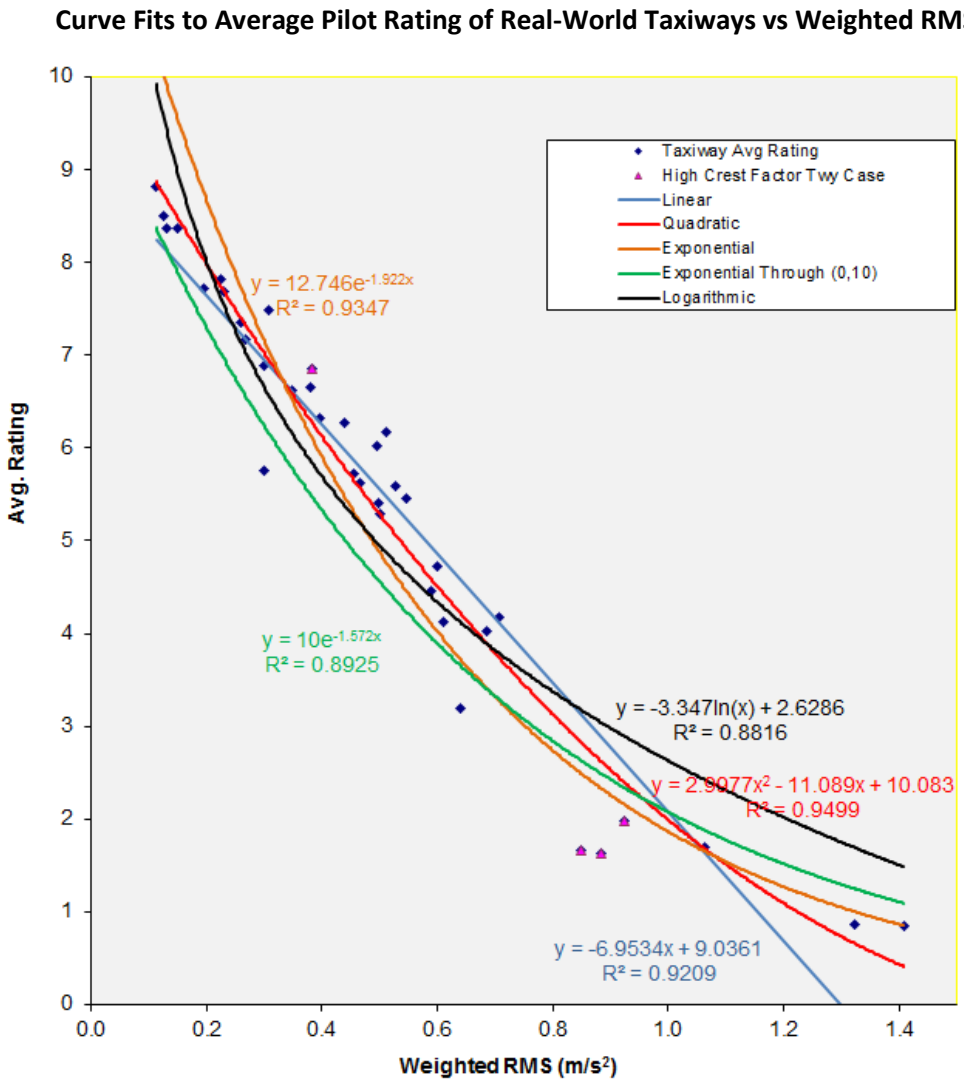

Figure 14. Various Curve Fits by Least Squares to Pilot Average Taxiway Ratings

[5] Fits by Stevens' power law for human perception ($y = ax^b$) were also attempted but found to be inaccurate and are not presented.

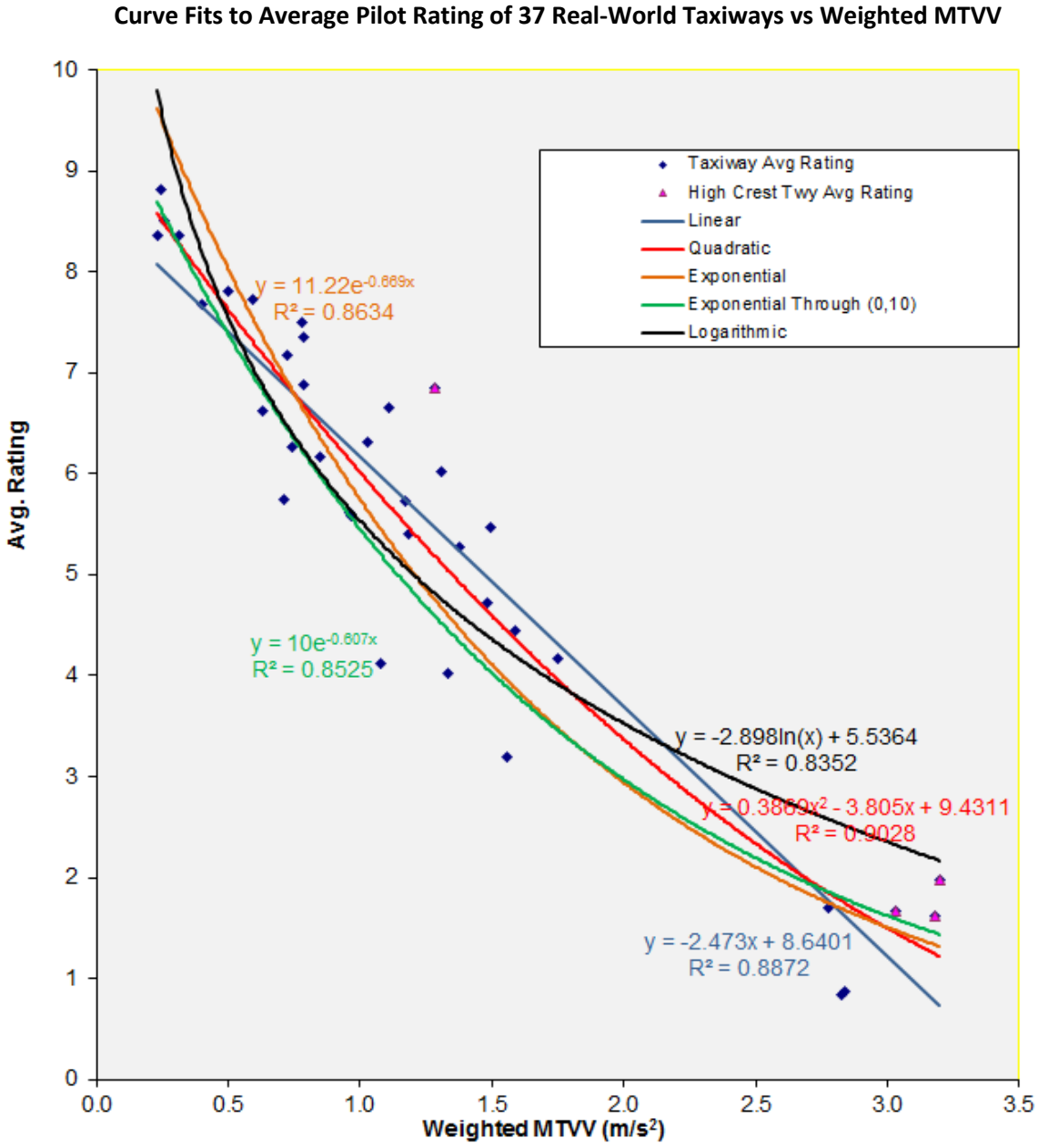

Figure 14. Various Curve Fits by Least Squares to Pilot Average Taxiway Ratings (Continued)

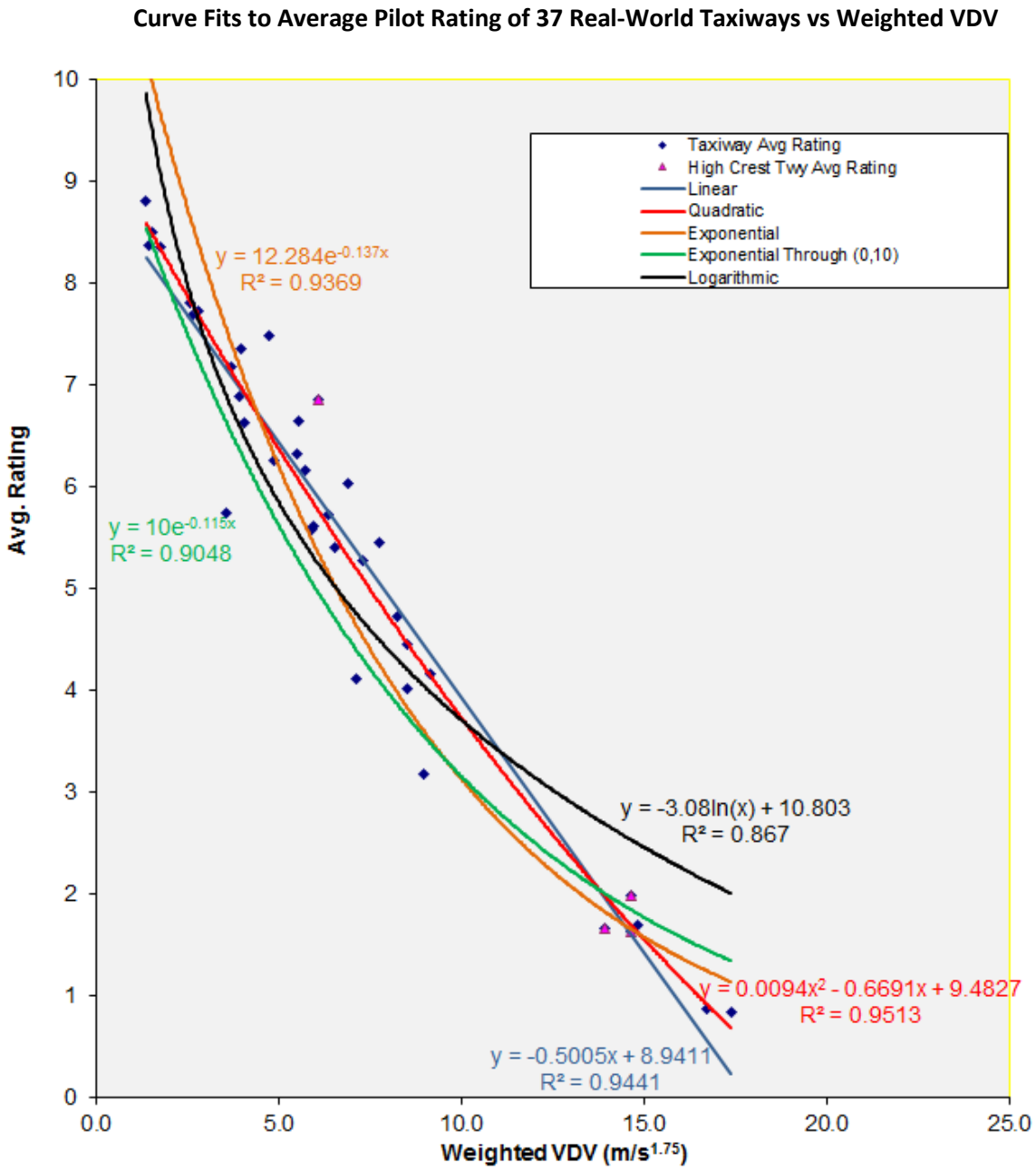

Figure 14. Various Curve Fits by Least Squares to Pilot Average Taxiway Ratings (Continued)

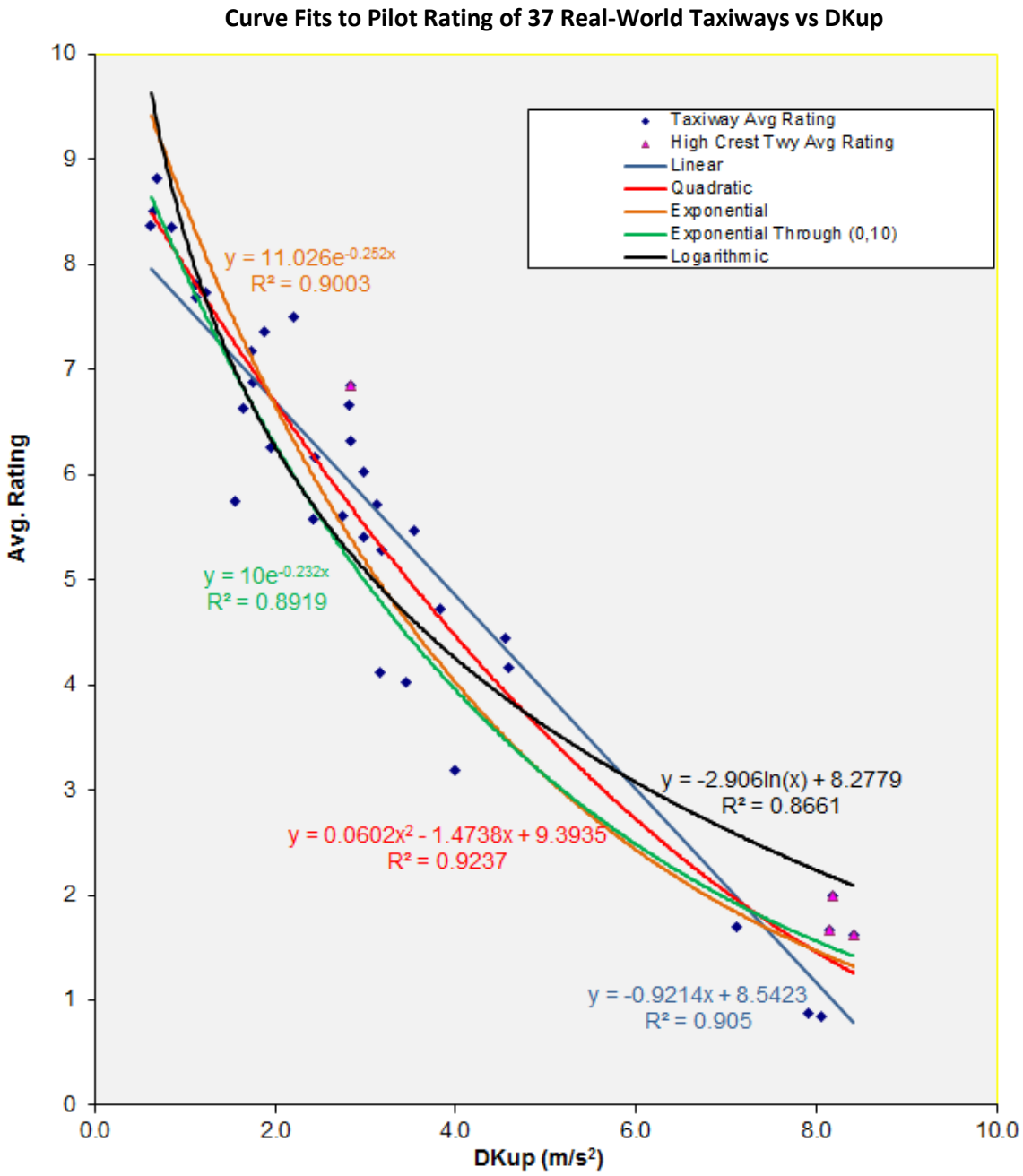

Figure 14. Various Curve Fits by Least Squares to Pilot Average Taxiway Ratings (Continued)

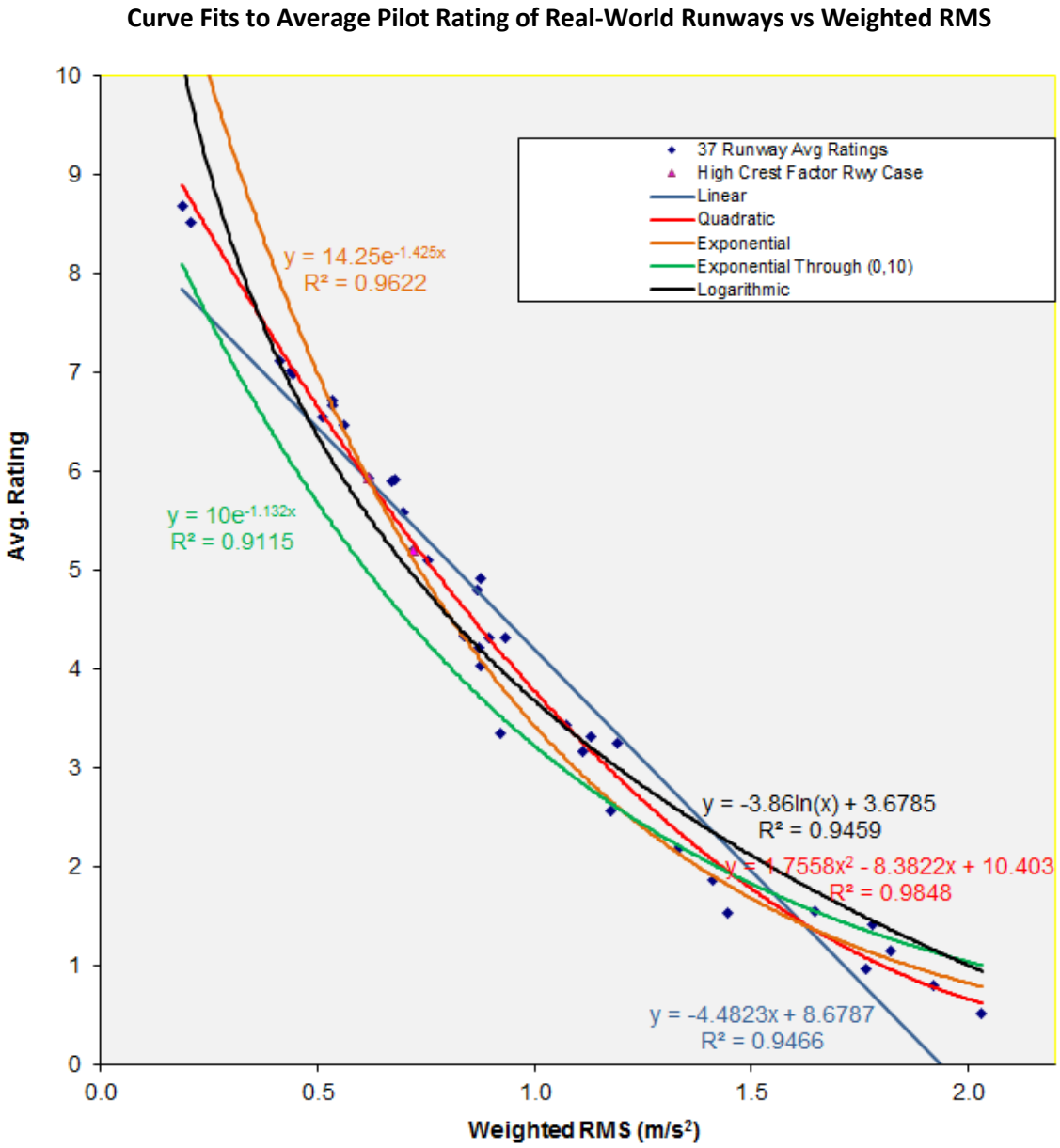

Figure 15. Various Fits of Average Runway Rating vs ISO Index by Least Squares

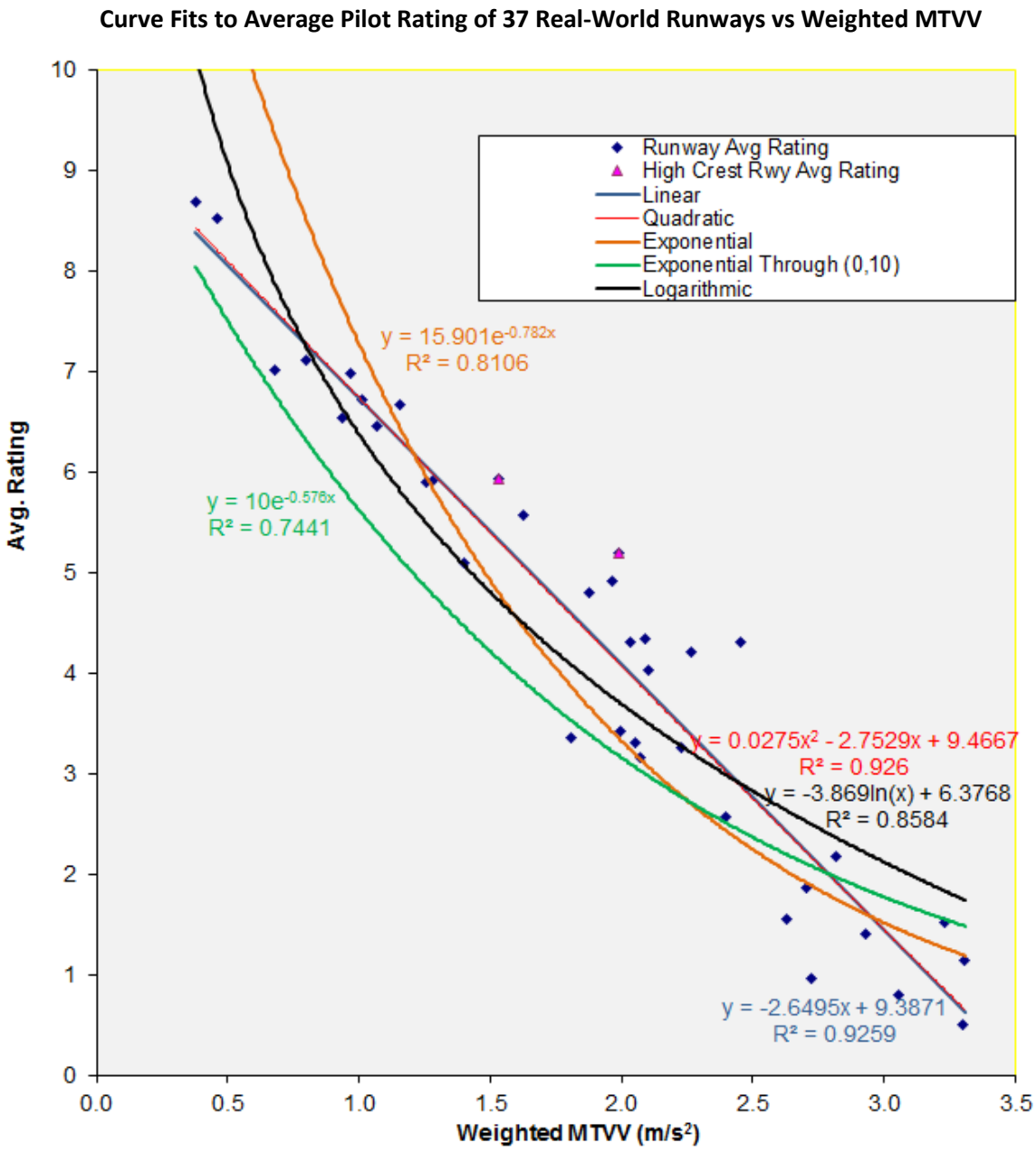

Figure 15. Various Fits of Average Runway Rating vs ISO Index by Least Squares (Continued)

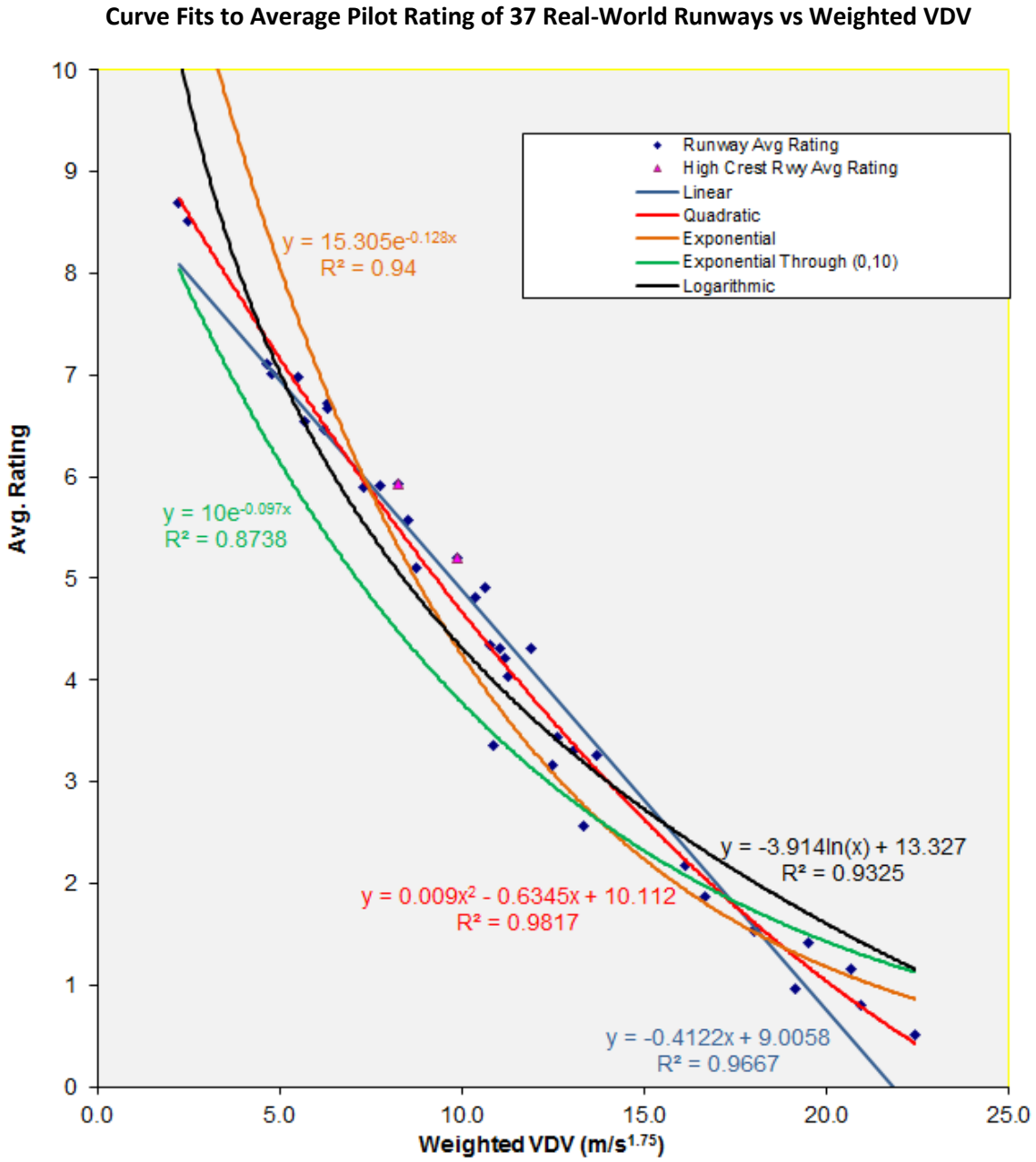

Figure 15. Various Fits of Average Runway Rating vs ISO Index by Least Squares (Continued)

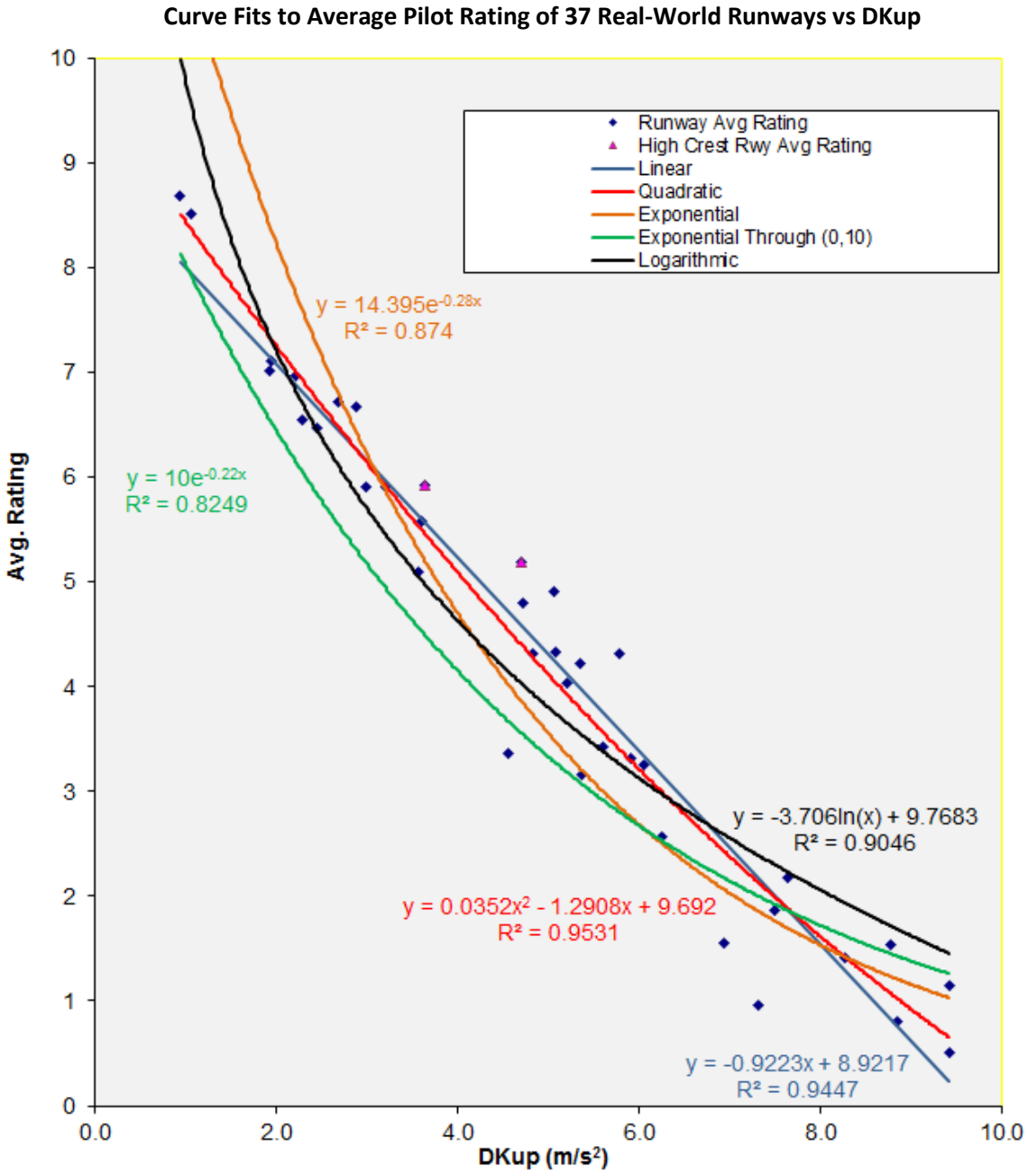

Figure 15. Various Fits of Average Runway Rating vs ISO Index by Least Squares (Continued)

The R^2 (R squared, or coefficient of determination) value of each fit shows the goodness of fit; in that the closer R^2 is to 1.0, the better the fit, and indicates that the quadratic fit is the best of the five curve fits shown.

To capture the closer fit of the quadratic function while preserving the more logarithmic behavior for extrapolation at larger index values, a fit that captures the curvature capability of the quadratic while preserving the decaying nature of the logarithmic fit on the right was introduced in the form of a shifted logarithmic fit: $y = a \ln(x+c) + b$, in which y is the pilot average numerical rating and x is an ISO index (to which "shift" c is added before taking the logarithm). The actual curve fit is unknown since subjective human evaluation is involved, but the shifted logarithmic fit provides the best combination of R^2 near 1 and decaying behavior for larger ISO index values from among the fits tested. An example is shown in figure 16 for weighted VDV.

Unlike the quadratic fit, the shifted logarithmic fit can be extrapolated to $y = 0$ (pilot numerical rating equal to zero) on the right because it is strictly decreasing. Furthermore, a shifted logarithmic fit is still simple enough to be amenable to analysis by a confidence interval for the fitted curve and a predictive interval for the samples. The confidence interval is an interval within which a fitted curve is likely to lie with a given probability under the assumption that the data points would fit the curve type, except they include normally distributed noise. The predictive interval shows where similarly generated data points would lie with a given likelihood under the same assumptions. A Matrix Laboratory (MATLAB®) program was generated to compute optimal shifts such that the least squares fit made R^2 as close as possible to 1.0 in the shifted logarithm fits.

Each ISO index may be considered to be best depending upon the particular application desired. Therefore, no ISO index is preferred here—despite the fits to weighted RMS and weighted VDV are somewhat closer (by R^2 values and reference 9). However, weighted RMS is the most commonly considered and frequently used indicator and provides an estimate of the average roughness of a ride. Weighted VDV is often considered in the analysis of rides containing non-uniform shocks and may provide "more cautious assessments of the limiting daily exposure duration" than weighted RMS methods [10]. Finally, weighted MTVV provides a maximum running value over a given period of weighted RMS, and DKup may be used as a spinal dose indicator.

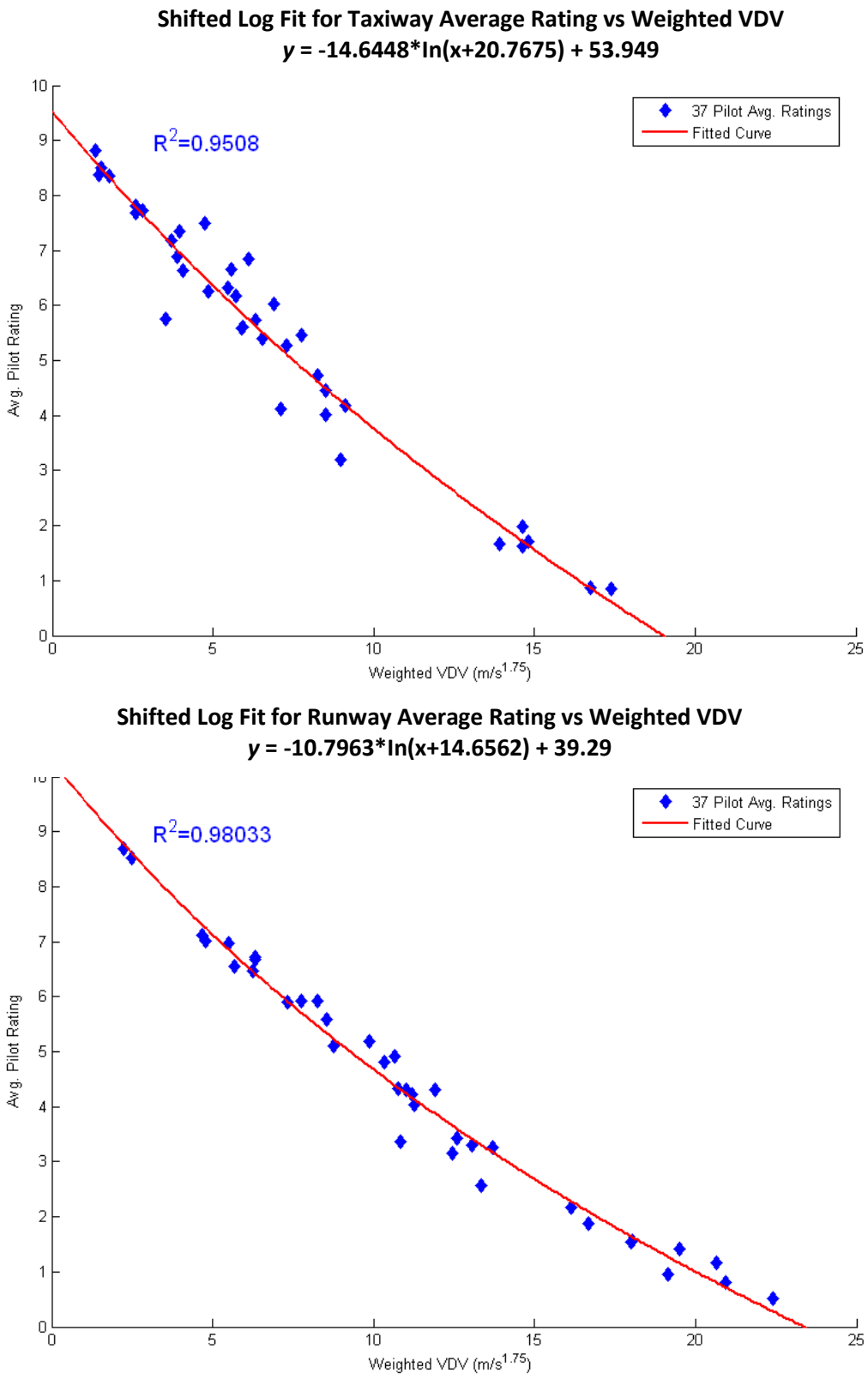

Figure 16. Shifted Logarithmic Fits of Taxiway (top) and Runway (bottom) Rating vs Weighted VDV

4.3 CALCULATION OF THE UNACCEPTABLE RANGE FOR EACH ISO INDEX.

Each pilot in the final surface roughness study rated each simulated taxiway and runway either as acceptable or unacceptable. This data was used to calculate acceptable values for the ISO roughness indices. Data from the preliminary surface roughness study could be combined because pilots in the preliminary surface roughness study were allowed a third acceptability option of uncomfortable.

4.3.1 The Numerical Rating at Which a Ride Becomes Unacceptable.

The percentage of pilots stating that a test ride was unacceptable was plotted as a function of pilot (average) numerical rating and is shown in figure 17(a). A more in-depth view, close to where the unacceptable rating declines to zero, is shown in figure 17(b).

The correlation coefficient between average taxiway rating and percentage of pilots rating the taxiway as unacceptable was -0.960 and the coefficient for runways was -0.973. These strong correlations show that a fit of percentage of pilots rating a ride as unacceptable as a function of pilot average numerical rating is reasonable. Consequently, logistic regression and simple polynomial fits that could accommodate the general behavior of each data trend (taxiway or runway) were made, with y representing the percent of pilots rating a ride as unacceptable versus x the average pilot numerical rating (0-10). These were subject to the requirement that $y = 100$ (percent unacceptable) when $x = 0$ (the lowest numerical rating). For taxiways, the logistic regression was

$$y = \frac{100}{1 + e^{-4.308+1.063x}} \tag{1}$$

and for runways

$$y = \frac{100}{1 + e^{-3.831+.891x}} \tag{2}$$

Figure 17 shows that logistic regression is slightly conservative in the tails, so polynomial fits are also given (appendix A) for a less conservative (slightly slimmer tails on the right) comparison. By solving equations 1 and 2, the numerical pilot rating at which any percentage of pilots rates taxiways or runways as unacceptable can be deduced (see table 4).

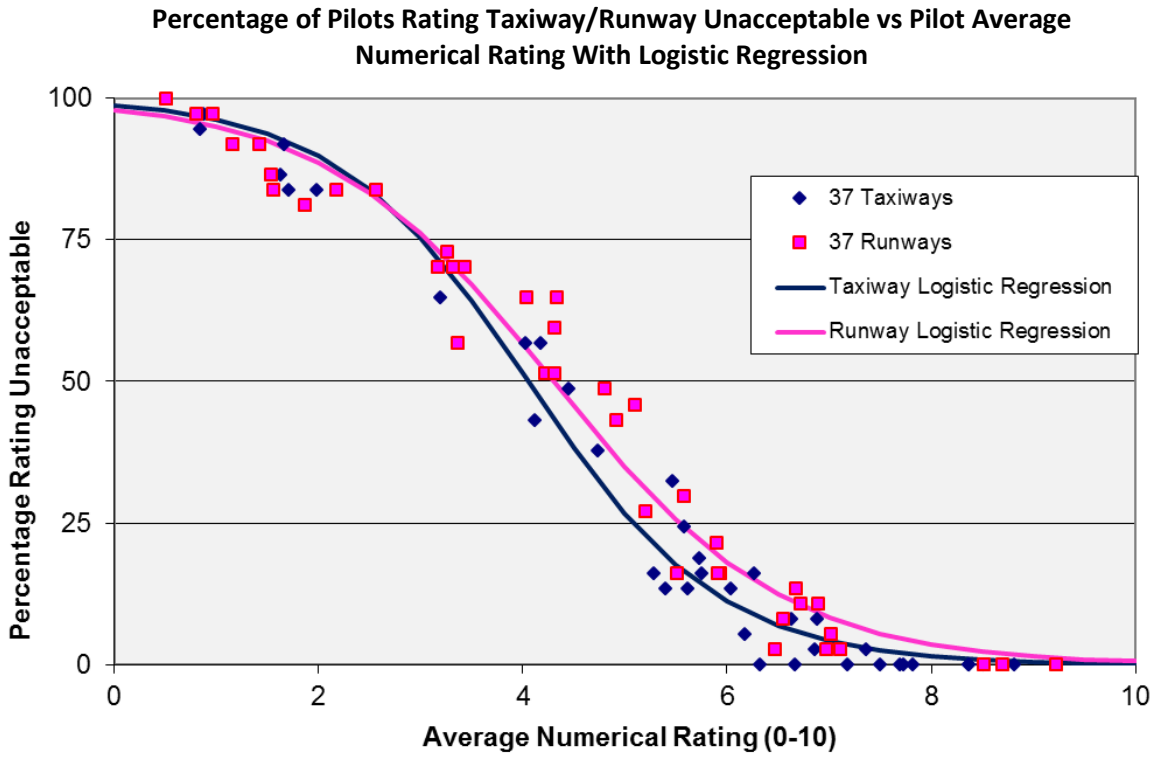

(a) Full view

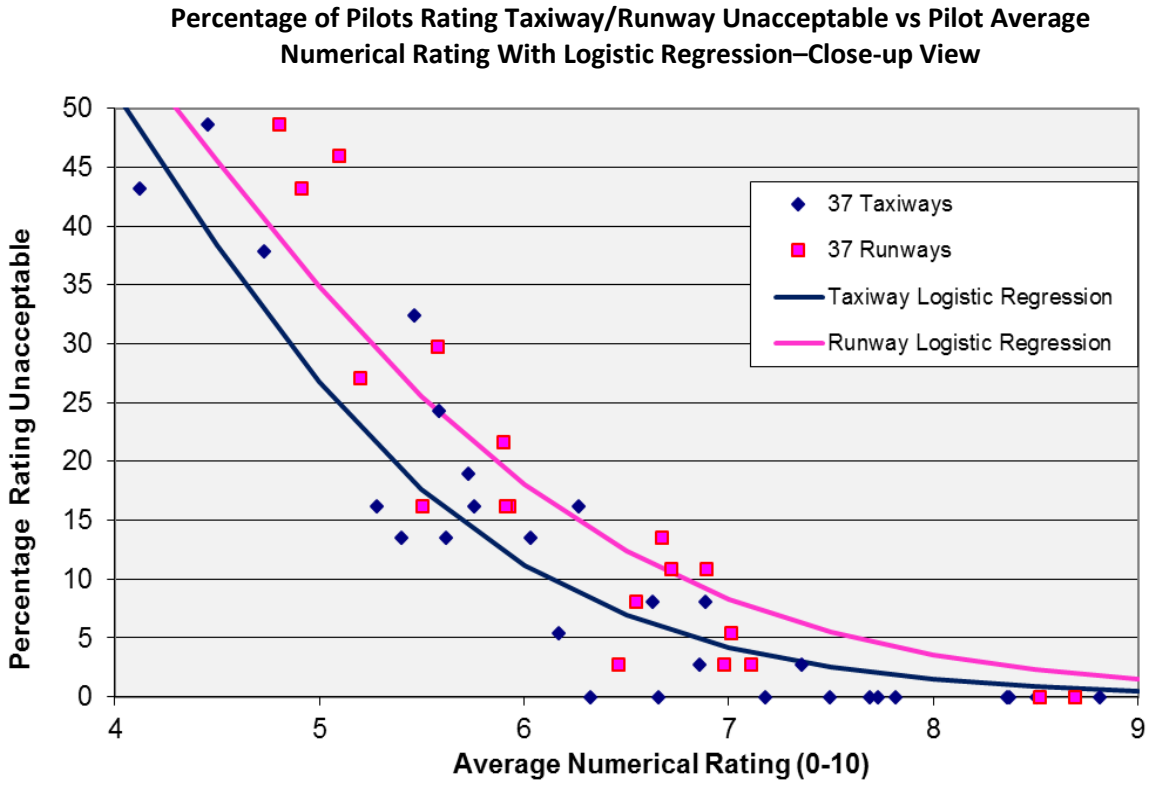

(b) Close-up view

Figure 17. Percentage of Taxiways and Runways Rated Unacceptable vs Numerical Rating

Table 4. Pilot Average Numerical Rating of a Taxiway or Runway When 5%, 10%, or 50% of Pilots Rate the Ride as Unacceptable

Amount Unacceptable	Taxiway Rating (0-10)	Runway Rating (0-10)
5%	6.88	7.60
10%	6.18	6.77
50%	4.11	4.30

If taxiways and runways are considered unacceptable when 5% of pilots rate them as unacceptable, then a taxiway becomes unacceptable at a pilot average numerical rating of approximately 6.88 and a runway becomes unacceptable at a pilot average numerical rating of approximately 7.60.

4.3.2 The Unacceptable Range for Each ISO Index.

It is desirable to predict the discomfort level that will be felt and the point at which a ride becomes unacceptable on an aircraft pavement as a function of each ISO index. To predict this, apply the curve fits of figure 17 (equations 1 and 2 or table 4) to find the average pilot numerical ratings 0-10 that correspond to 5%, 10%, or 50% of the pilots declaring a taxiway or runway ride unacceptable (figure 17). Then, apply the previous curve fits of pilot average numerical rating to the ISO indices (as shown in figure 16 for the shifted logarithmic case of weighted VDV) to find the value of each index that caused 5%, 10%, or 50% of pilots in the final data set to rate a ride as unacceptable. Figures 16, 18, 19, and 20 show the fits of pilot average numerical rating to each index by the shifted logarithm method that together with equations 1 and 2 determine the index values at which pilot average rating indicates taxiways and runways are unacceptable[6] (see table 5).

[6] Table 2 was generated using the shifted logarithmic fits of average pilot rating versus ISO parameter because the shifted logarithm provided a good overall fit, but a similar table can be generated using any of the curve fits. Most exponential fits have substantial unconservative deviations from the data at small pilot percentages, however, and should not be used.

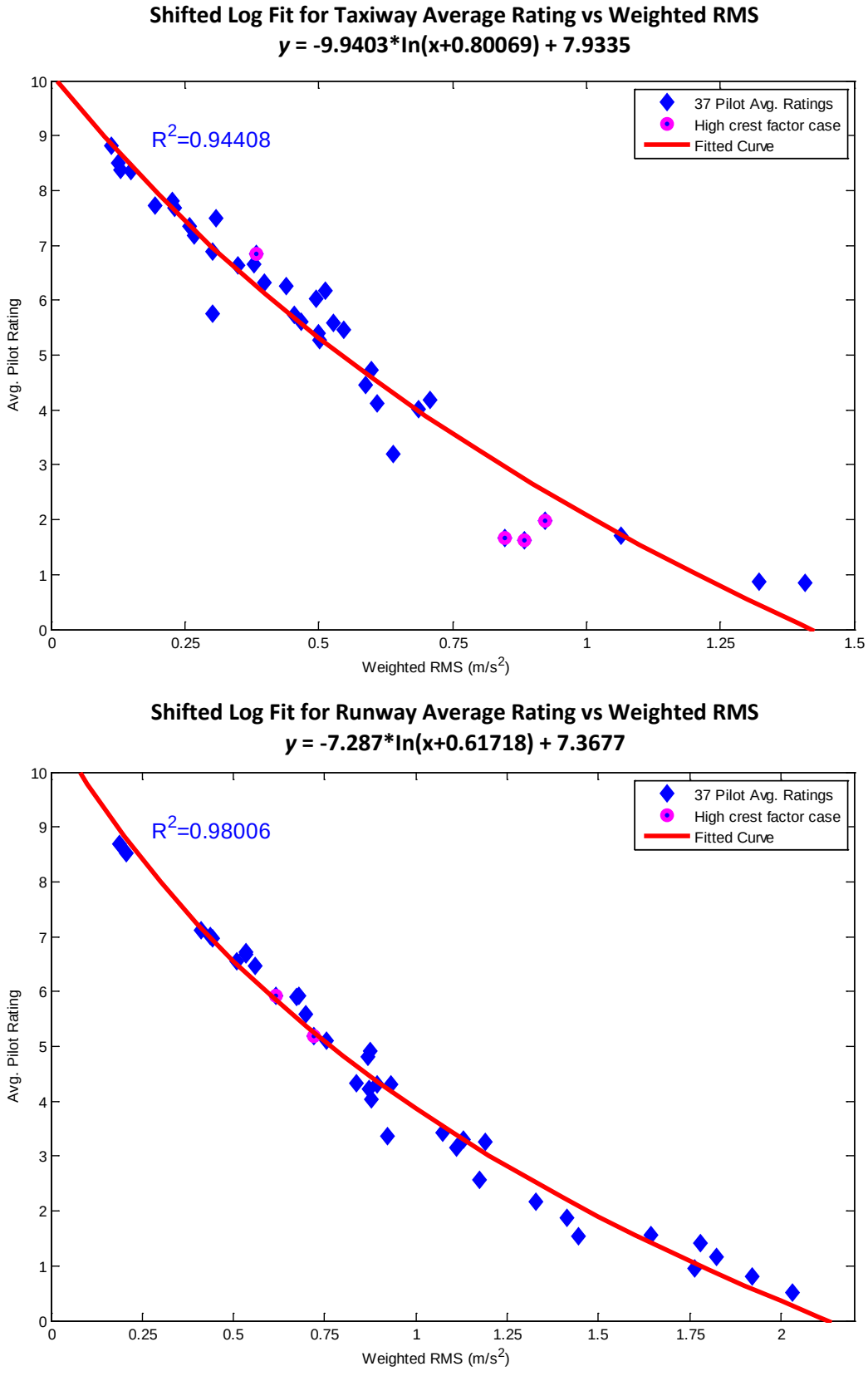

Figure 18. Average Pilot Taxiway (top) and Runway (bottom) 0-10 Rating vs Weighted RMS

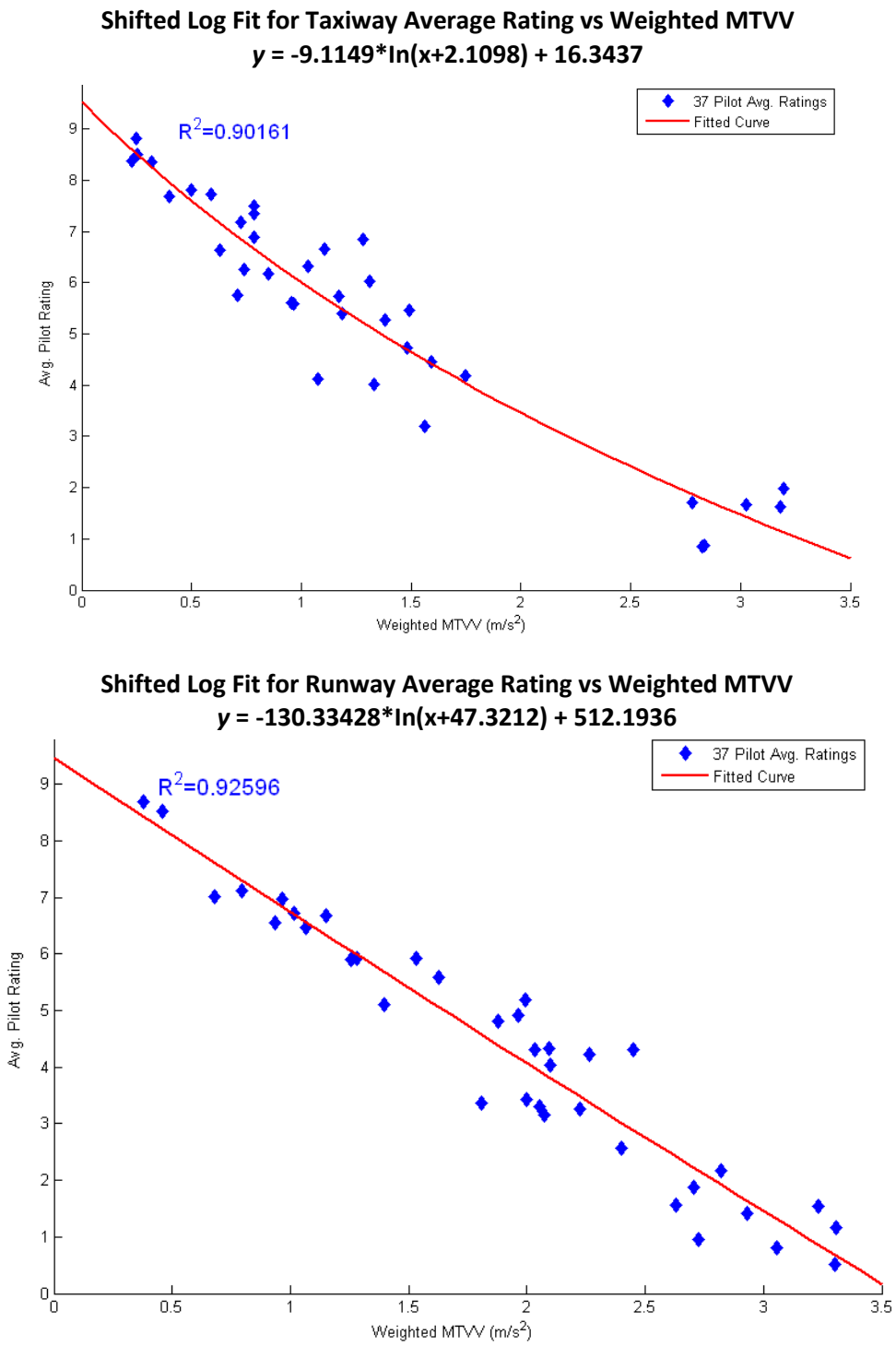

Figure 19. Average Pilot Taxiway (top) and Runway (bottom) 0-10 Rating vs Weighted MTVV

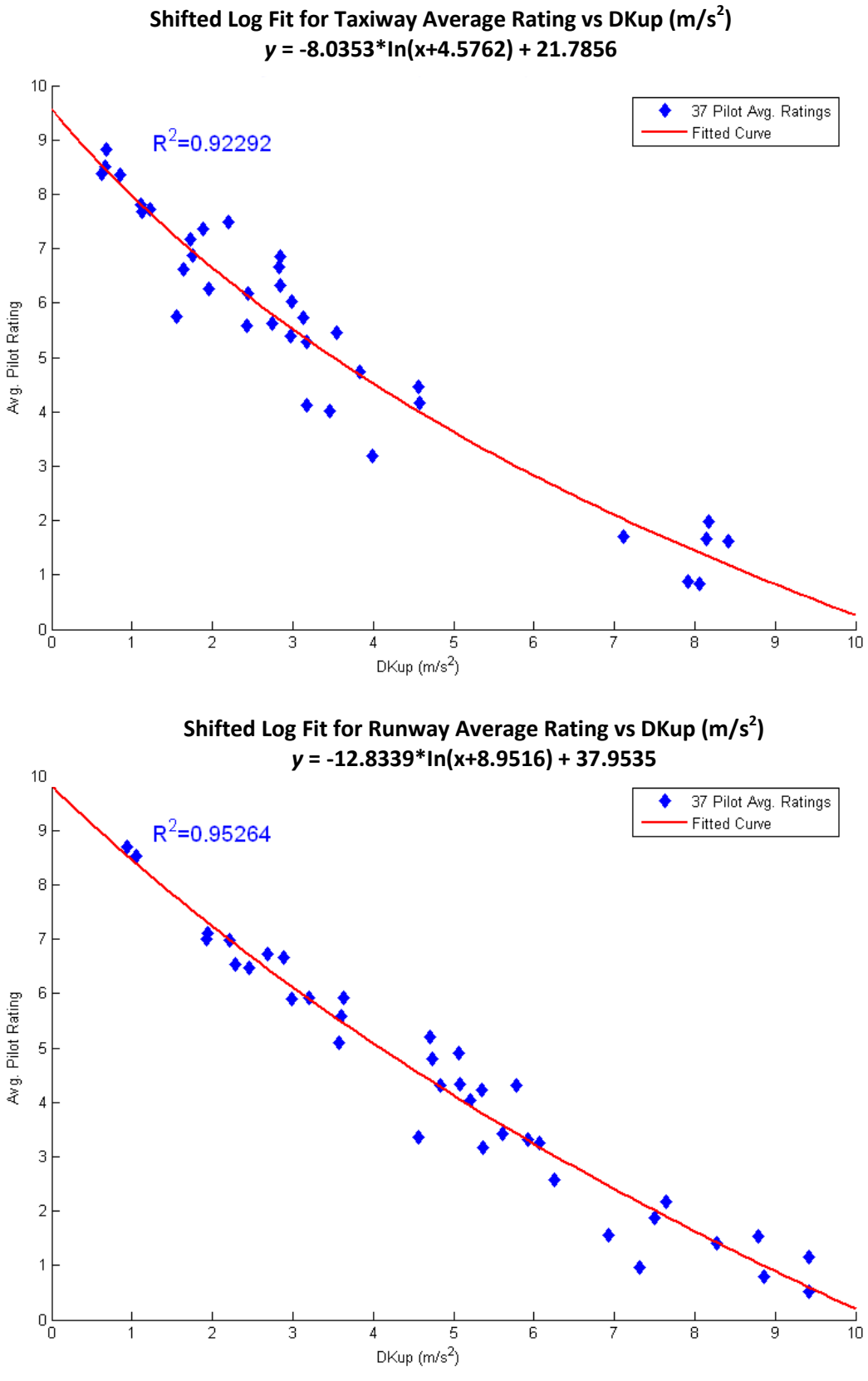

Figure 20. Average Pilot Taxiway (top) and Runway (bottom) 0-10 Rating vs DKup

Table 5. The ISO Index Values at Which 5%, 10%, and 50% of Pilots are Estimated to Rate a Taxiway or Runway as Unacceptable

ISO Roughness Index	Index Value When 5% of Pilots Rate the Taxiway as Unacceptable	Index Value When 10% of Pilots Rate the Taxiway as Unacceptable	Index Value When 50% of Pilots Rate the Taxiway as Unacceptable	Index Value When 5% of Pilots Rate the Runway as Unacceptable	Index Value When 10% of Pilots Rate the Runway as Unacceptable	Index Value When 50% of Pilots Rate the Runway as Unacceptable
Weighted RMS (m/s^2)	0.31	0.39	0.67	0.35	0.47	0.91
Weighted MTVV (m/s^2)	0.71	0.94	1.72	0.68	0.99	1.91
Weighted VDV ($m/s^{1.75}$)	4.11	5.32	9.29	4.16	5.66	10.88
DKup (m/s^2)	1.82	2.40	4.45	1.69	2.40	4.81

If the index value leading to 5% of pilots rating a ride as unacceptable is used as the threshold[7] for calling a taxiway or runway unacceptable, then table 5 shows the unacceptable index ranges. A similar table can be generated for any percentage of pilots rating a ride as unacceptable.

Table 6 indicates that for each index, the value at which a runway or taxiway becomes unacceptable to 5% of pilots is similar; however, the value at which 50% of pilots find a taxiway unacceptable is uniformly lower for the taxiways. During post-test evaluations, some pilots expressed concern about flight attendants during taxiway maneuvers because they were not seat-belted; it is likely that the lower taxiway thresholds resulted at least partly from concern for flight attendant safety.

Table 6. Index Values at Which Taxiways and Runways Become Unacceptable Based Upon the Index Values at Which 5% of Pilots Rated Rides Unacceptable

ISO Roughness Index	Unacceptable Taxiway Range	Unacceptable Runway Range
Weighted RMS (m/s^2)	$\geq$0.31	$\geq$0.35
Weighted MTVV (m/s^2)	$\geq$0.71	$\geq$0.68
Weighted VDV ($m/s^{1.75}$)	$\geq$4.11	$\geq$4.16
DKup (m/s^2)	$\geq$1.82	$\geq$1.69

4.4 COMPARISON OF PILOT RATINGS FOR RIDES WITH HIGH CREST FACTOR.

The crest factor for each taxiway and runway in the final roughness study was evaluated. A high crest factor is an indication that a ride has some sharp jolts. There were no tests that had a crest

[7] Five percent is not necessarily recommended as a criterion for accepting or rejecting a runway, but there is a lack of data to make approximations of unacceptability at much lower percentages (e.g., 1%), thus 5% was chosen as the smallest possible commonly used value for statistical acceptability in hypothesis tests.

factor greater than the ISO standard value of 9.0; but figure 21 shows the 37 final surface roughness study taxiway average ratings and highlights the four taxiway ratings, shown in magenta, that are from taxiways with crest factors greater than 7 (7.63, 8.10, 8.62, and 8.77). Similar plots for runways were constructed but do not appear here, because only two runways had crest factors greater than 5.5 (5.67 and 6.36).

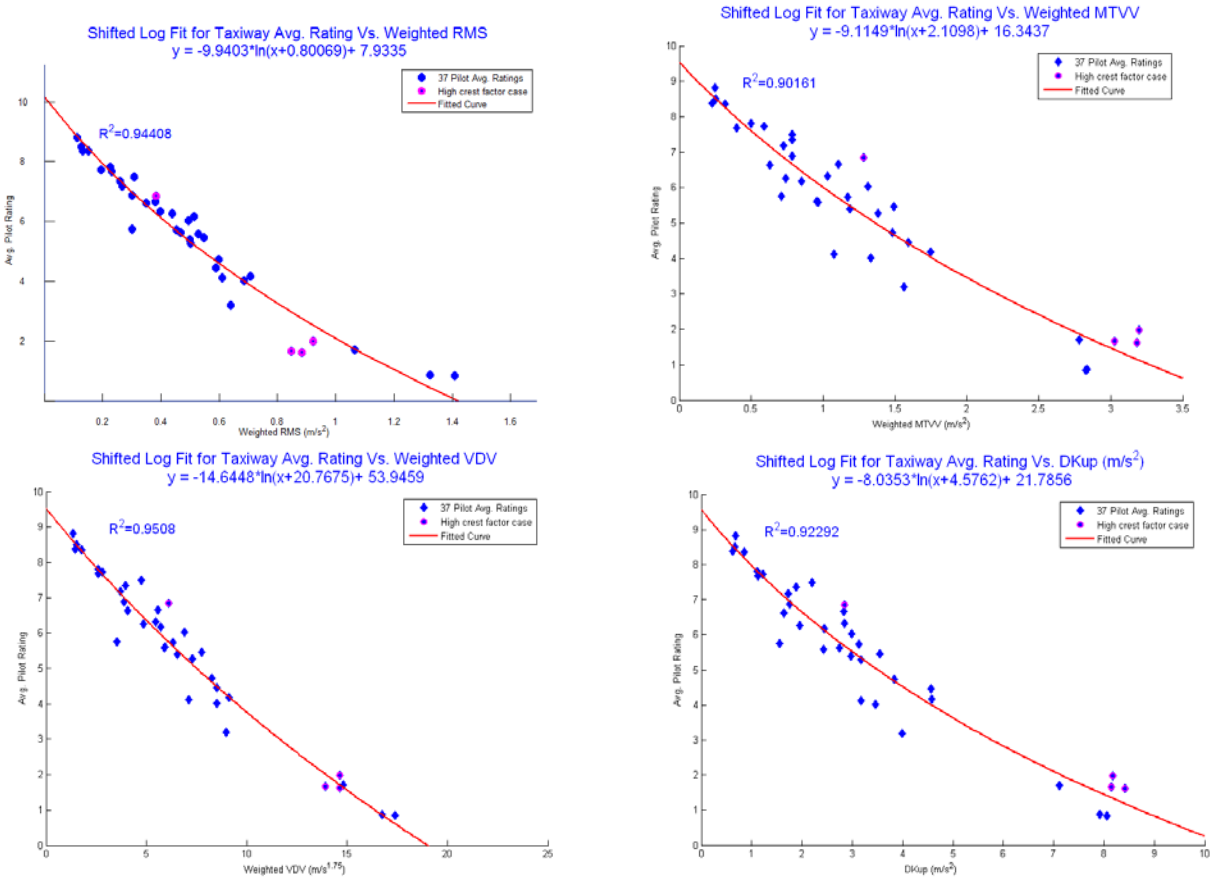

Figure 21. Shifted Logarithmic Fits Highlighting Taxiways With High Crest Factor

For the four taxiways with the high crest factor ratings (magenta), it is apparent that pilot rating given as a function of weighted RMS or weighted VDV provides the best fit.

4.5 MILITARY AND REPEAT PILOT BIAS.

A number of pilots were classified as flying for a branch of the military, and it was considered that these pilots might have different ride expectations. Therefore, the military pilots' responses were separated from the non-military pilots and compared (see figures 22 and 23 and appendix A).

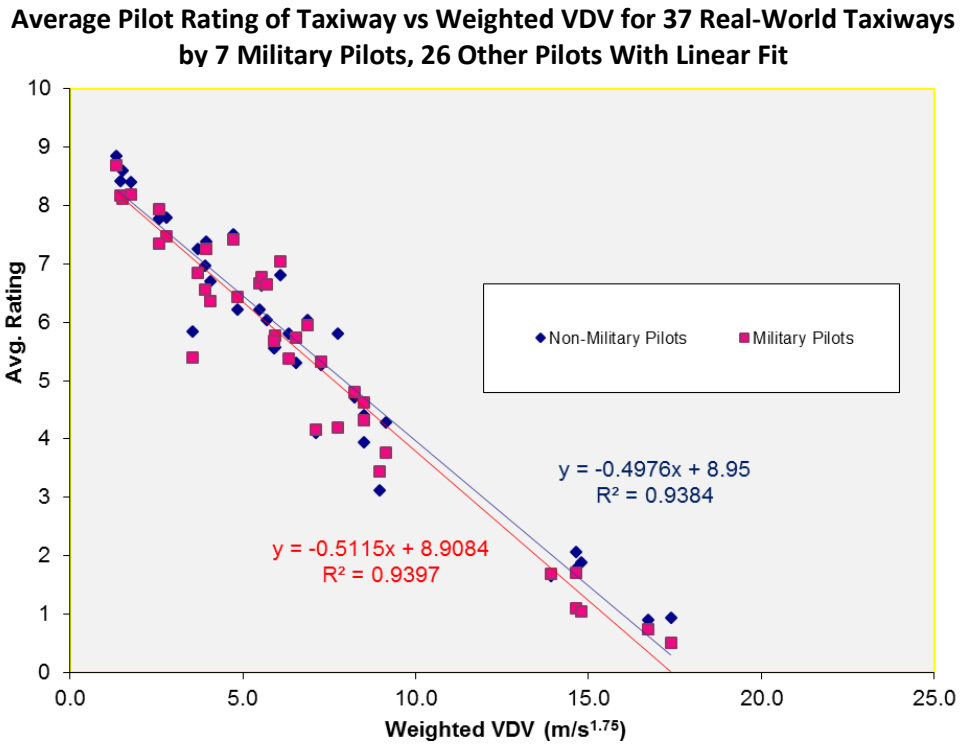

Figure 22. Linear Fits of Average Pilot Rating on 37 Taxiways to Weighted VDV for Military and Non-Military Pilots

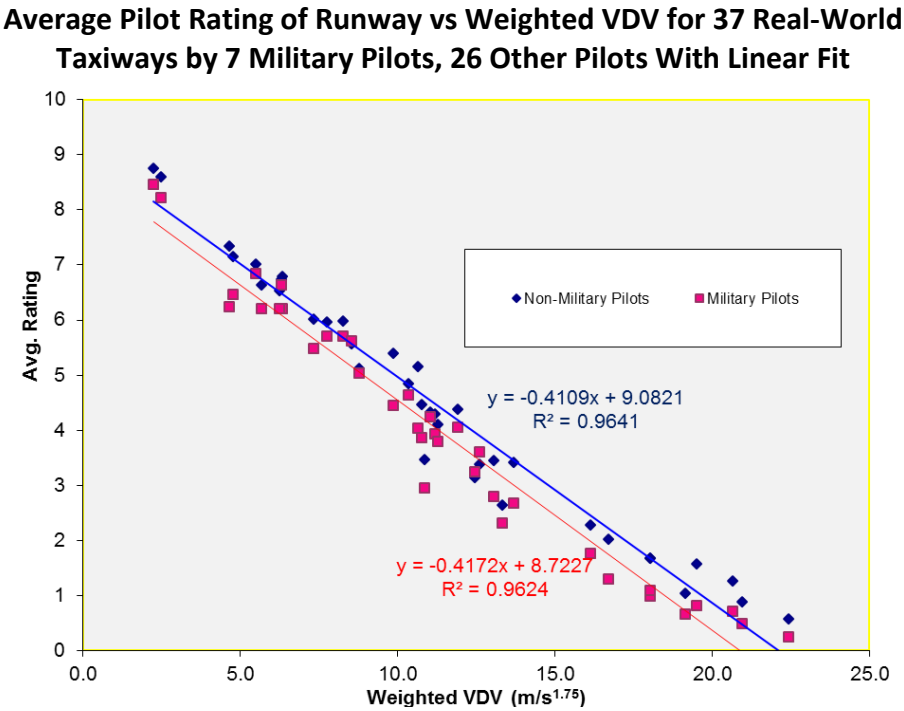

Figure 23. Linear Fits of Average Pilot Rating on 37 Runways to Weighted VDV for Military and Non-Military Pilots

Weighted VDV fits were used for this analysis because the fits were closer to linear than the weighted RMS fits, and the linear fits were more easily evaluated for the possibility of bias.

It was decided that having so many military pilots among the test pilots could bias the results; therefore, hypothesis tests at the 5% level were conducted. For these tests, it is easiest to consider only simple linear fits. For the linear fits, in which $y = mx + b$ is the form of the fitted line of slope m and y-intercept b, a hypothesis test that the y-intercept was the same for taxiways or runways could not be rejected at the 5% level. This indicates that it is more than 5% likely that the separation between the lines in figures 22 and 23 could have happened by chance. The hypothesis that the y-intercept was the same for runways was, however, not far from being rejected.

It is speculated, but not with 95% confidence, that there is a slight military bias on runways that occurs because many of the military test pilots in this study fly KC-135 refueling aircraft.

Similar hypothesis tests were performed at the 5% level for repeat pilots. Repeat pilots are test pilots who had previously been involved in a flight simulator evaluation of taxiways and/or runways. Trend lines for repeat pilots were found to cross in the middle of the rating range with the trend lines for non-repeat/non-military pilots (see figures 24 and 25 and appendix A).

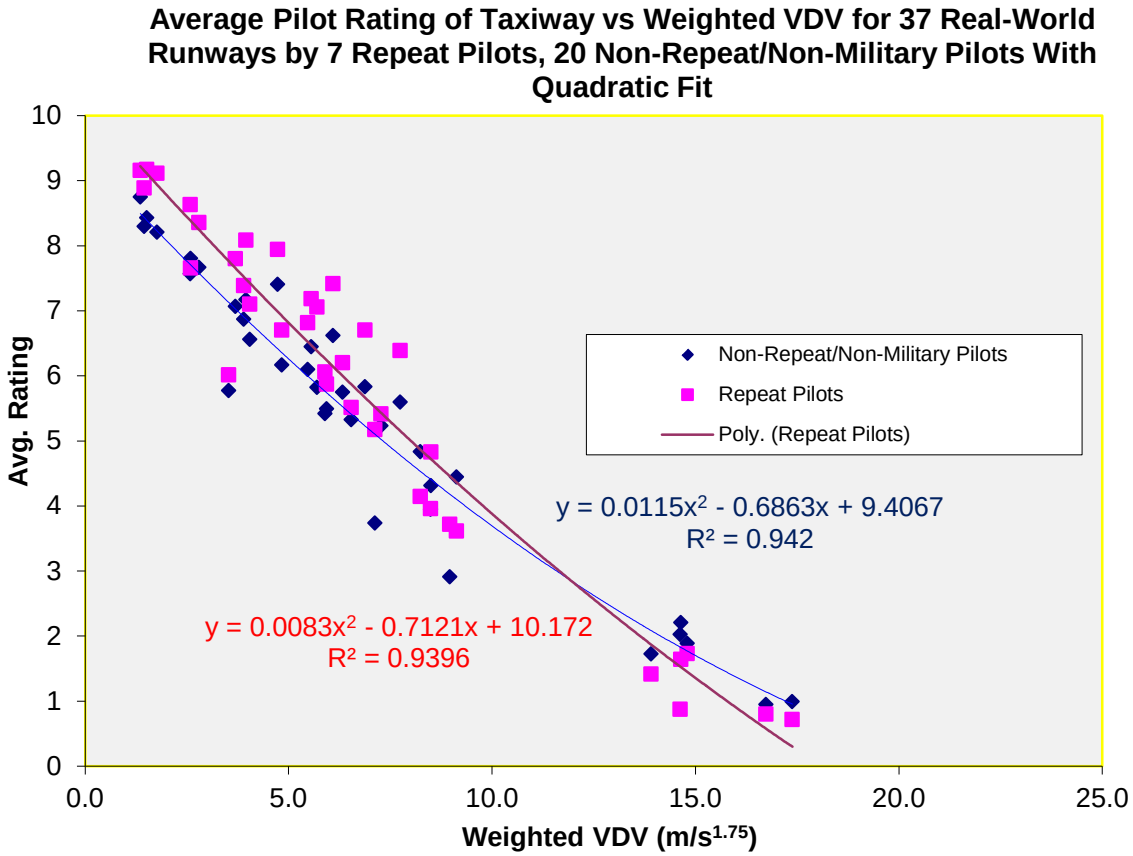

Figure 24. Linear Fits of Average Pilot Rating on 37 Taxiways to Weighted VDV for Repeat Pilots and Non-Repeat/Non-Military Pilots

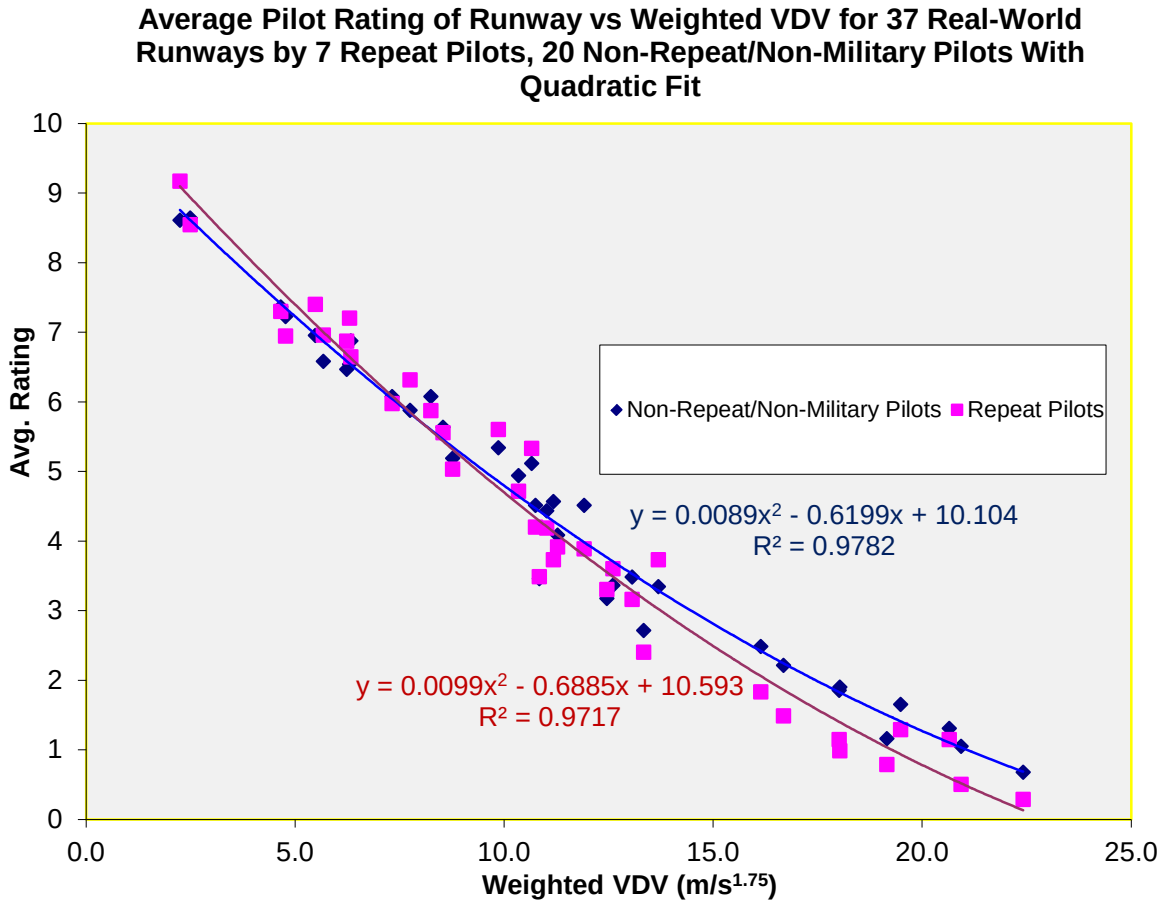

Figure 25. Linear Fits of Average Pilot Rating on 37 Runways to Weighted VDV for Repeat Pilots and Non-Repeat/Non-Military Pilots

The hypothesis that the fitted lines for the average ratings of repeat pilots and for non-repeat/non-military pilots had the same slope was rejected at the 5% level for both taxiways and runways.

It is more than 95% likely that repeat pilots had some anticipation of rating the taxiways and runways that caused them to rate the smoother surfaces in the study slightly higher and the rough surfaces slightly lower than the other pilots.

The biases were not considered significant enough to remove the repeat pilots from the data set but are presented because they constitute a human factor[8] that slightly influenced the data.

[8] Seat number in the simulator was also considered as a human factor, but not found to have influenced pilot responses. (Graphs are shown in appendix A.)

4.6 HUMAN VIBRATION LIMITS.

The first row of table 7 (the weighted RMS line) may be compared with the numbers in Subclause 2.3 of Annex C (informative) of the ISO standard [8], which for weighted RMS provides "approximate indications of likely reactions to various magnitudes of overall vibration total values in public transport" [8].

Table 7. The ISO Standards for Discomfort

Weighted RMS m/s^2	Discomfort Level
0-0.315	Not uncomfortable
0.315-0.63	A little uncomfortable
0.5-1.0	Fairly uncomfortable
0.8-1.6	Uncomfortable
1.25-2.5	Very uncomfortable
>2.0	Extremely uncomfortable

The range of the weighted acceleration RMS values reported in this study is from 0.11 m/s^2 to 2.03 m/s^2. Considering that the cockpit accelerations were measured on the floor of the simulator cockpit below the pilot's seat, not at the seat (as required by the ISO standard), and that the measured signal bandwidth was somewhat limited compared to the ISO standard, the range of the reported RMS values is compatible with what would be expected from the values in Annex C of the ISO standard 2631. [8]

- At a weighted RMS value of 0.31, approximately 5% of pilots rated a taxiway ride as unacceptable. This is where the ISO standard for general vibration indicates the vibration becomes "a little uncomfortable." At a weighted RMS of 0.67, approximately 50% of pilots rated a taxiway ride as unacceptable. The ISO standard says vibration is "fairly uncomfortable" at this level. [8]

- Runways were rated unacceptable by 5% of pilots when their weighted RMS value was 0.35. The ISO standard 2631 says general vibration is "a little uncomfortable" at this level. About 50% of pilots rated a runway as unacceptable when its weighted RMS was 0.91 (m/s^2). This is where the ISO standard classifies vibration as transitioning from fairly uncomfortable to uncomfortable. [8]

These numbers suggest that the "a little uncomfortable" level of the ISO standard is closely related to the point at which 5% of pilots rated taxiways and runways as unacceptable, and the "fairly uncomfortable" level is closely related to the point at which 50% of pilots rated taxiways and runways as unacceptable.

The ISO standard 2631 [8] also provides a health guideline for (shock-related) vibration, stating that "caution with respect to health risks is indicated" for VDV exposures from 8.5 and 17 $m/s^{1.75}$. Tables 4 and 6 together show that approximately half of the pilots rated taxiway and runway rides as unacceptable when vibrations reached into the lower end of the VDV caution range.

4.7 COMPUTATION OF BEST FIT SHIFTED LOGARITHMIC CURVES TO DATA.

The MATLAB code in appendix H was used to compute a shift to be added to each ISO index to provide the best possible least squares logarithmic fit to numerical pilot ratings in the final roughness study as a function of roughness index. The program computes the least squares fit; a 95% confidence interval for the fit; and 50%, 90%, and 95% prediction intervals. The confidence intervals represent intervals within which it is 95% likely the true trend points should lie, given that the fitted curve is of the type assumed—linear, quadratic, etc.—when noise (errors in measurement) has been removed. The prediction intervals provide ranges within which approximately 95% of data points should fall when 33 pilots rate taxiways or runways and their average numerical rating is calculated.

The shifted logarithmic intervals assume that

- the data follows a shifted logarithmic trend with the given shift, and
- the difference between the taxiway or runway average rating and the actual trend has a (bell-shaped) normal distribution with its mean on the trend and a standard deviation that is constant overall index values.

Another notable feature of the shifted logarithmic fit is that it is very close to the quadratic fit and that these two curves provide the smallest R^2 values over all fits attempted, which is not surprising since these fits have three free constants but the others have only two or one.

The closeness of the quadratic and shifted logarithmic fits, as best fits, suggest that the true trend of the data is very close to these curves (see figure 26).

The assumptions for the shifted logarithmic fits and intervals cannot be precisely true. For example, when the trend curve for taxiways or runways is near a rating of 0 or 10, the rating uncertainty cannot vary symmetrically about the trend (fit) as the model requires. However, the fact that the 95% prediction intervals contain about 95% of the averages in the data above suggests that the normality assumption of the model is not too far from correct (see figures 27 through 34).

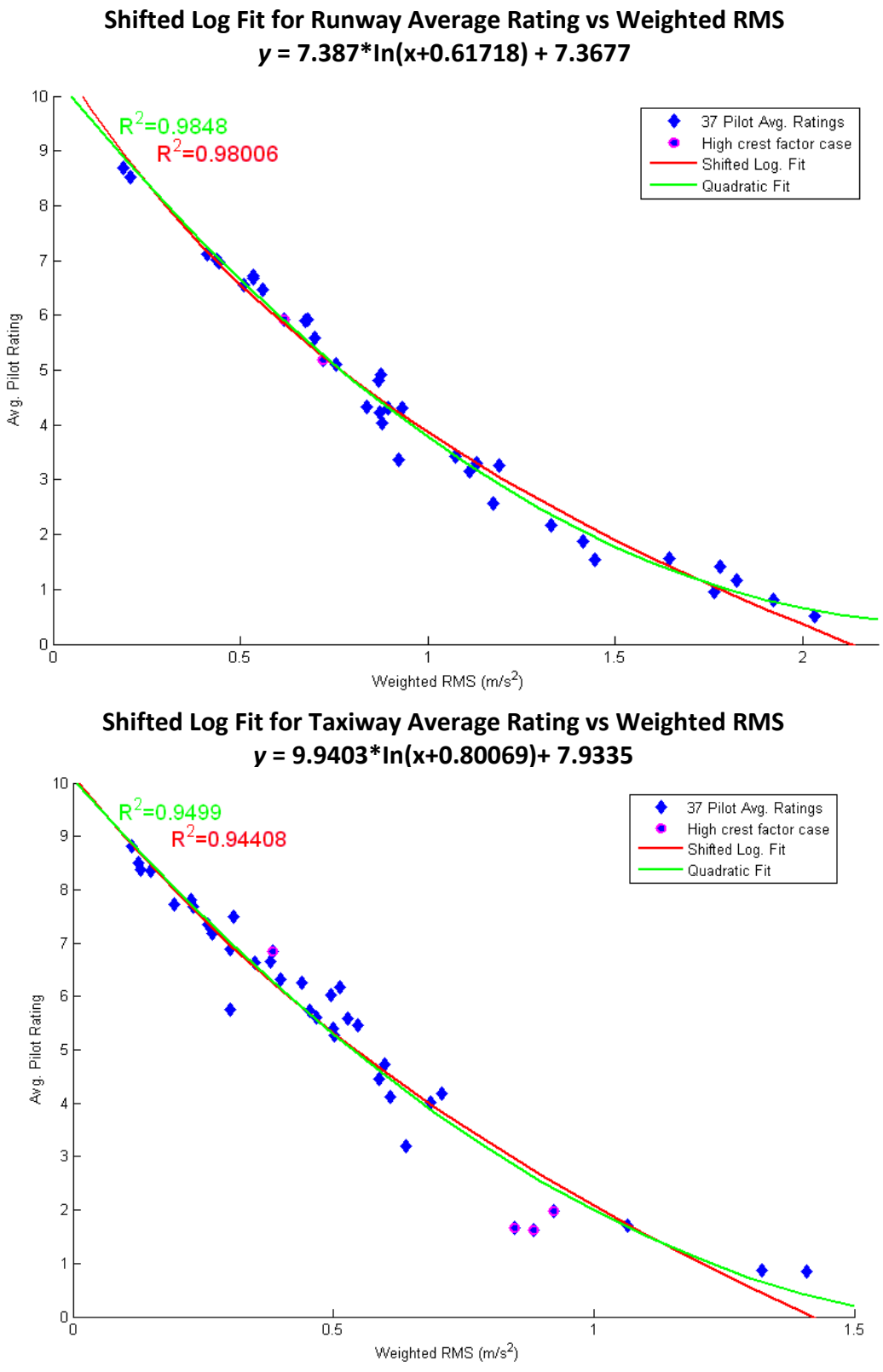

Figure 26. Comparison of the Quadratic and Shifted Logarithmic Fits to Pilot Runway Average (top) and Taxiway Average (bottom) Ratings vs Weighted RMS

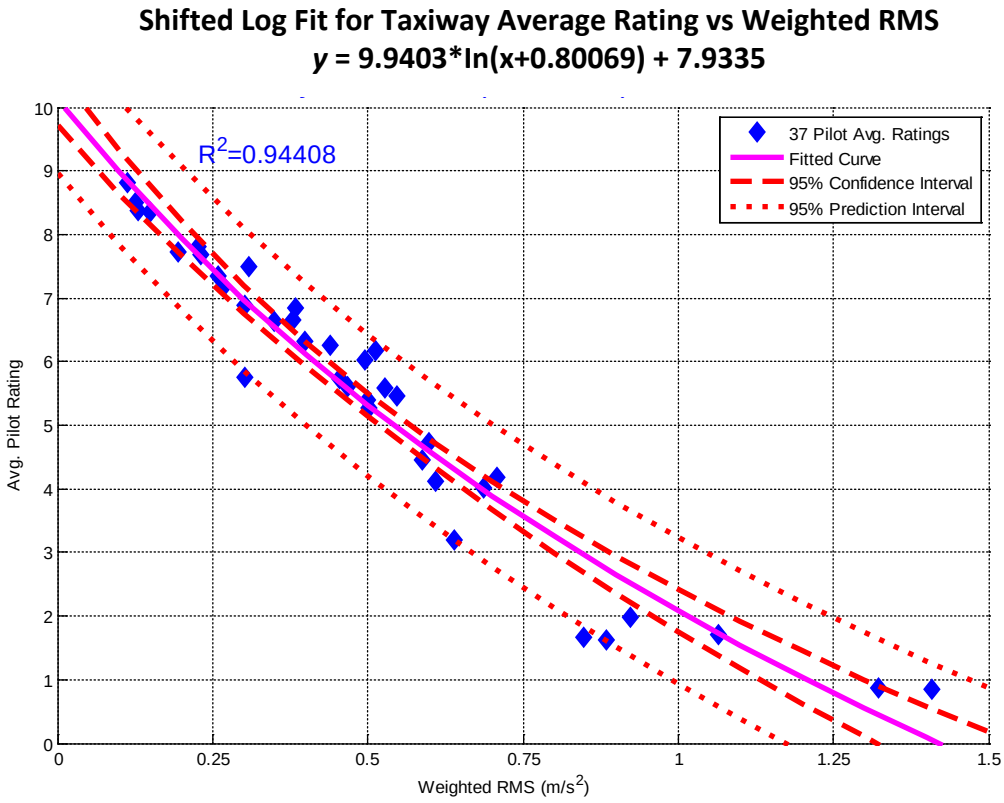

Figure 27. Shifted Logarithmic Fit for Pilot Average Taxiway Rating vs Weighted RMS

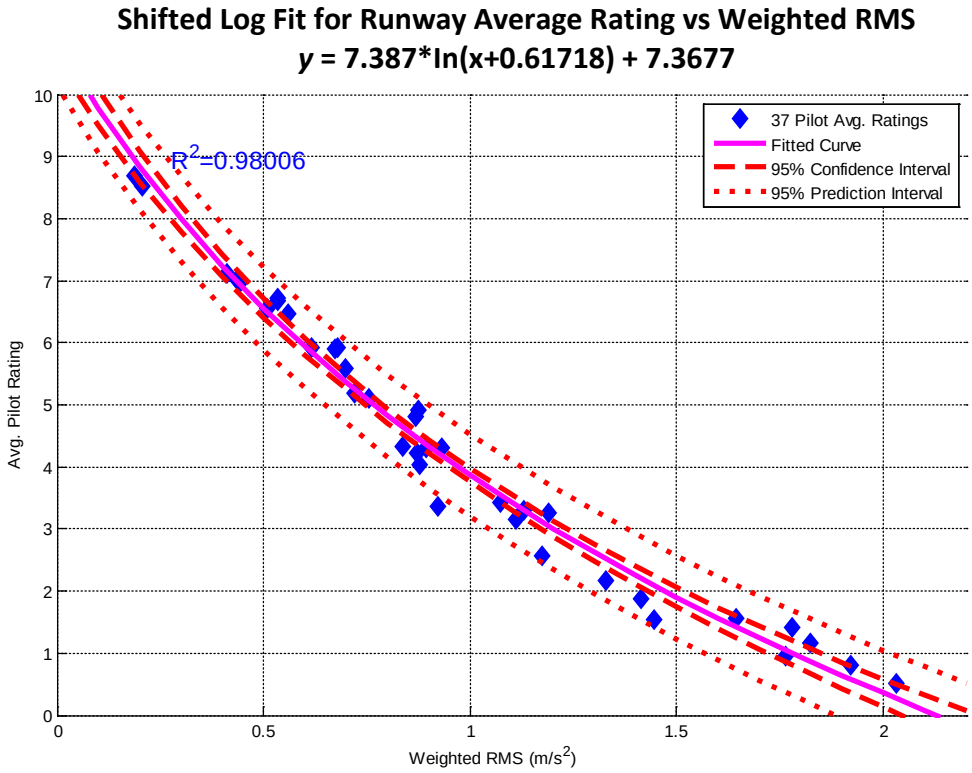

Figure 28. Shifted Logarithmic Fit for Pilot Average Runway Rating vs Weighted RMS

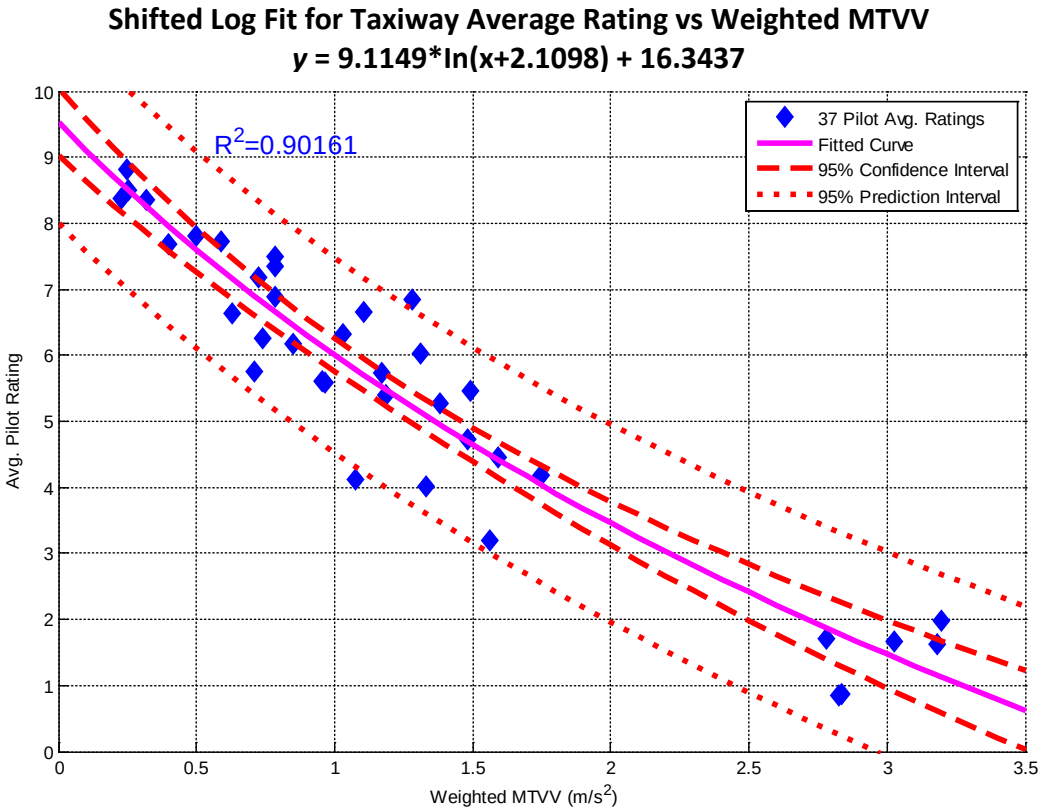

Figure 29. Shifted Logarithmic Fit for Pilot Average Taxiway Rating vs Weighted MTVV

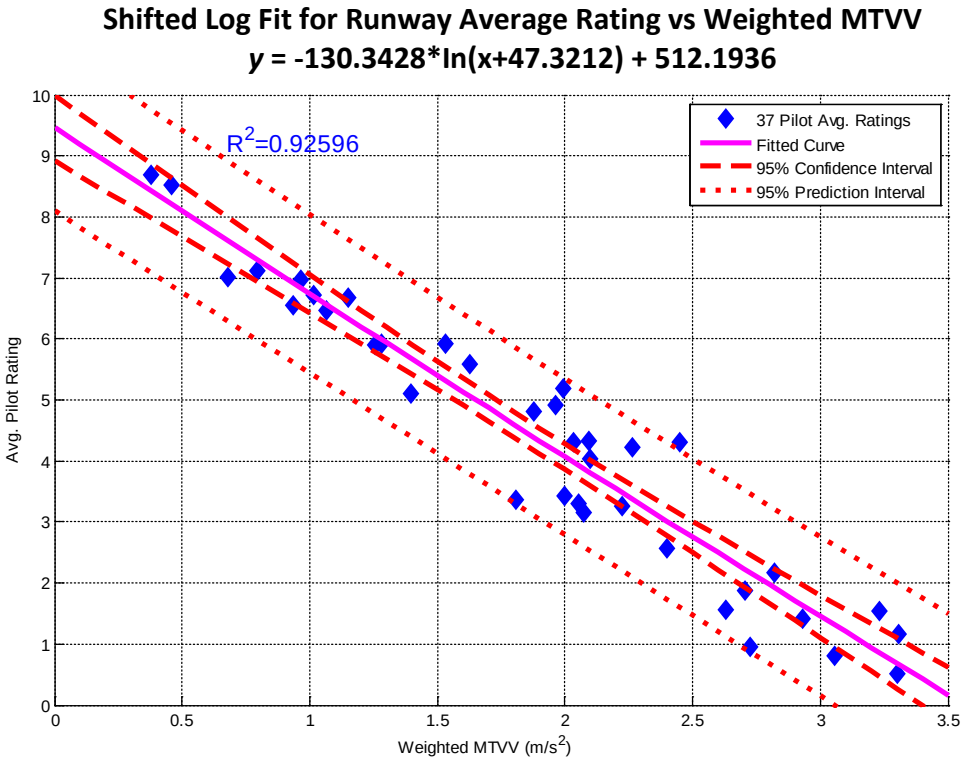

Figure 30. Shifted Logarithmic Fit for Pilot Average Runway Rating vs Weighted MTVV

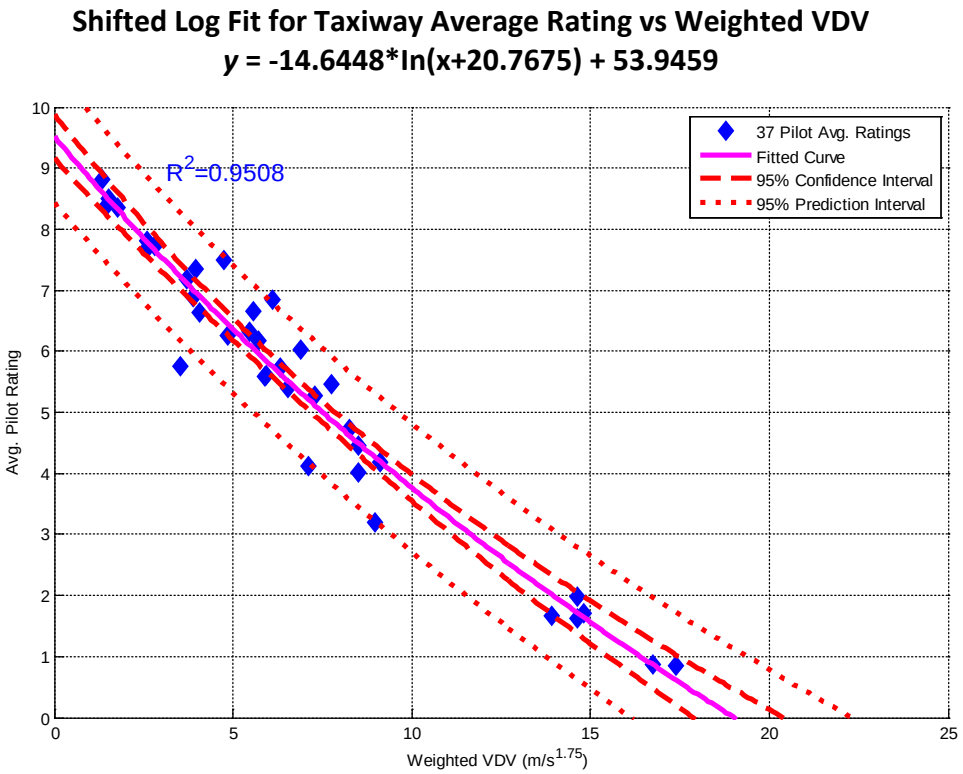

Figure 31. Shifted Logarithmic Fit for Pilot Average Taxiway Rating vs Weighted VDV

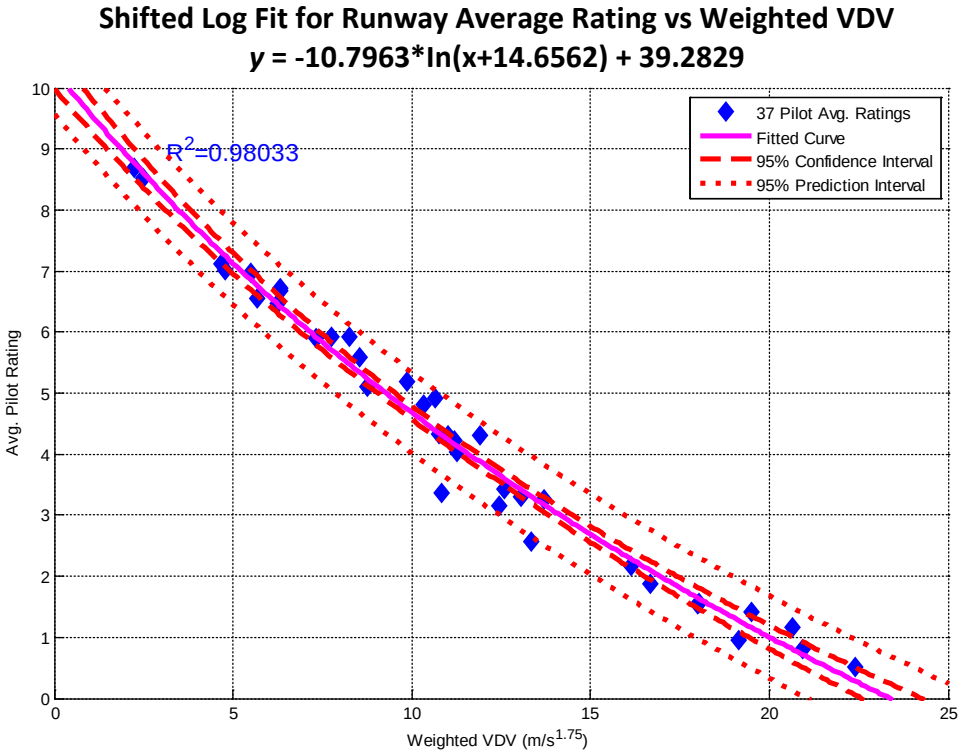

Figure 32. Shifted Logarithmic Fit for Pilot Average Runway Rating vs Weighted VDV

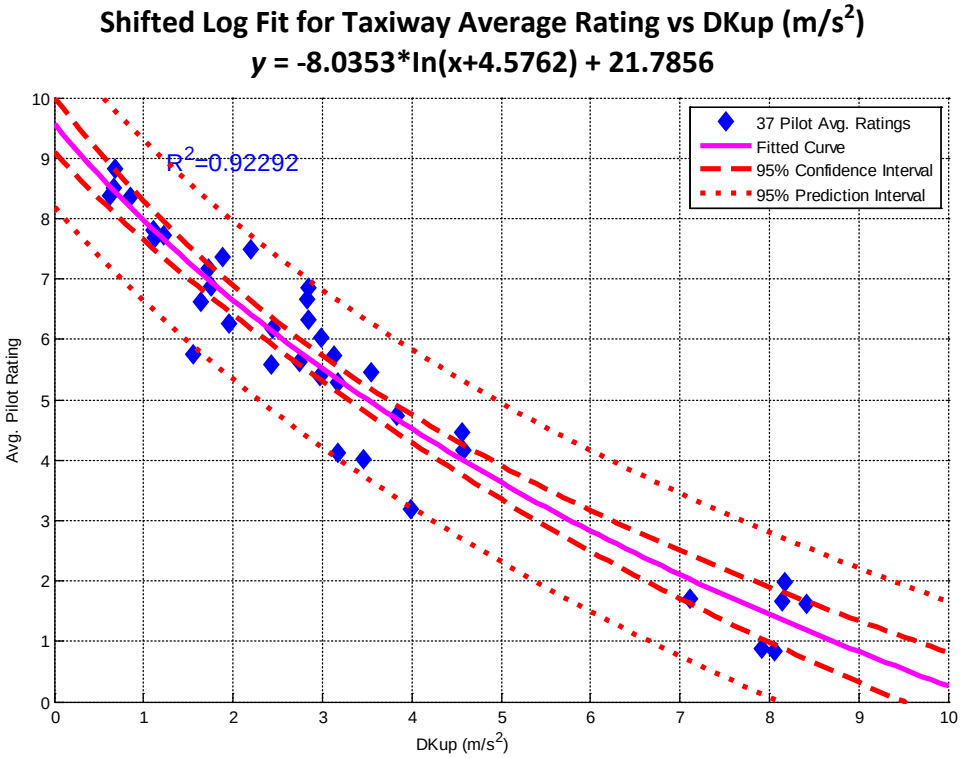

Figure 33. Shifted Logarithmic Fit for Pilot Average Taxiway Rating vs DKup

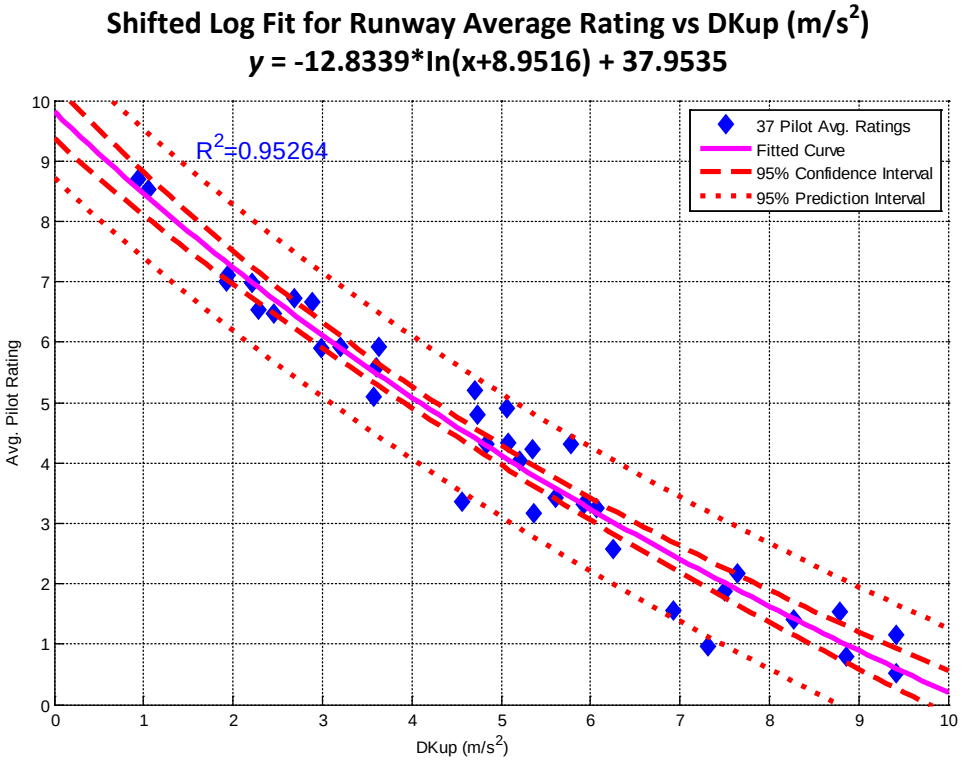

Figure 34. Shifted Logarithmic Fit for Pilot Average Runway Rating vs DKup

In these plots,

- the narrower confidence and prediction intervals in the runway cases indicate that pilots were more uniform in their ratings of runways.

- the narrower intervals in the fits versus weighted RMS and weighted VDV indicate that pilot responses follow a more well-defined trend when plotted against these indices (as anticipated from the correlation coefficients of section 4.2).

- the large shift for the runway weighted MTVV fit occurs because the best fit is nearly linear (and the shifted logarithmic fit is not appropriate in such a case).

4.8 COMPARISON OF THE BEST SHIFTED LOGARITHMIC FIT TO OTHER FITS.

Confidence and prediction intervals were also calculated for the linear, exponential, and logarithmic fits with the final surface roughness study data set. These intervals for fits of average pilot rating as a function of weighted RMS are shown in figures 35 through 37.

The prediction intervals help determine where a fit is insufficient by indicating when data points are substantially off to one side of the trend. For example, the linear fits have many data points well above the trend line at small and large values of weighted RMS and well below the trend line in the middle. The exponential and unshifted logarithmic fits similarly display too much curvature for small values of weighted RMS.

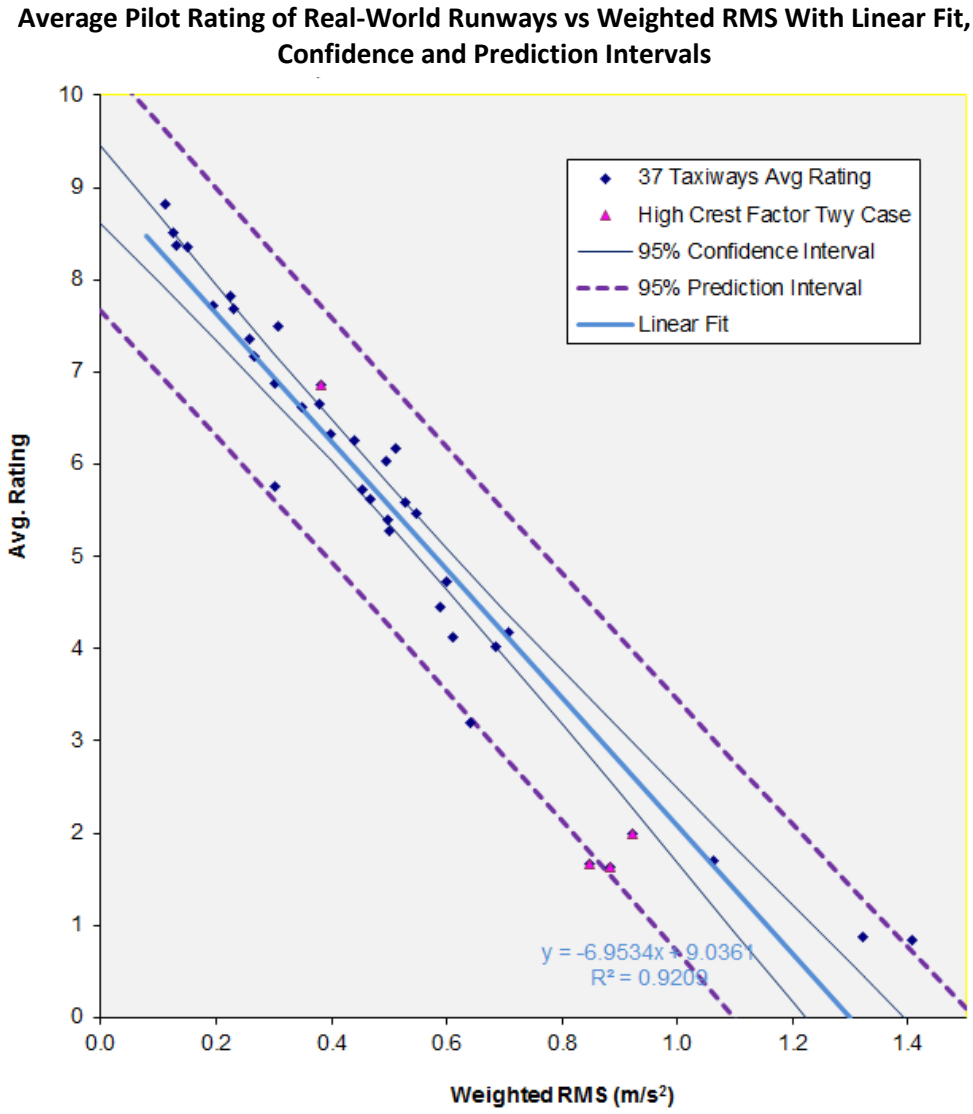

Figure 35. Linear Fit of Rating vs Weighted RMS With Confidence and Prediction Intervals

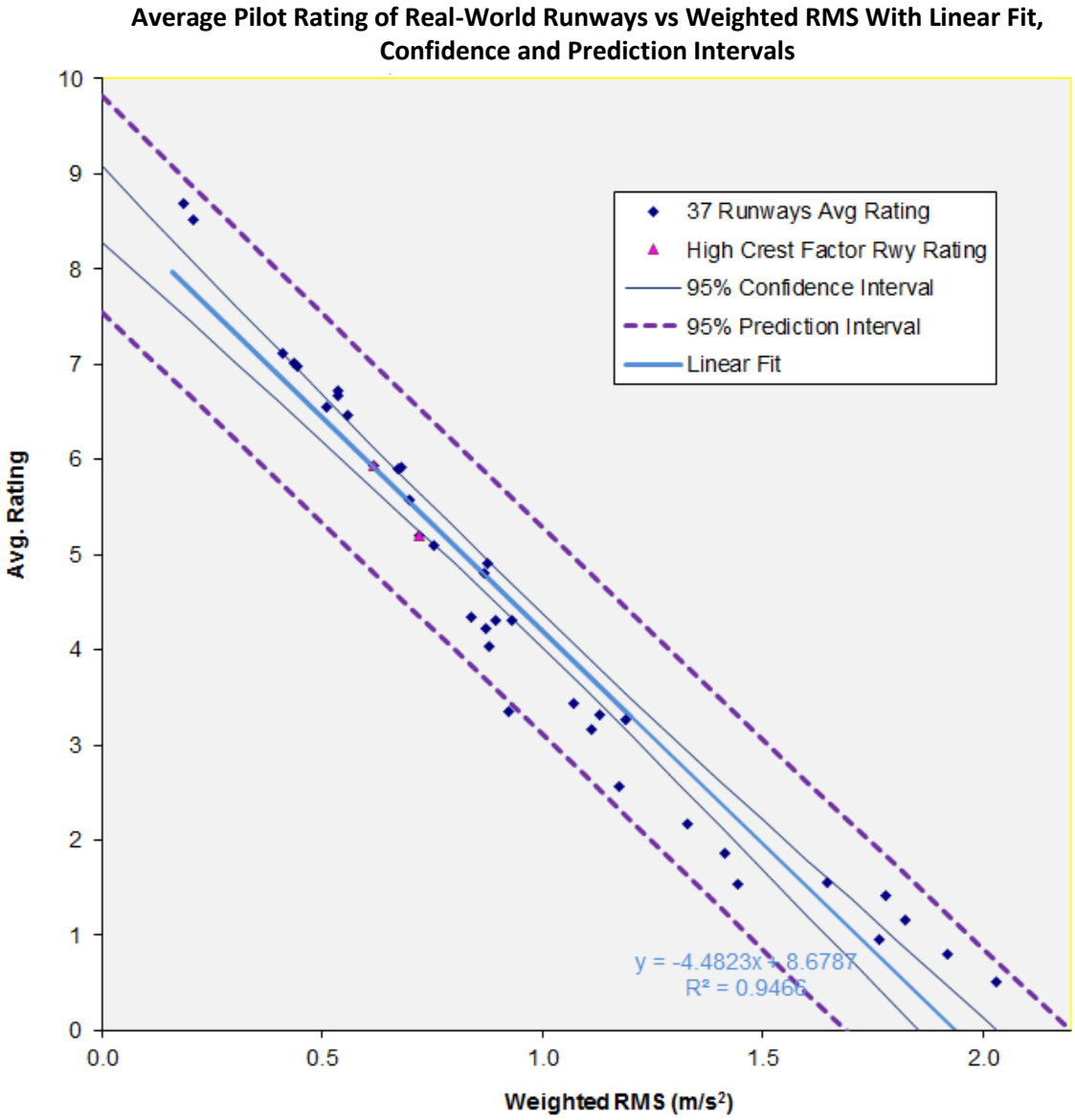

Figure 35. Linear Fit of Rating vs Weighted RMS With Confidence and Prediction Intervals (Continued)

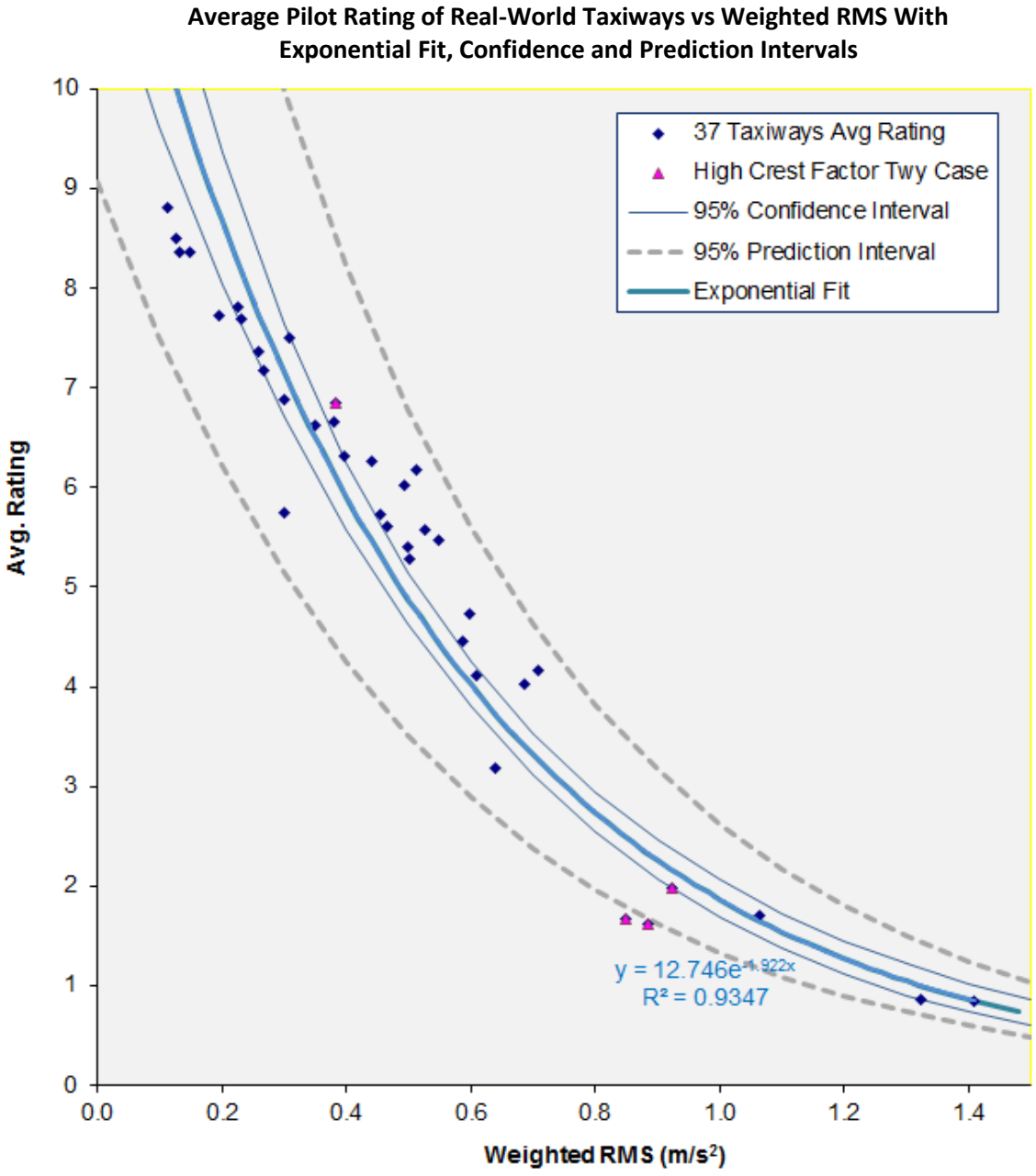

Figure 36. Exponential Fit of Rating vs Weighted RMS With Confidence and Prediction Intervals

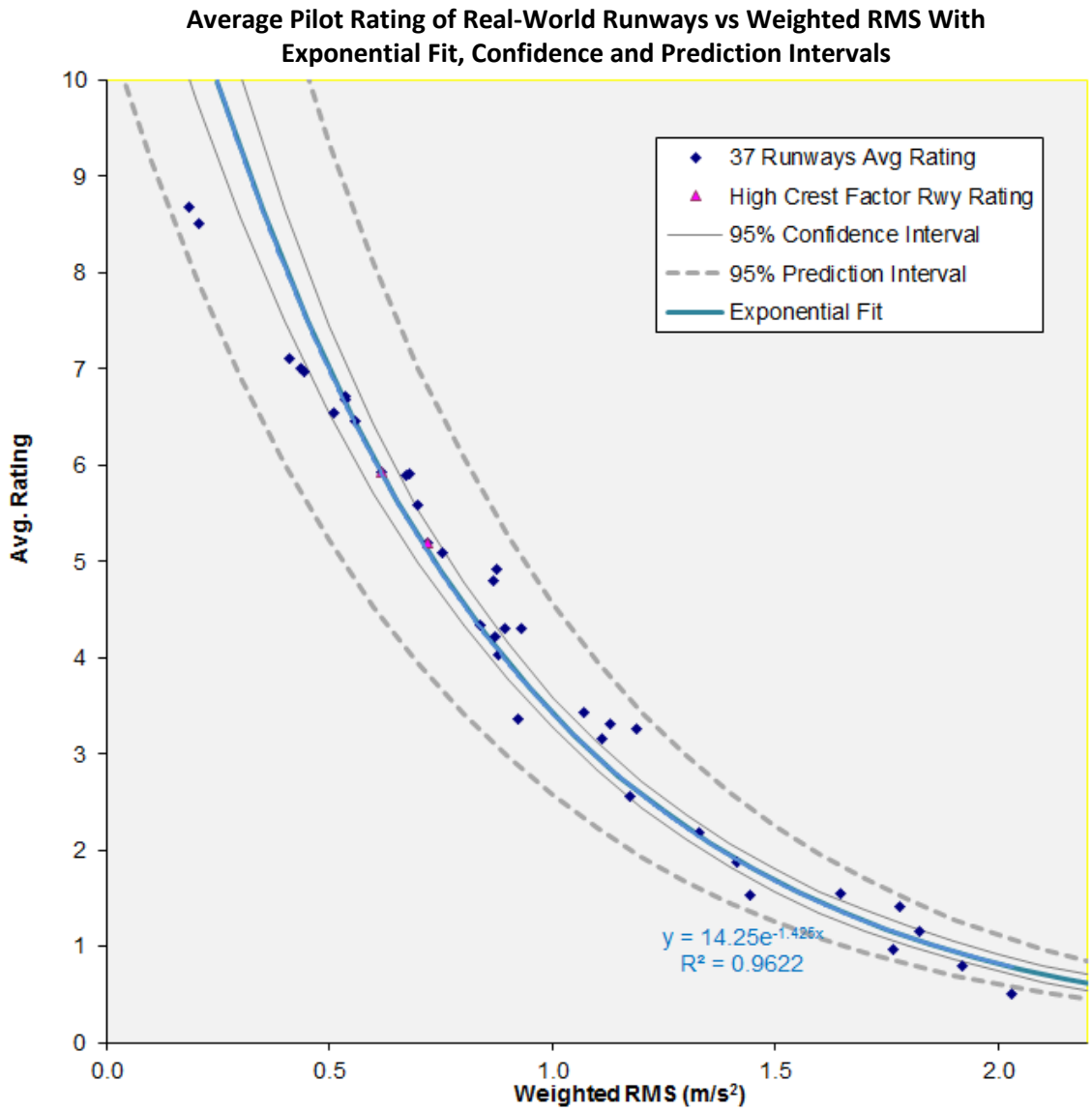

Figure 36. Exponential Fit of Rating vs Weighted RMS With Confidence and Prediction Intervals (Continued)

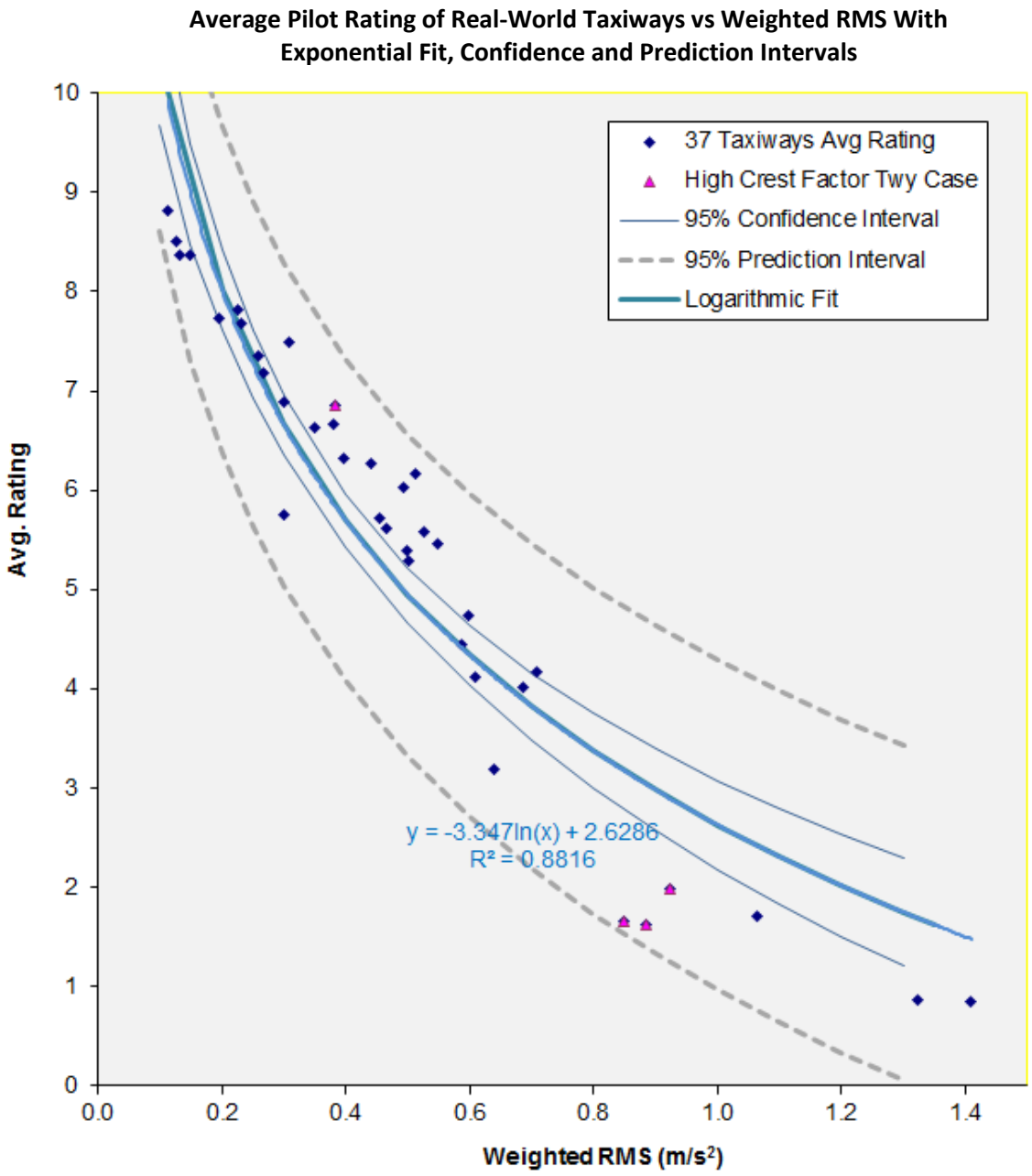

Figure 37. Logarithmic Fit of Rating vs Weighted RMS With Confidence and Prediction Intervals

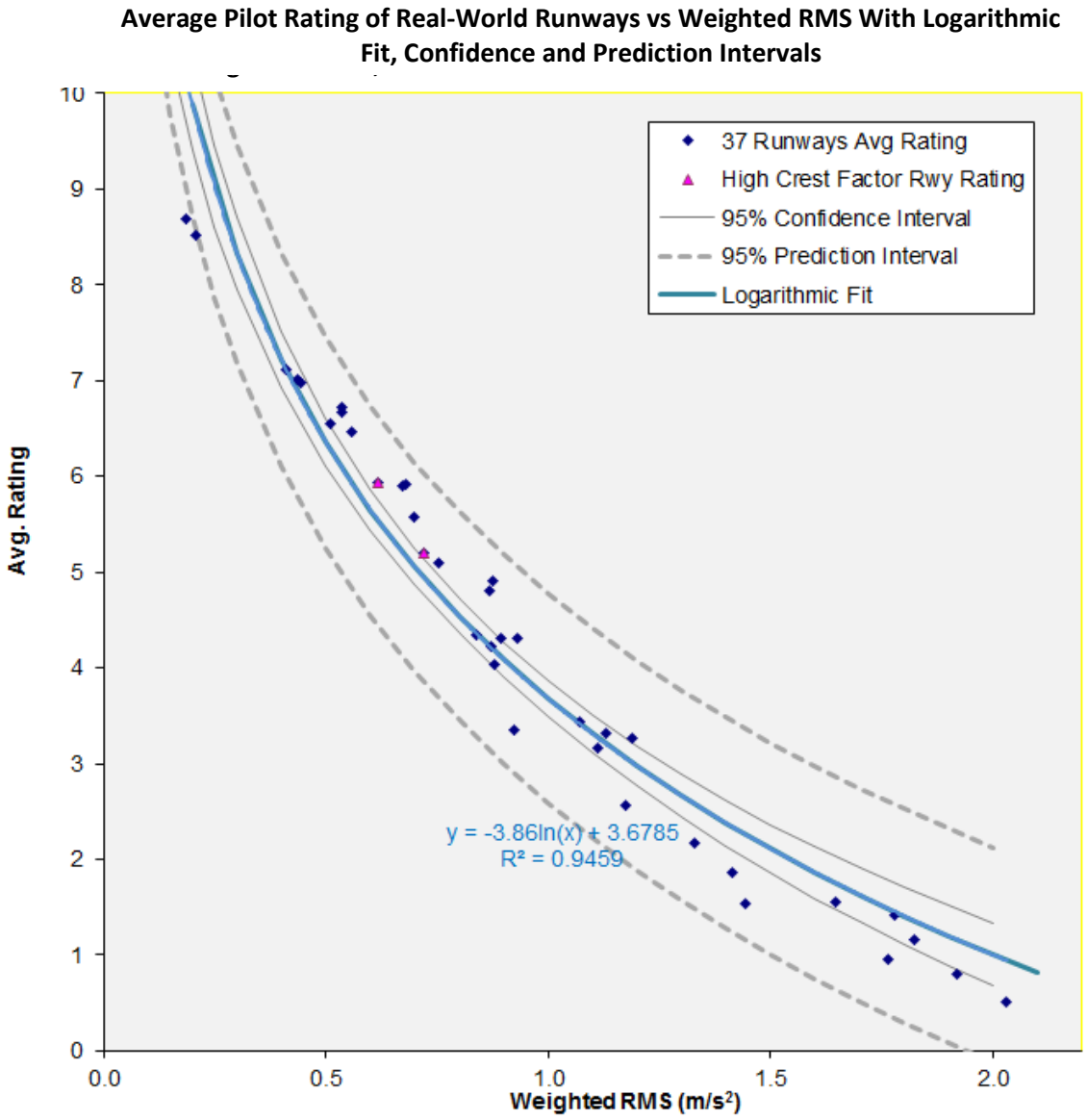

Figure 37. Logarithmic Fit of Rating vs Weighted RMS With Confidence and Prediction Intervals (Continued)

4.9 COMPARISON OF BEST FITS WHEN DATA FROM THE PRELIMINARY ROUGHNESS STUDY IS INCLUDED.

Figure 38 shows the combined quadratic trends[9] for runways as a function of weighted RMS when the 20 average numerical ratings from runways in the preliminary roughness study tests and from 37 runways in the final roughness study tests are all fit.

[9] The trend equations are not given here because the fits shown used equal weighting for averages computed with 33 pilots from the final roughness study and averages computed using 12 pilots from the preliminary roughness study and are not valid.

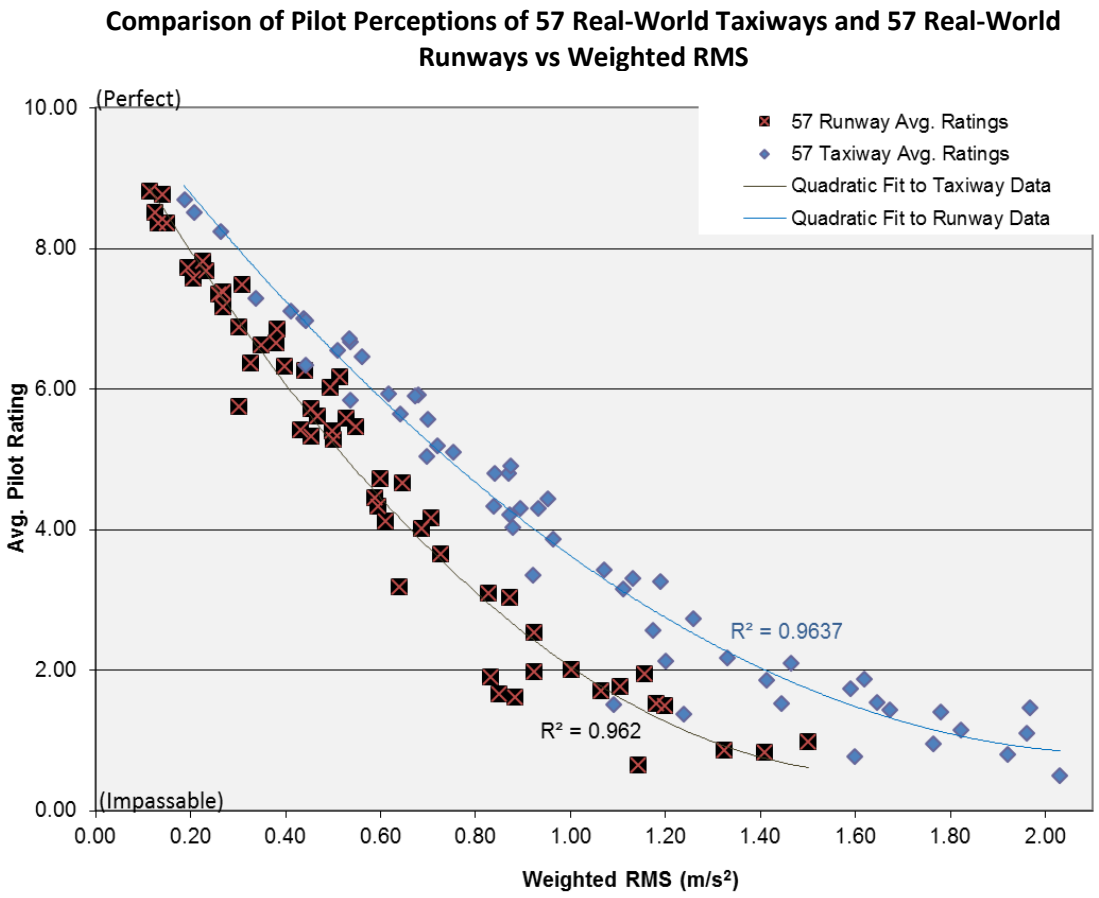

Figure 38. Combined Preliminary and Final Roughness Study Runway Average Ratings vs Weighted RMS

Figure 38 illustrates that combining runway average ratings from the final and preliminary roughness study tests yields a single trend line for taxiways and runways, indicating consistency in both test sessions.

When all 1572 individual pilot numerical ratings of taxiways or runways (from 36 pilots × 37 taxiways/runways plus 12 pilots × 20 taxiways/runways) are combined, the confidence and prediction intervals for individual pilot responses are obtained for the shifted logarithm fits, as shown in figures 39 through 42.

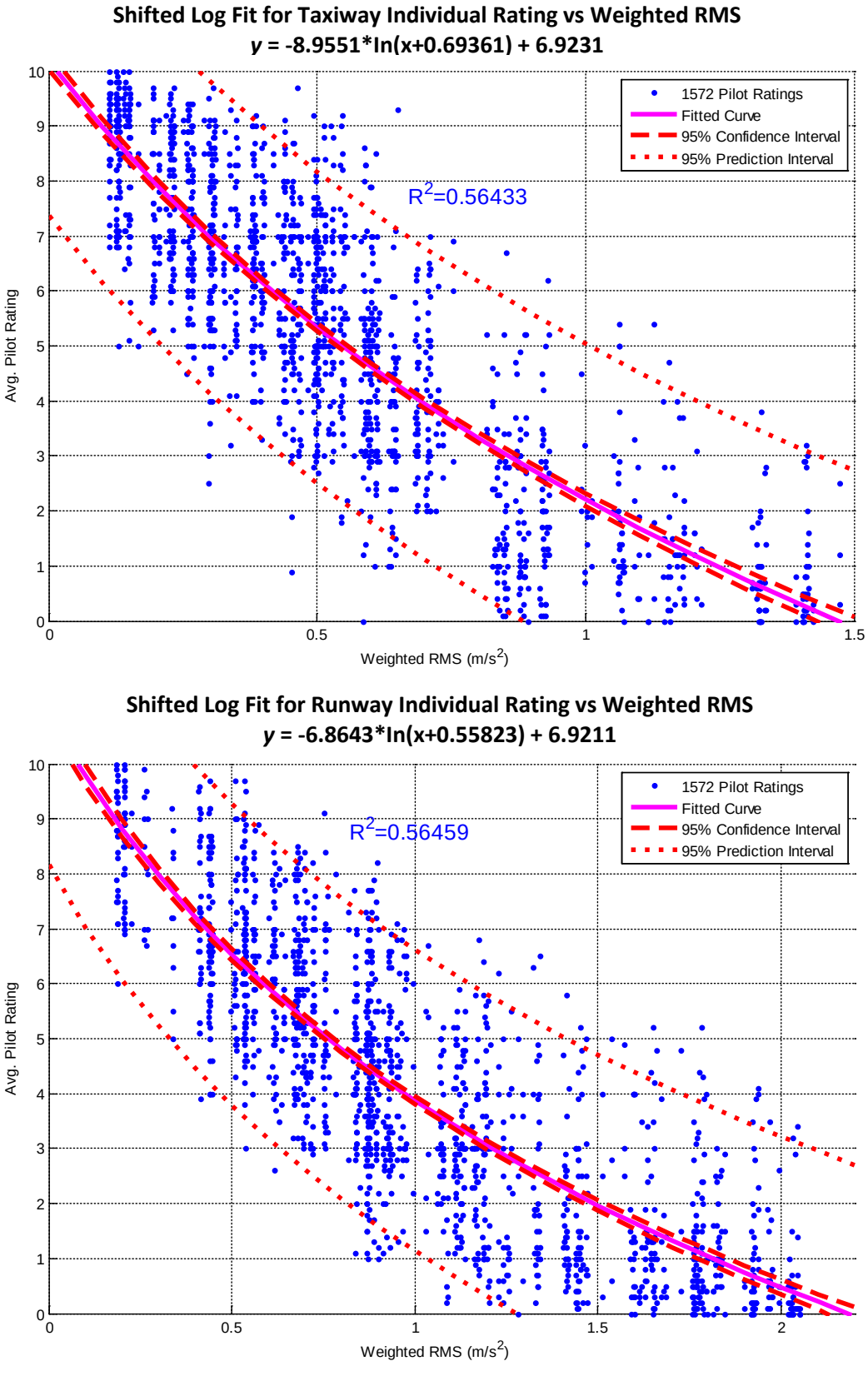

Figure 39. Confidence and Prediction Intervals for Logarithmic Fits With Weighted RMS

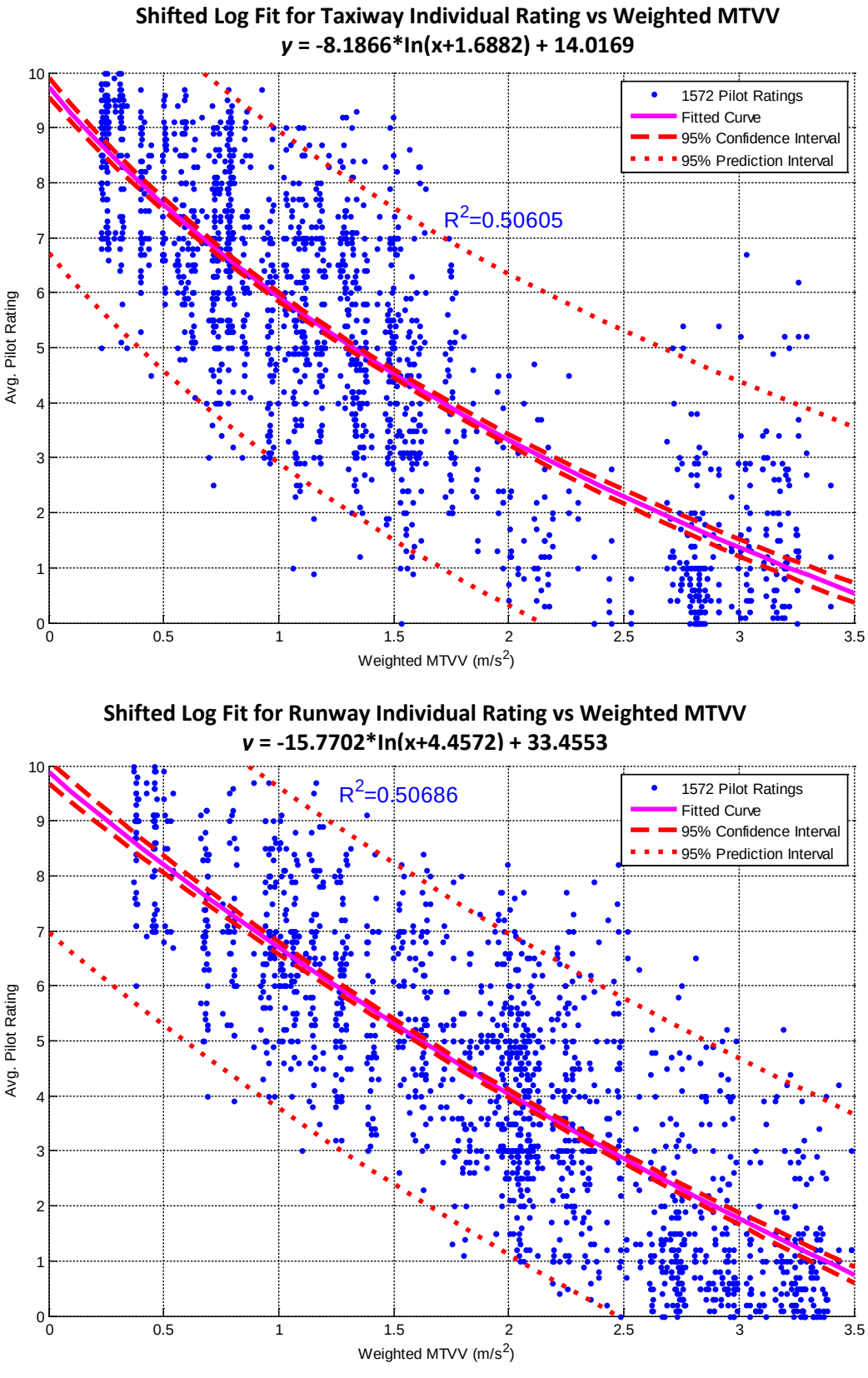

Figure 40. Confidence and Prediction Intervals for Logarithmic Fits With Weighted MTVV

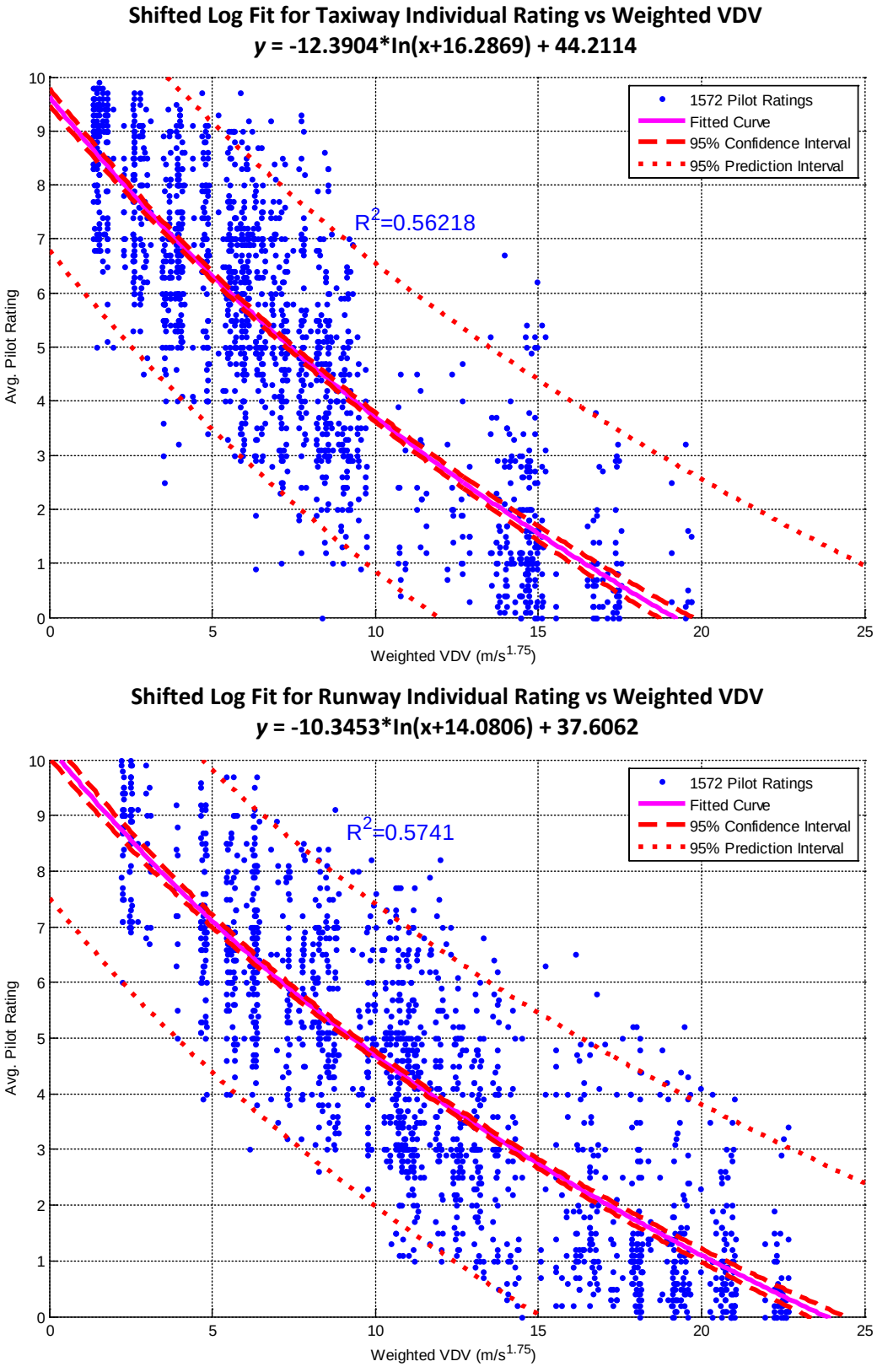

Figure 41. Confidence and Prediction Intervals for Logarithmic Fits With Weighted VDV

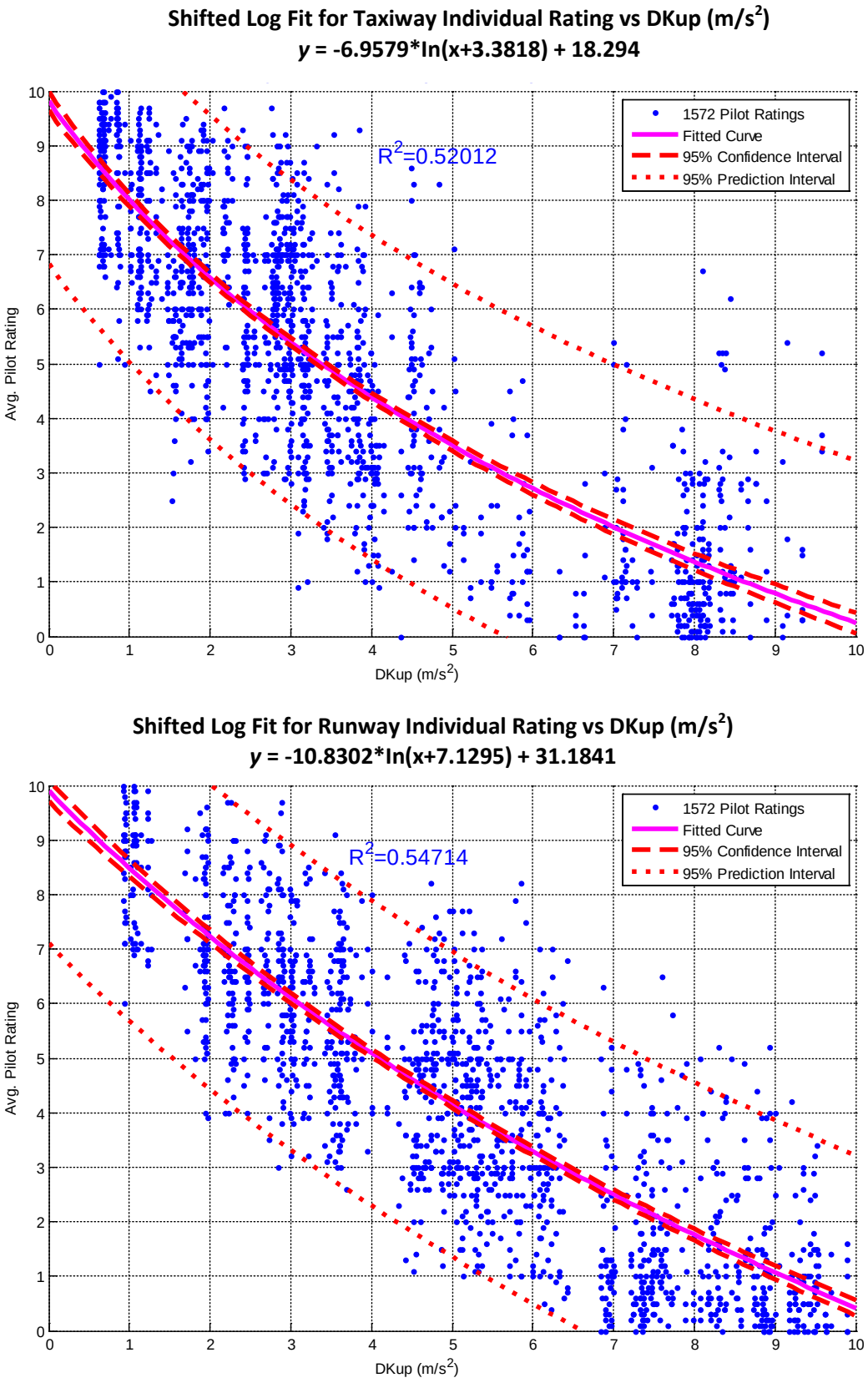

Figure 42. Confidence and Prediction Intervals for Logarithmic Fits With DKup

Each dot in these figures represents an individual pilot response. The confidence intervals are narrow because of the large number of samples. Many dots coincide—especially in the cases of pilot responses of 0 or 10—therefore, it is not possible to count 1572 points or to determine precisely how many are on each side of the trend from the figure alone.

The least squares shifted logarithmic fits to the 1572 individual pilot numerical ratings and to the 37 taxiways and runways of the final roughness study tests with pilot average ratings nearly coincide. Figure 43 compares such trends for the case of fits using weighted RMS and shows that the blue and red trends (for individual and average pilot responses) nearly coincide.

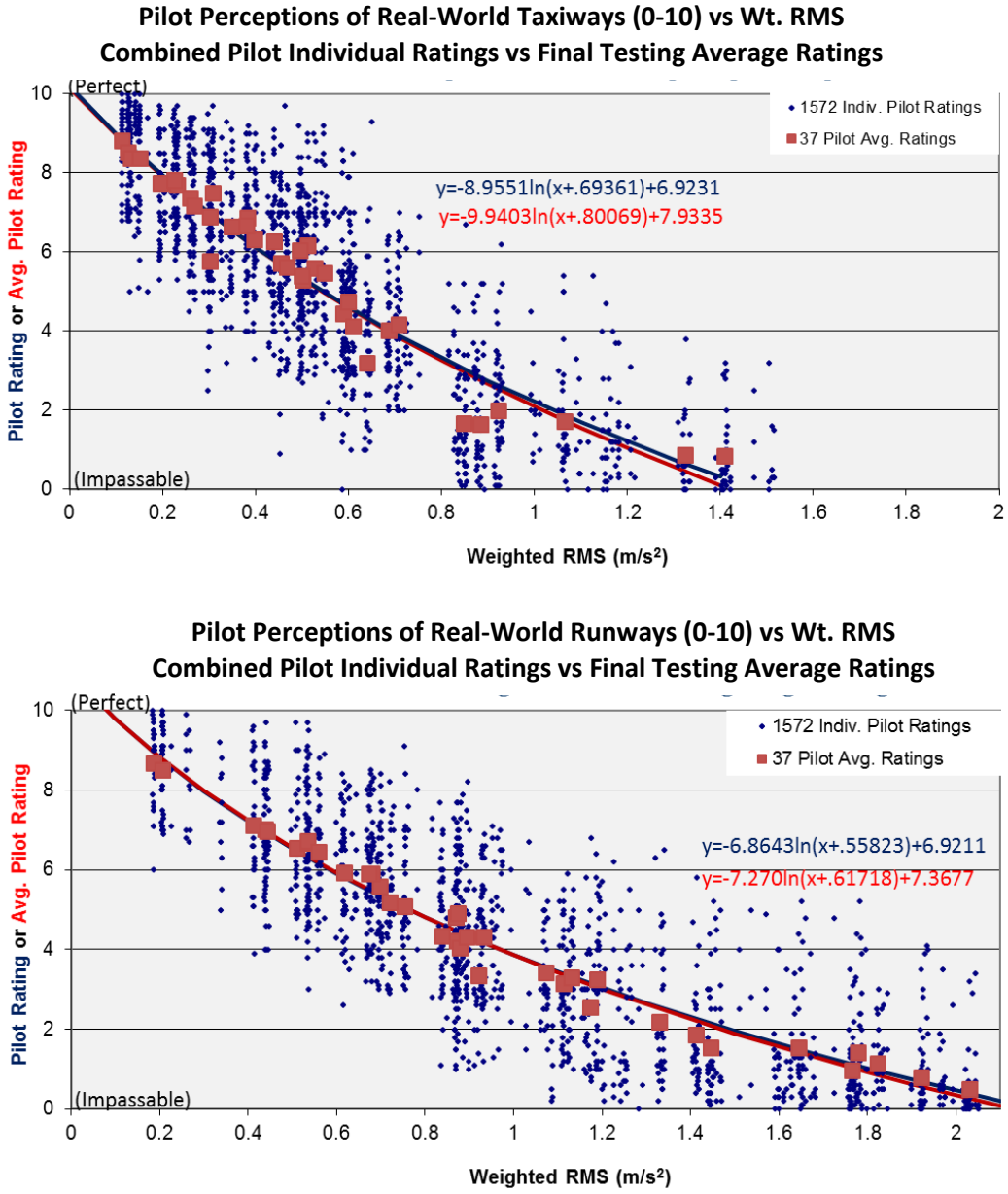

Figure 43. Comparison of Shifted Logarithmic Trends Using all Pilot Numerical Ratings vs Pilot Average Ratings From Final Simulator Runs

The scatter in individual pilot responses, the same that appears in figure 39, has a trend with very little uncertainty—as indicated by the narrow confidence interval, despite the wide range of individual responses. Figure 43 shows agreement of the trend of individual responses with the trend of the average pilot responses. The wide range of responses is in agreement with the wide prediction interval shown in figure 39.

4.10 VARIATION IN PILOT RATINGS.

Similar prediction intervals to the 95% intervals in figure 42 can be constructed for any percentage. For example, figure 44 shows the 95%, 90%, and 50% intervals as a function of weighted RMS.

These prediction intervals provide, for each value of an ISO index, a response range within which approximately 95%, 90%, and 50% of individual pilots are expected to rate a ride given its weighted RMS value.

For example, a taxiway with a weighted RMS rating of 0.5 will have approximately a 95% chance of a random pilot rating it between 2.5 and 8.2 on the 0-10 scale, a 90% chance of a rating between 3.0 and 7.7, and a 50% chance of a rating between 4.4 and 6.4. Similarly, a runway with a weighted RMS rating of 0.5 will have a 95% chance of a random pilot rating it between 3.8 and 9.2 on the 0-10 scale, a 90% chance of a rating between 4.2 and 8.8, and a 50% chance of a rating between 5.6 and 7.5.

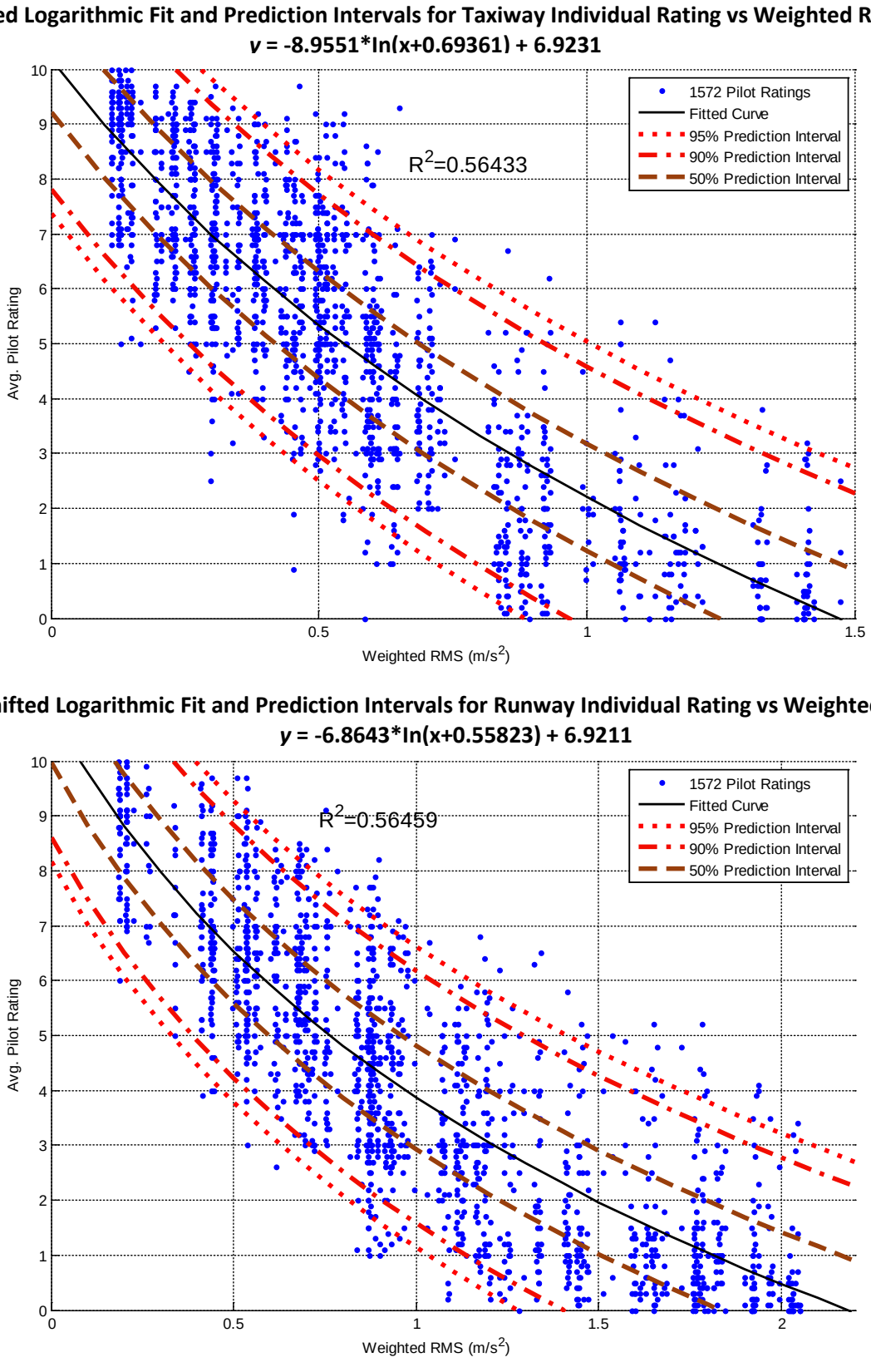

Figure 44. The 95%, 90%, and 50% Prediction Intervals for Logarithmic Fits vs Weighted RMS

4.11 COMPARISON OF B737-800 SIMULATOR AND ProFAA ROUGHNESS MODEL RESULTS.

B737-800 simulator cockpit vertical acceleration values were compared with predicted ProFAA cockpit accelerations using final surface roughness study taxiway and runway surface profiles. The ProFAA B737 surface roughness model was created by modifying the existing ProFAA B727 surface roughness model to adjust the wheelbase and aircraft weight to match those of a B737-800. Otherwise, the ProFAA B737 surface roughness model is the same as the ProFAA B727 roughness model. The major differences between the ProFAA model and the B737-800 simulator output are:

- The ProFAA profile sample spacing is 250 mm (0.82 feet) compared with the B737-800 simulator's 2.0-foot runway and 0.4-foot taxiway sample spacing.

- The ProFAA strut force calculation update rate is 400 Hz compared with a 60-Hz update rate used in the B737-800 simulator.

- The strut and tire-ground contact models are different.

Weighted RMS acceleration indices were used for the comparisons. As shown in figure 45, the B737-800 simulator cockpit accelerations are higher than those modeled by ProFAA with the difference in acceleration increasing with the increase in profile roughness.

ProFAA and the B737-800 simulator incorporate rigid-body and flexible mode simulation of the aircraft reaction to surface roughness. Additional ProFAA versus B737-800 simulator comparisons were performed using cockpit acceleration data collected with the B737-800 simulator flexible mode model disabled to determine the relative contribution of B737-800 simulator rigid and flexible mode models toward the increase in cockpit acceleration over that predicted by ProFAA. The no-flex simulator data were collected for ten real-world taxiway and eight real-world runway profiles. Figure 46 shows the relative cockpit accelerations for the ProFAA and B737-800 simulator with flexible mode models enabled and disabled.

The comparisons between the ProFAA and B737-800 simulator cockpit accelerations show the following:

- For rigid-body simulations (no flex modes), the B737 simulator cockpit accelerations are at the same level or lower than the ProFAA cockpit accelerations.

- For combined rigid-body and flexible mode simulations, the B737-800 simulator cockpit accelerations are higher than the ProFAA cockpit accelerations.

- The variance between the B737-800 simulator and ProFAA accelerations increases for rougher profiles.

- For rigid-body simulations, the B737-800 simulator and ProFAA accelerations are more closely aligned for taxiway profiles than for runway profiles.

The differences in cockpit acceleration between the B737-800 simulator and ProFAA may be due to the differences in strut models and roughness profile sample spacing.

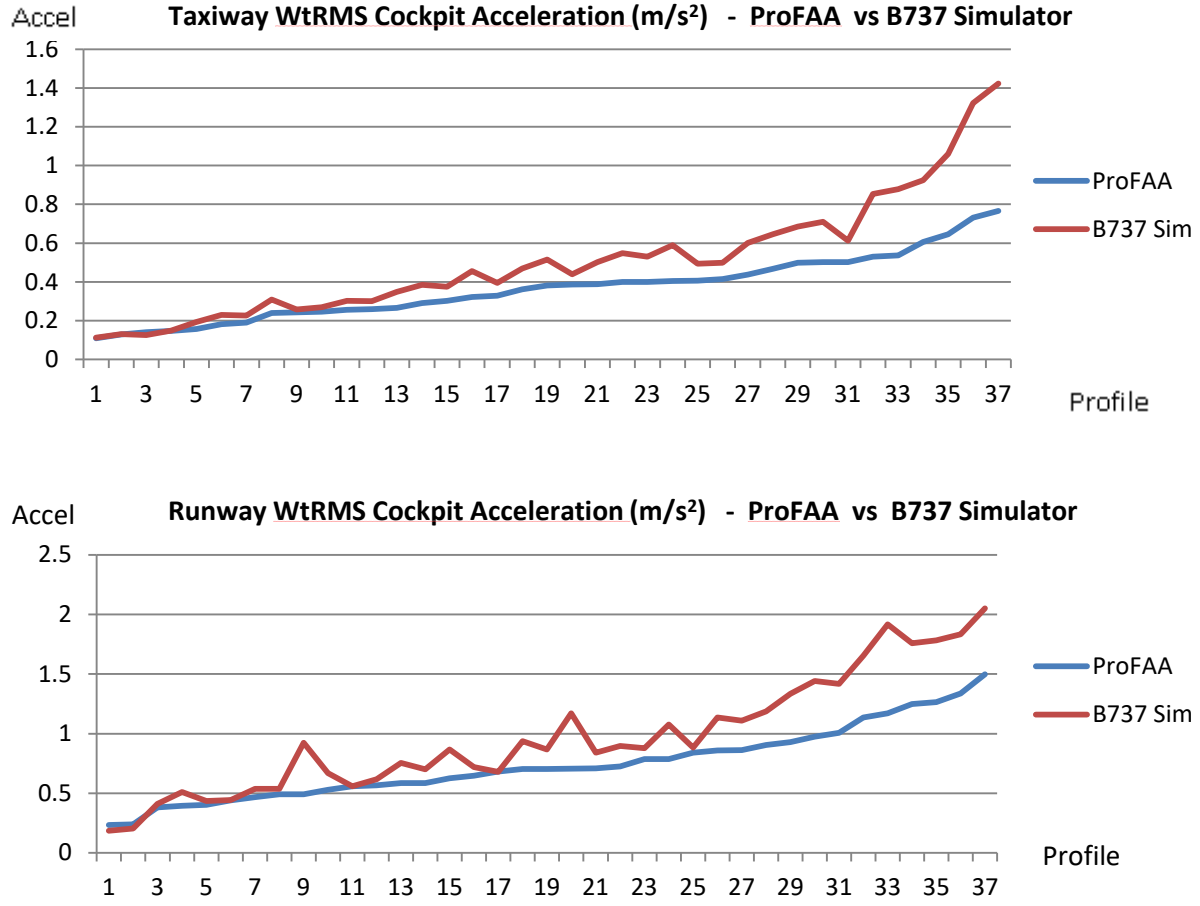

Figure 45. Cockpit Weighted RMS Acceleration—ProFAA vs B737-800 Simulator

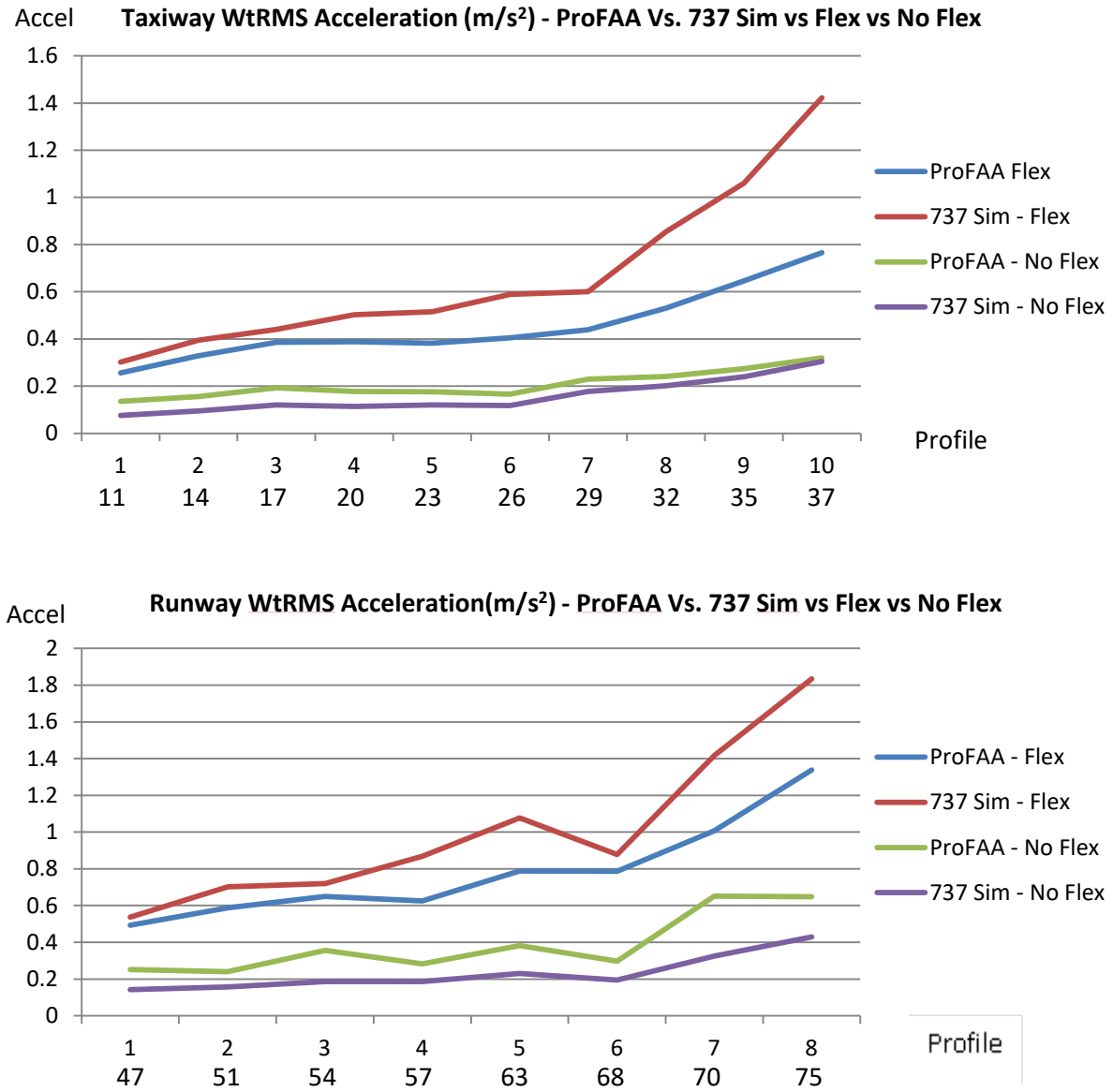

Figure 46. Cockpit Weighted RMS Acceleration—ProFAA vs B737-800 Simulator vs Flex vs no Flex for a Sample of Ten Final Roughness Study Taxiways and Eight Final Roughness Study Runways

5. SUMMARY.

Roughness testing was completed in a final data collection effort conducted at the MMAC in Oklahoma City, Oklahoma. Measured real-world airport taxiway and runway surface profiles were used to create 37 taxiway and runway roughness scenarios on the FAA B737-800 simulator. Thirty-three commercial pilots provided subjective ratings of surface rideability rating (on a scale of 0 to 10) and an acceptable/not acceptable rating for each ride.

A numerical score for the cockpit vertical accelerations resulting from each ride was calculated in terms of four ISO standard estimators of ride roughness: weighted RMS, weighted MTVV, weighted VDV, and DKup. The following comparisons of pilot ratings versus cockpit acceleration ISO indices were performed.

- Average pilot ratings versus weighted RMS acceleration allowed comparison of ratings with overall vibration discomfort levels.

- Average pilot ratings versus weighted VDV acceleration provided a comparison with a shock-related health standard.

- Average pilot ratings versus weighted MTVV acceleration compared ratings with the highest running value of weighted RMS acceleration.

- Average pilot ratings versus DKup acceleration constituted a comparison of ratings with a spinal response acceleration dose.

Analysis of the data provided the following observations:

- High correlations were found between the pilot ratings and the four ISO measures of total acceleration experienced, with different trends for taxiways and runways.

- The numerical 0 to 10 ratings were highly correlated with ride acceptability ratings using a ratings sheet with strong similarity to a previous effort [1] for evaluation of highway pavement.

- Objective indicators of subjective human ratings of rideability were deduced in terms of functions of the ISO indices with confidence intervals for the fits.

- Limits for cockpit vibration were suggested by identifying index values at which it was estimated that a desired percentage of pilots would rate a taxiway or runway as unacceptable.

This approach to data collection differs from many past efforts to evaluate the discomfort to humans imparted by whole-body vibration, such as NCHRP tests [1], in which the International Roughness Index (IRI) or the Ride Number value was used as a roughness indicator. This effort is also the first to apply ISO standard indices to determine airport pavement roughness limits for in-service pavement.

It was observed that the pilot numerical ratings and computed ISO roughness index values were highly correlated (correlation coefficients ranging from -0.942 to -0.983, with negative coefficients because pilot rating decreases corresponding to roughness index increases). Because of these strong correlations, reasonable fits could be made to express pilot average numerical rating as a function of each of the four ISO roughness indices.

The least scatter occurred in fitting the pilot ratings as a function of weighted RMS or weighted VDV by a quadratic fit or a shifted logarithmic fit, as shown in figures 47 and 48. Of these two

fits, the shifted logarithmic fit had the better extrapolation capability on the right because it was strictly decreasing. For both of these fits, the coefficient of determination R^2 ranged from 0.941 (for the shifted logarithmic fit of taxiway rating versus weighted RMS) to 0.985 (for the quadratic fit of runway rating versus weighted RMS), indicating very reasonable approximations since $R^2 = 1$ indicates a perfect fit.

Possible biases for military and repeat pilots were tested by hypothesis tests at the 95% level. It was observed that pilots who had previously participated in rating taxiway and runway roughness were more than 95% likely to have slight biases towards rating less rough surfaces better and rough surfaces lower compared with the ratings of the other pilots. However, the biases were not large, so the repeat pilots were included in the analysis. It was reasonable to consider, but with less than 95% confidence, that military pilots had a slight bias to rate the runway rides lower than other pilots.

The ISO crest factor was computed for each taxiway and runway profile because a large crest factor indicates large individual jolts in the ride. For the four taxiway rides with a high crest factor, the best fit of pilot average numerical rating was achieved using weighted VDV as the roughness indicator. Therefore, it is reasonable to consider the use of the weighted VDV for surfaces with single events. Runway profiles did not contain examples of crest factors significant enough to warrant analysis.

From the acceptable/unacceptable ratings given by pilots, fits were made to estimate the percentage of pilots rating each taxiway or runway acceptable as a function of the ISO roughness indices. If at least 5% of pilots rated a taxiway or runway as unacceptable, then the corresponding ISO roughness index unacceptable values are those shown in table 8.

Table 8. The ISO Index Values for Which Taxiways and Runways are Unacceptable to 5% of Pilots

ISO Roughness Index*	Unacceptable Taxiway Limits	Unacceptable Runway Limits
Weighted RMS (m/s^2)	≥0.31	≥0.35
Weighted MTVV (m/s^2)	≥0.71	≥0.68
Weighted VDV ($m/s^{1.75}$)	≥4.11	≥4.16
DKup (m/s^2)	≥1.82	≥1.69

* The ISO standard states that, in addition to the weighted RMS, one of the alternative indices should be reported when the crest factor of the acceleration record is approximately 9.0 or greater.

It was also observed that the RMS values shown in table 8 correspond roughly to the standardized RMS values found in reference 3 at which vibration is considered “a little uncomfortable” and that the VDV values are well below the 8.5 to 17 range at which caution with respect to health risks is indicated (for persons subjected to strong vibration shocks).

Additional pilot numerical ratings of real-world taxiways and runways from a preliminary surface roughness study collection effort for this study together with some final study pilot

ratings that were not usable in the final study average ratings were combined with the final study data to generate a total of 1572 taxiway ratings and 1572 runway ratings from the test pilots. From these, statistics for individual pilot ratings (as opposed to pilot average ratings) were calculated. The fits to the combined individual pilot ratings closely matched the fits to average pilot ratings of rides in the final test data set (figures 47 and 48).

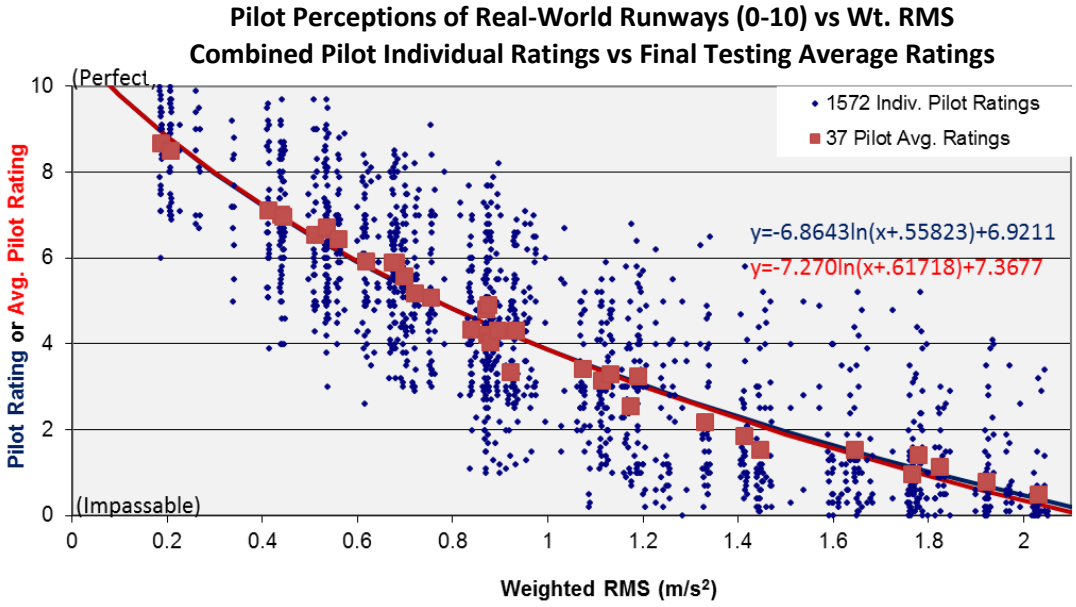

Figure 47. Shifted Logarithmic Trend Comparison: All Pilots' Runway Ratings vs Final Testing Average Runway Ratings

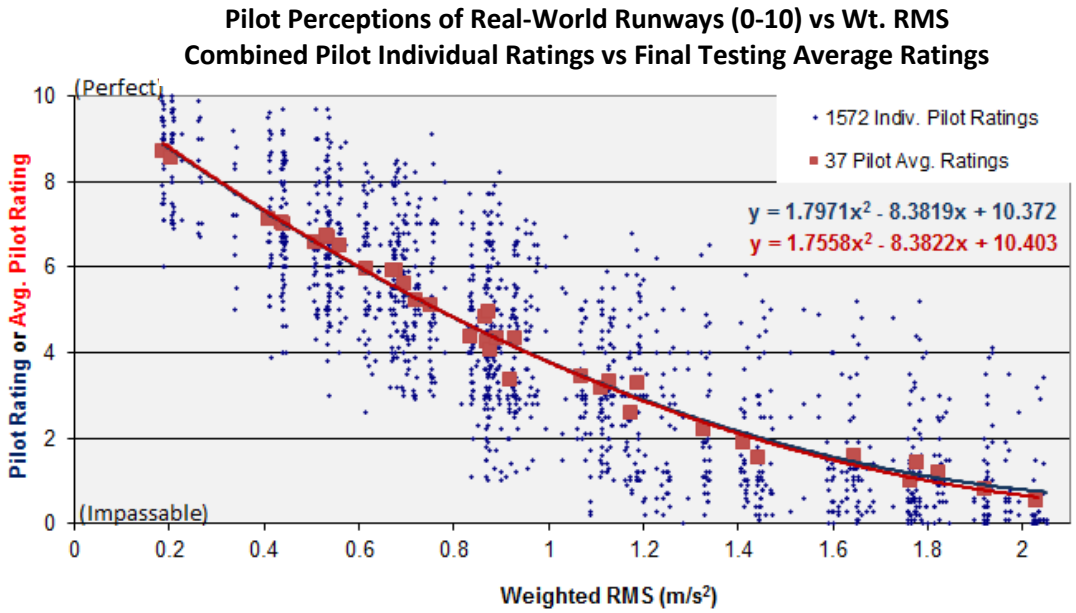

Figure 48. Quadratic Trend Comparison: All Pilots' Runway Ratings vs Final Testing Average Runway Ratings

Confidence intervals for the fits and predictive intervals for individual pilot numerical ratings were computed as a function of each roughness parameter and show that despite the substantial variation in individual pilot ratings the confidence interval for average pilot rating is narrow and various percentage levels (such as 5%) of pilots rating surfaces as unacceptable can be reasonably approximated.

No recommendation of a best ISO roughness index was made because different indices may be better indicators of roughness in different circumstances.

However, one reasonable strategy for maintaining in-service pavement would be to service the pavement when any one of the four indices (weighted RMS, weighted MTVV, weighted VDV, or DKup) exceeded some threshold value, such as the 5% level in table 8.

Another reasonable strategy would be to service pavement only when a threshold value for weighted RMS or weighted VDV was exceeded because these two indices have the best fit statistics, appear more frequently in literature, and estimate discomfort from overall vibration and from occasional shocks, respectively.

6. FUTURE WORK.

The following areas have been identified for future research:

- Simulator roughness testing for other aircraft types.
- Incorporate pilot seat accelerometer for future testing.
- Correlate pilot ratings with standard surface roughness indices (Boeing Bump, IRI, etc.).
- Evaluate new pavement construction limits for surface roughness.
- Analyze rideability ratings for asphalt versus concrete surfaces.
- Analyze recommended ISO indices.

7. REFERENCES.

1. http://ww.airporttech.tc.faa.gov/Airport-Pavement/Nondestructive-Pavement-Testing/AirportPavementRoughnessResearch (date last visited 01/23/18).

2. Federal Aviation Administration (FAA), "Standards for Specifying Construction of Airports," Advisory Circular (AC) 150/5270-10F, September 20. 2011.

3. FAA, "Guidelines and Procedures for Measuring Airfield Pavement Roughness," AC 150/5380-9, September 30, 2009.

4. Janoff, M.S., National Cooperative Highway Research Program (NCHRP) Report 308, "Pavement Roughness and Rideability Field Evaluation," National Research Council Transportation Research Board, Washington, DC, September 26, 1988.

5. Cherokee CRC, LLC, "FAA Surface Roughness Preliminary Study Data Collection Report" (Draft), March 1, 2012.

6. ProFAA, "The Federal Aviation Administration's Computer Program for Roughness Index Analysis User's Manual" (Draft), Mike Monroney Aeronautical Center, 6500 S. MacArthur Blvd., Oklahoma City, Oklahoma, available via http://www.airporttech.tc.faa.gov/Airport-Pavement/Nondestructive-Pavement-Testing/Runway-Roughness-Criteria (date last visited 10/26/16).

7. American Society for Testing and Materials (ASTM) E1927-98, "Standard Guide for Conducting Pavement Ride Quality Ratings," January 1998 (Reapproved 2012).

8. International Organization for Standardization (ISO) 2631 "Mechanical Vibration and Shock – Evaluation of Human Exposure to Whole-Body Vibration," May 1, 1997: 2631-1:1997 "Part 1: General Requirements," 2631-4:2001 "Part 4: Guidelines for the Evaluation of the Effects of Vibration and Rotational Motion on Passenger and Crew Comfort in Fixed-Guideway Transport Systems," and 2631-5:2004 "Part 5: Method for Evaluation Containing Multiple Shocks."

9. Lewis, C. and Griffin, M., "A Comparison of Evaluations and Assessments Obtained Using Alternative Standards for Predicting the Hazards of Whole-Body Vibration and Repeated Shocks," *Journal of Sound and Vibration*, Vol. 215, Issue 4, August 27, 1998, pp. 915-926.

10. Mansfield, N., Holmlund, P., and Lundstrom, R., "Comparison of Subjective Responses to Vibration and Shock With Standard Analysis Methods and Absorbed Power," *Journal of Sound and Vibration*, Vol. 230, Issue 3, February 24, 2000, pp. 477-491.

APPENDIX A—ADDITIONAL STATISTICAL GRAPHS

This appendix provides statistical graphs compiled in a separate spreadsheet that are pertinent to discussions found in the main body of this report. .

Regarding the possibility of a bias in military taxiway and runway ratings, figures A-1 and A-2 show the comparison of military ratings with ratings by other pilots versus weighted root-mean-square (RMS).

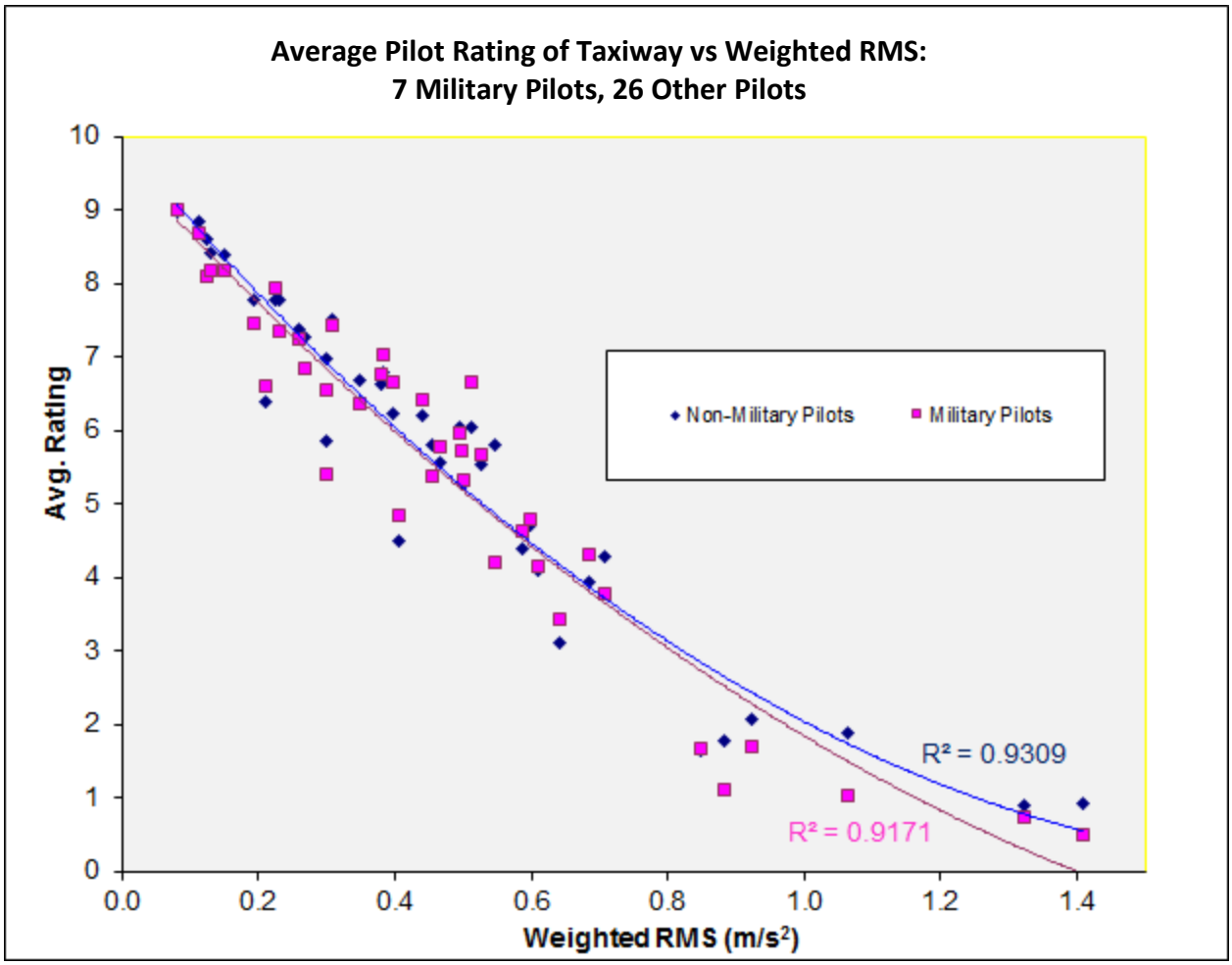

Figure A-1. Military and Non-Military Average Pilot Numerical Taxiway Ratings vs Weighted RMS

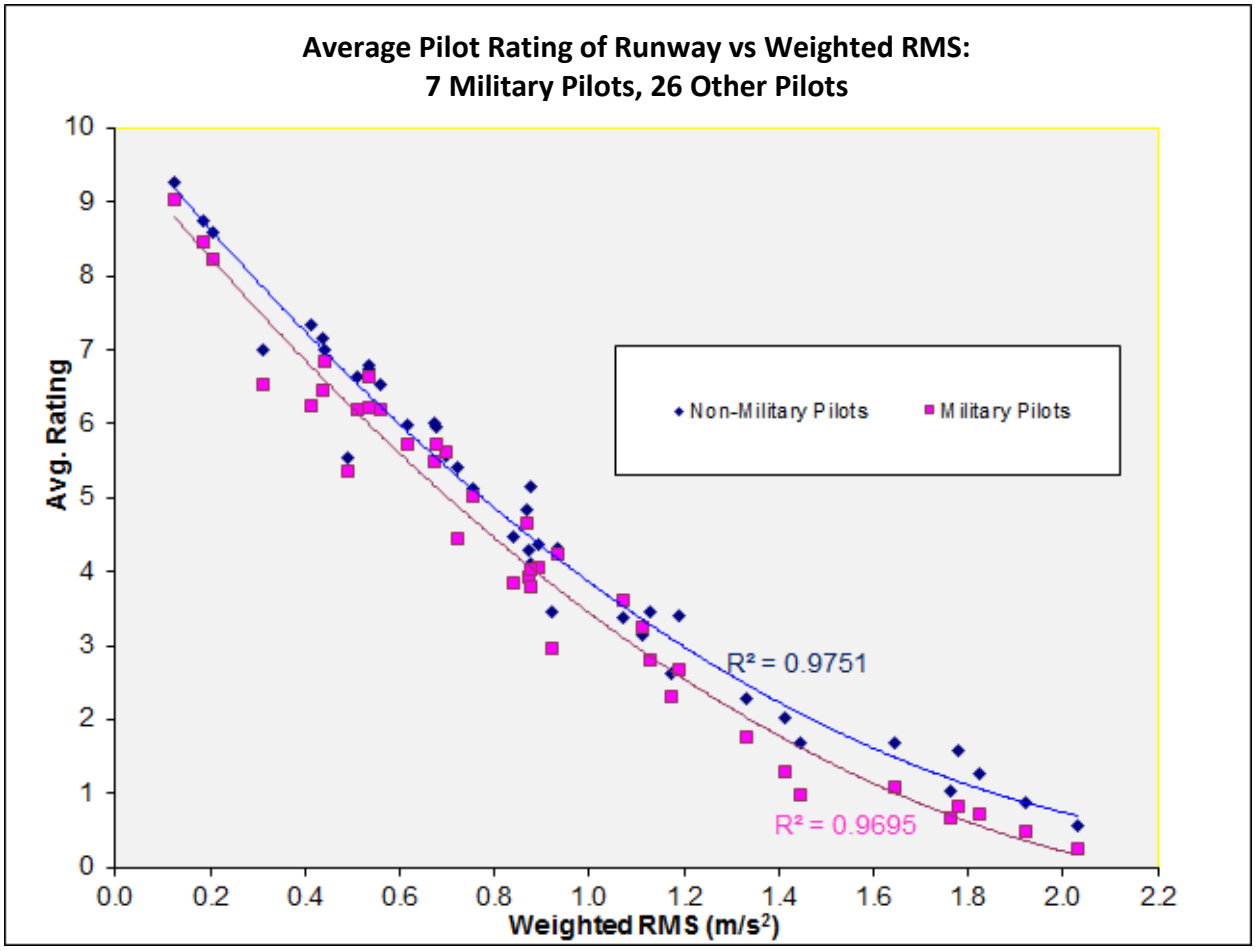

Figure A-2. Military and Non-Military Average Pilot Numerical Runway Ratings vs Weighted RMS

These runway data fits are separated similarly to the linear fits to runway data versus weighted fourth-power vibration does value (VDV) (section 4.5 of the main document), similarly suggesting a slight bias between military and non-military pilots. The coefficient of determination (R^2) values are as similar as expected, since only seven sample points for military pilots were available, which indicates reasonable fits were accomplished.

Regarding the possibility of a bias in taxiway and runway ratings by pilots who had participated in a simulator evaluation before, figures A-3 and A-4 show the comparison of these repeat ratings with ratings by other pilots versus weighted RMS with similar apparent biases in the slope of the fits to those encountered in the weighted VDV case.

An analysis of bias of the linear fit of pilot rating to weighted VDV had graphs with similarly differing slopes that were evaluated for bias by hypothesis tests.

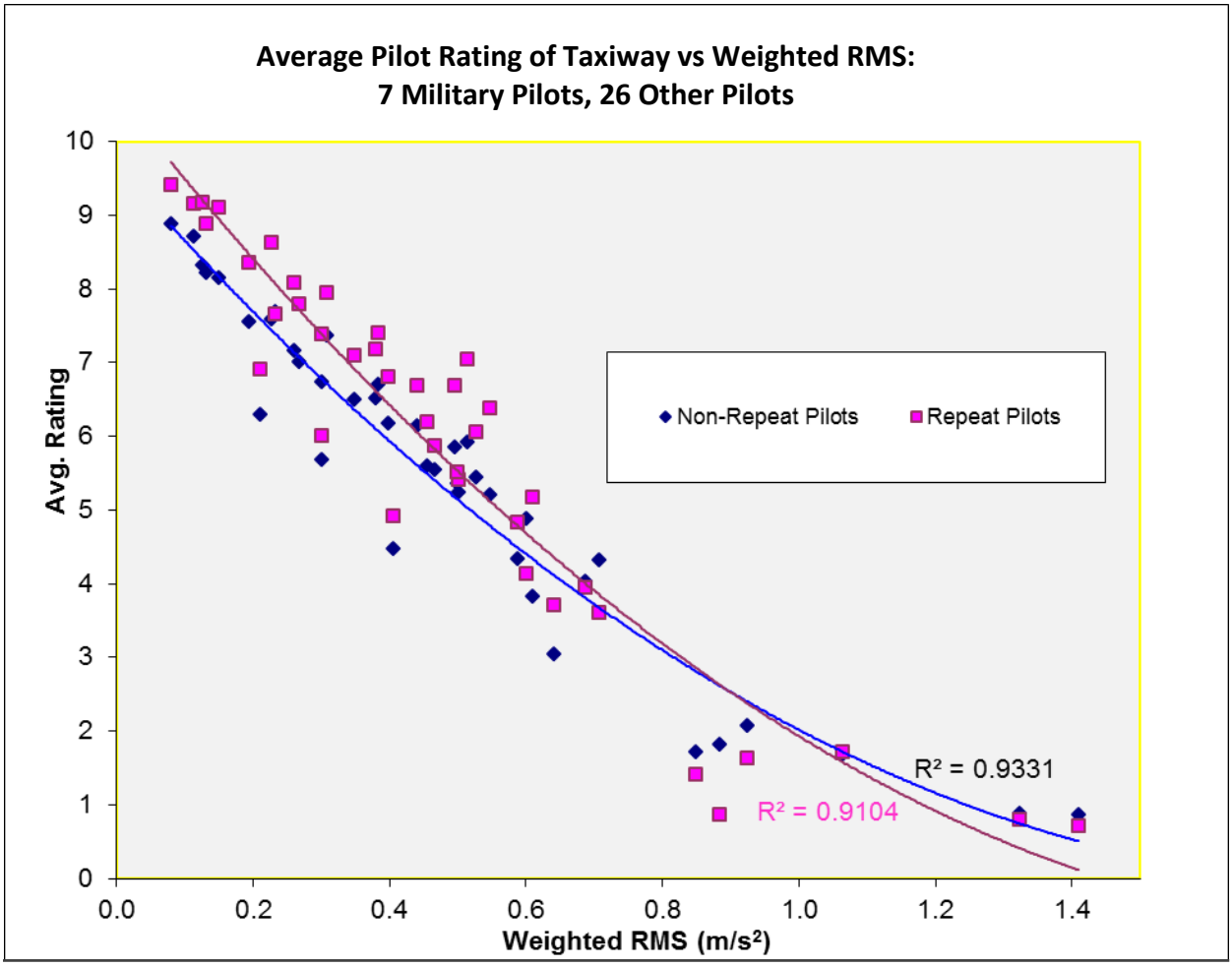

Figure A-3. Repeat and Non-Repeat Average Pilot Numerical Taxiway Ratings vs Weighted RMS

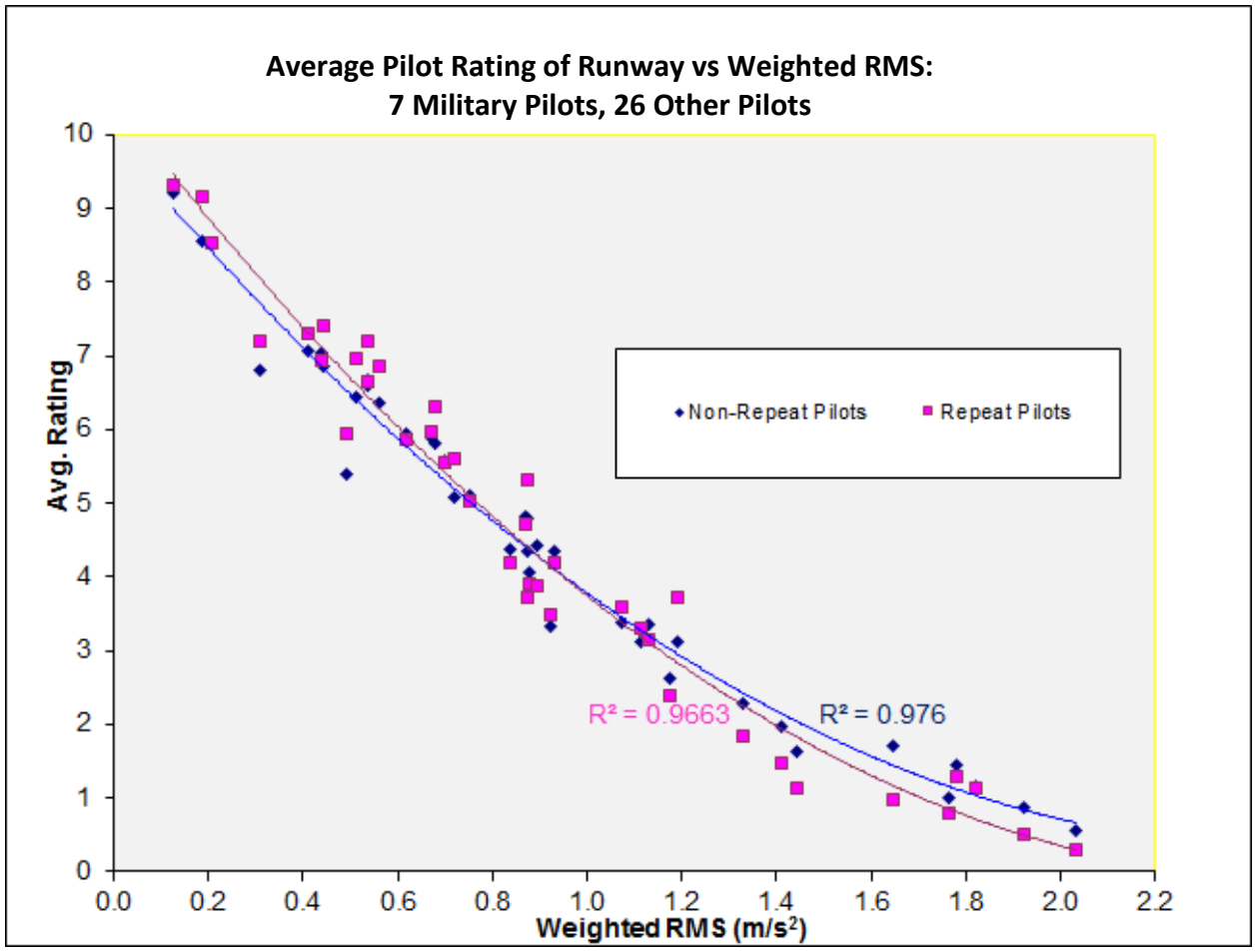

Figure A-4. Repeat and Non-Repeat Average Pilot Numerical Runway Ratings vs Weighted RMS

Regarding the possibility of bias in ratings as a function of simulator seating position, in addition to the correlation coefficients that appear in tables 1 and 2 of the main document, figures A-5 and A-6 graphically compares the average ratings by seat number. The same pilot subjective numerical ratings versus weighted RMS curve fits demonstrated consistent agreement regardless of seat number.

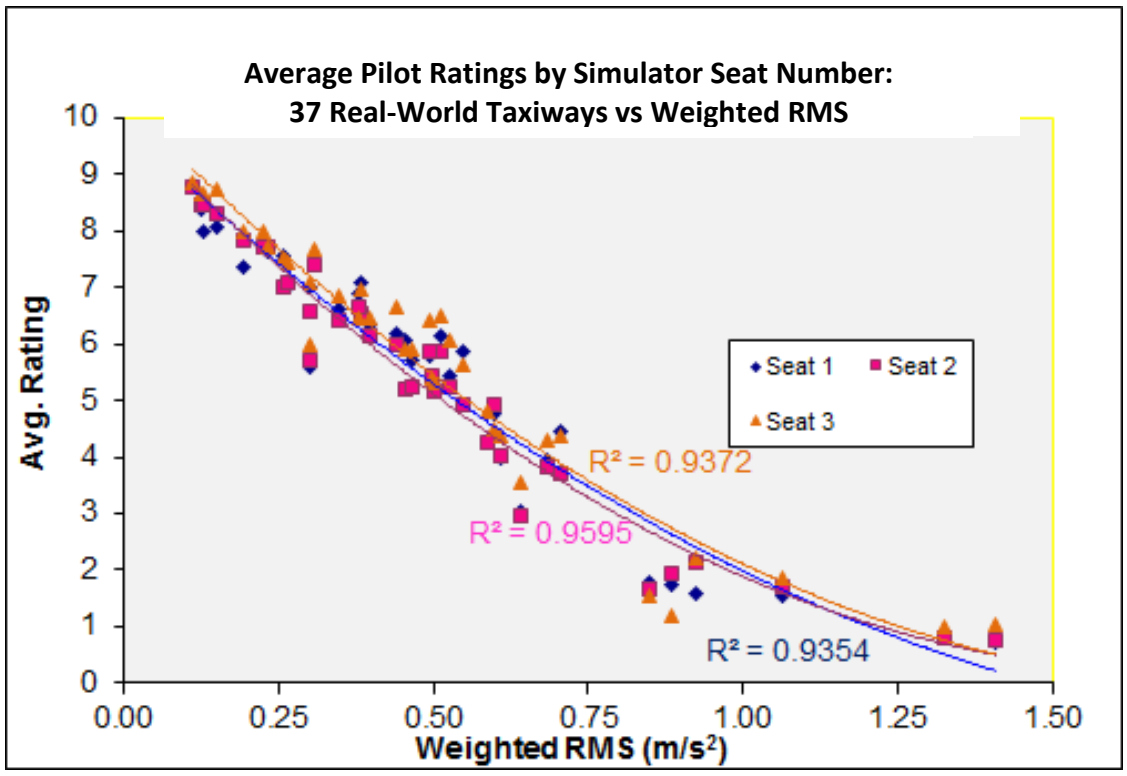

Figure A-5. Average Pilot Numerical Taxiway Ratings vs Weighted RMS by Seat Number

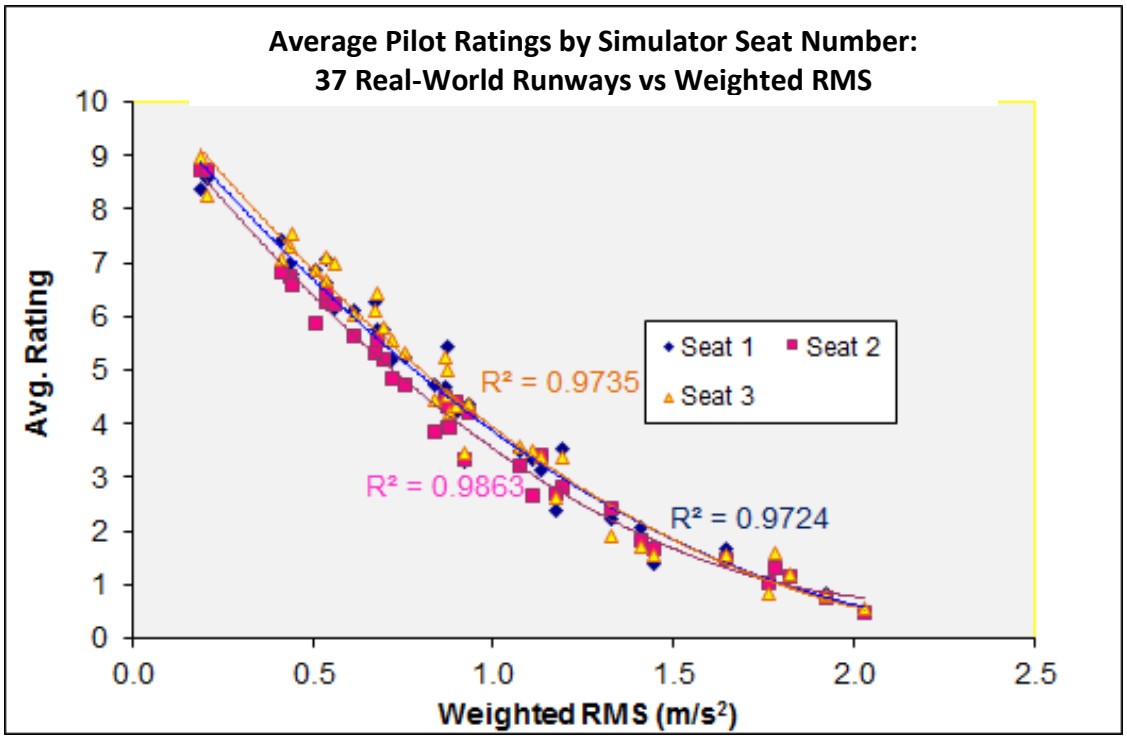

Figure A-6. Average Pilot Numerical Runway Ratings vs Weighted RMS by Seat Number

Figures A-7 and A-8 show generic taxiway and runway data combined with real-world data.

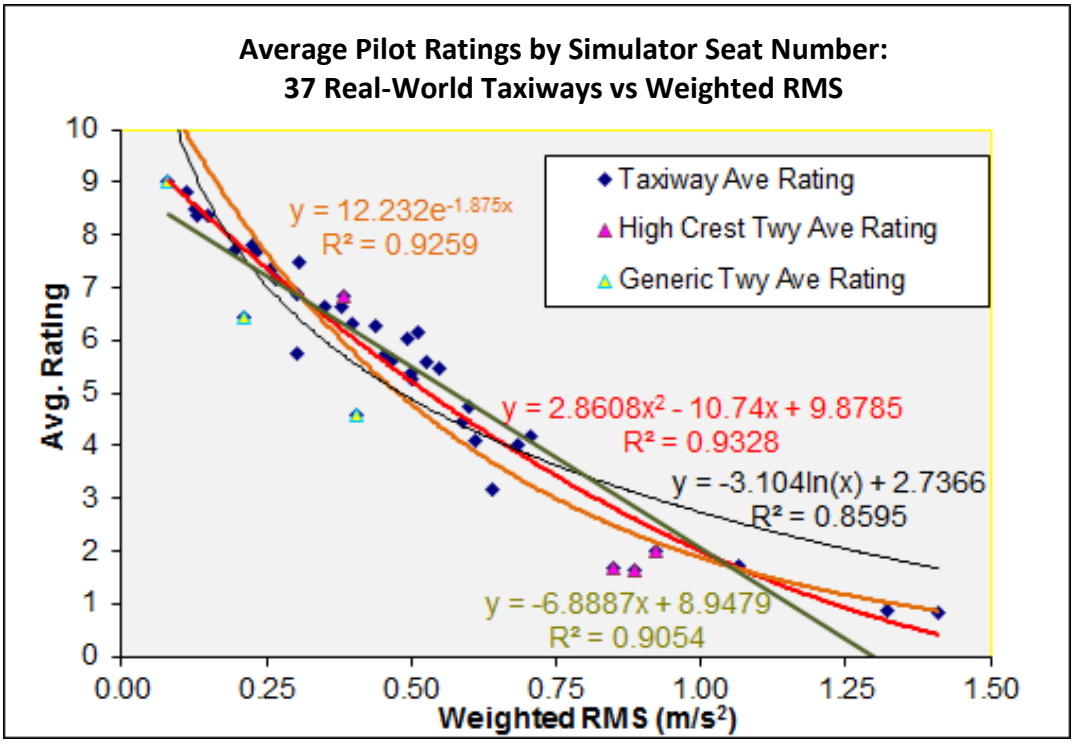

Figure A-7. The Off-Trend Behavior of Generic Taxiway Average Ratings vs Weighted RMS

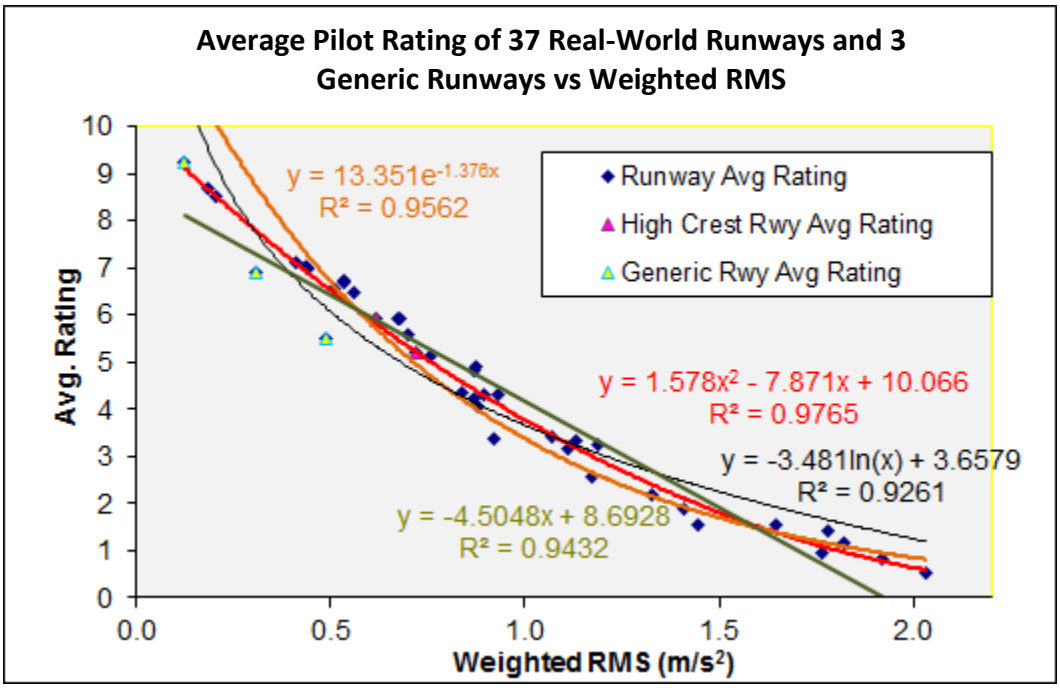

Figure A-8. The Off-Trend Behavior of Generic Runway Average Ratings vs Weighted RMS

Simple (cubic) polynomial fits were made for comparison with the logistic regression to fit percent of pilots rating a taxiway or runway acceptable (y) as a function of pilot average numerical rating (x). For taxiways, the polynomial fit was

$$y = \begin{cases} 100 & (0 \le x < 0.2132) \\ 0.4222x^3 - 5.1001x^2 + 1.068x + 100 & (0.2132 \le x \le 7.3447) \\ 0 & (x > 7.3447) \end{cases} \quad \text{(A-1)}$$

and for runways, the fit was

$$y = \begin{cases} 100 & (0 \le x < 0.3940) \\ 0.3479x^3 - 4.5896x^2 + 1.7543x + 100 & (0.3940 \le x \le 7.7315) \\ 0 & (x > 7.7315) \end{cases} \quad \text{(A-2)}$$

Figures A-9 and A-10 show the graphs of these fits. Figure A-10 shows a close-up view of figure A-9 in the critical region.

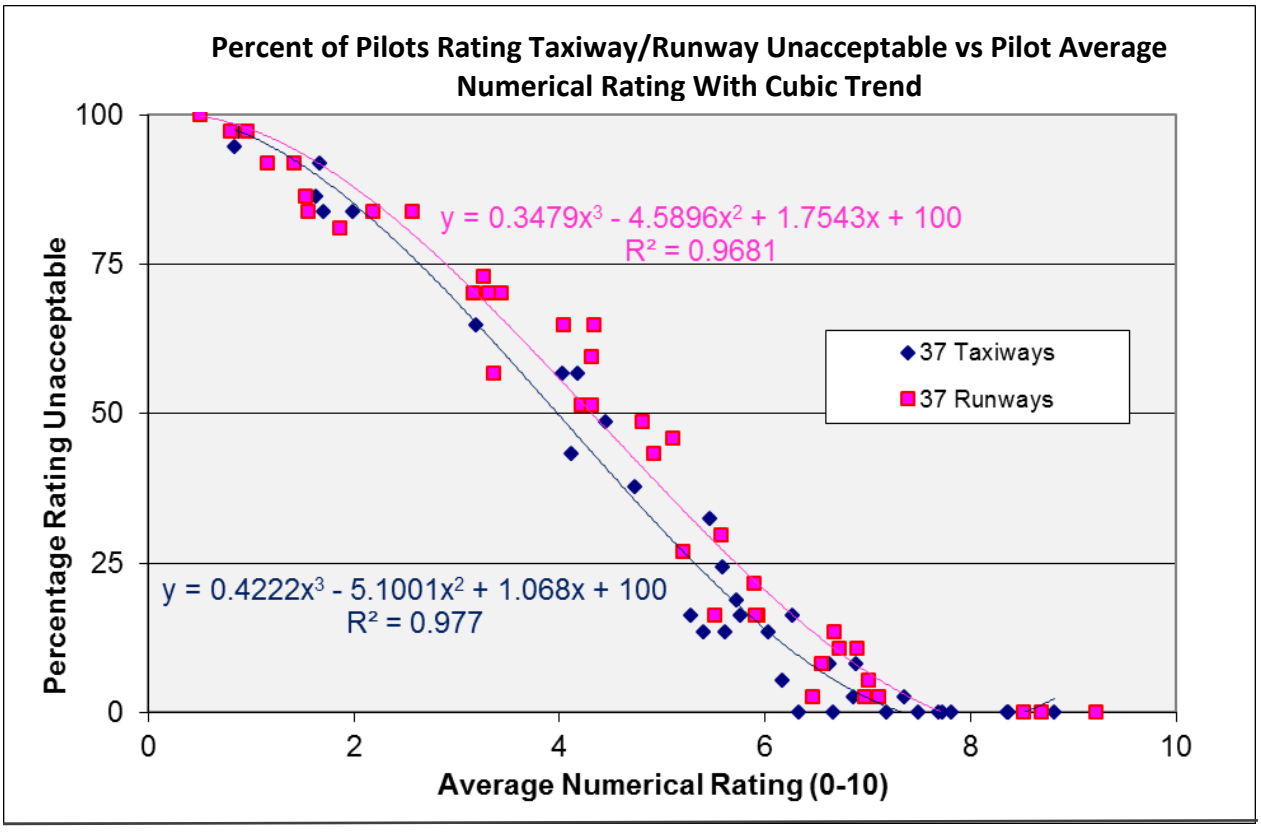

Figure A-9. Cubic Polynomial Fits to Percent Acceptable Ratings vs Numerical Ratings

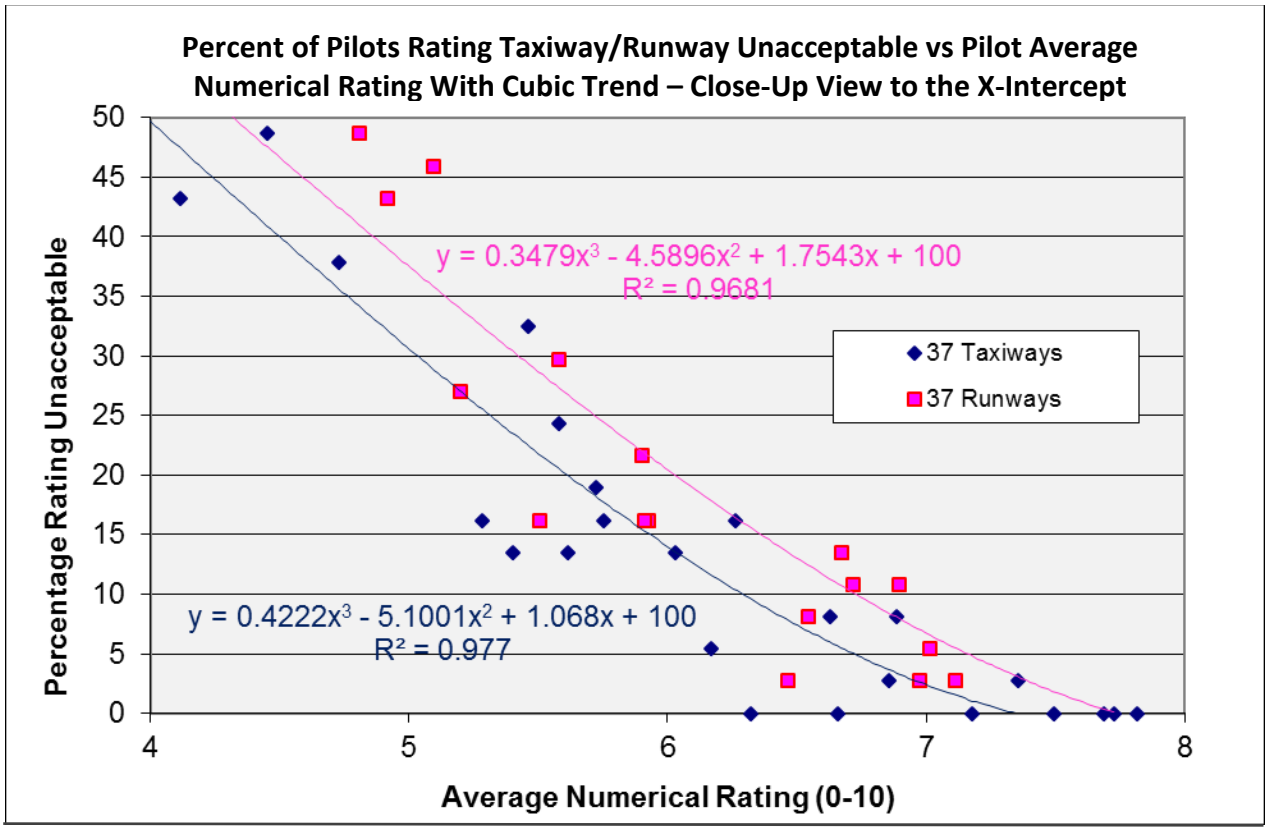

Figure A-10. Closeup of Cubic Polynomial Fits to Percent Acceptable Ratings vs Numerical Ratings

Table A-1 extracts some specific numerical ratings at which rides become unacceptable by these polynomial fits.

Table A-1. Pilot Average Numerical Rating of a Taxiways or Runway When 5%, 10%, or 50% of Pilots Rate the Ride as Unacceptable Estimated by Cubic Polynomial Fits

Amount Unacceptable	Taxiway Rating (0-10)	Runway Rating (0-10)
5%	6.7188	7.1574
10%	6.2904	6.7282
50%	3.9841	4.3186

Hence, if taxiways and runways are considered unacceptable when 5% of pilots rate them as unacceptable, then by means of polynomial approximation, a taxiway becomes unacceptable at a pilot average numerical rating of approximately 6.7 and a runway becomes unacceptable at a pilot average numerical rating of approximately 7.2. If the 5% criterion is used as a threshold for calling a taxiway or runway unacceptable and the polynomial fit of percent unacceptable versus average numerical rating is applied, then table A-1 provides the ranges of unacceptable International Organization for Standardization (ISO) index values.

Table A-1 should to be compared with table 2 of the main document, in which the (usual) logistic regression was made to the same data points. The actual function to fit human unacceptability versus numerical rating is unknown; therefore, this alternative interpolation is provided in order to provide an estimate of the uncertainty in table 2.

Table A-2 should be compared with table 3 of the main document, which was computed using logistic regression. The different values here are the result of using a cubic polynomial instead of a logistic regression to fit pilot unacceptability percentage versus ISO indices. This method of interpolation gives the reader an idea of how much uncertainty is possible in the numbers of tables 3 and 4, since the exact form of an interpolating function to subjective human response is unknown. Table 3 is preferred to table A-2 because the logistic fit has better end behavior (better behavior for large and small pilot percentages). Confidence intervals to better quantify uncertainty in the index values shown in table 3 are considered unreliable and were not calculated.

Table A-2. ISO Index Values at Which 5%, 10%, and 50% of Pilots are Estimated by Cubic Polynomial Fit to Rate a Taxiway or Runway as Unacceptable

ISO Roughness Index	Index Value When 5% of Pilots Rate the Taxiway as Unacceptable	Index Value When 10% of Pilots Rate the Taxiway as Unacceptable	Index Value When 50% of Pilots Rate the Taxiway as Unacceptable	Index Value When 5% of Pilots Rate the Runway as Unacceptable	Index Value When 10% of Pilots Rate the Runway as Unacceptable	Index Value When 50% of Pilots Rate the Runway as Unacceptable
Weighted RMS (m/s^2)	0.33	0.38	0.69	0.41	0.47	0.90
Weighted MTVV* (m/s^2)	0.76	0.90	1.77	0.85	1.00	1.91
Weighted VDV ($m/s^{1.75}$)	4.38	5.13	9.55	4.95	5.74	10.84
DKup** (m/s^2)	1.95	2.30	4.59	2.07	2.44	4.79

*MTVV = Maximum transient vibration value from a running RMS computation
**DKup = Spinal response acceleration dose

APPENDIX B—REAL-WORLD TAXIWAY AND RUNWAY PROFILES

Profile Number	Profile Type	Airport Type	Profile Source	Runway Intersection	Profile Gain	Weighted Crest Factor
1	Taxiway	Domestic	FAA		0.80	4.7702
2	Taxiway	Domestic	FAA		0.85	4.5086
3	Taxiway	International	FAA		0.90	4.055
4	Taxiway	Domestic	FAA		0.90	4.0675
5	Taxiway	Domestic	FAA		0.90	6.8529
6	Taxiway	Domestic	FAA		0.90	3.4313
7	Taxiway	Domestic	FAA	x	0.90	3.8845
8	Taxiway	Domestic	FAA	x	0.90	5.6931
9	Taxiway	Domestic	FAA	x	0.90	6.1859
10	Taxiway	International	FAA		0.90	5.1845
11	Taxiway	Domestic	FAA		1.00	3.9377
12	Taxiway	Domestic	FAA	x	1.00	6.2471
13	Taxiway	Domestic	FAA		1.00	3.9933
14	Taxiway	Domestic	FAA		1.00	6.7417
15	Taxiway	Domestic	FAA		1.00	7.7475
16	Taxiway	Domestic	FAA		1.00	6.2149
17	Taxiway	Domestic	FAA		1.00	3.3419
18	Taxiway	Domestic	FAA	x	1.00	4.9543
19	Taxiway	Domestic	FAA		1.00	4.7831
20	Taxiway	Domestic	FAA		1.00	6.5274
21	Taxiway	Domestic	FAA		1.00	3.3011
22	Taxiway	Domestic	FAA		1.00	5.0539
23	Taxiway	Domestic	FAA		1.00	3.5494
24	Taxiway	Domestic	FAA		1.00	6.2093
25	Taxiway	International	FAA	x	1.00	5.9554
26	Taxiway	Domestic	FAA		1.00	6.3879
27	Taxiway	Domestic	FAA		1.00	5.667
28	Taxiway	Domestic	FAA		1.00	4.1005
29	Taxiway	Domestic	FAA	x	1.00	5.3076
30	Taxiway	Domestic	FAA		1.00	4.4206
31	Taxiway	Domestic	FAA		1.10	5.0849
32	Taxiway	Domestic	FAA		1.00	8.7003
33	Taxiway	Domestic	FAA		1.05	9.1693
34	Taxiway	Domestic	FAA		1.10	8.6623
35	Taxiway	Domestic	FAA		1.00	5.3498
36	Taxiway	Domestic	FAA		1.00	4.2676
37	Taxiway	Domestic	FAA		1.00	3.9542

Profile Number	Profile Type	Airport Type	Profile Source	Runway Intersection	Profile Gain	Weighted Crest Factor
38	Runway	International	FAA		0.90	3.8756
39	Runway	International	FAA		0.90	4.3736
41	Runway	Domestic	FAA		0.70	3.1376
42	Runway	Domestic	FAA		0.70	3.7343
43	Runway	Domestic	FAA		0.70	5.3492
44	Runway	Domestic	FAA	x	0.75	3.2223
45	Runway	Domestic	FAA		0.80	4.8551
46	Runway	Domestic	FAA		0.80	4.4619
47	Runway	Domestic	FAA		0.80	4.0656
48	Runway	Domestic	FAA	x	0.80	5.8144
49	Runway	Domestic	FAA		0.80	4.5739
50	Runway	RWY 2_CL	Gerardi		0.80	3.4114
51	Runway	International	FAA		0.80	3.6595
52	Runway	Domestic	FAA		0.80	6.18
53	Runway	Domestic	FAA	x	0.80	5.1776
54	Runway	Domestic	FAA	x	0.80	4.5239
55	Runway	Domestic	FAA	x	0.80	5.575
56	Runway	Domestic	FAA		0.80	4.8569
57	Runway	Domestic	FAA	x	0.80	5.2135
58	Runway	Domestic	FAA		0.80	3.4487
59	Runway	International	FAA	x	0.80	4.5881
60	Runway	Domestic	FAA		0.80	3.7879
61	Runway	Domestic	FAA		0.80	4.0296
62	Runway	Domestic	FAA	x	0.80	3.4079
63	Runway	Rwy 1 LOC 0 - 5100	Gerardi		0.80	3.9844
64	Runway	International	FAA		0.80	4.1298
65	Runway	Domestic	FAA		0.80	3.8626
66	Runway	Domestic	FAA	x	0.80	5.1694
67	Runway	International	?		0.80	4.2703
68	Runway	International	?		0.80	4.0416
69	Runway	International	?		0.85	5.4214
70	Runway	International	Boeing		0.85	3.2731
71	Runway	International	Boeing		0.90	3.5965
72	Runway	International	Boeing		0.90	3.4653
73	Runway	International	Boeing		0.90	3.3232
74	Runway	International	Boeing		0.90	2.9676
75	Runway	International	Boeing		0.90	3.6398

APPENDIX C—REAL-WORLD SURFACE PROFILE FORMATTING FOR SIMULATOR USE

This appendix provides details on the formatting of the real-world surface profiles for simulator use. Figure C-1 shows an example of a real-world runway profile prior to formatting. This profile was selected to provide an example of surface roughness due to intersecting runways. The surface elevation change at the runway intersection occurs between 3800 and 4000 feet along the profile. The vertical red lines delineate the 5100-foot section selected for use in this study.

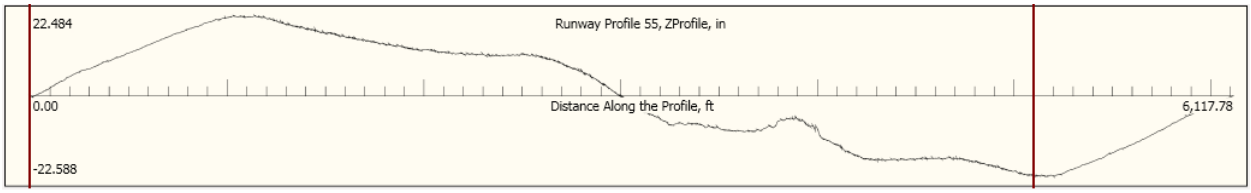

Figure C-1. Real-World Runway Profile Showing Selected 5100-Foot Section

Figure C-2 shows an expanded view of the selected 5100-foot profile section.

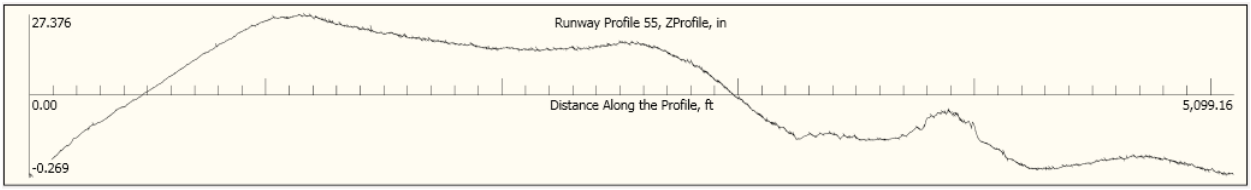

Figure C-2. Expanded View of Selected 5100-Foot Section

The profile was filtered using a 1000-foot cutoff high-pass filter to remove low-frequency height variations. Removal of low frequencies was necessary due to the flight simulator's inability to provide sustained low-frequency motion response. Figure C-3 shows the profile height and modeled accelerations after filtering.

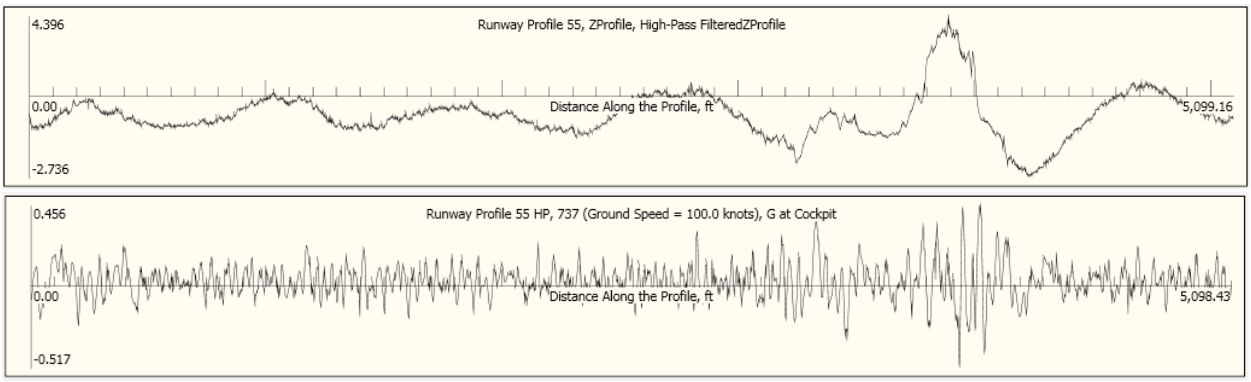

Figure C-3. Profile Height (top) and Cockpit Acceleration (bottom) After High-Pass Filtering

After high-pass filtering, the profile height units were converted from inches to feet, and the profile sample rate was changed to 2 feet to align with the flight simulator format. After conversion, the profile was loaded in the flight simulator for testing, and the ground model surface height and resulting cockpit accelerations were recorded. B737-800 simulator cockpit accelerations were obtained from the accelerometer installed below the pilot seats. Figure C-4 shows the recorded simulator surface height and cockpit vertical acceleration.

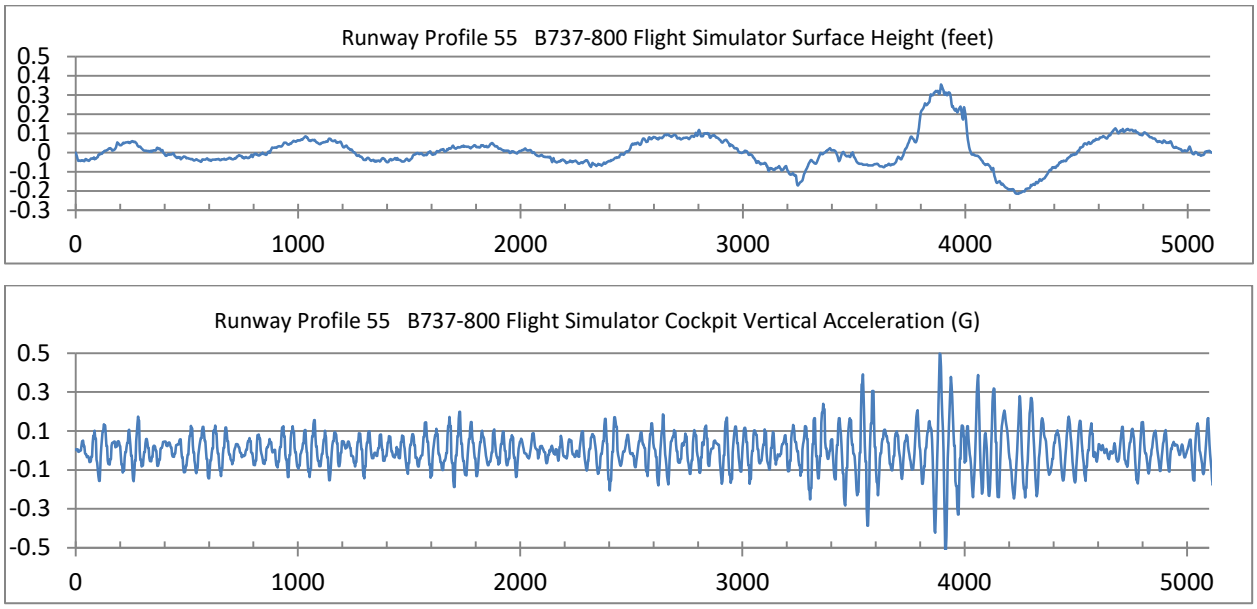

Figure C-4. The B737-800 Simulator Profile Height (top) and Cockpit Vertical Acceleration (bottom)

After the real-world profiles were installed in the B737-800 simulator, each profile was tuned using a profile height gain to provide a range of roughness levels. Figure C-5 shows the average cockpit acceleration after tuning for each of the 37 real-world taxiway and runway profiles.

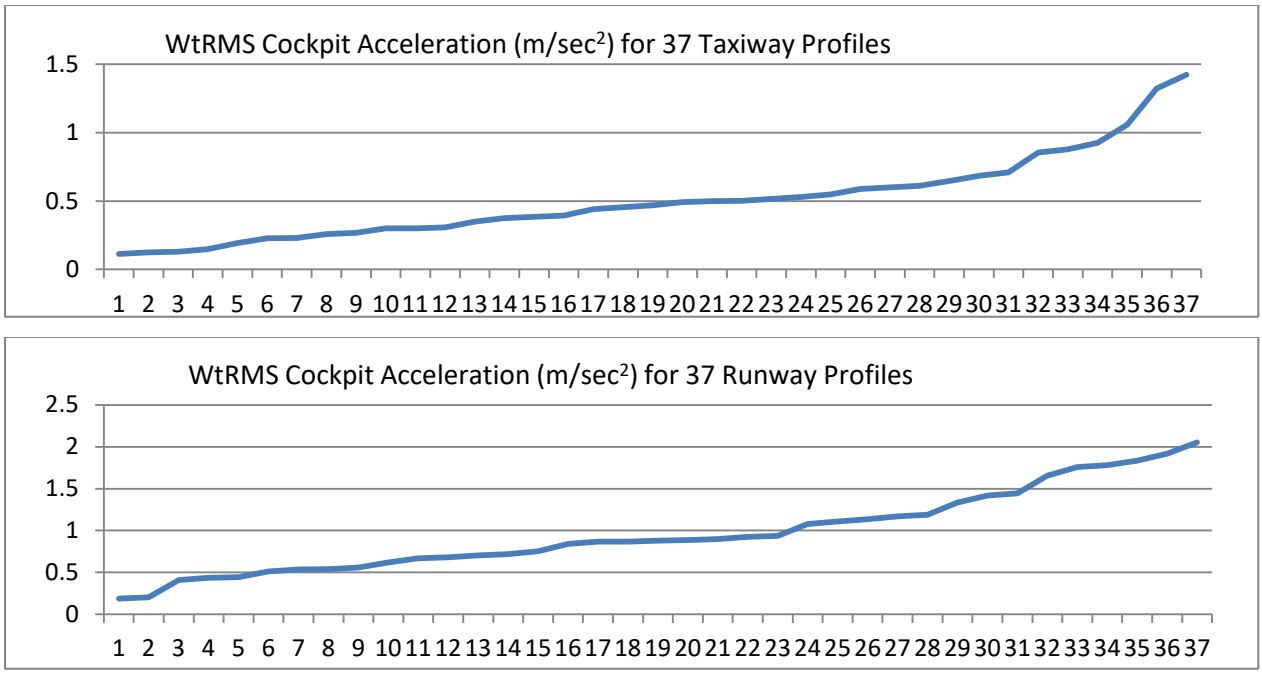

Figure C-5. The B737-800 Simulator Average Cockpit Acceleration for Tuned Taxiway (top) and Runway (bottom) Profiles

APPENDIX D—REAL-WORLD PROFILE HEIGHTS AND B737-800 SIMULATOR COCKPIT VERTICAL ACCELERATIONS

This appendix shows the graphs that provided time histories of the Boeing (B)737-800 simulator real-world taxiway and runway surface profile height and cockpit vertical acceleration captured during simulator test scenarios. The upper graph displays recorded surface height (feet) versus profile distance (feet). The bottom graph displays recorded cockpit vertical acceleration (g) versus profile distance (feet). Four International Organization for Standardization (ISO) indices of average cockpit acceleration for the time history are provided on the bottom graph. Full descriptions for each profile are provided in appendix B of this report.

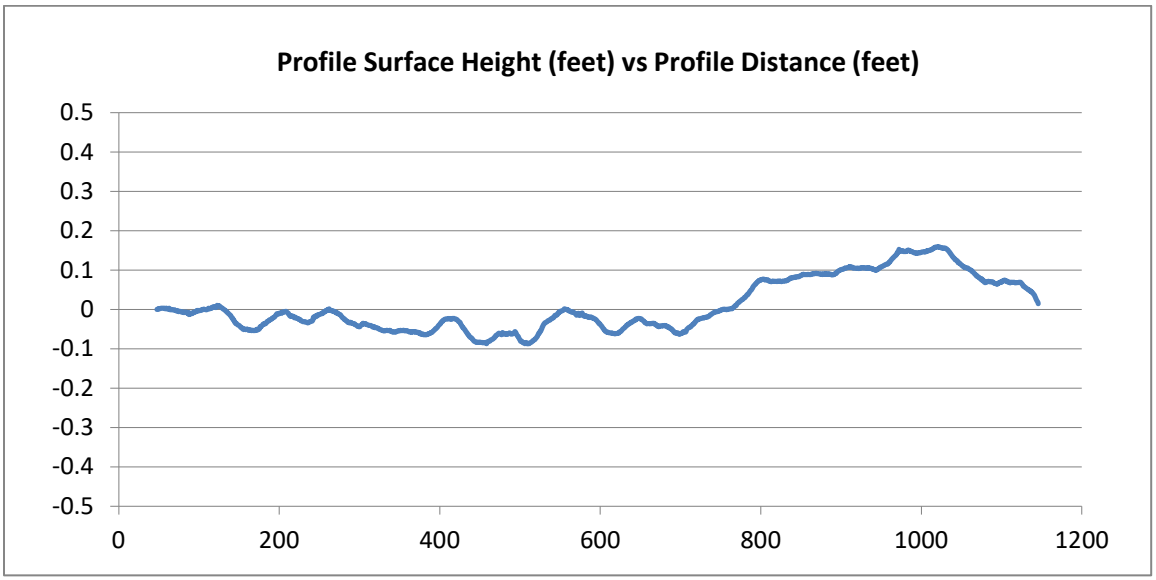

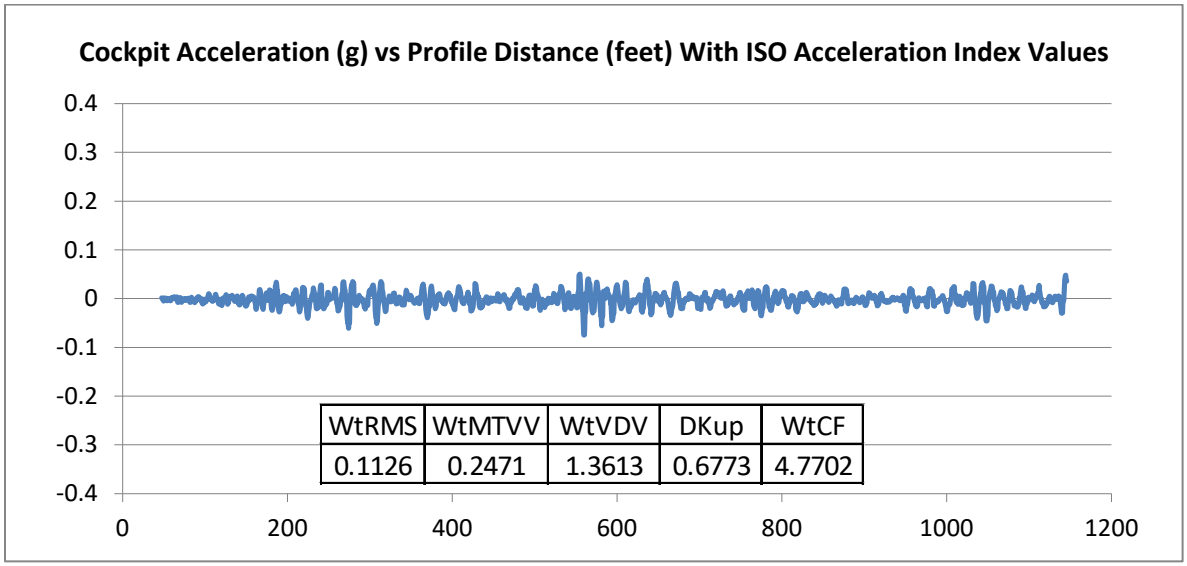

Figure D-1. Taxiway Profile 1—Profile Surface Height, Cockpit Acceleration, and Acceleration ISO Indices

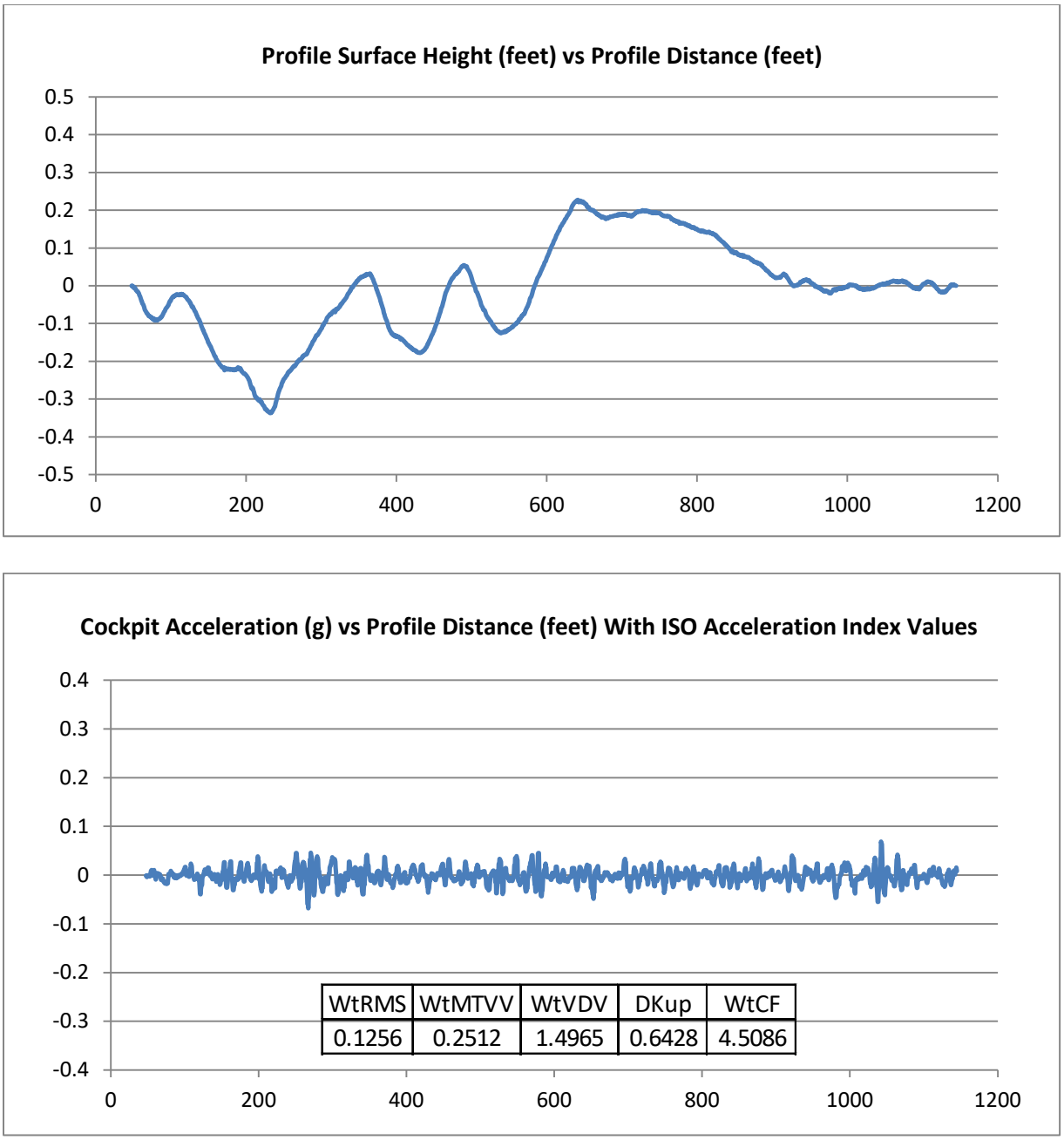

Figure D-2. Taxiway Profile 2—Profile Surface Height, Cockpit Acceleration, and Acceleration ISO Indices

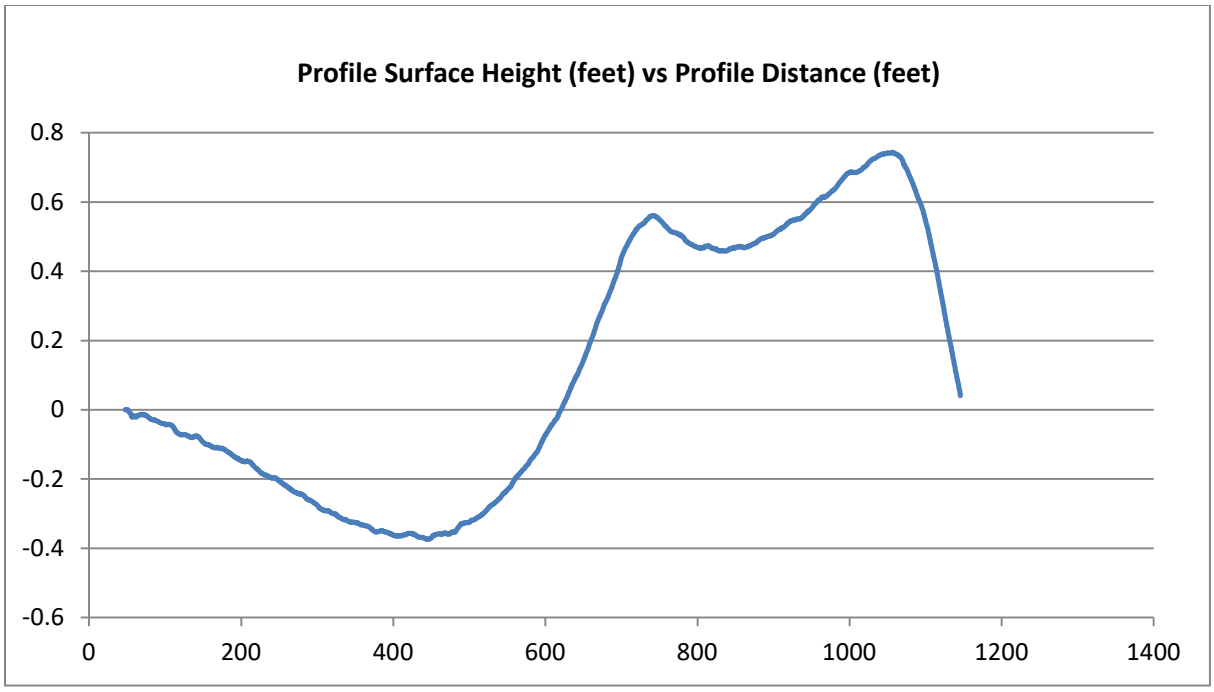

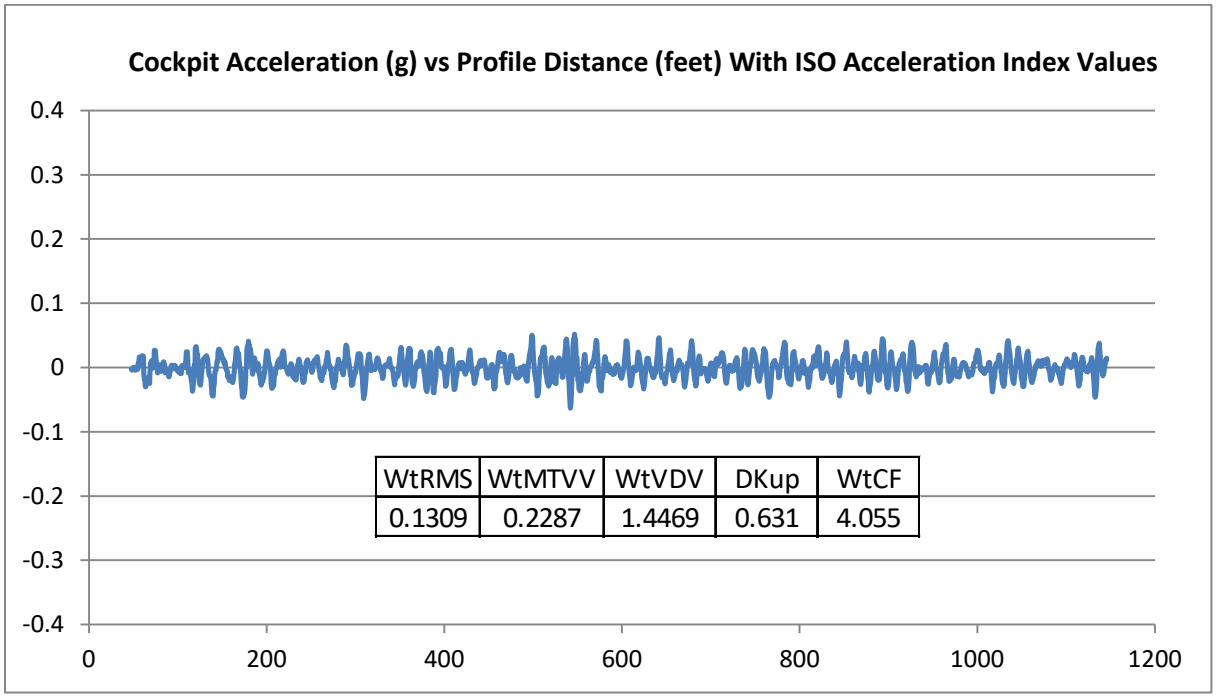

Figure D-3. Taxiway Profile 3—Profile Surface Height, Cockpit Acceleration, and Acceleration ISO Indices

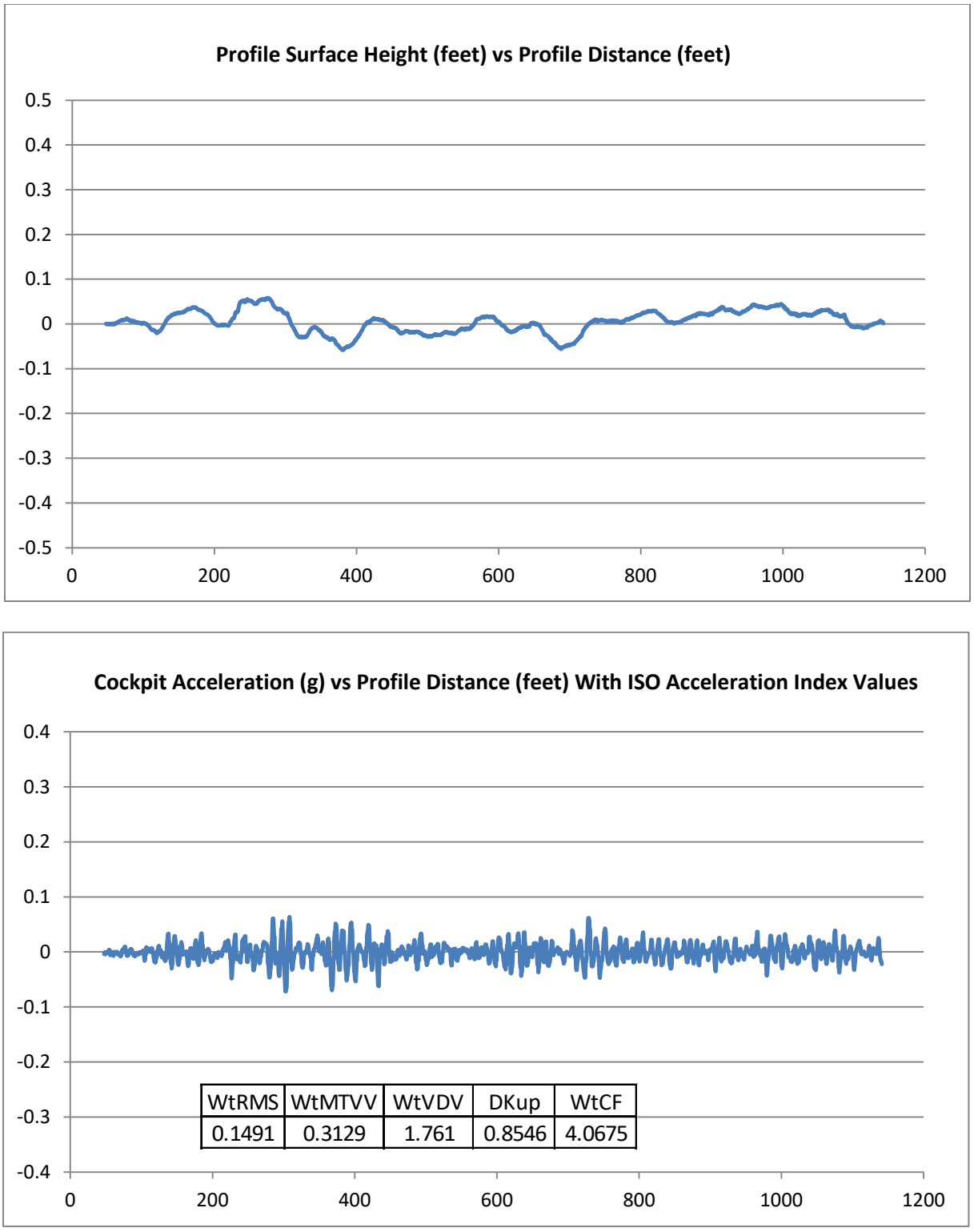

Figure D-4. Taxiway Profile 4—Profile Surface Height, Cockpit Acceleration, and Acceleration ISO Indices

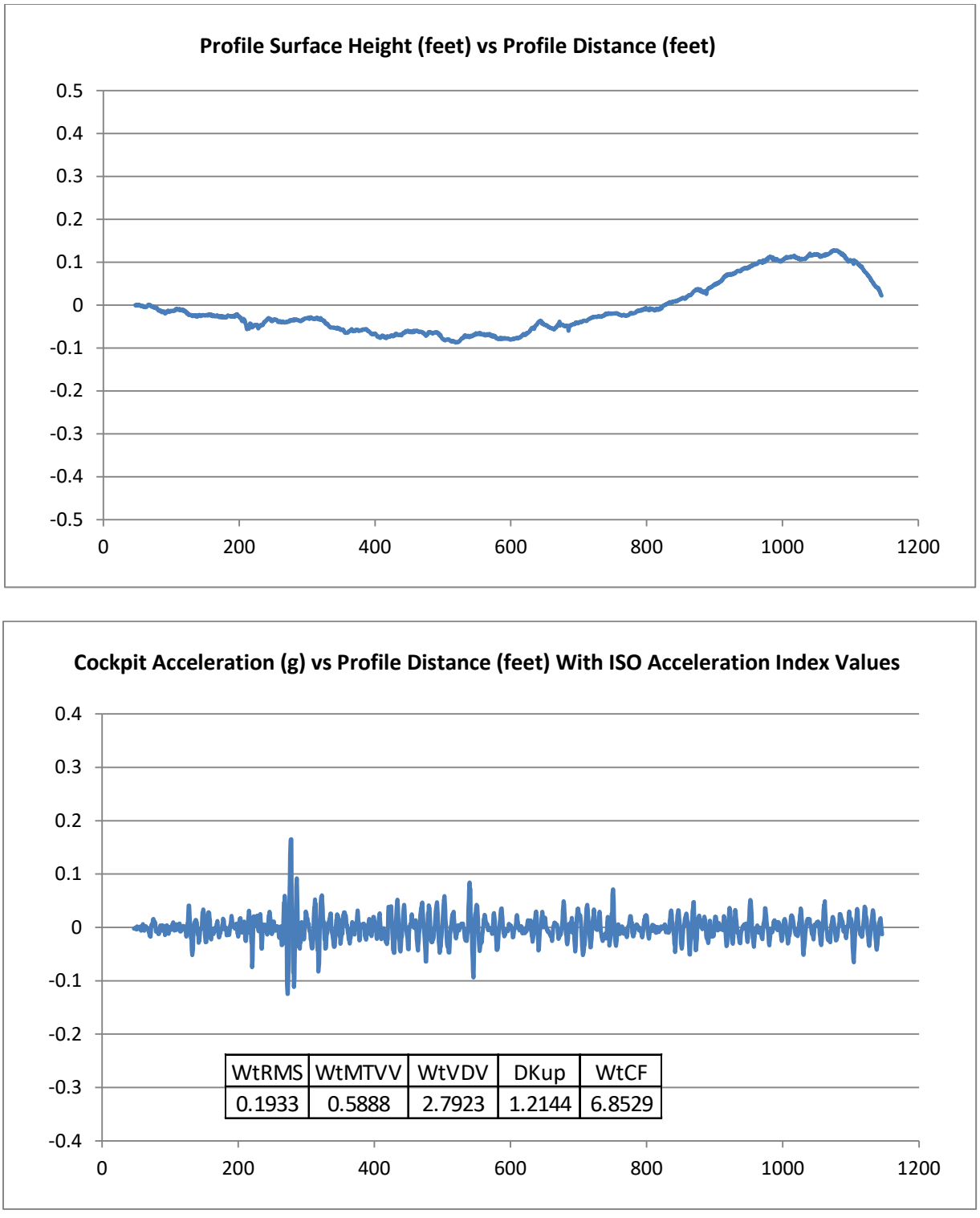

Figure D-5. Taxiway Profile 5—Profile Surface Height, Cockpit Acceleration, and Acceleration ISO Indices

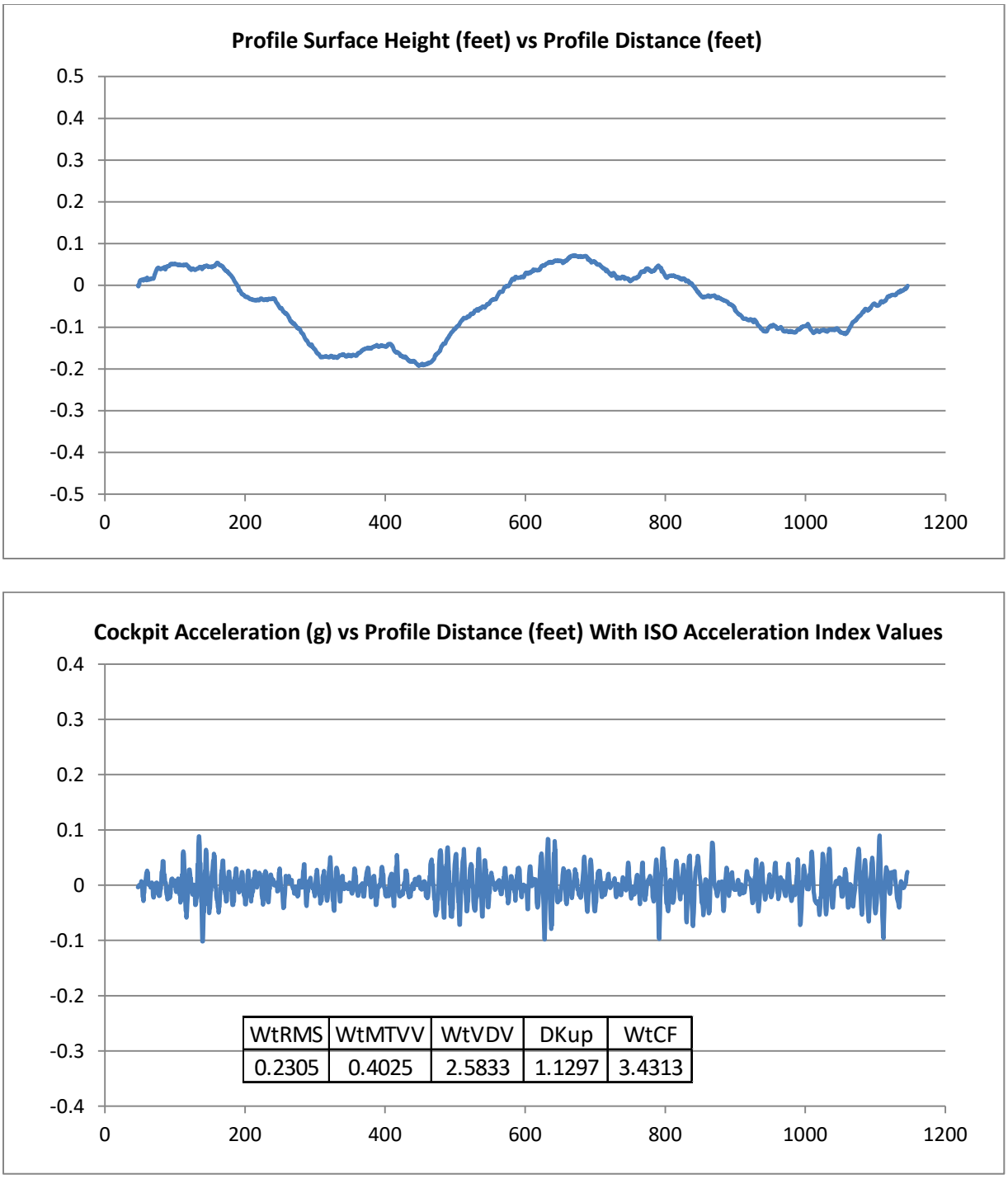

Figure D-6. Taxiway Profile 6—Profile Surface Height, Cockpit Acceleration, and Acceleration ISO Indices

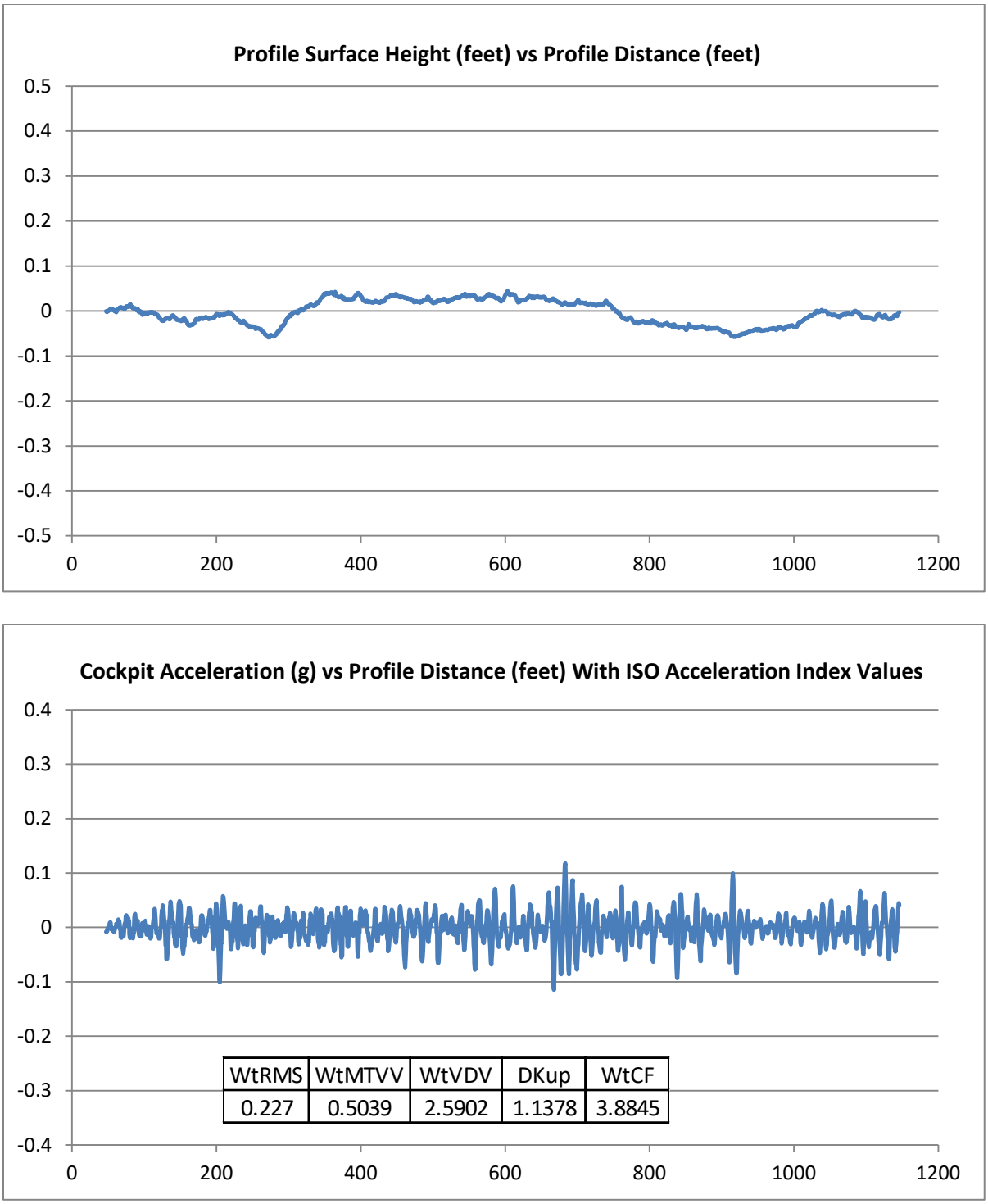

Figure D-7. Taxiway Profile 7—Profile Surface Height, Cockpit Acceleration, and Acceleration ISO Indices

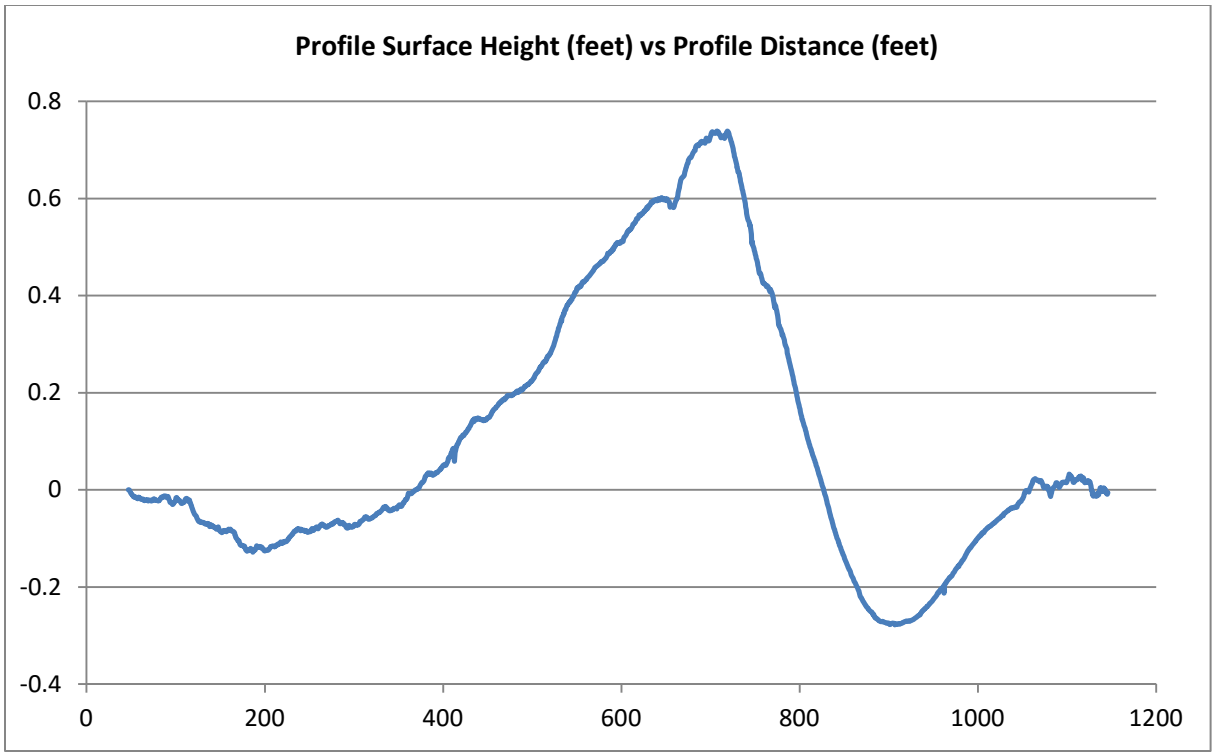

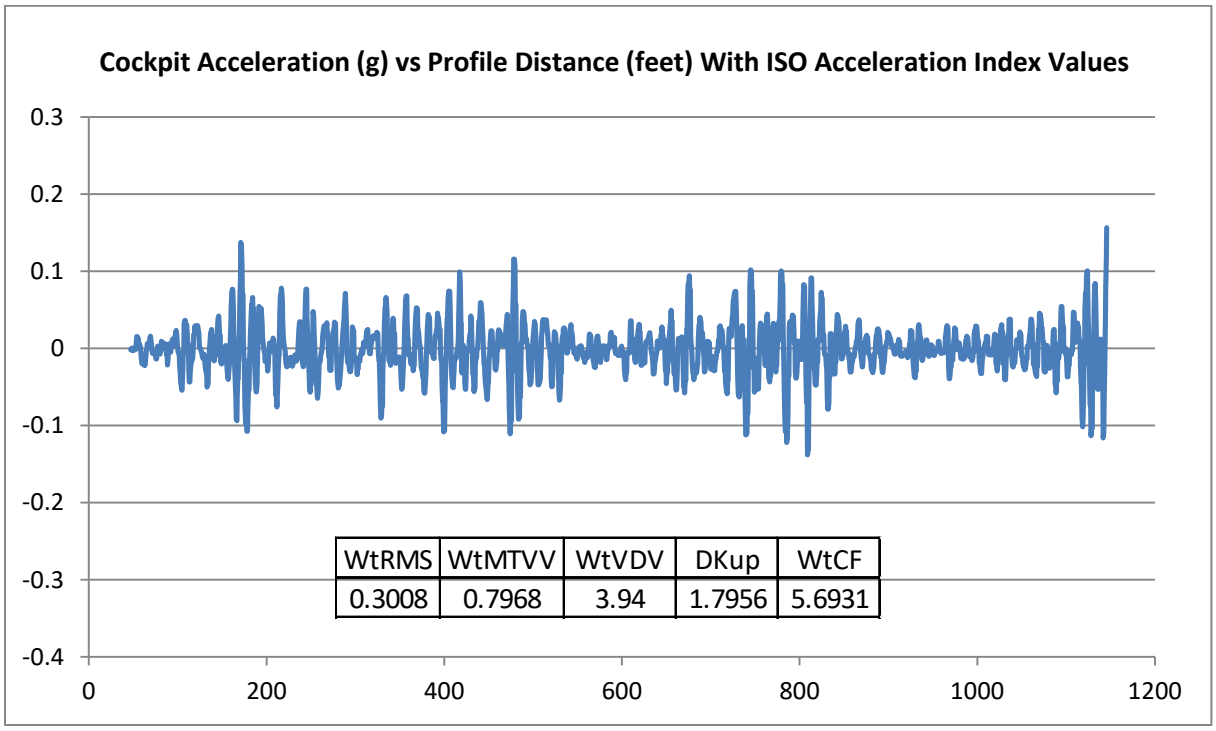

Figure D-8. Taxiway Profile 8—Profile Surface Height, Cockpit Acceleration, and Acceleration ISO Indices

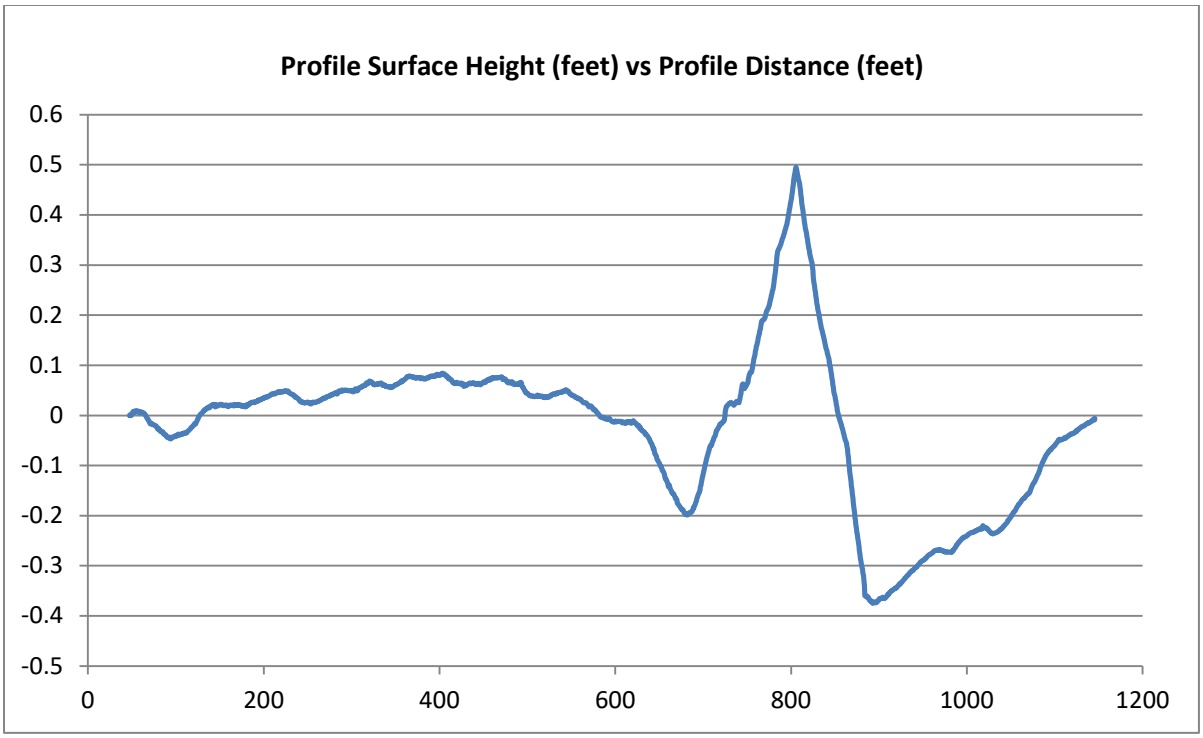

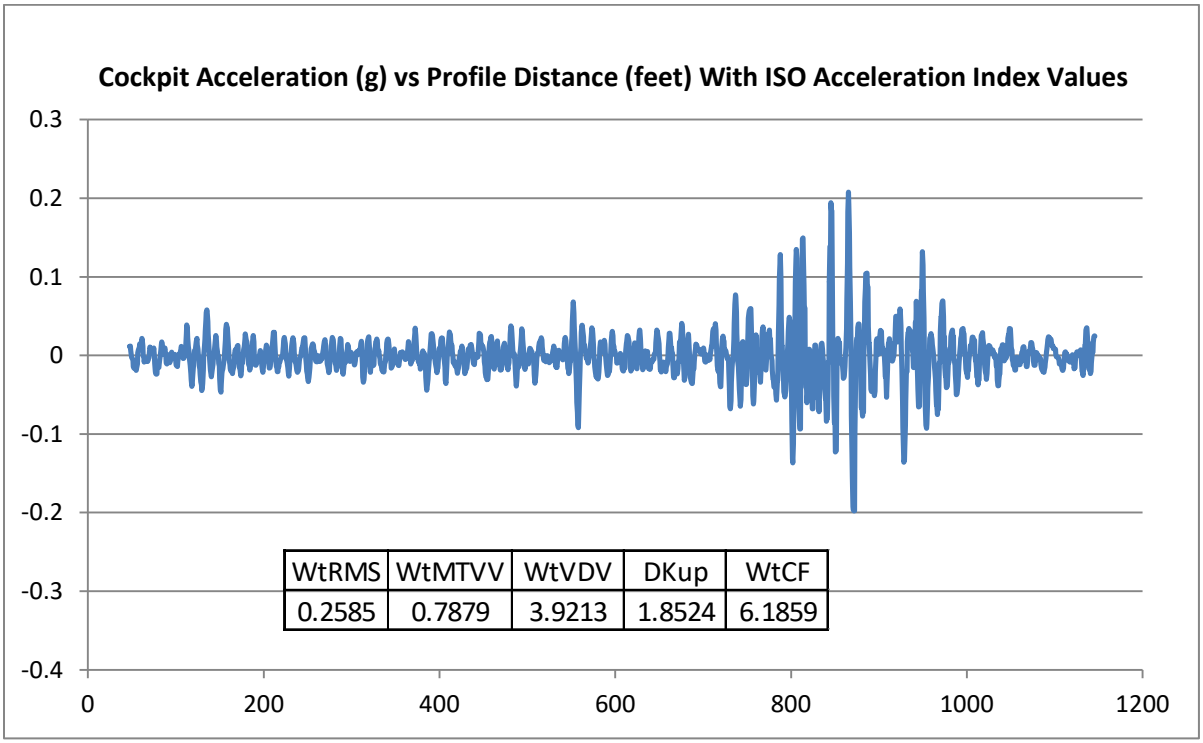

Figure D-9. Taxiway Profile 9—Profile Surface Height, Cockpit Acceleration, and Acceleration ISO Indices

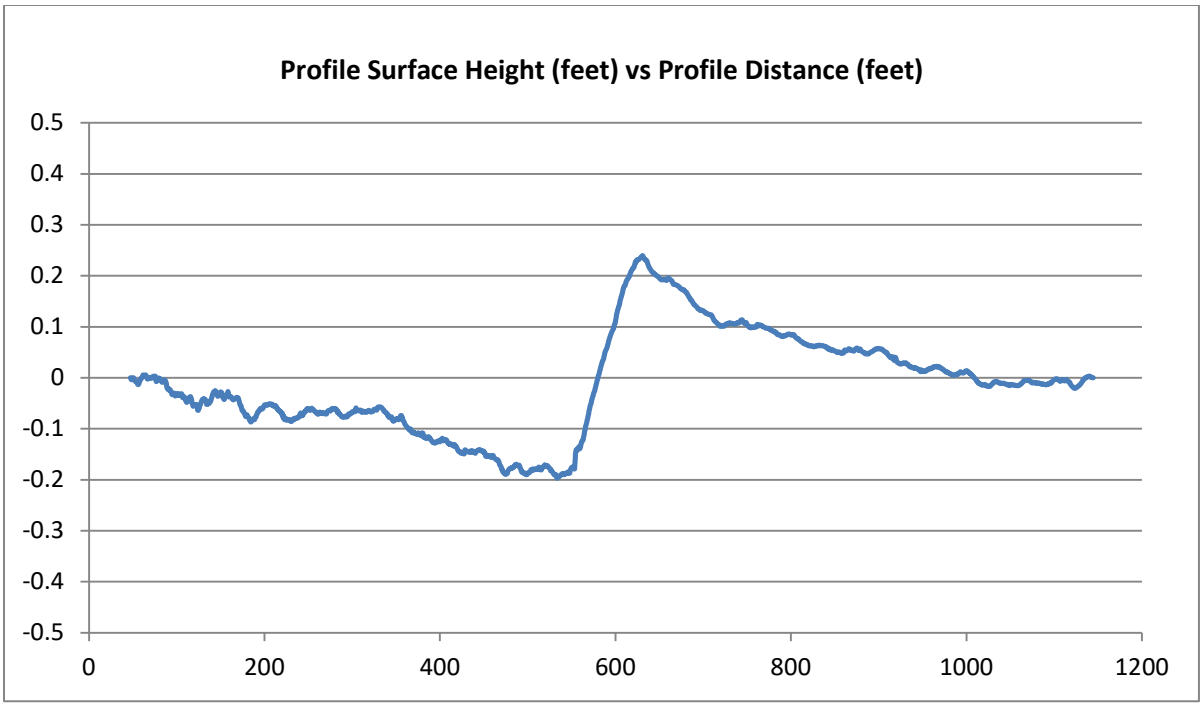

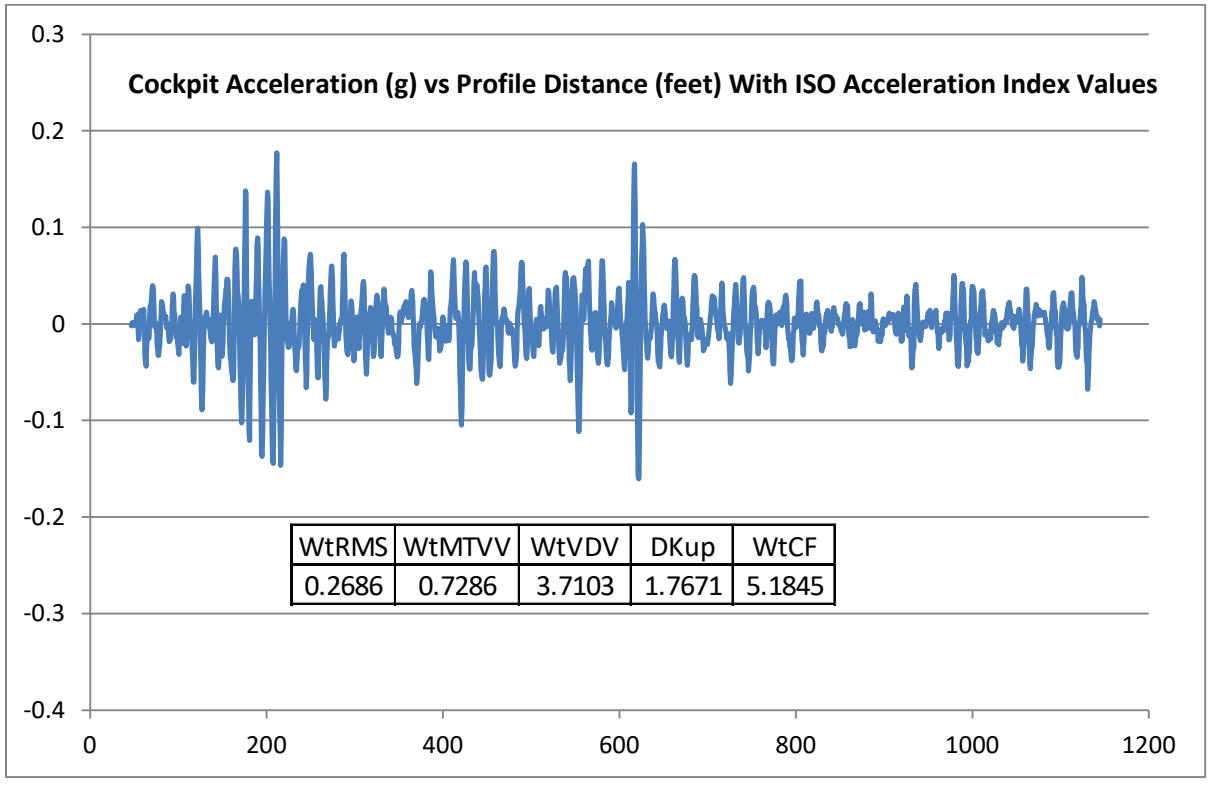

Figure D-10. Taxiway Profile 10—Profile Surface Height, Cockpit Acceleration, and Acceleration ISO Indices

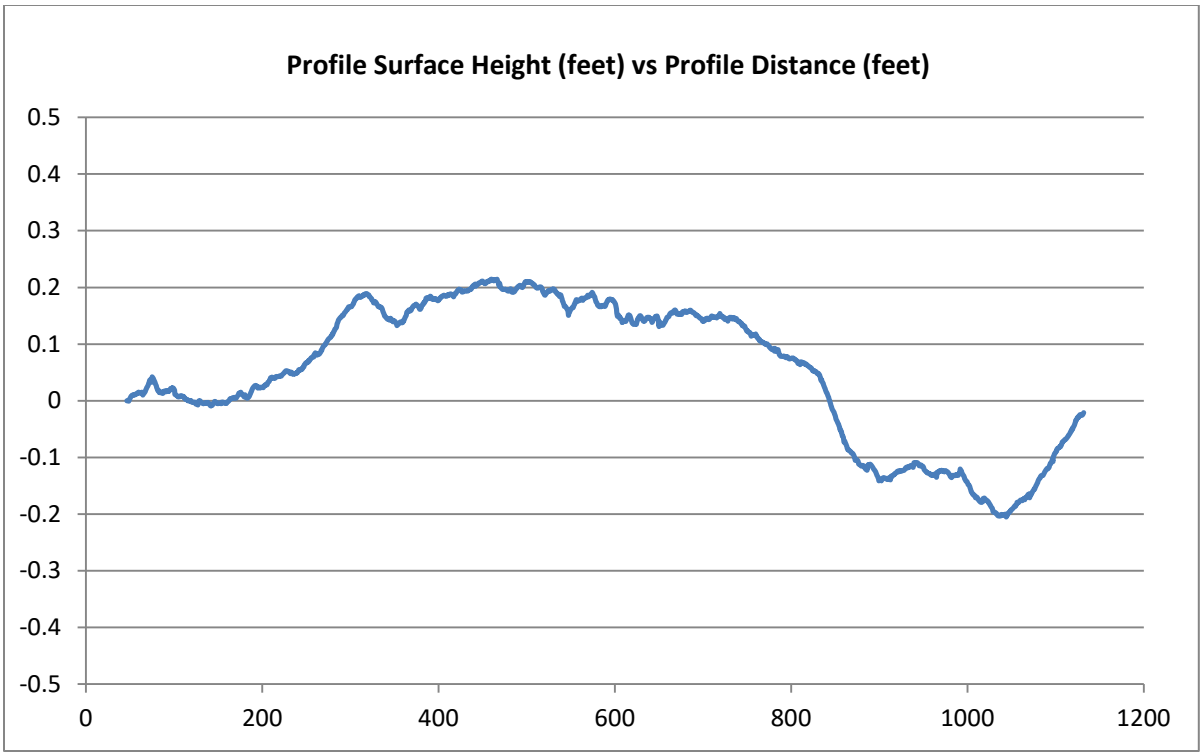

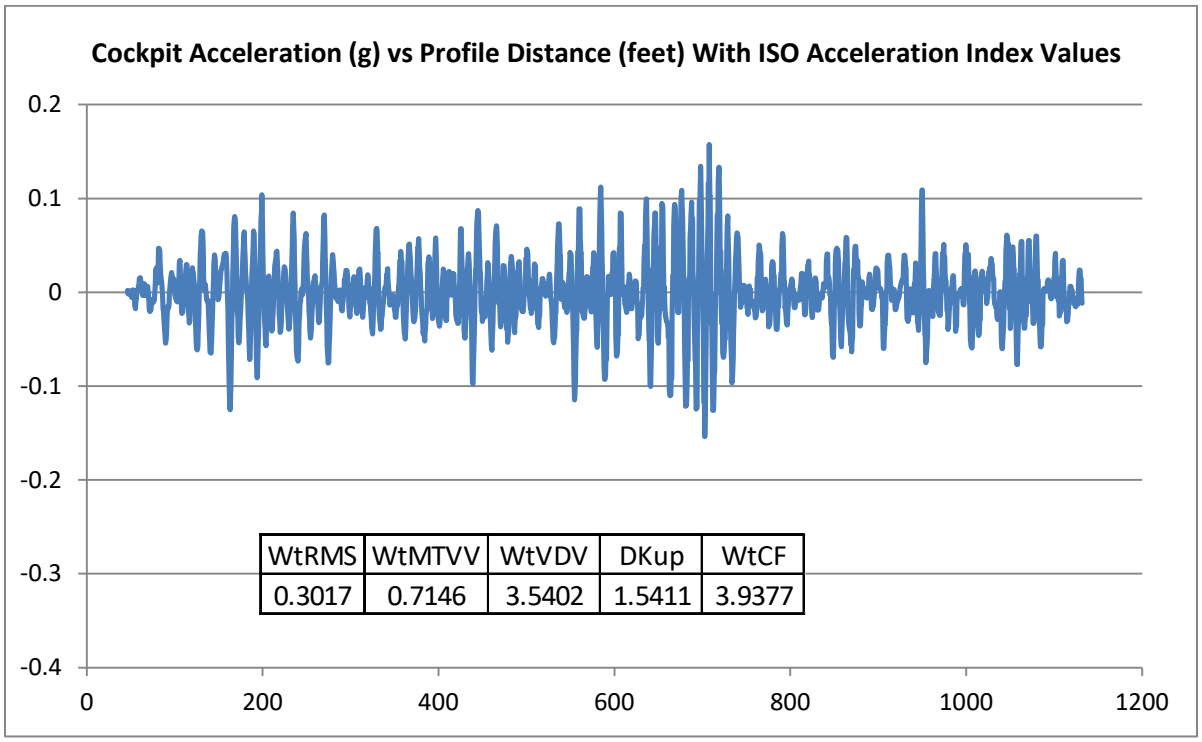

Figure D-11. Taxiway Profile 11—Profile Surface Height, Cockpit Acceleration, and Acceleration ISO Indices

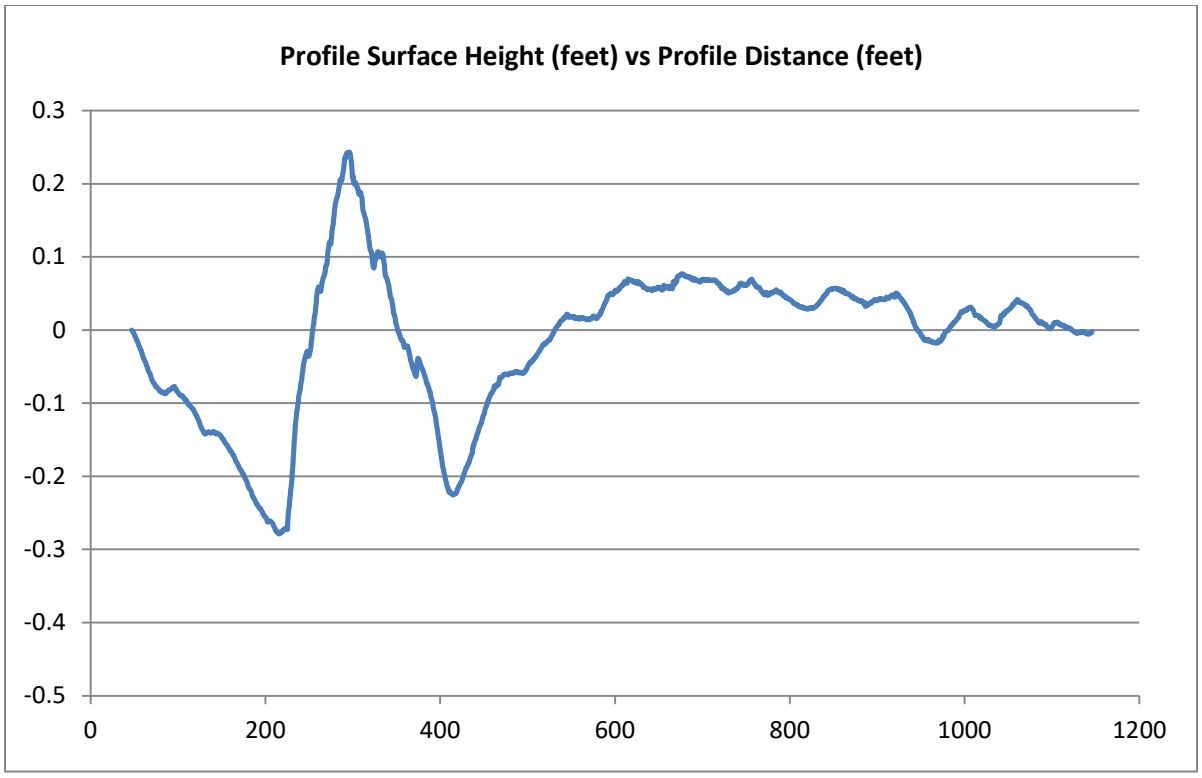

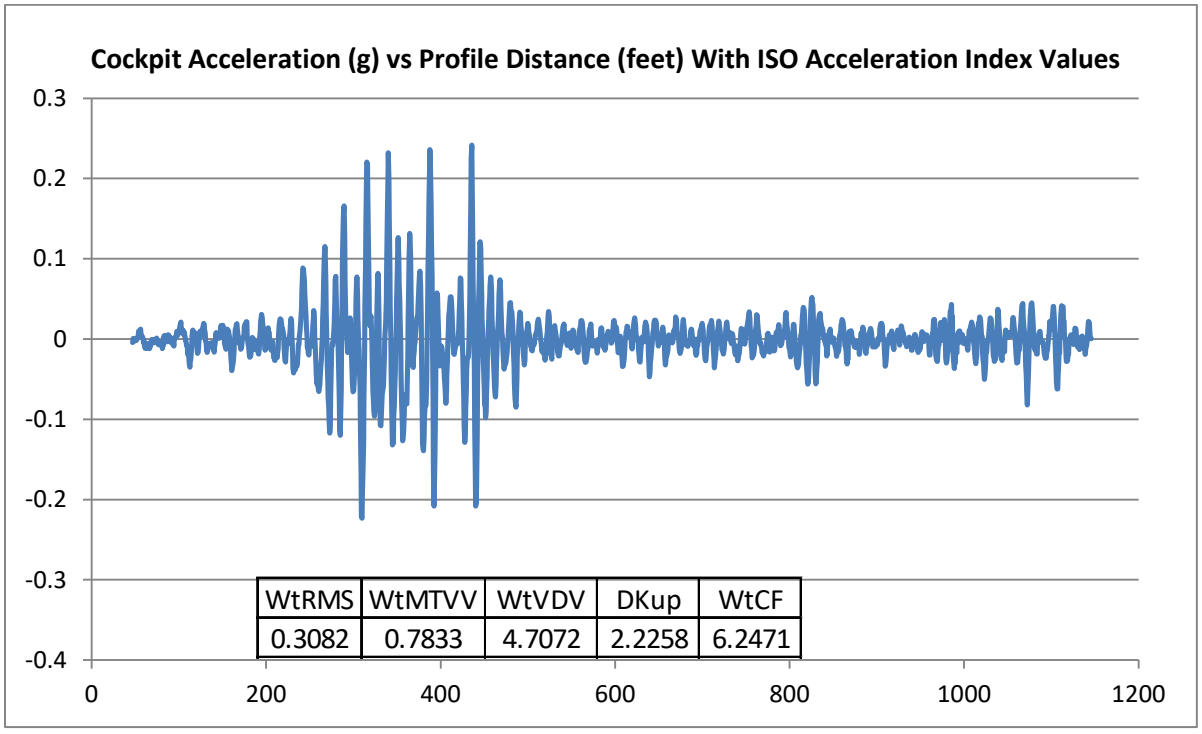

Figure D-12. Taxiway Profile 12—Profile Surface Height, Cockpit Acceleration, and Acceleration ISO Indices

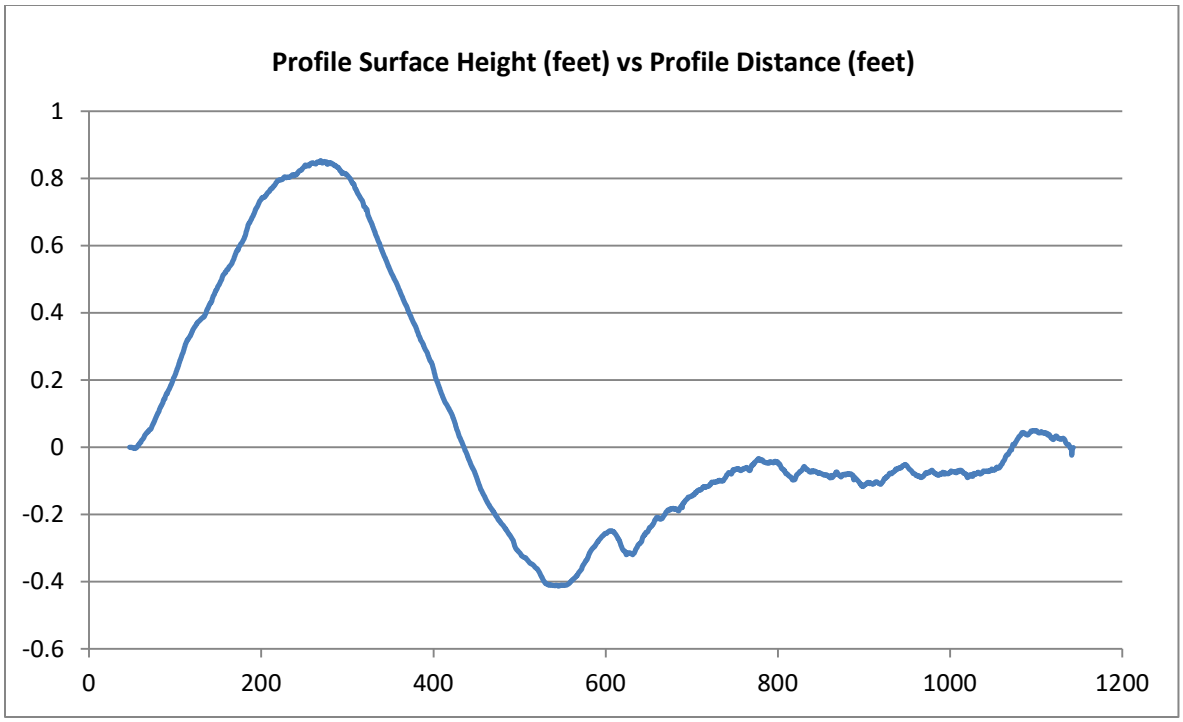

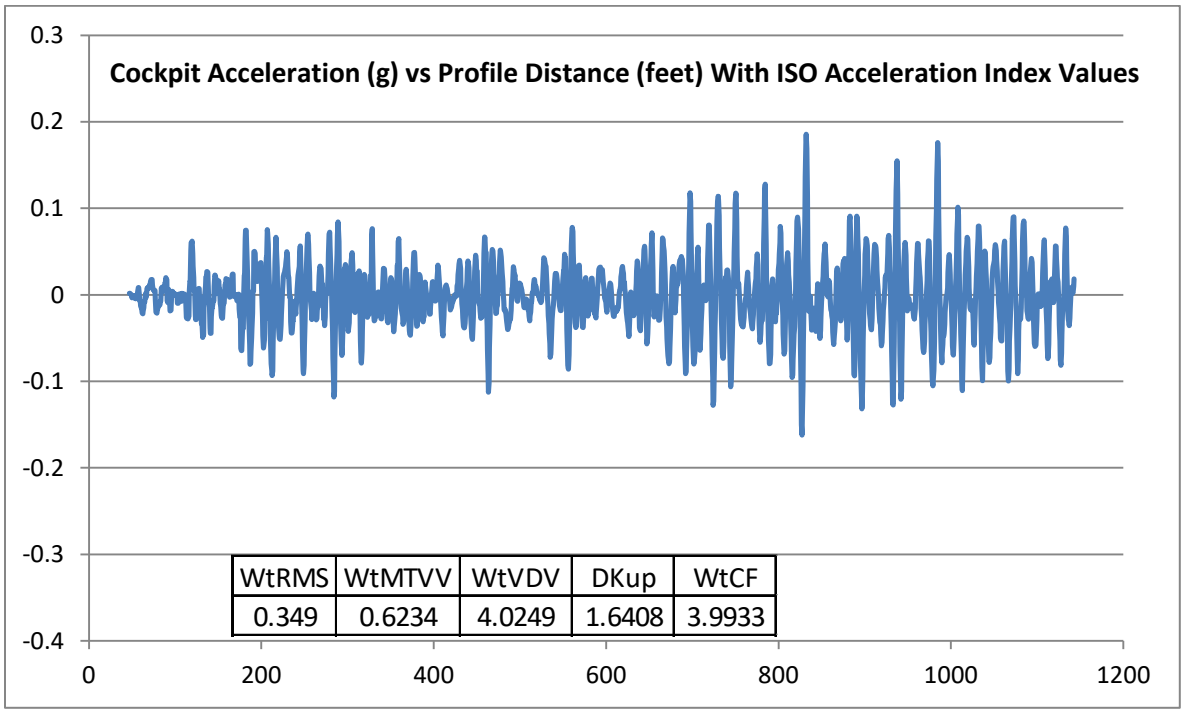

Figure D-13. Taxiway Profile 13—Profile Surface Height, Cockpit Acceleration, and Acceleration ISO Indices

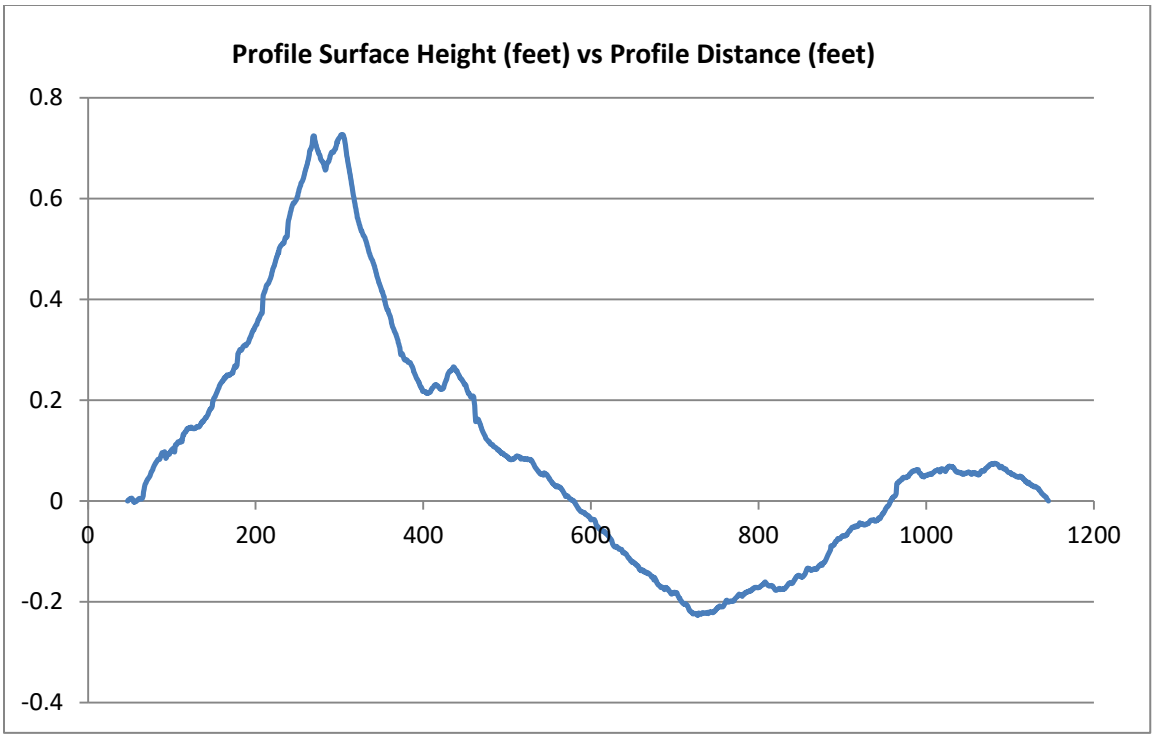

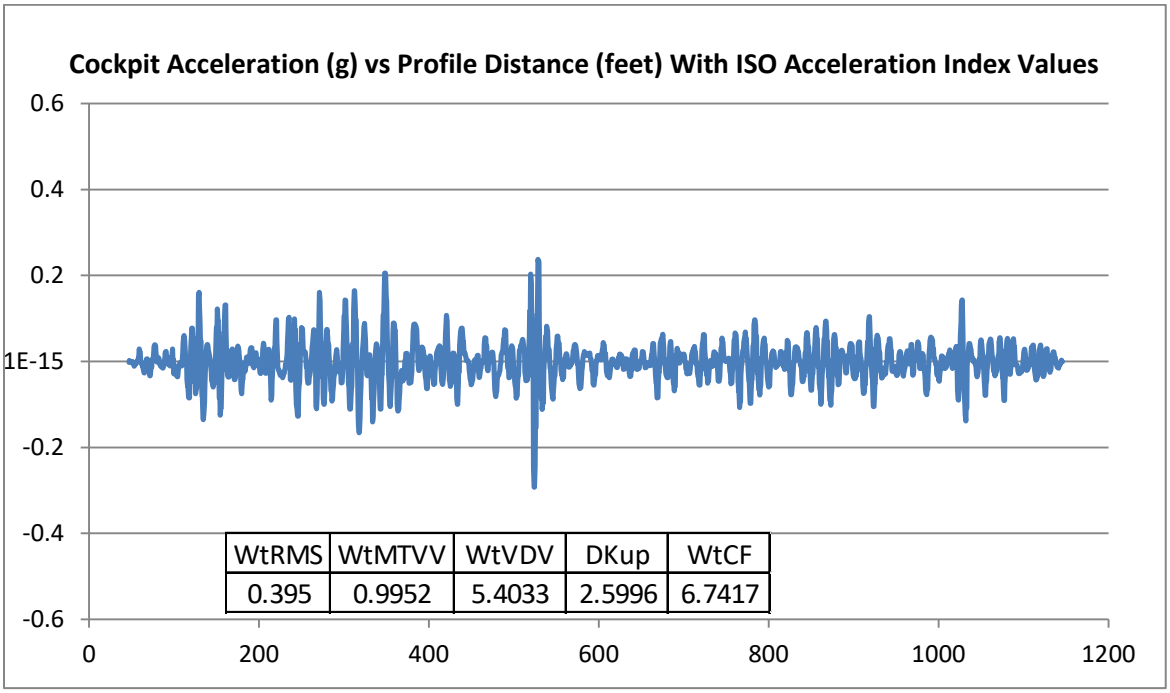

Figure D-14. Taxiway Profile 14—Profile Surface Height, Cockpit Acceleration, and Acceleration ISO Indices

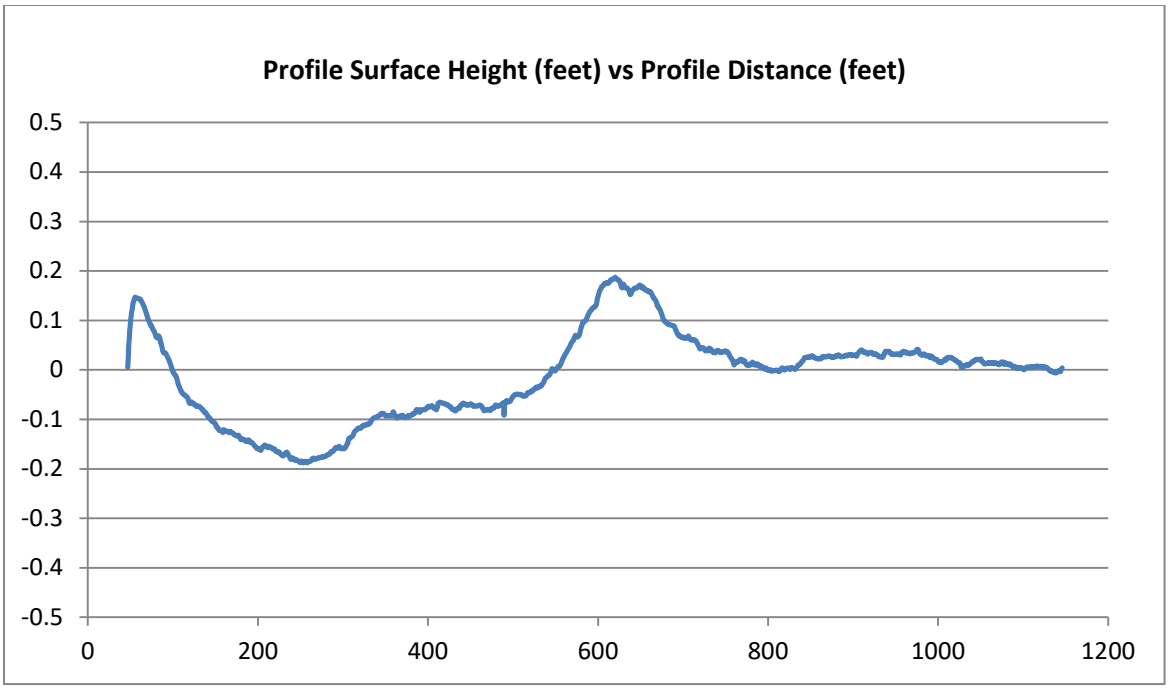

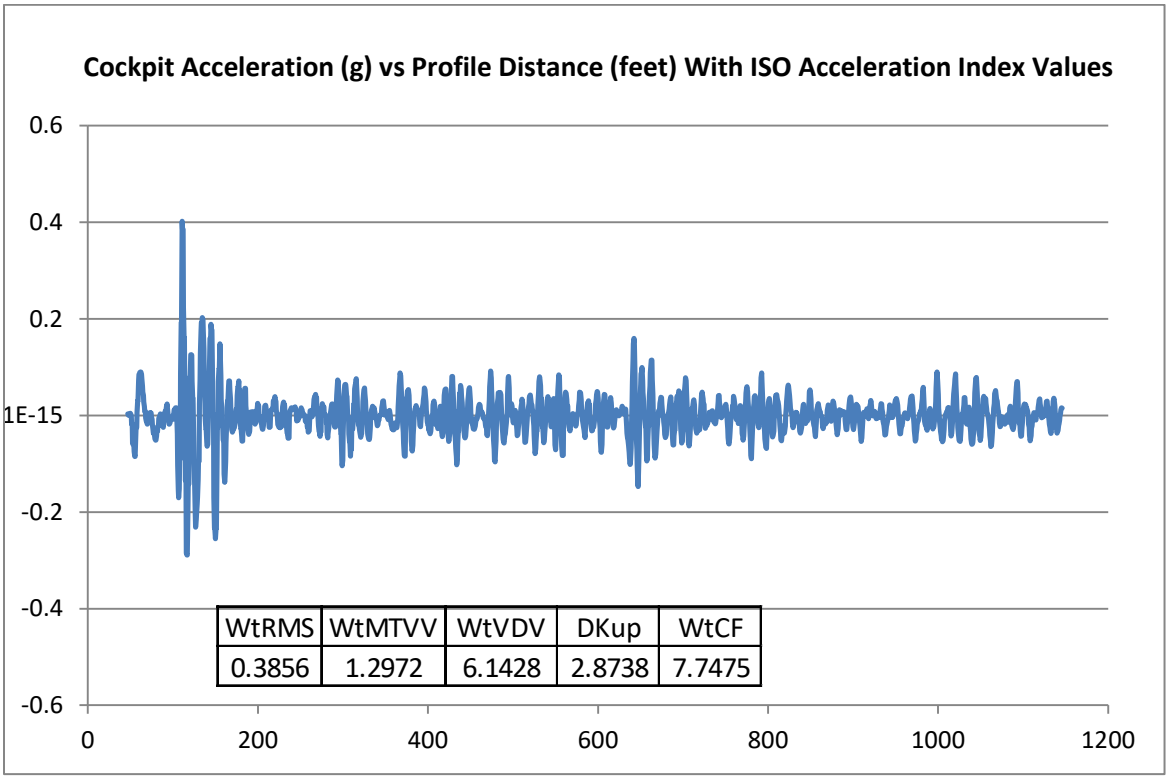

Figure D-15. Taxiway Profile 15—Profile Surface Height, Cockpit Acceleration, and Acceleration ISO Indices

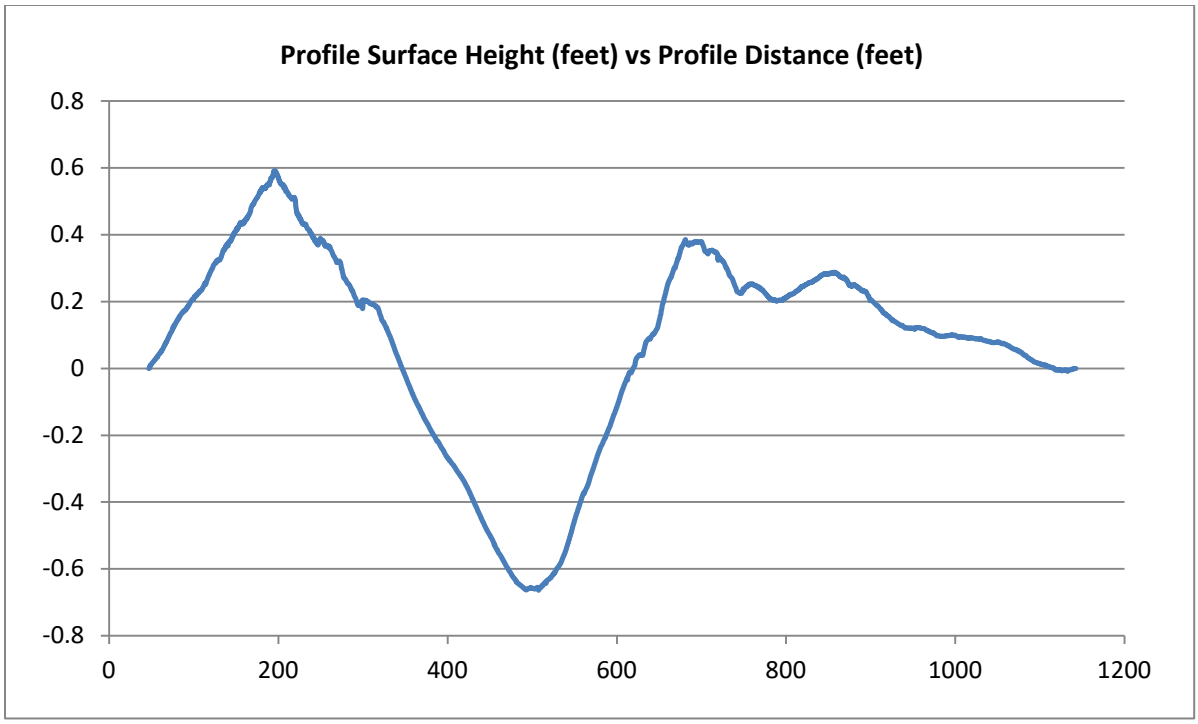

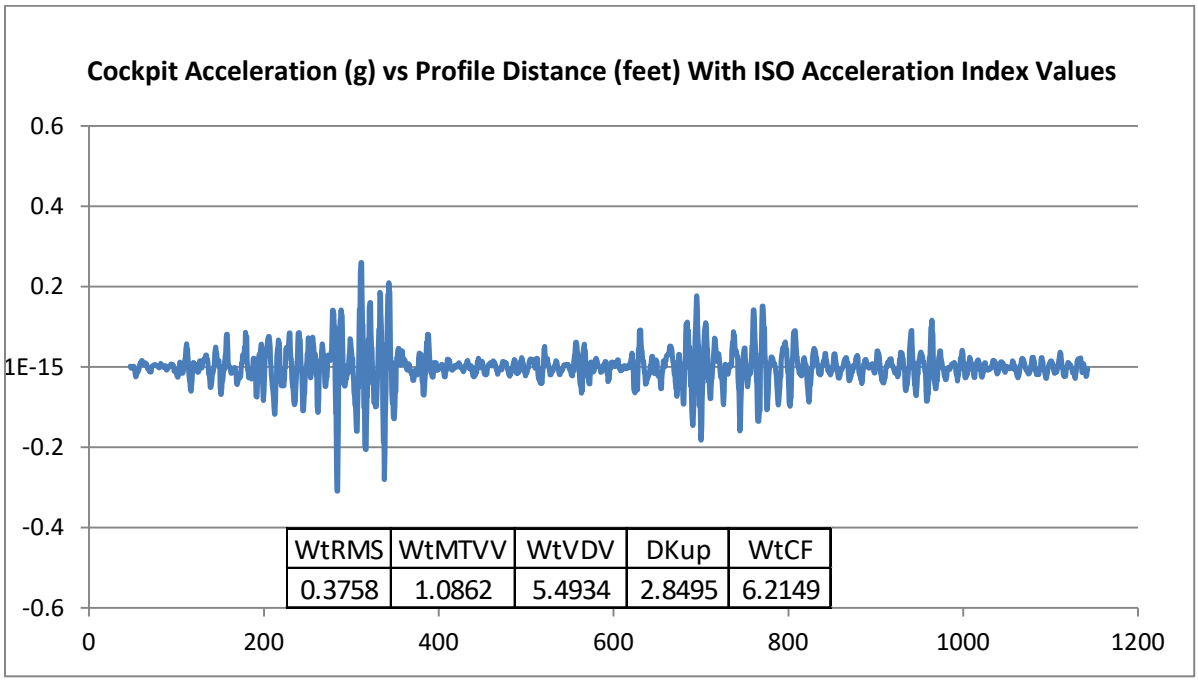

Figure D-16. Taxiway Profile 16—Profile Surface Height, Cockpit Acceleration, and Acceleration ISO Indices

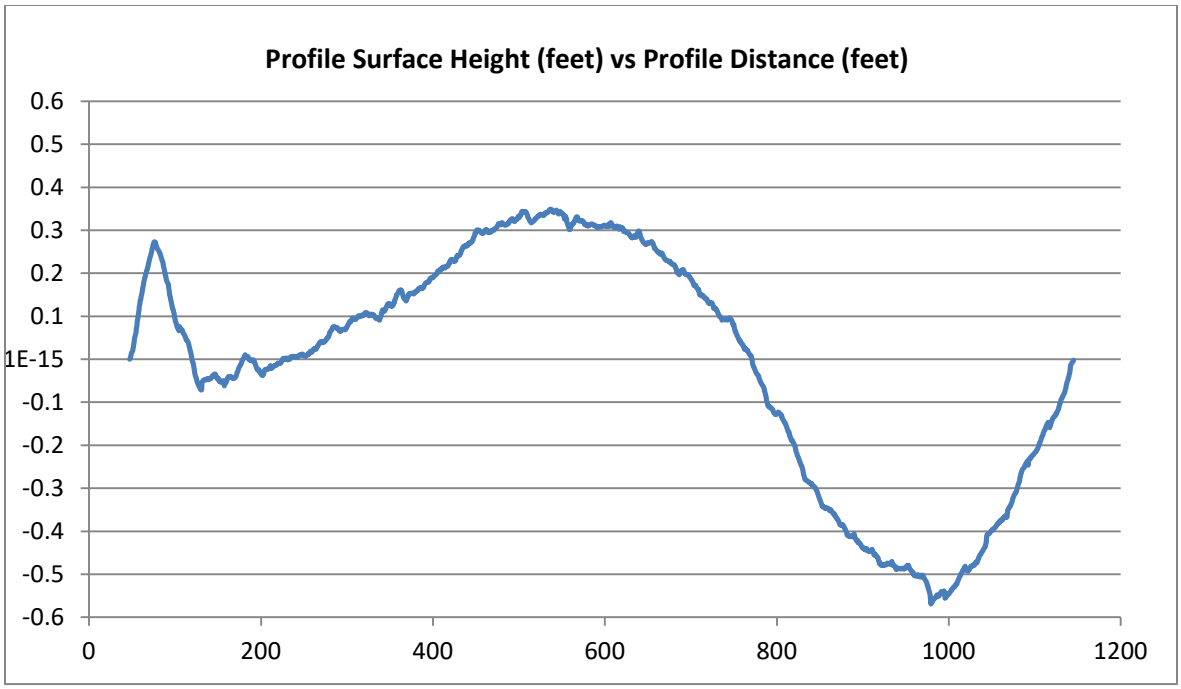

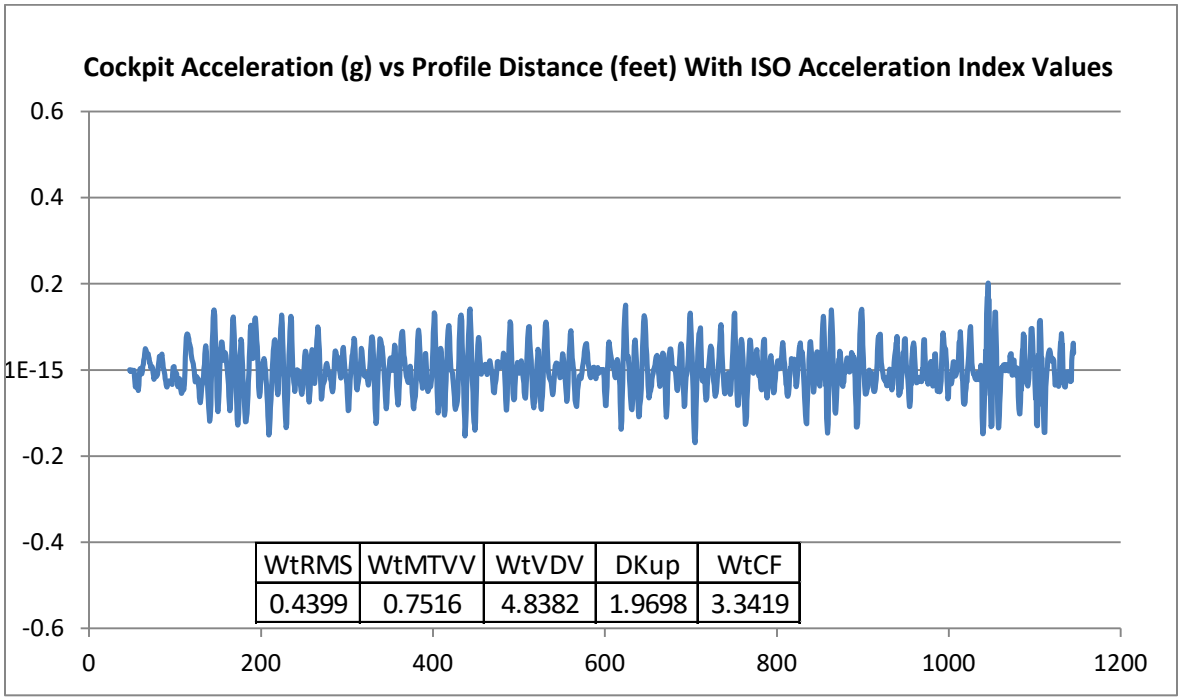

Figure D-17. Taxiway Profile 17—Profile Surface Height, Cockpit Acceleration, and Acceleration ISO Indices

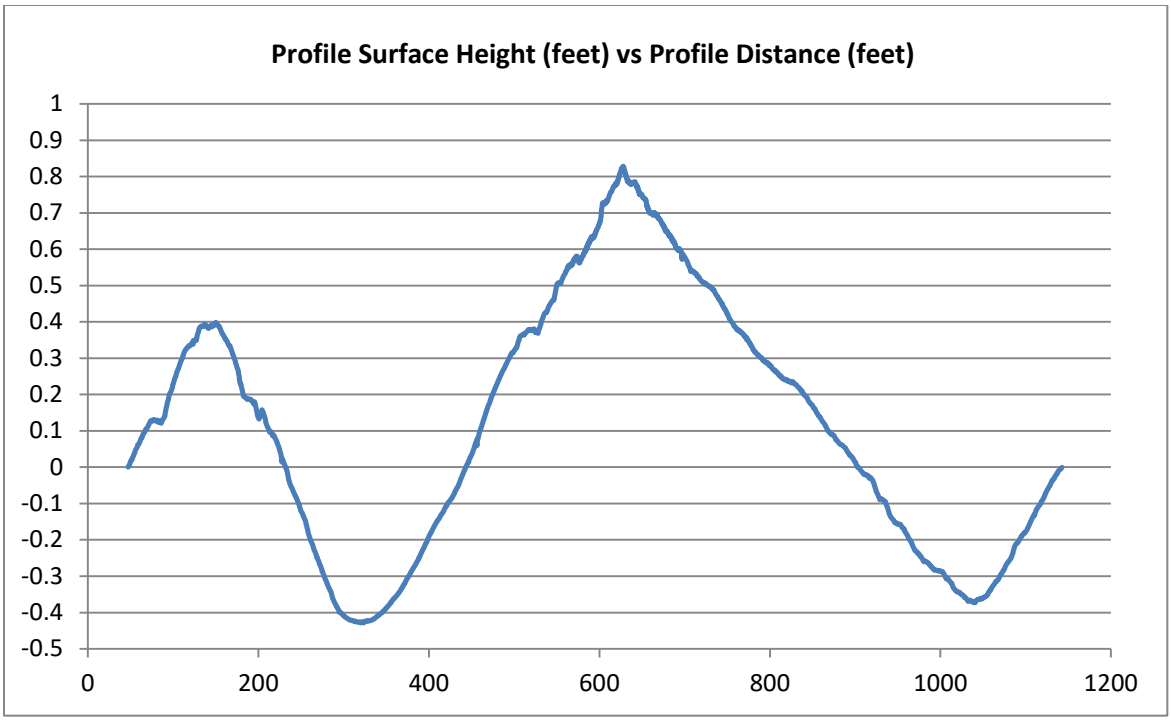

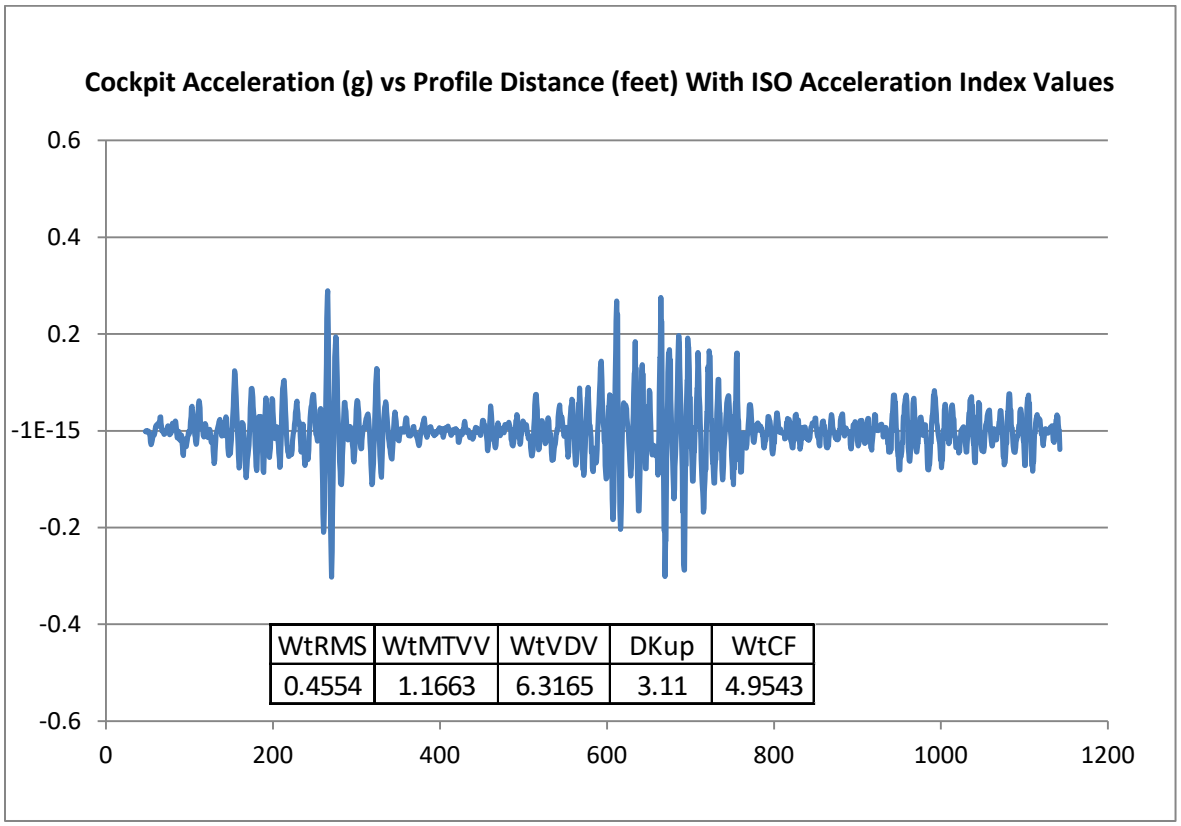

Figure D-18. Taxiway Profile 18—Profile Surface Height, Cockpit Acceleration, and Acceleration ISO Indices

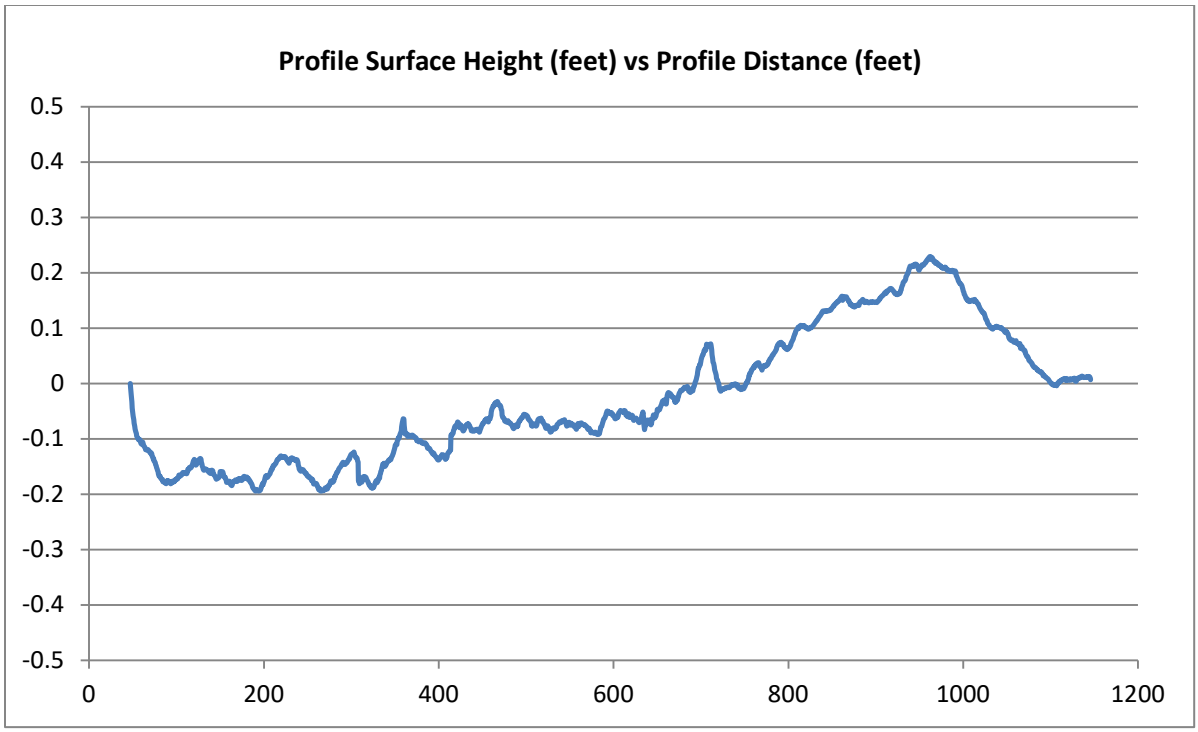

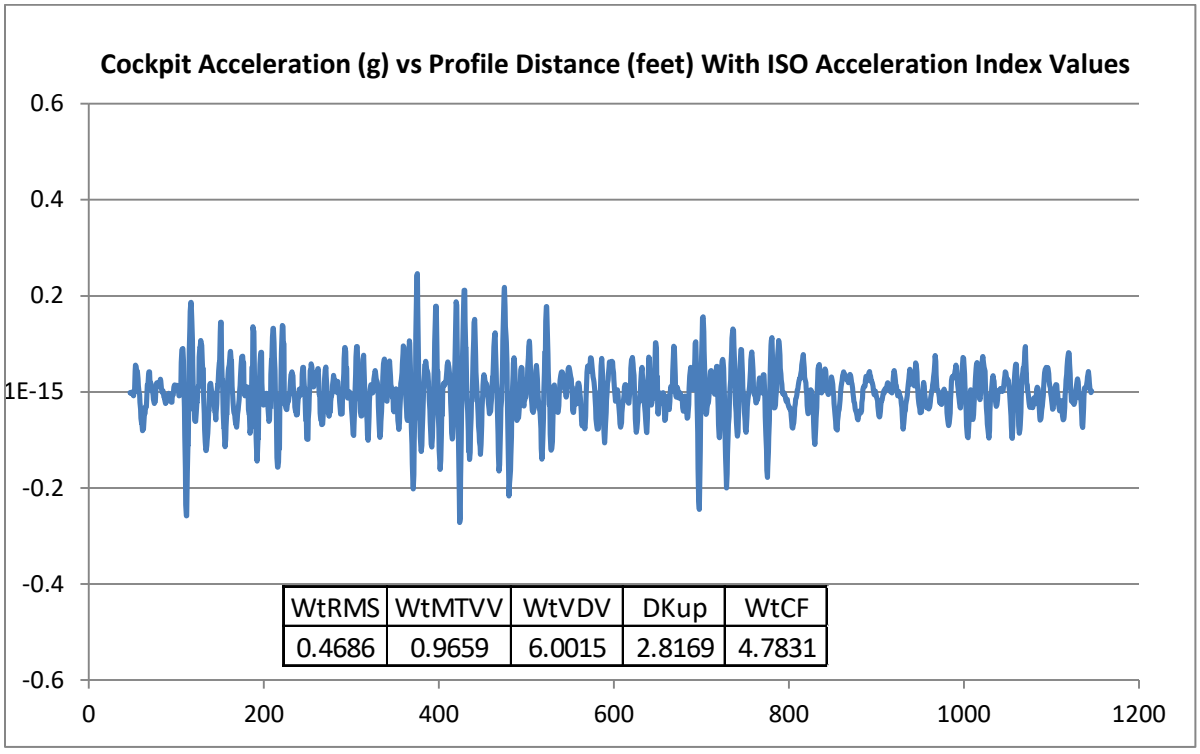

Figure D-19. Taxiway Profile 19—Profile Surface Height, Cockpit Acceleration, and Acceleration ISO Indices

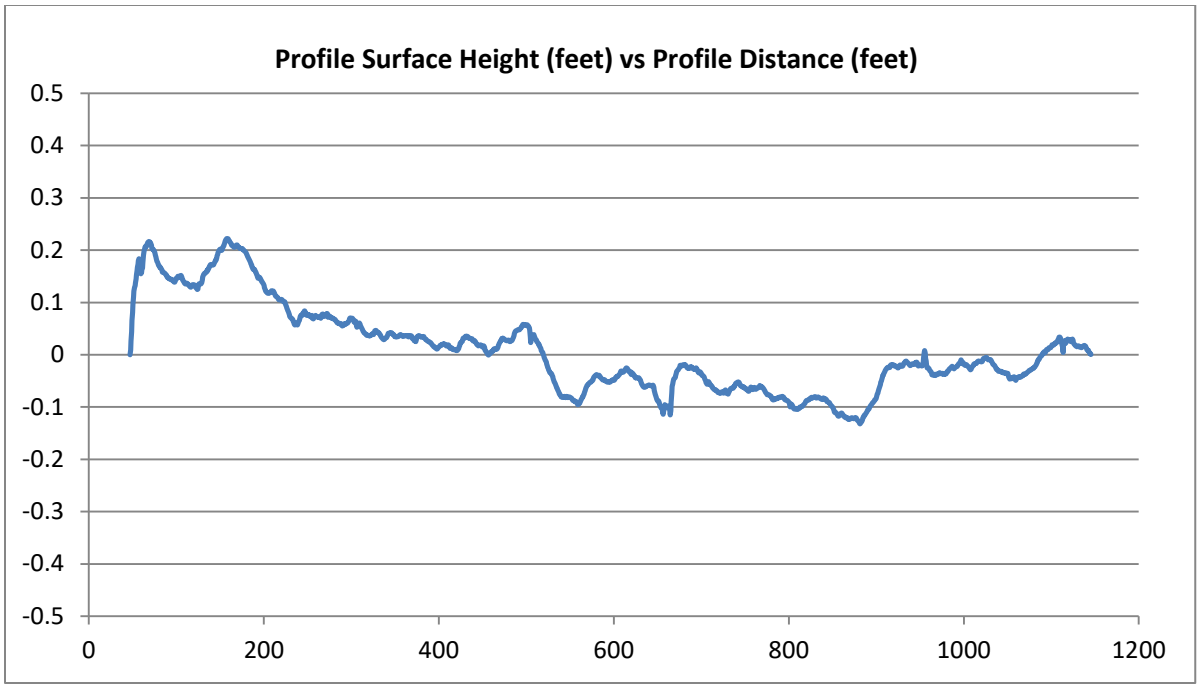

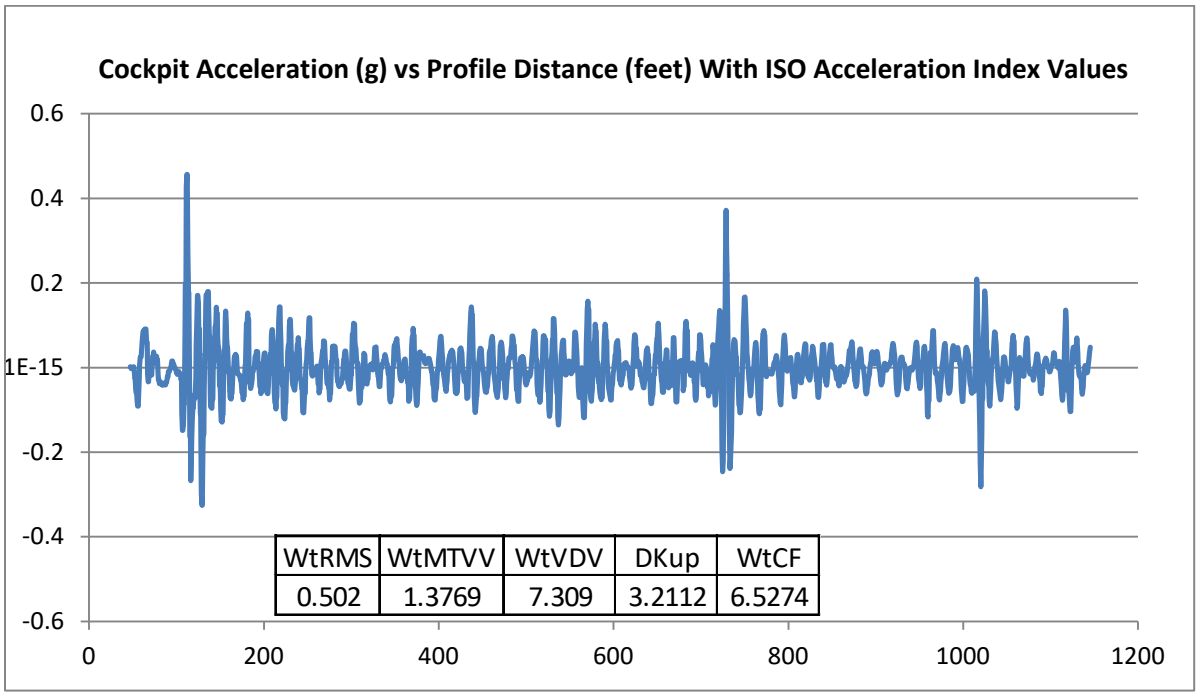

Figure D-20. Taxiway Profile 20—Profile Surface Height, Cockpit Acceleration, and Acceleration ISO Indices

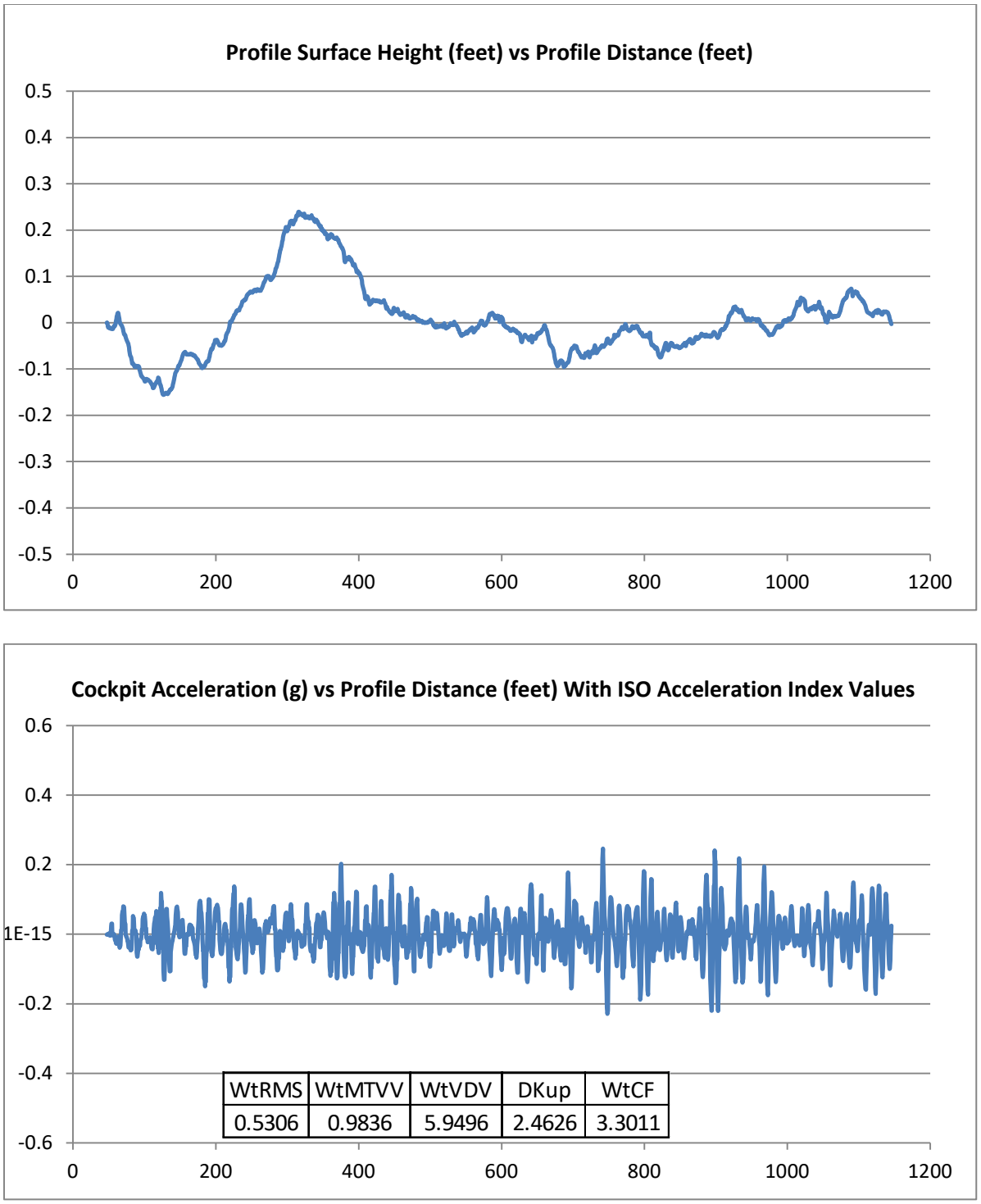

Figure D-21. Taxiway Profile 21—Profile Surface Height, Cockpit Acceleration, and Acceleration ISO Indices

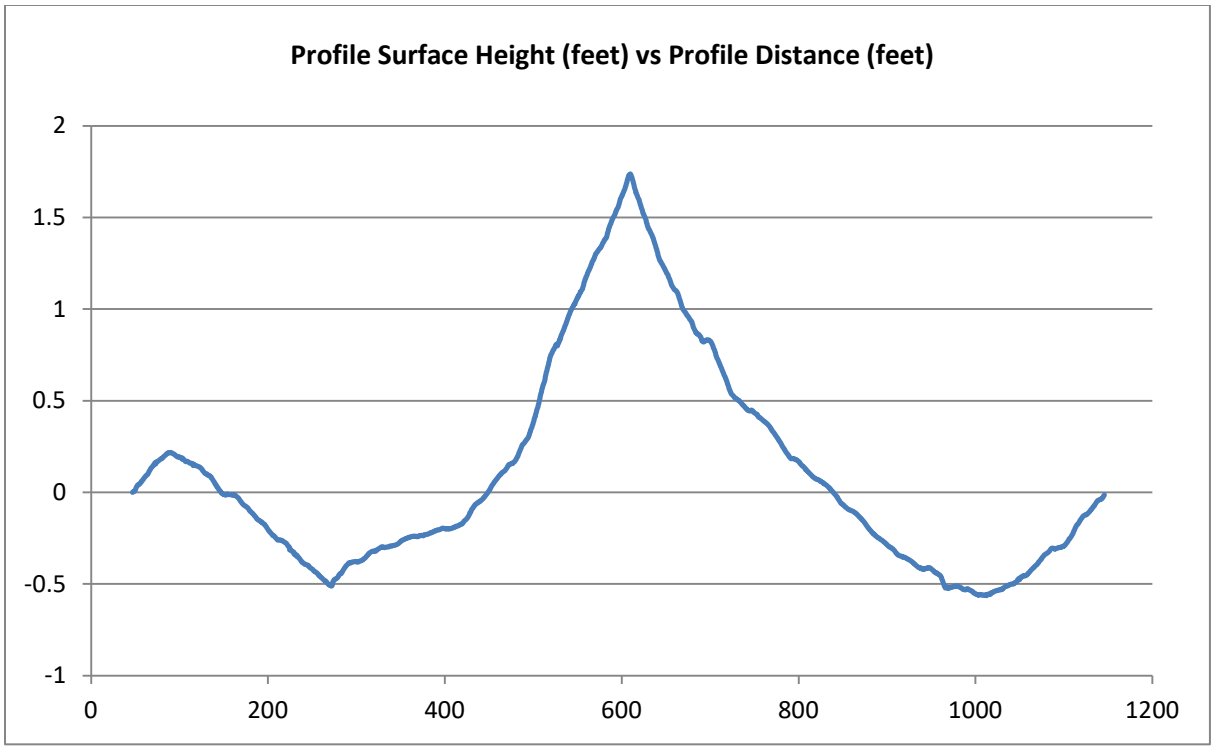

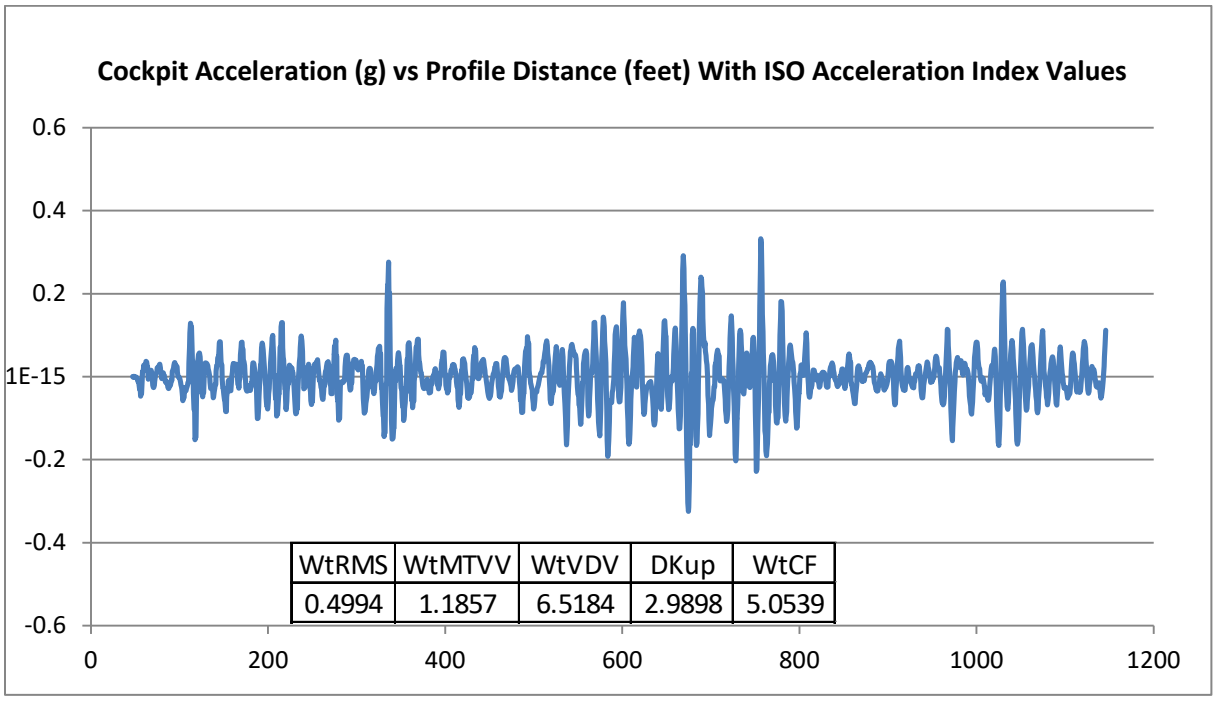

Figure D-22. Taxiway Profile 22—Profile Surface Height, Cockpit Acceleration, and Acceleration ISO Indices

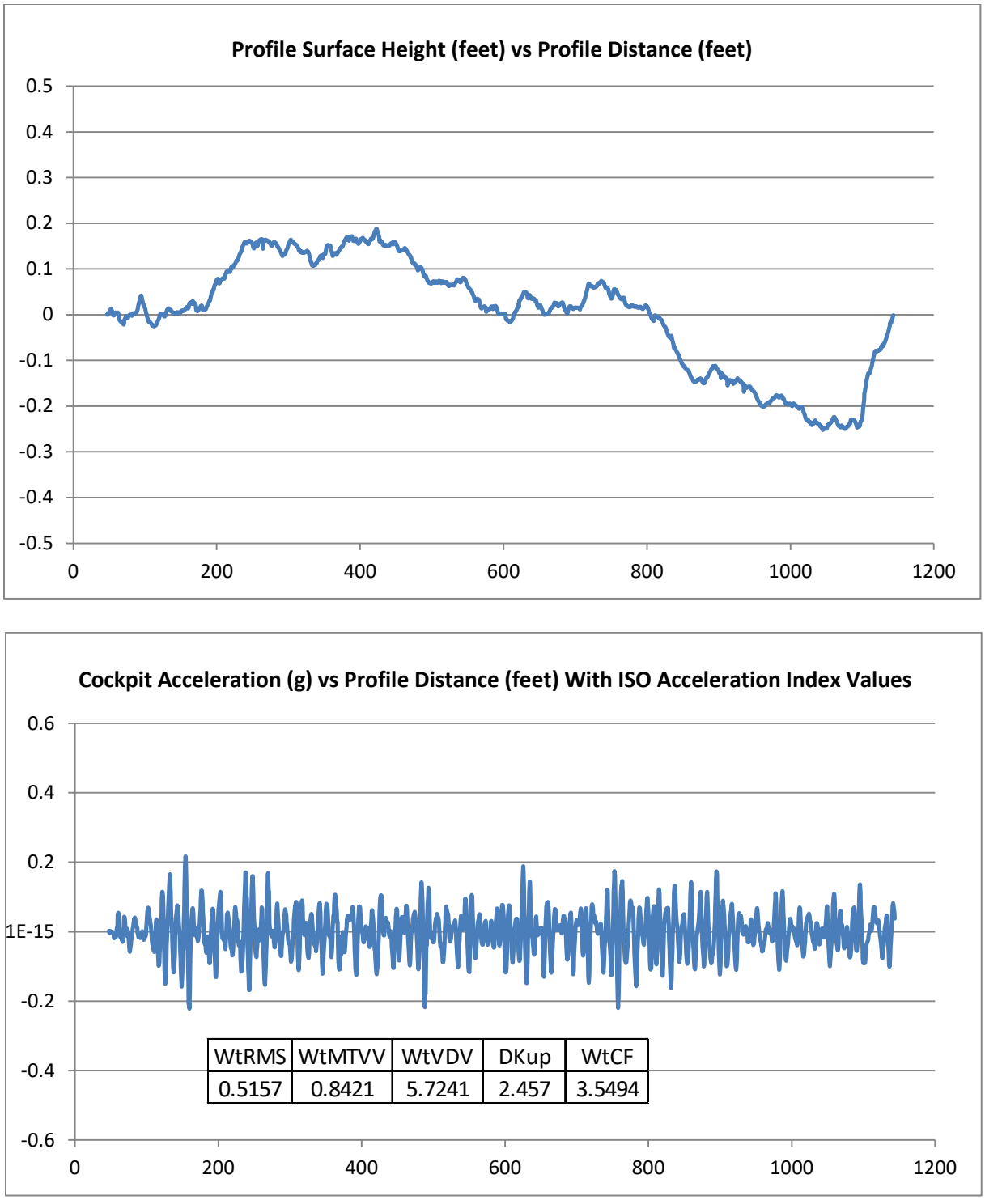

Figure D-23. Taxiway Profile 23—Profile Surface Height, Cockpit Acceleration, and Acceleration ISO Indices

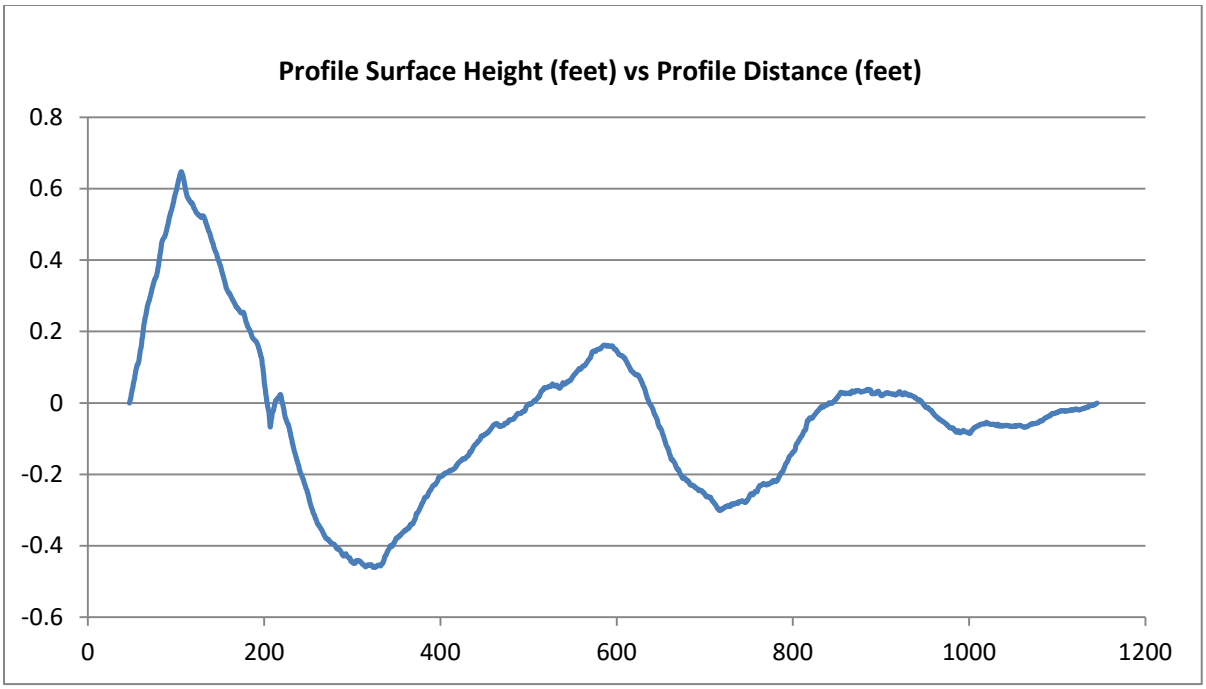

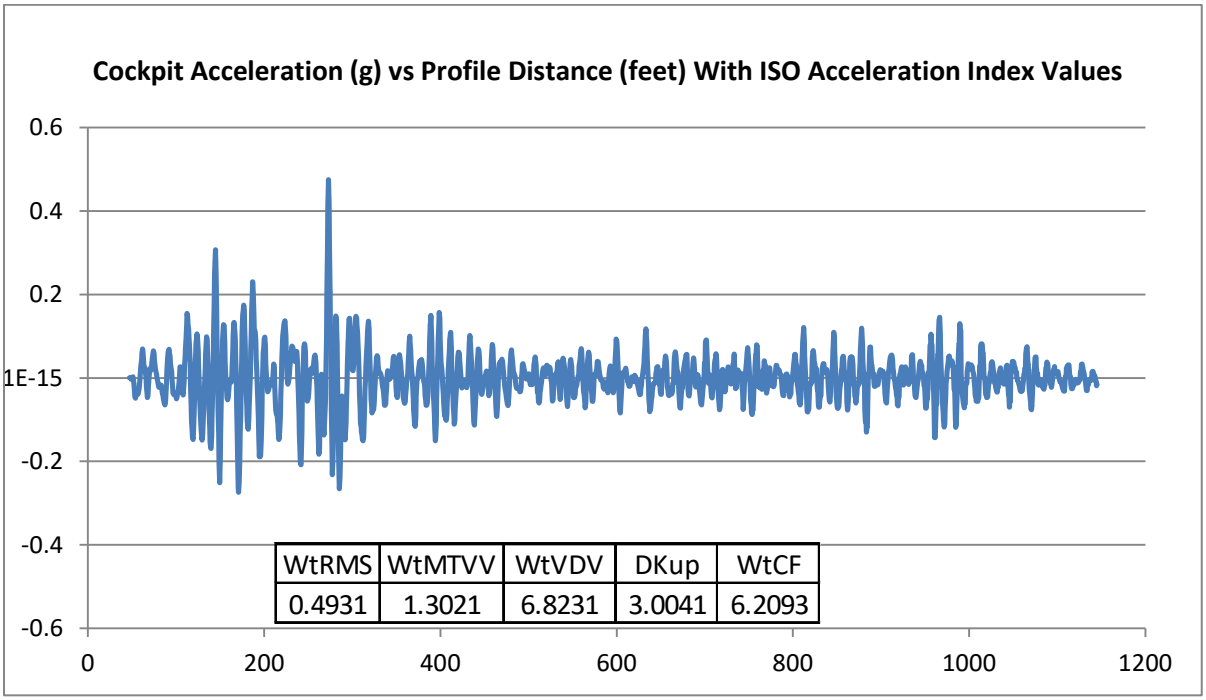

Figure D-24. Taxiway Profile 24—Profile Surface Height, Cockpit Acceleration, and Acceleration ISO Indices

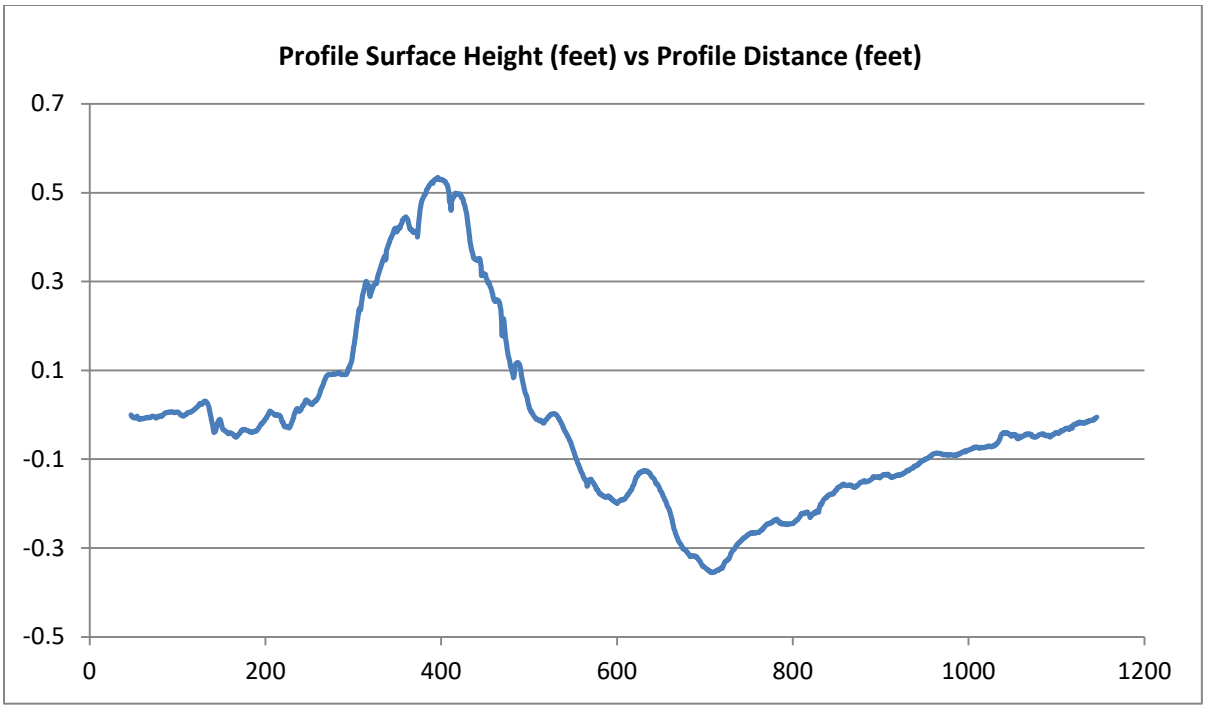

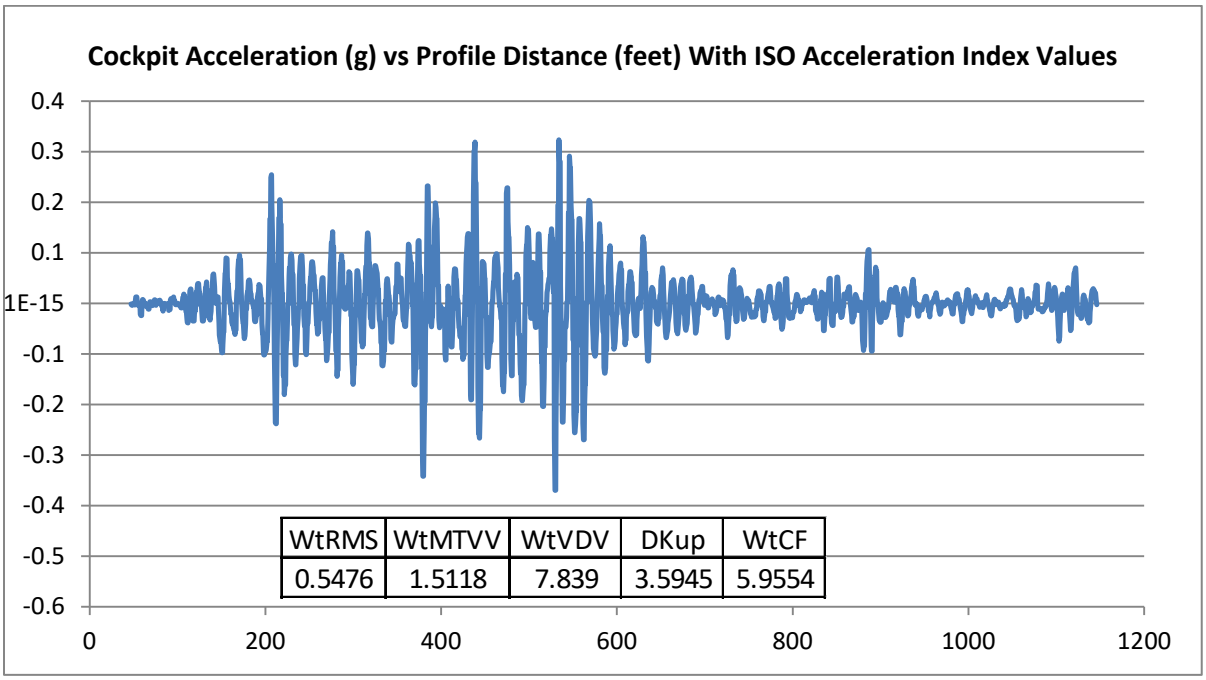

Figure D-25. Taxiway Profile 25—Profile Surface Height, Cockpit Acceleration, and Acceleration ISO Indices

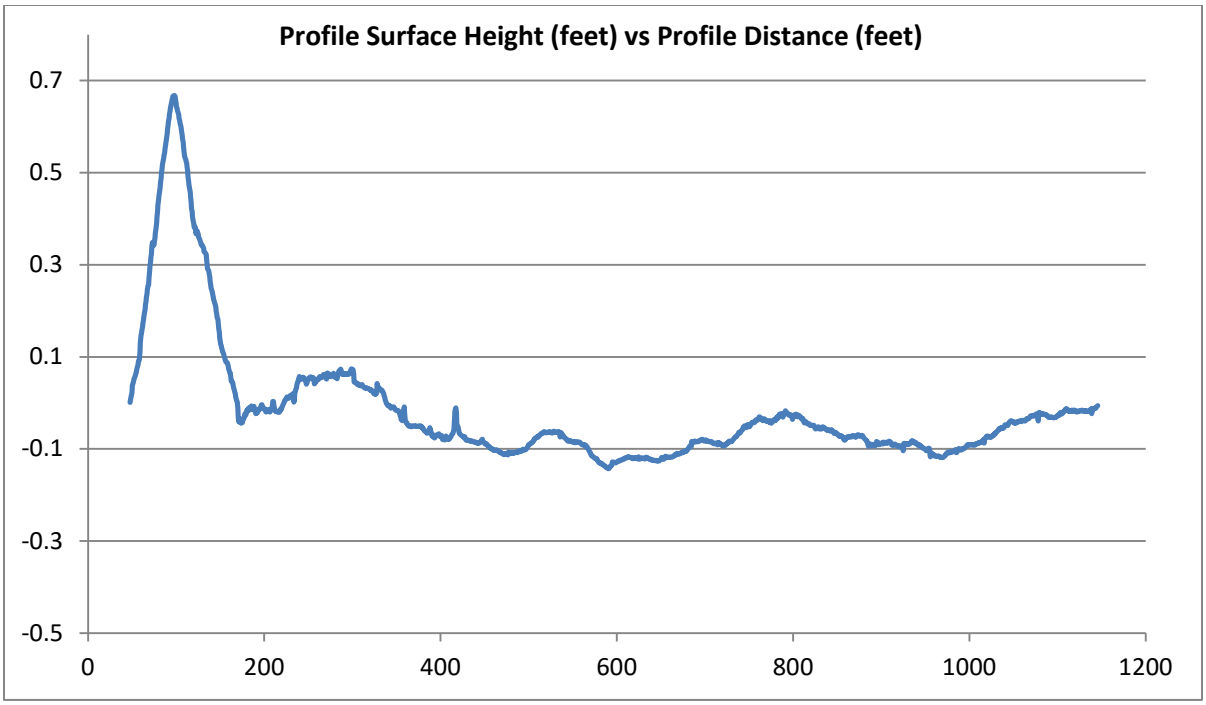

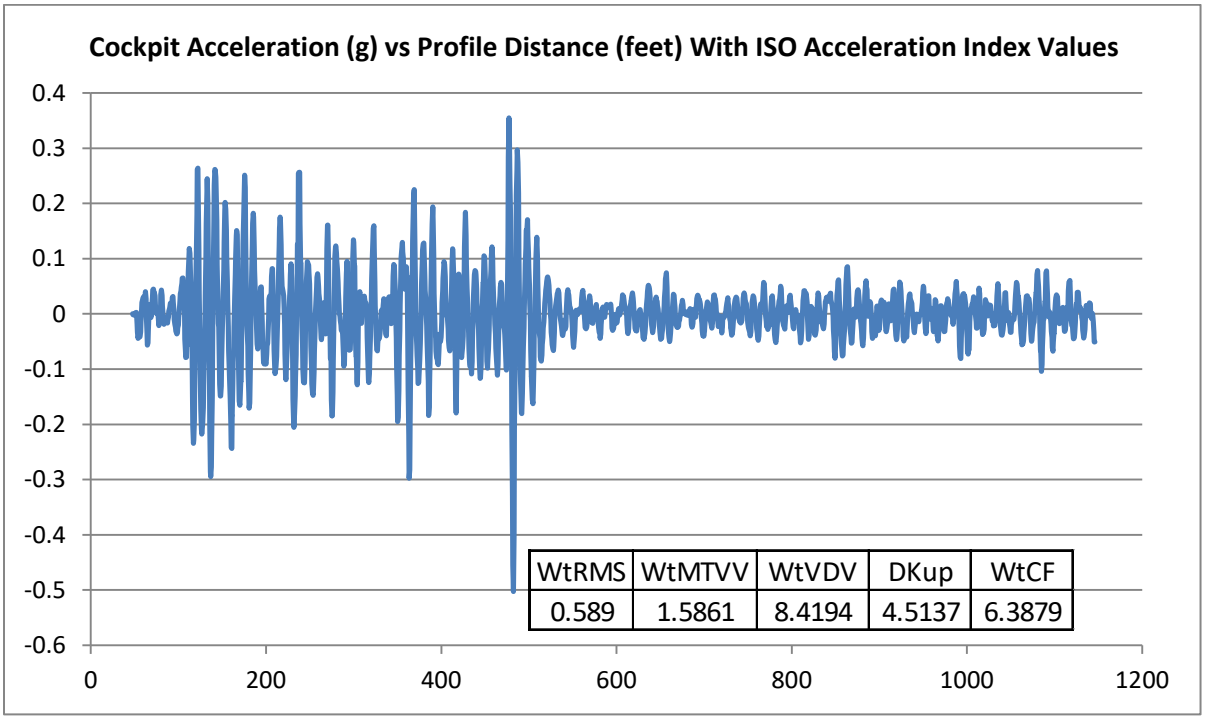

Figure D-26. Taxiway Profile 26—Profile Surface Height, Cockpit Acceleration, and Acceleration ISO Indices

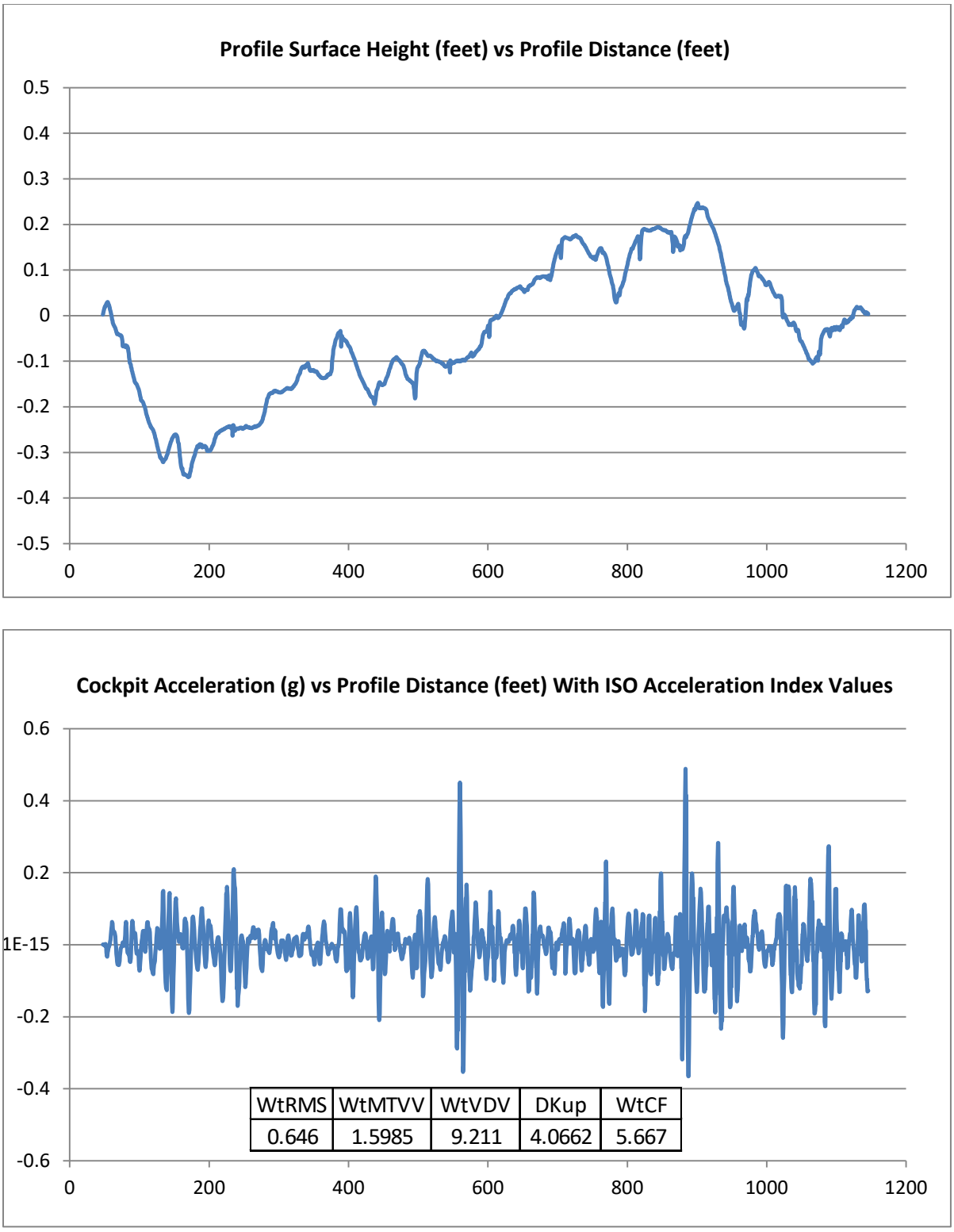

Figure D-27. Taxiway Profile 27—Profile Surface Height, Cockpit Acceleration, and Acceleration ISO Indices

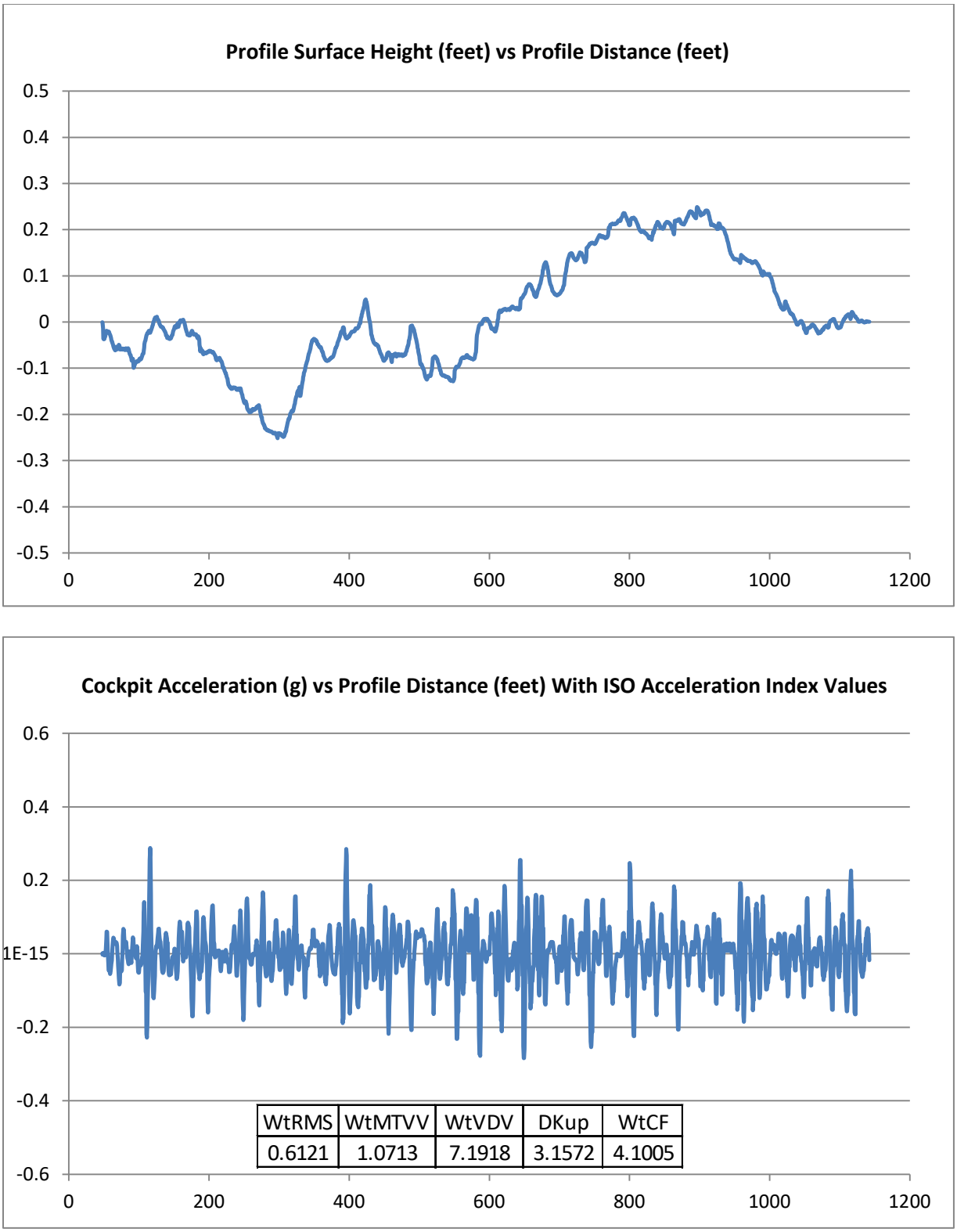

Figure D-28. Taxiway Profile 28—Profile Surface Height, Cockpit Acceleration, and Acceleration ISO Indices

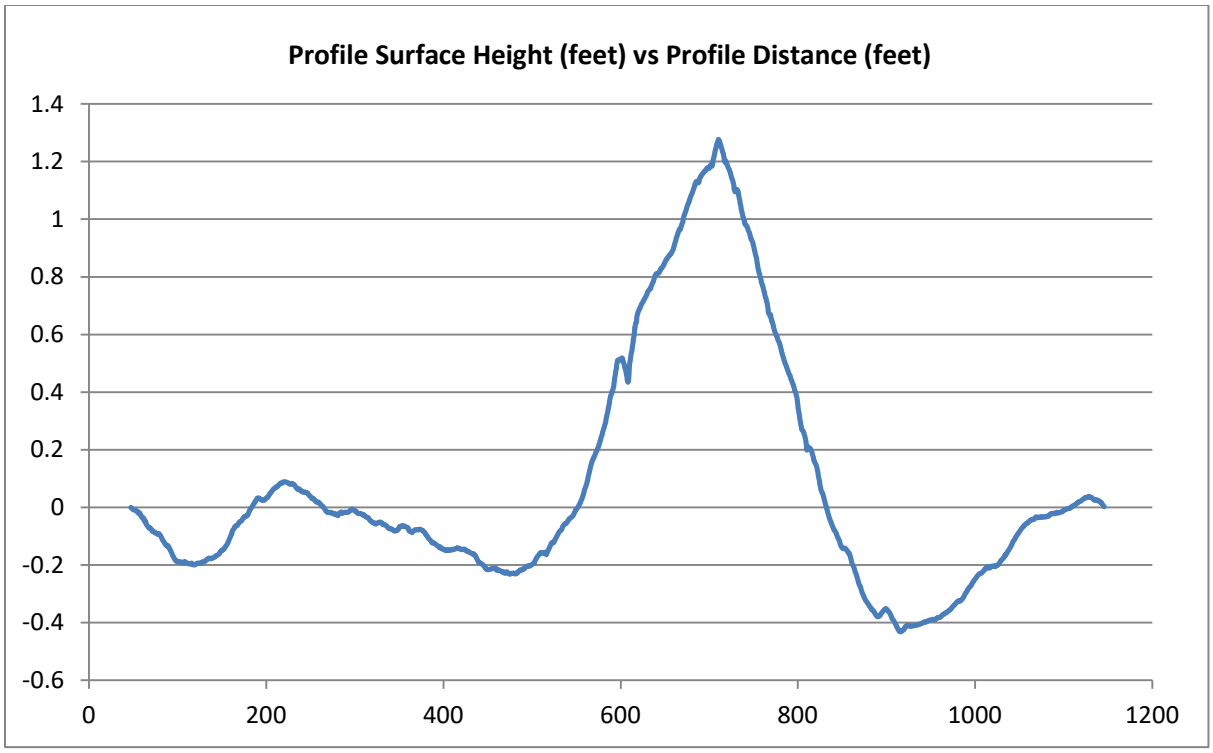

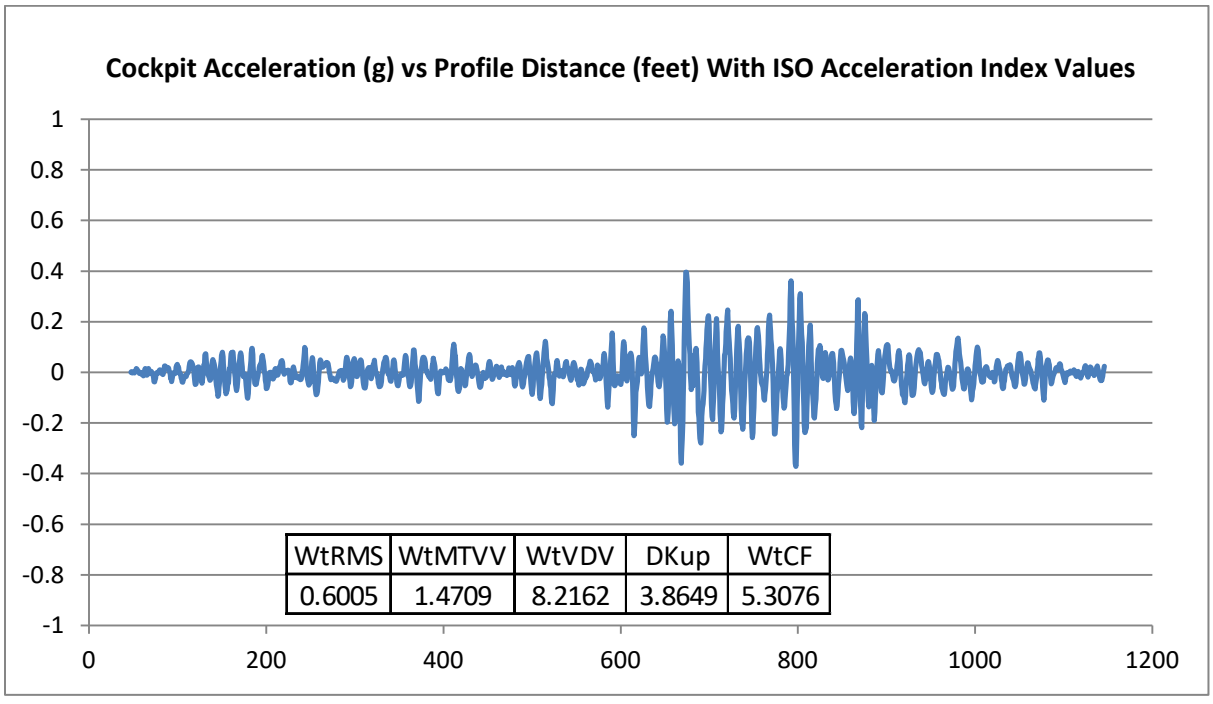

Figure D-29. Taxiway Profile 29—Profile Surface Height, Cockpit Acceleration, and Acceleration ISO Indices

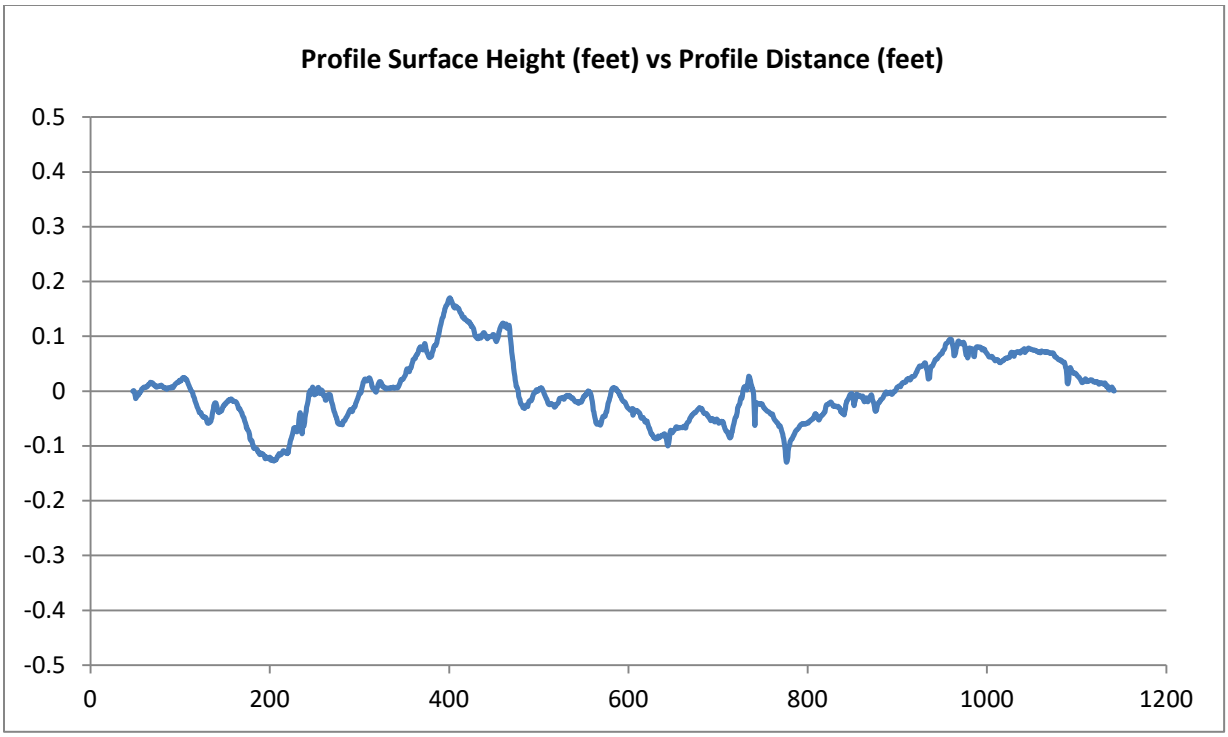

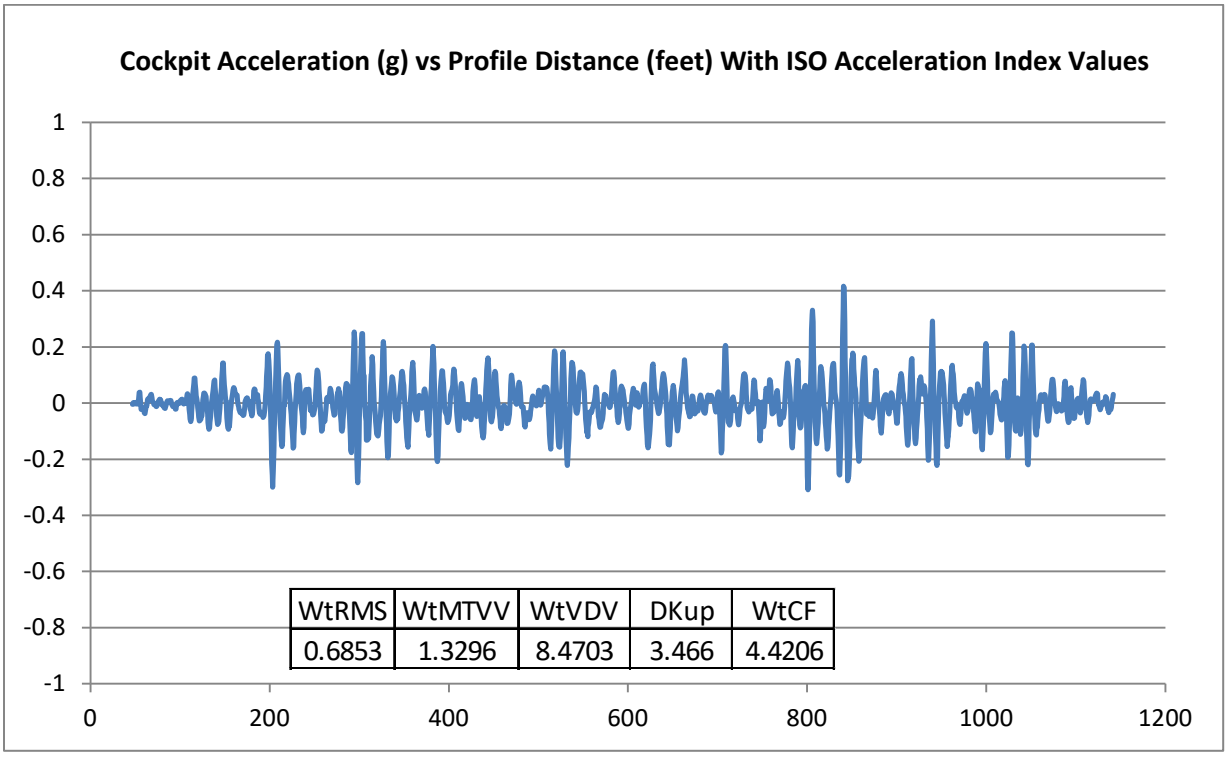

Figure D-30. Taxiway Profile 30—Profile Surface Height, Cockpit Acceleration, and Acceleration ISO Indices

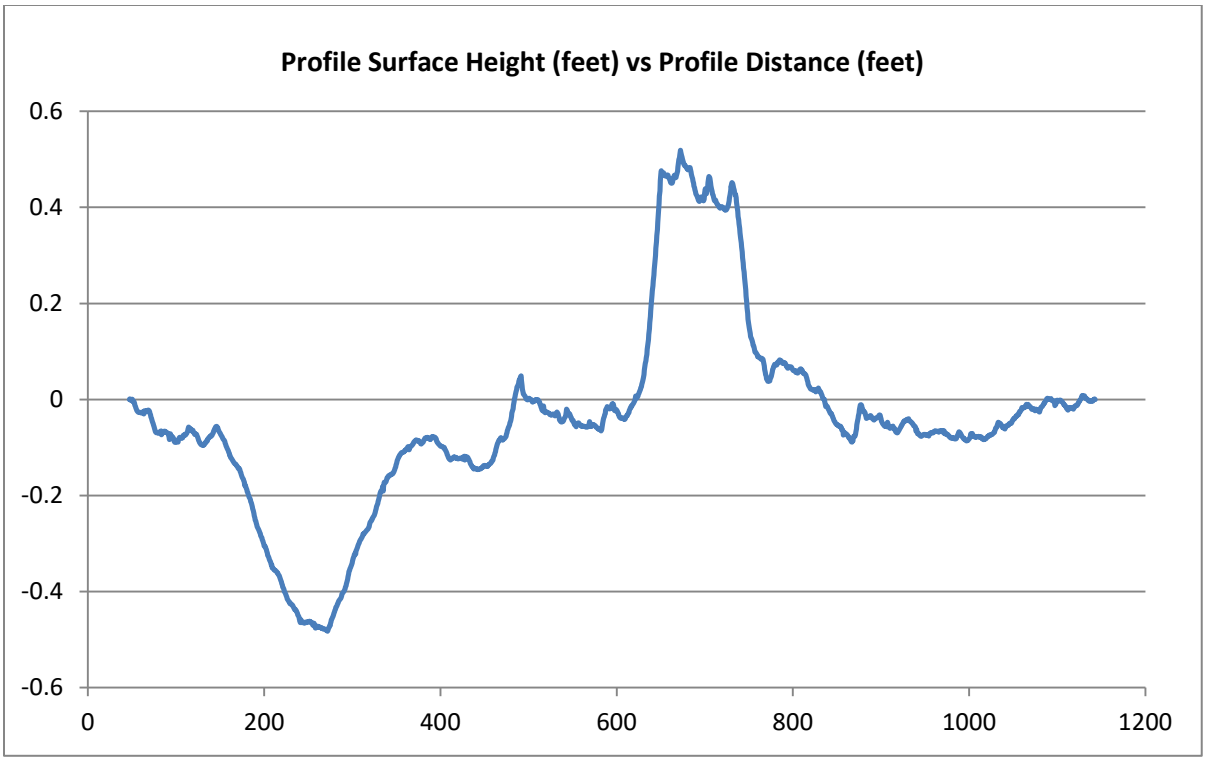

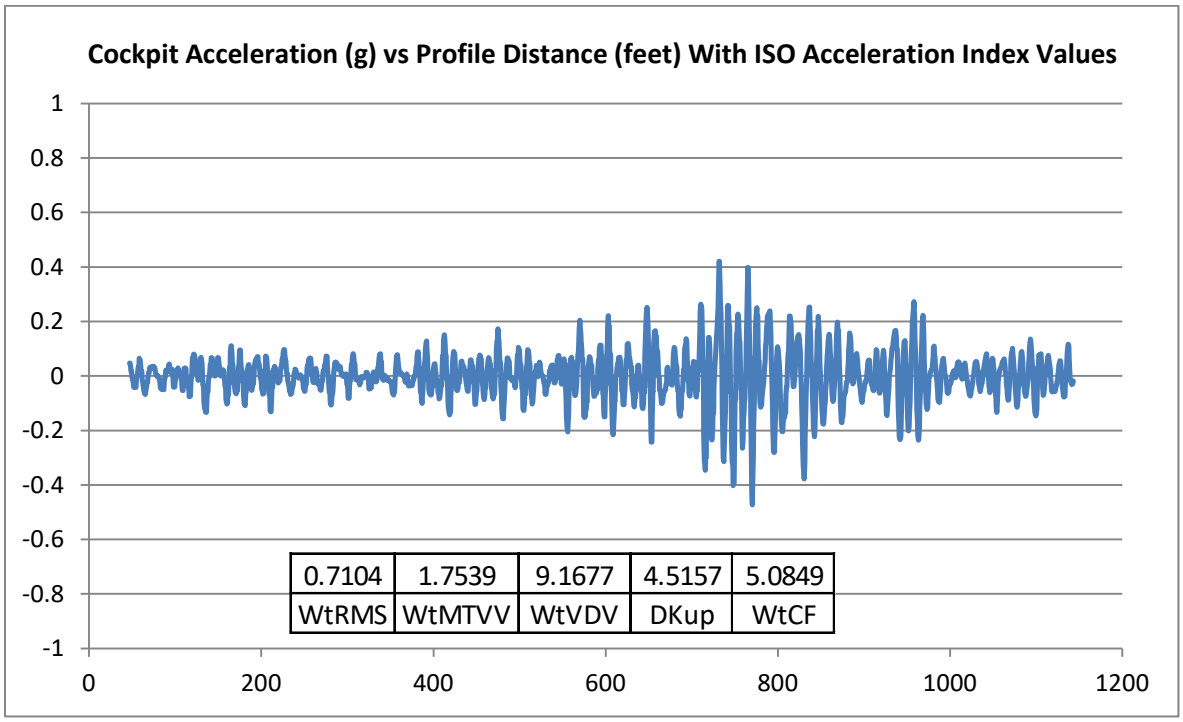

Figure D-31. Taxiway Profile 31—Profile Surface Height, Cockpit Acceleration, and Acceleration ISO Indices

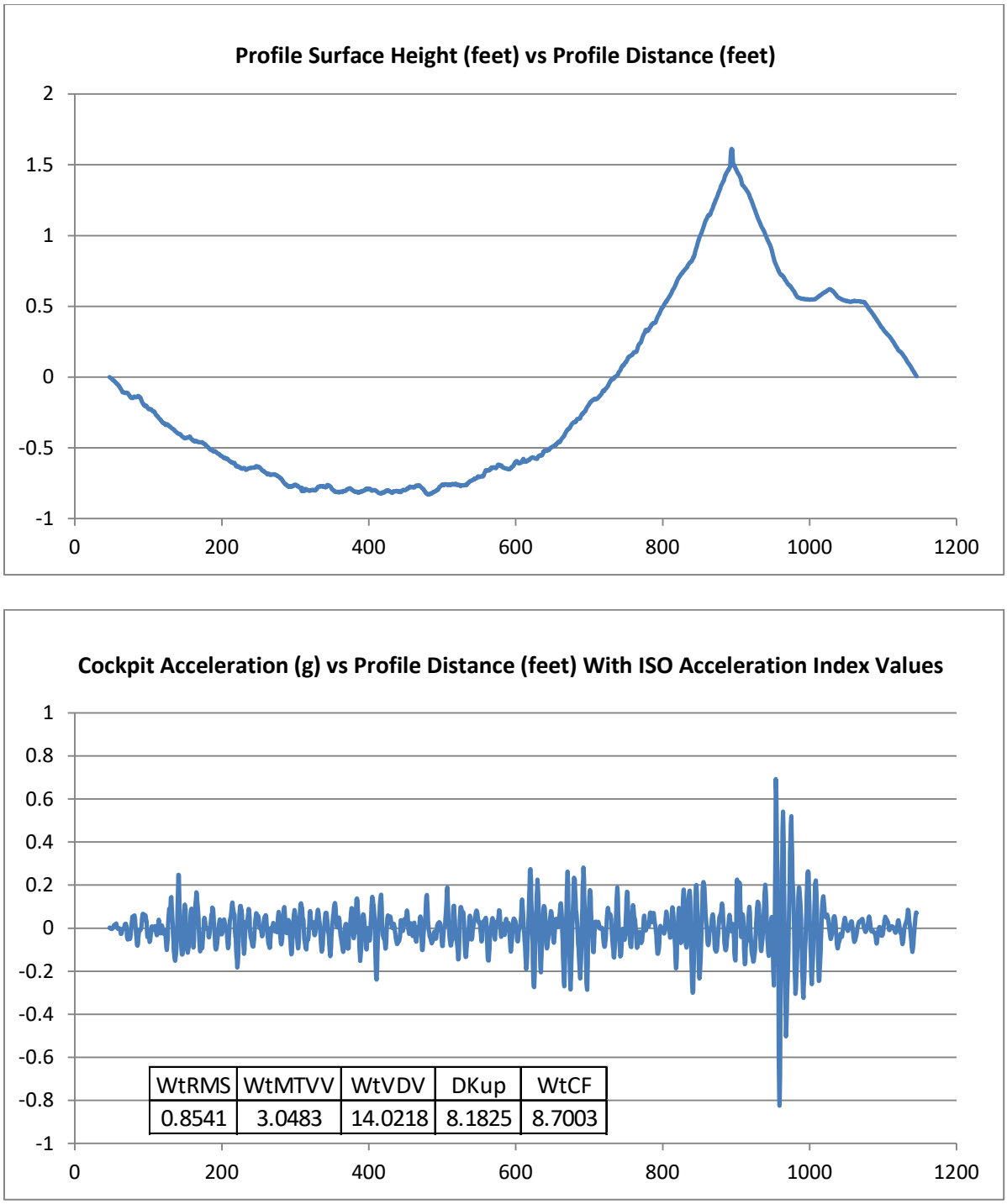

Figure D-32. Taxiway Profile 32—Profile Surface Height, Cockpit Acceleration, and Acceleration ISO Indices

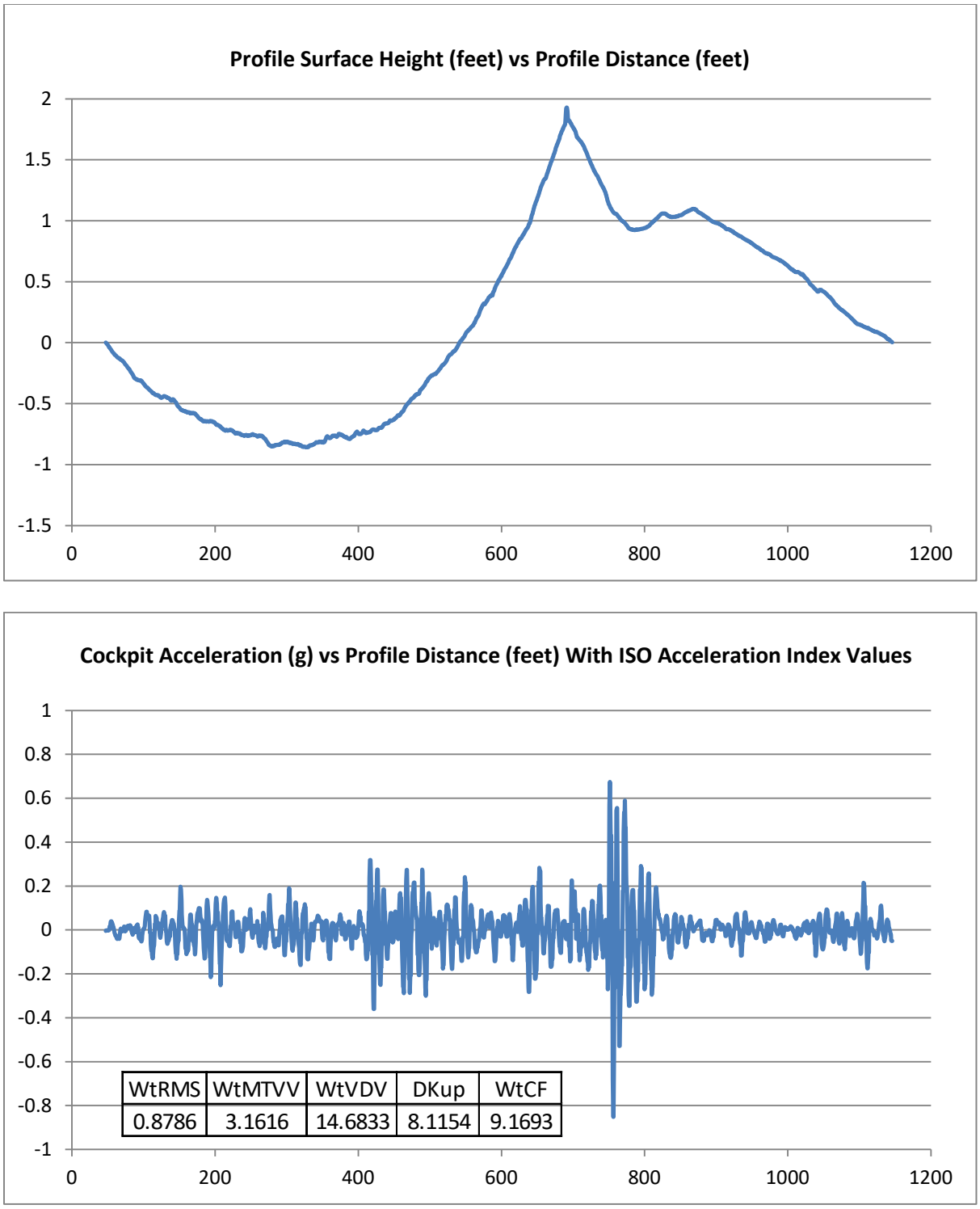

Figure D-33. Taxiway Profile 33—Profile Surface Height, Cockpit Acceleration, and Acceleration ISO Indices

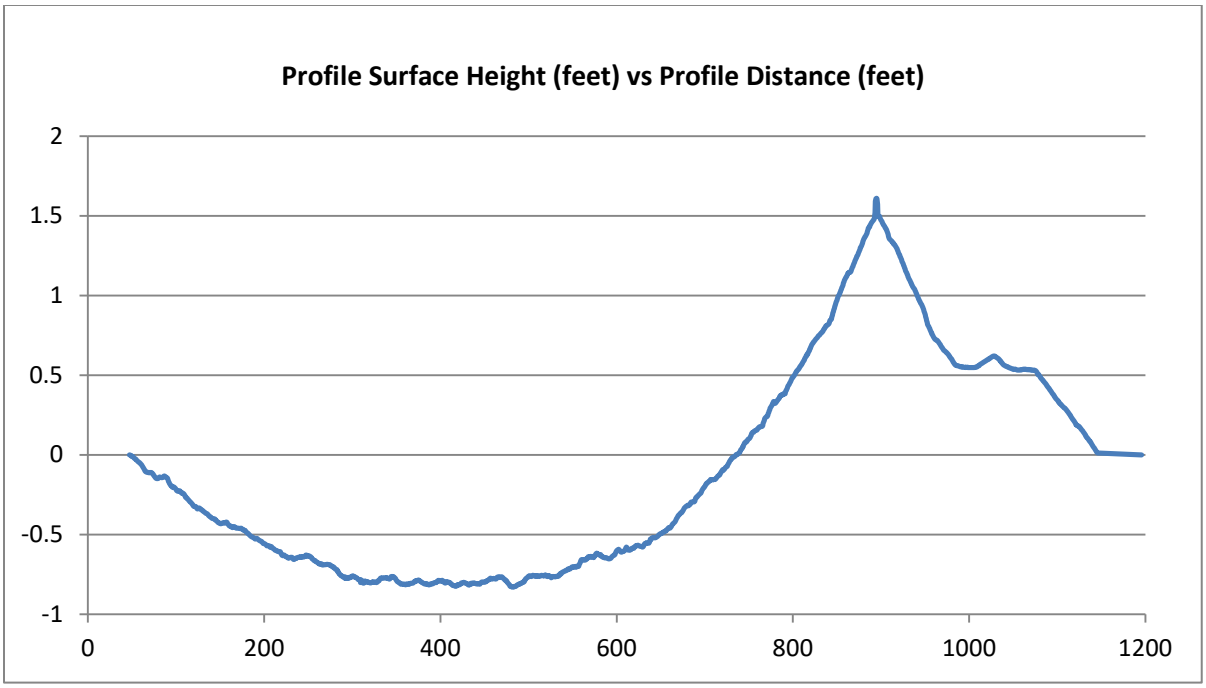

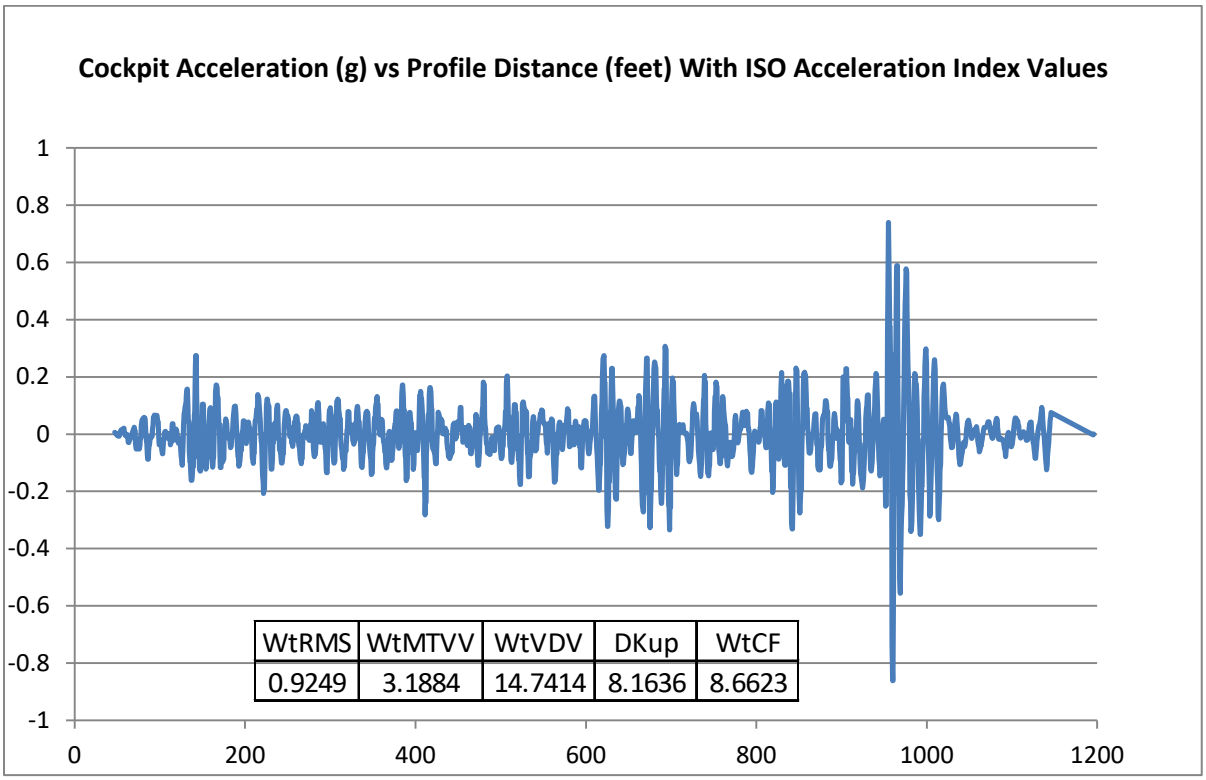

Figure D-34. Taxiway Profile 34—Profile Surface Height, Cockpit Acceleration, and Acceleration ISO Indices

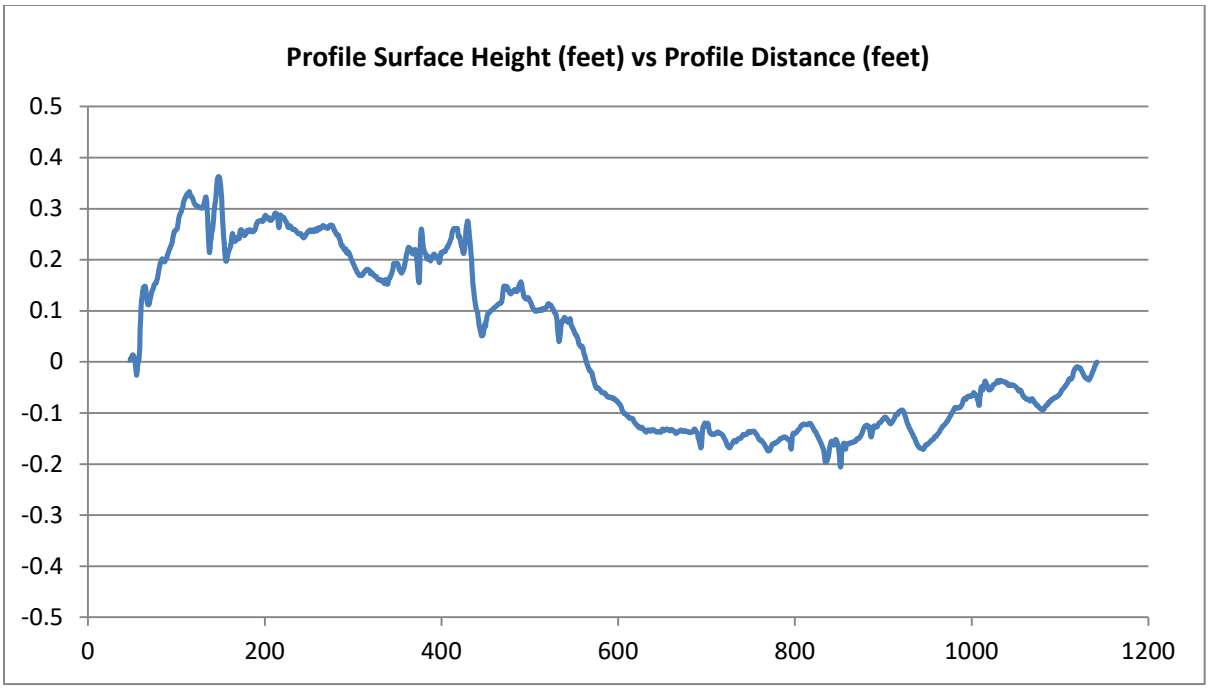

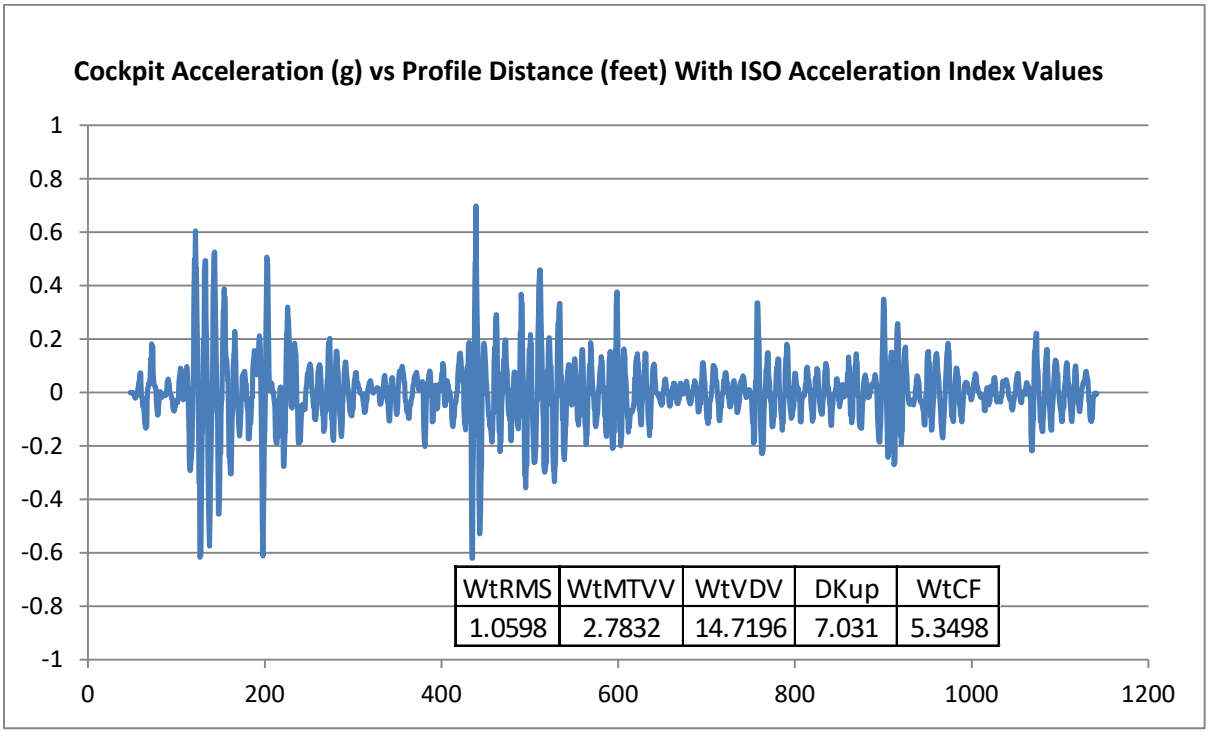

Figure D-35. Taxiway Profile 35—Profile Surface Height, Cockpit Acceleration, and Acceleration ISO Indices

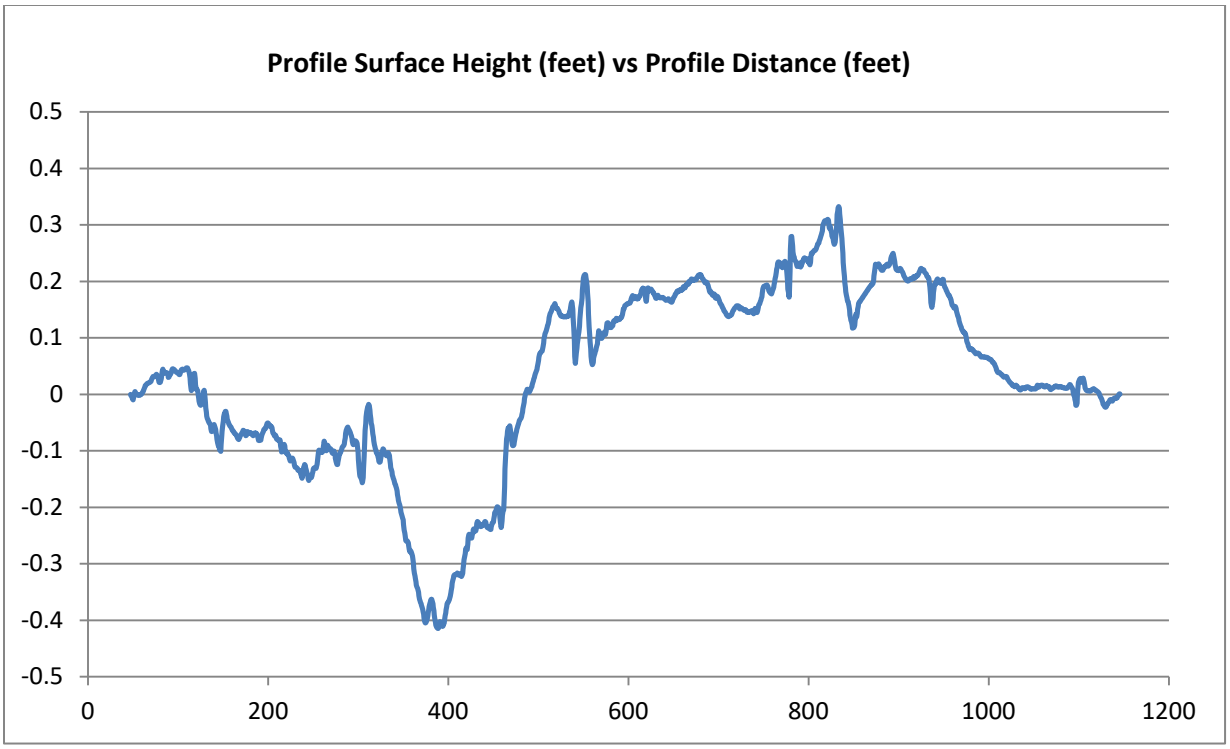

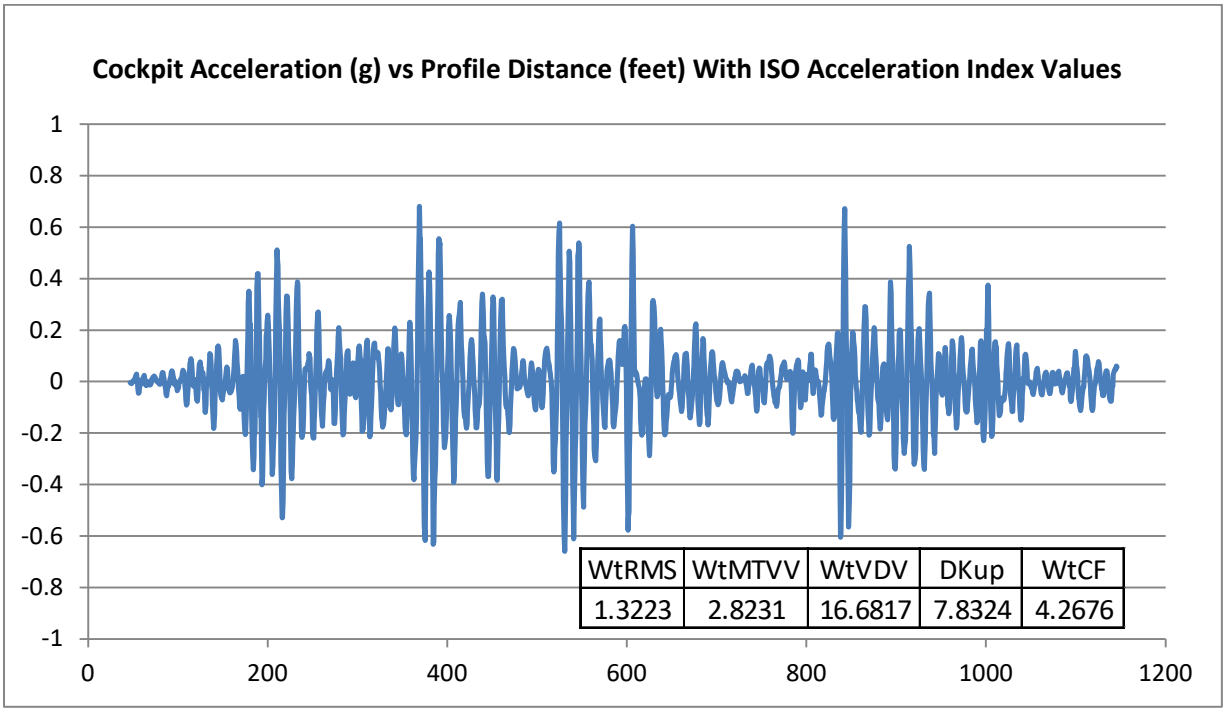

Figure D-36. Taxiway Profile 36—Profile Surface Height, Cockpit Acceleration, and Acceleration ISO Indices

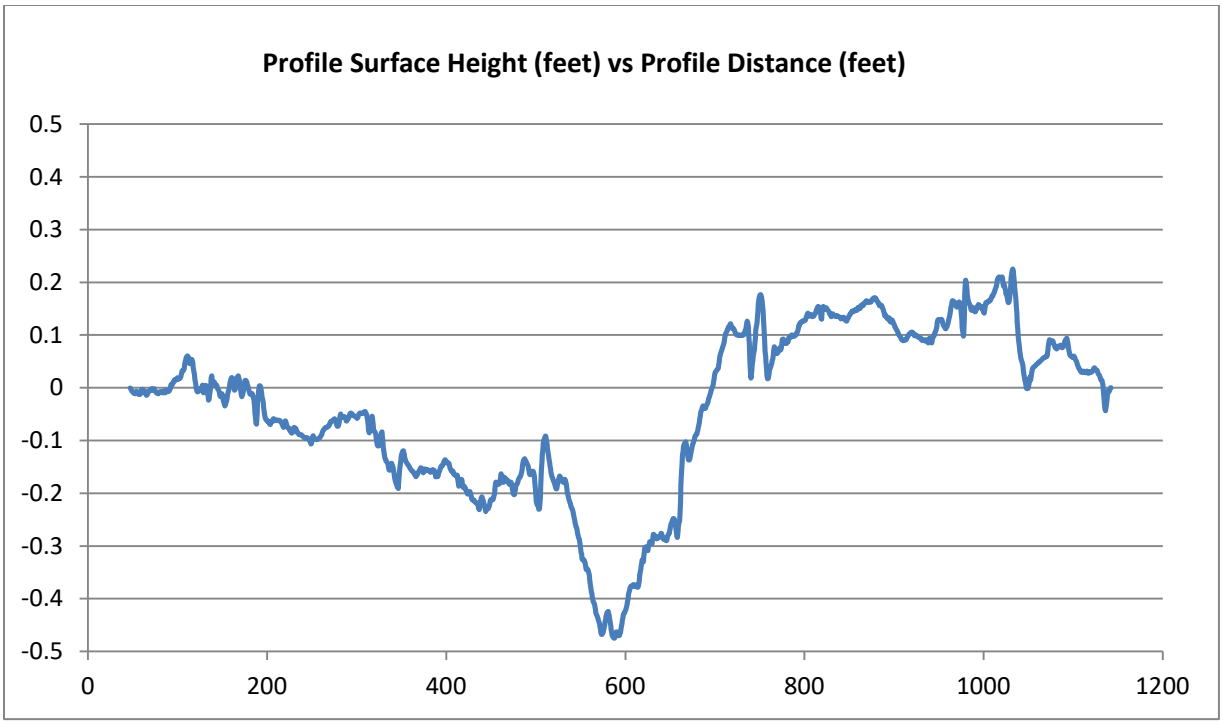

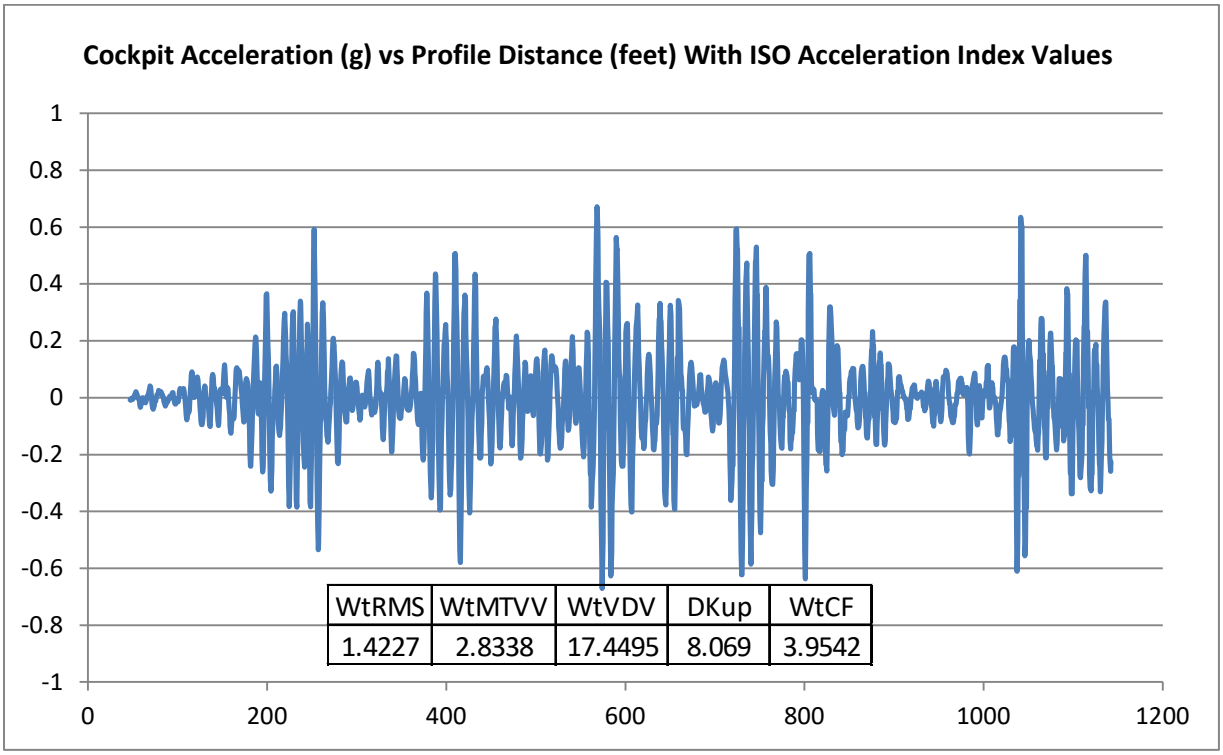

Figure D-37. Taxiway Profile 37—Profile Surface Height, Cockpit Acceleration, and Acceleration ISO Indices

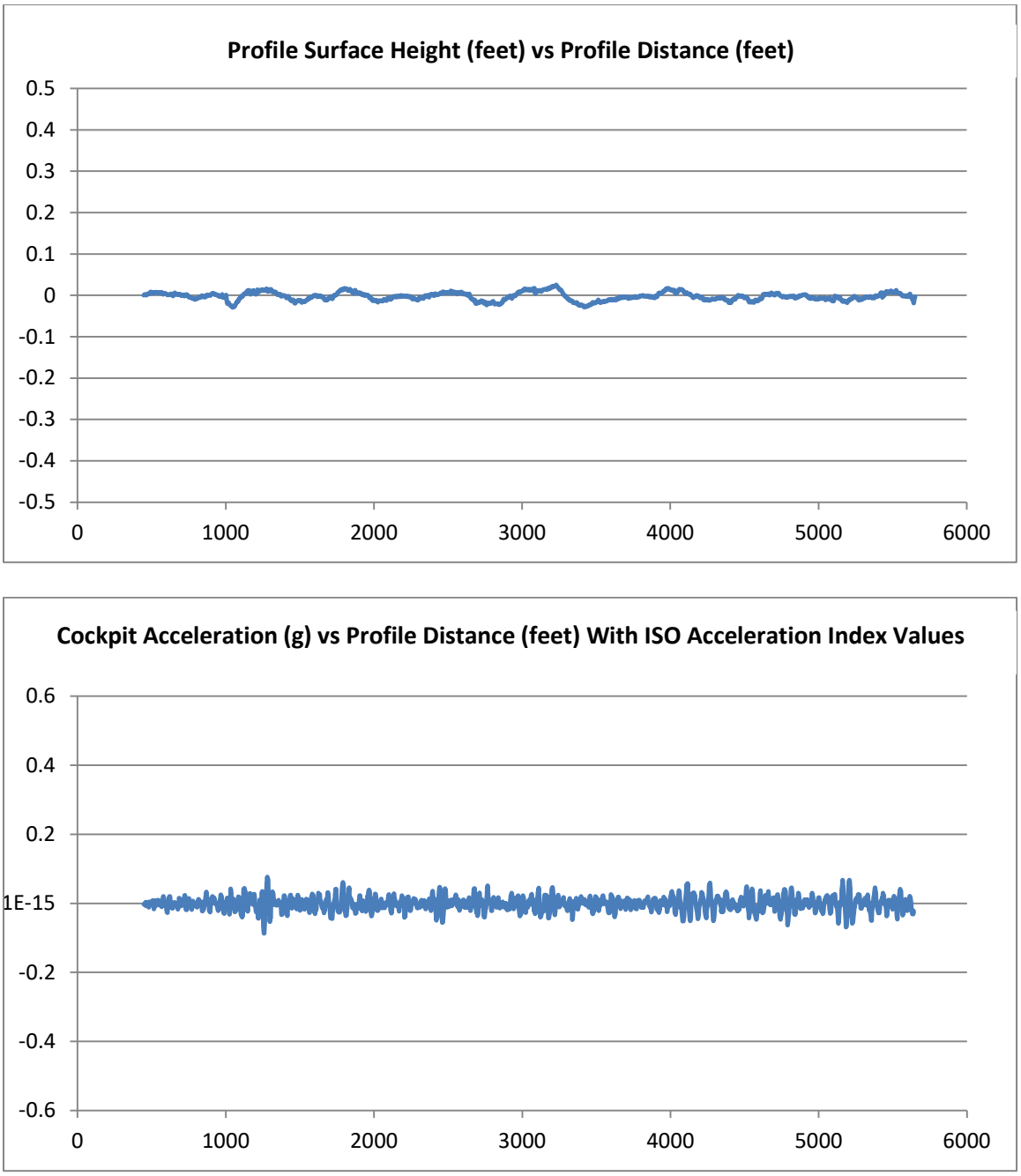

Figure D-38. Runway Profile 38—Profile Height, Cockpit Acceleration, and Acceleration ISO Indices

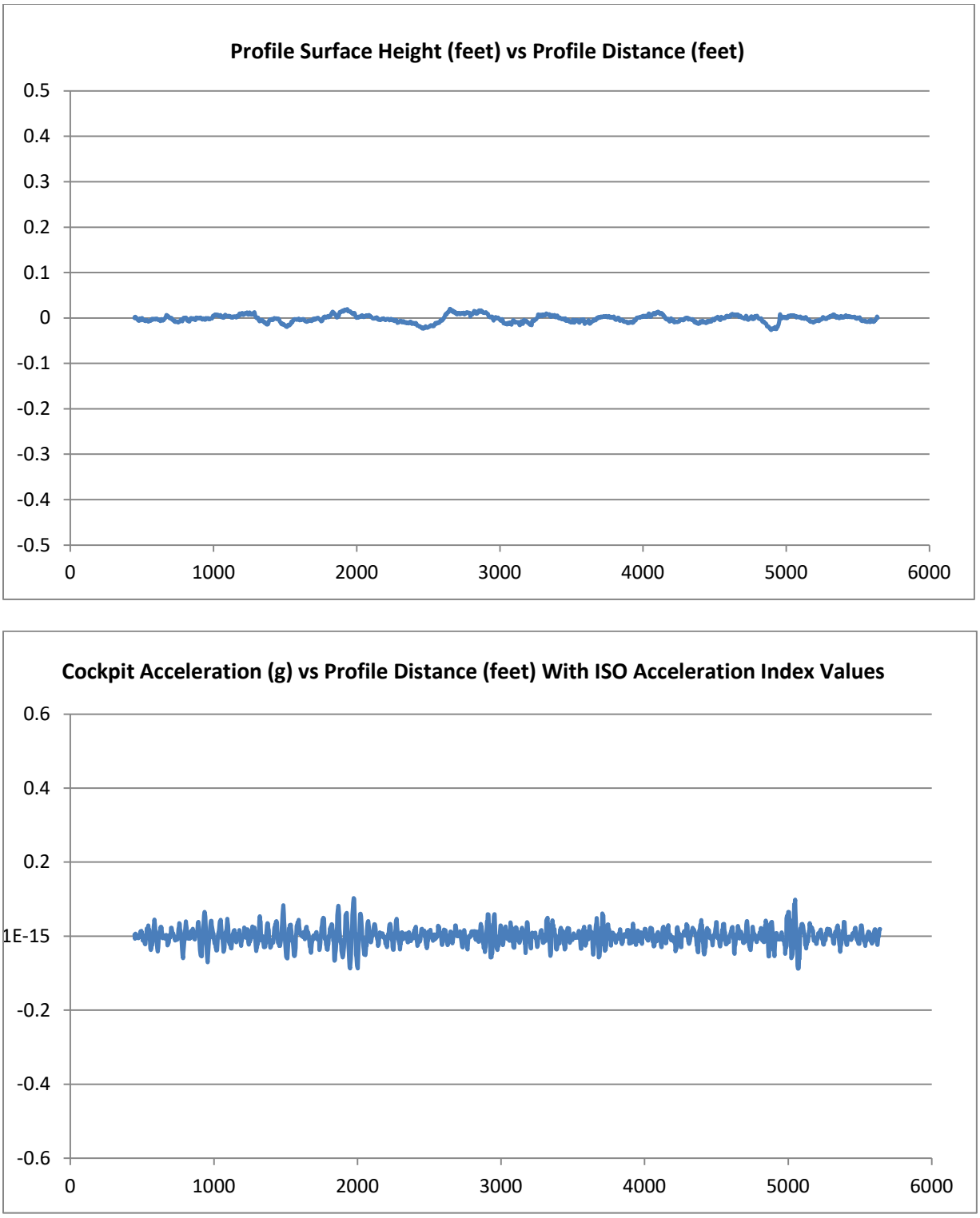

Figure D-39. Runway Profile 39—Profile Height, Cockpit Acceleration, and Acceleration ISO Indices

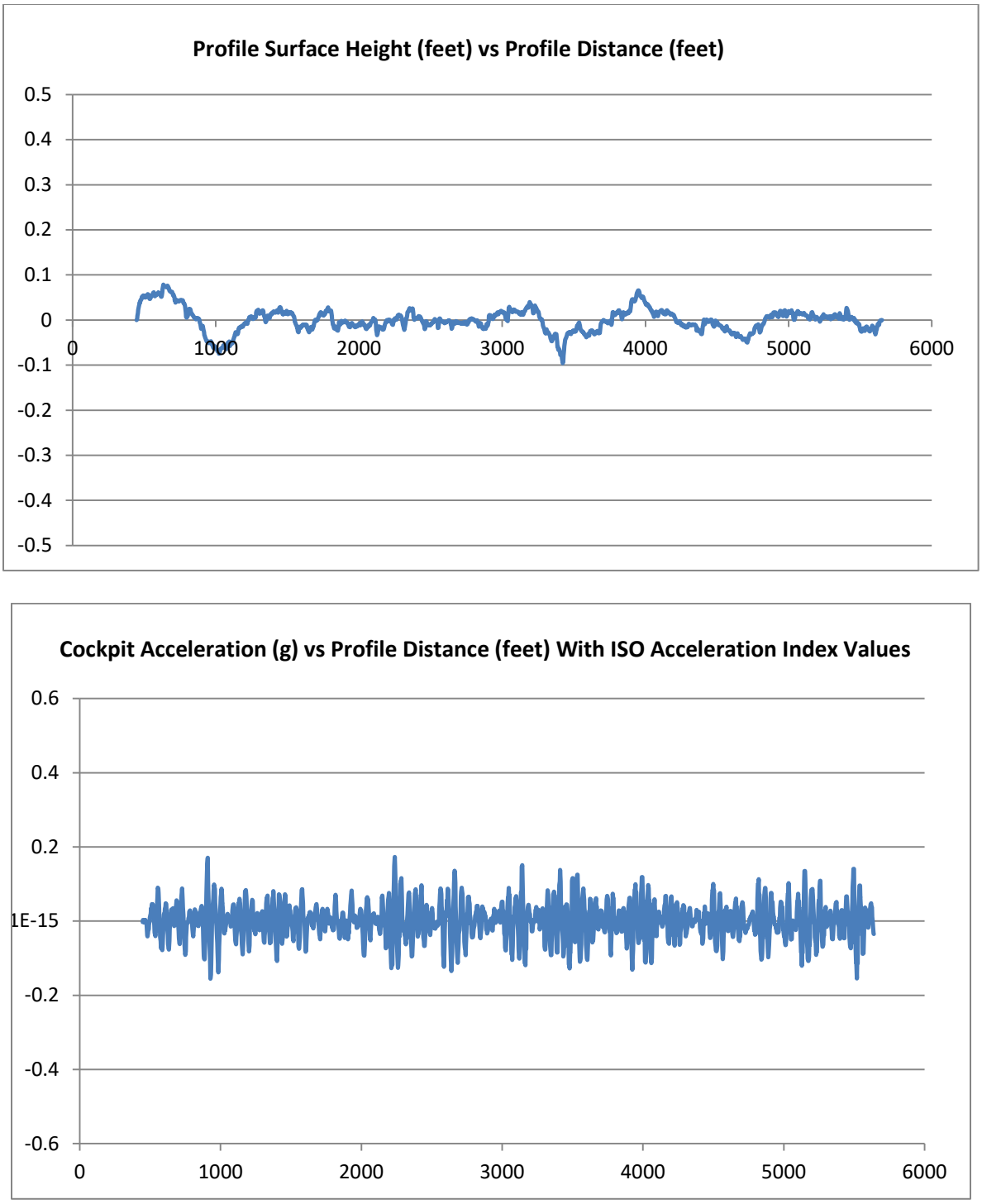

Figure D-40. Runway Profile 40—Profile Height, Cockpit Acceleration, and Acceleration ISO Indices

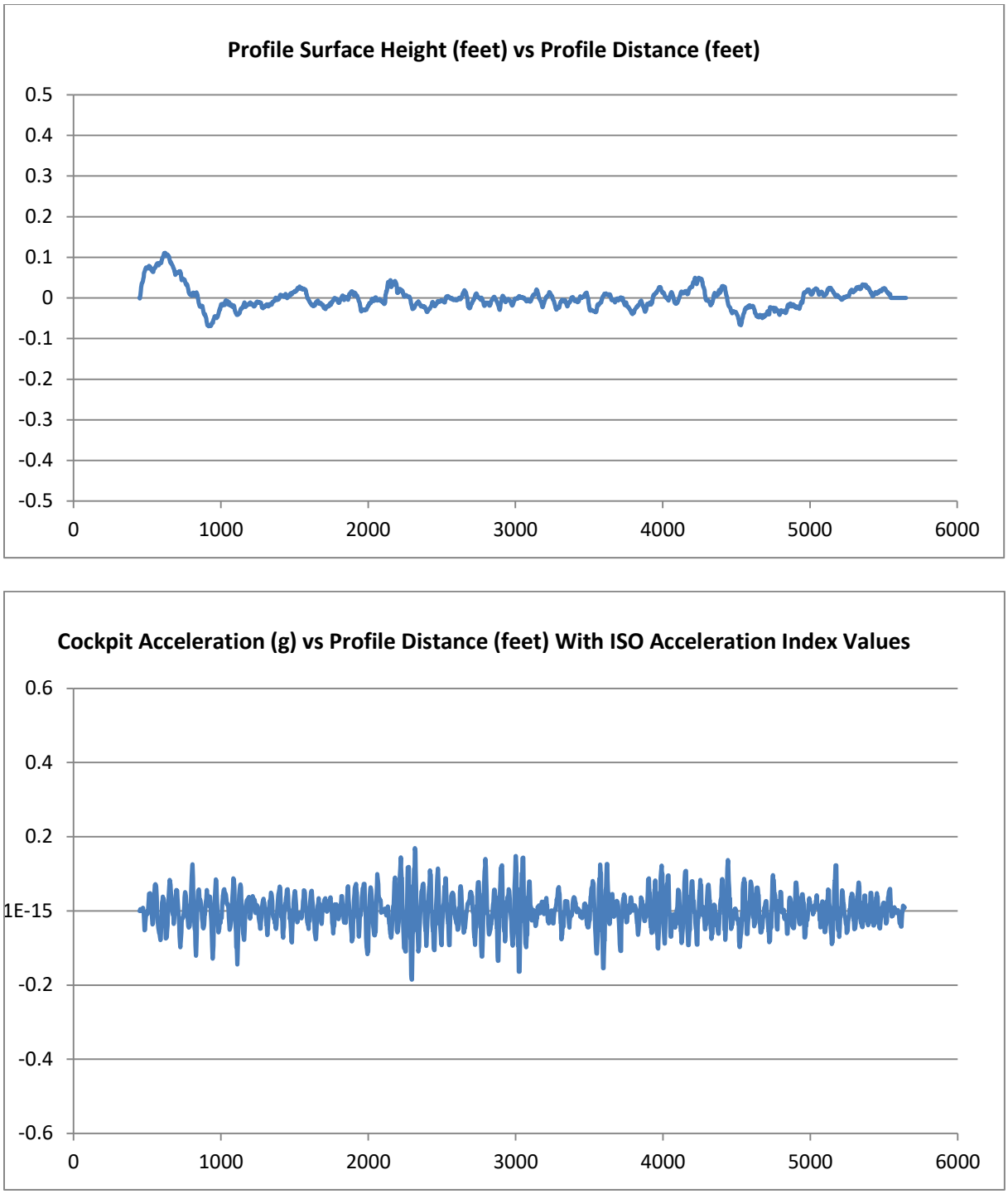

Figure D-41. Runway Profile 41—Profile Height, Cockpit Acceleration, and Acceleration ISO Indices

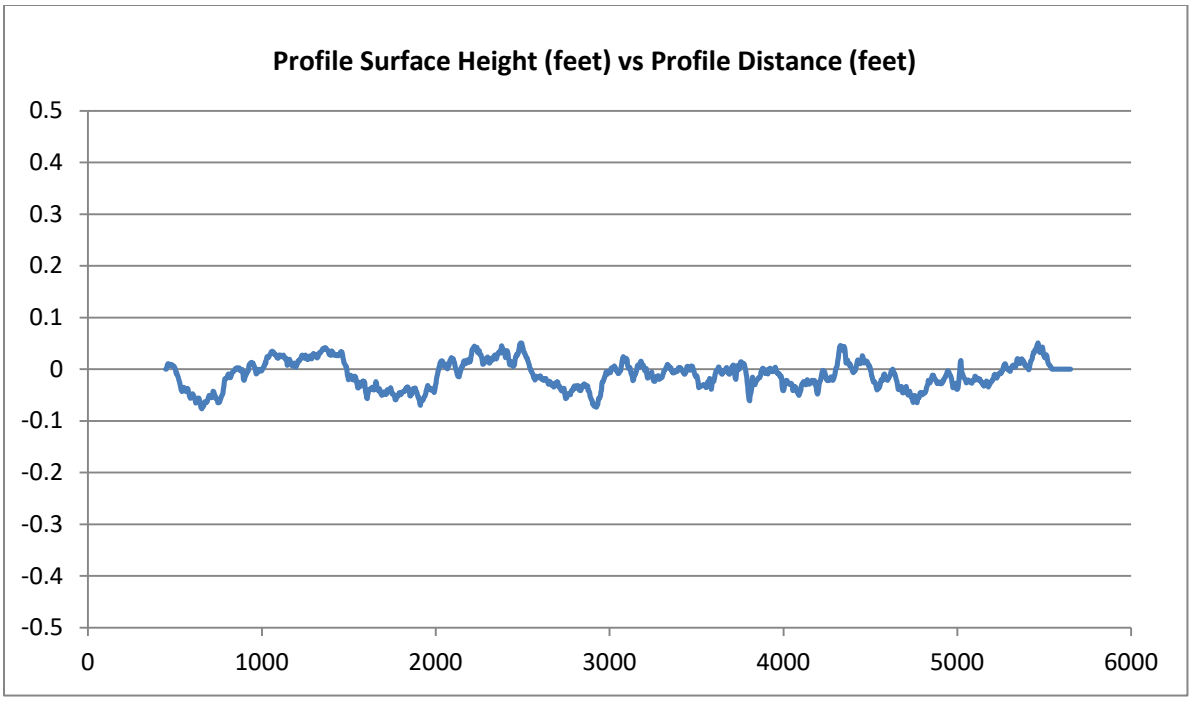

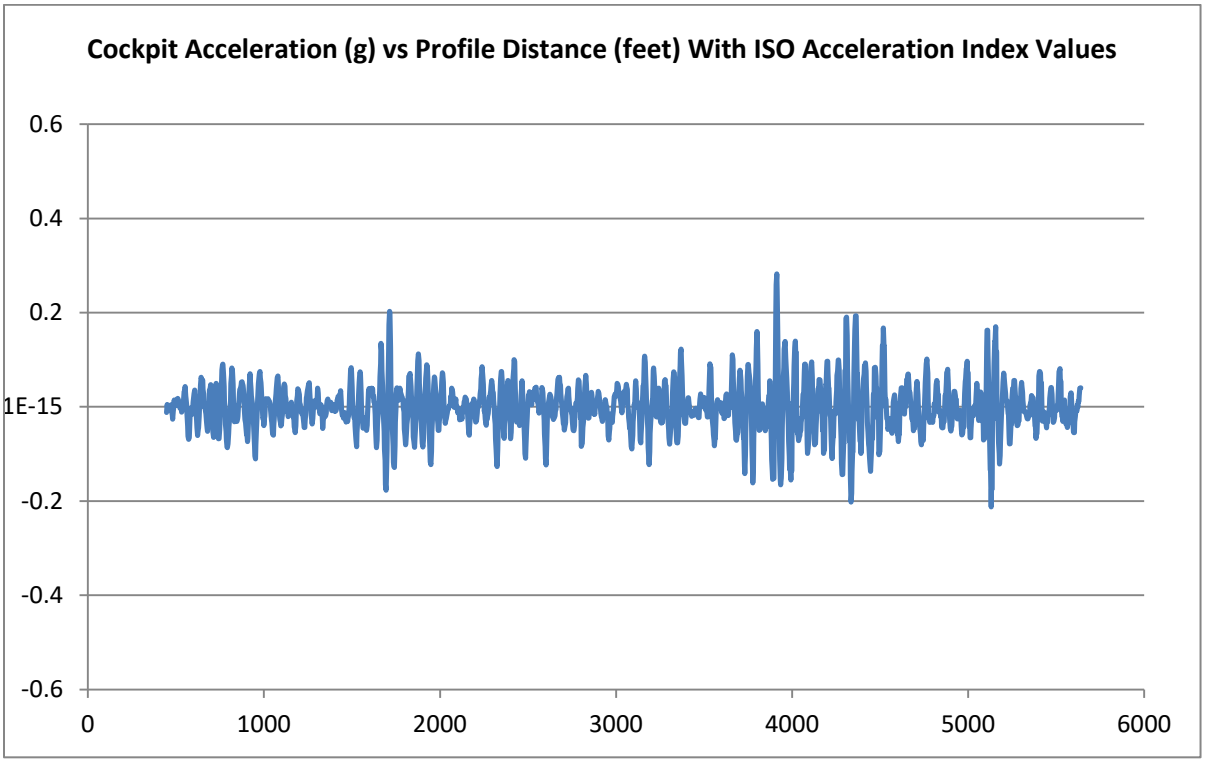

Figure D-42. Runway Profile 42—Profile Height, Cockpit Acceleration, and Acceleration ISO Indices

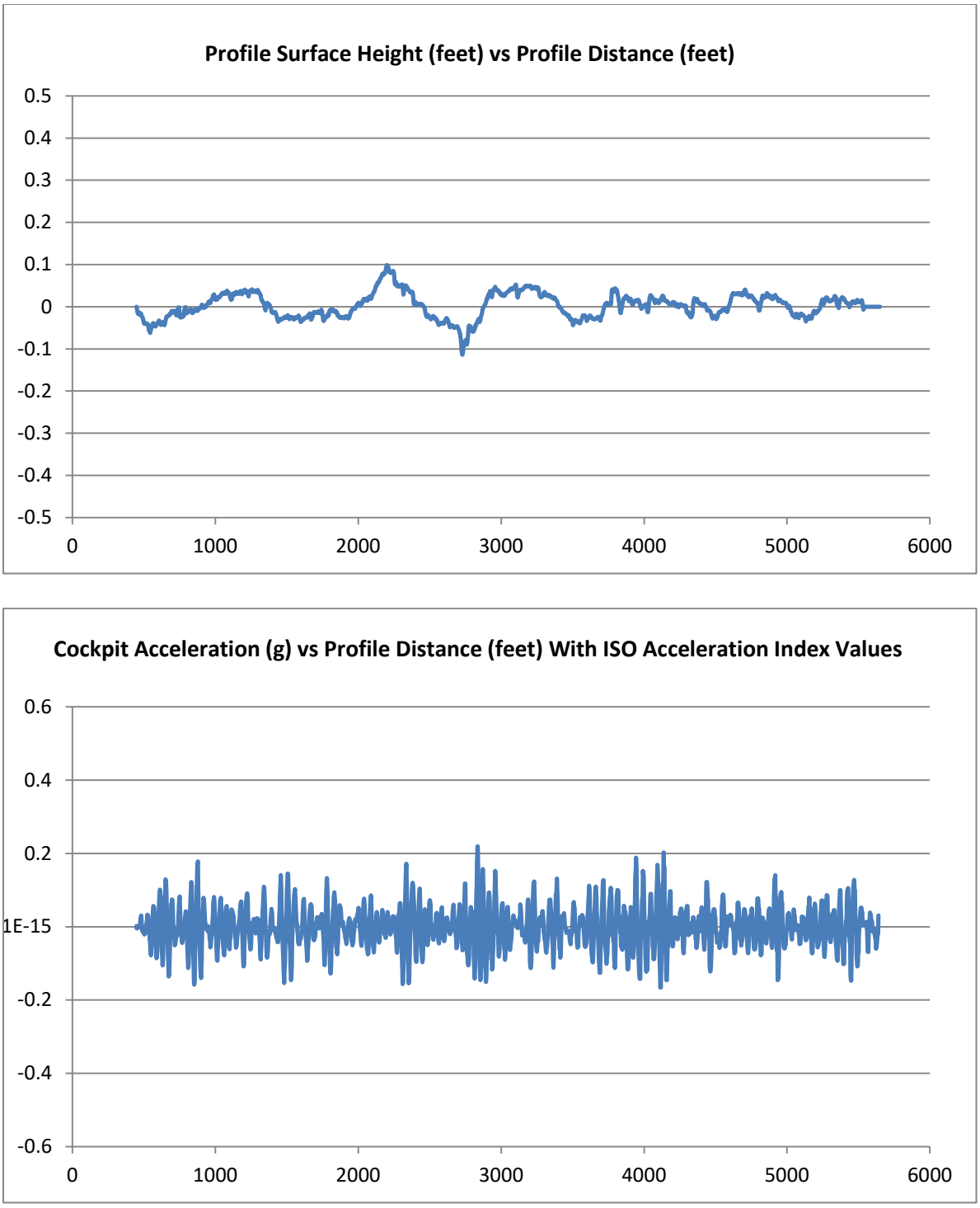

Figure D-43. Runway Profile 43—Profile Height, Cockpit Acceleration, and Acceleration ISO Indices

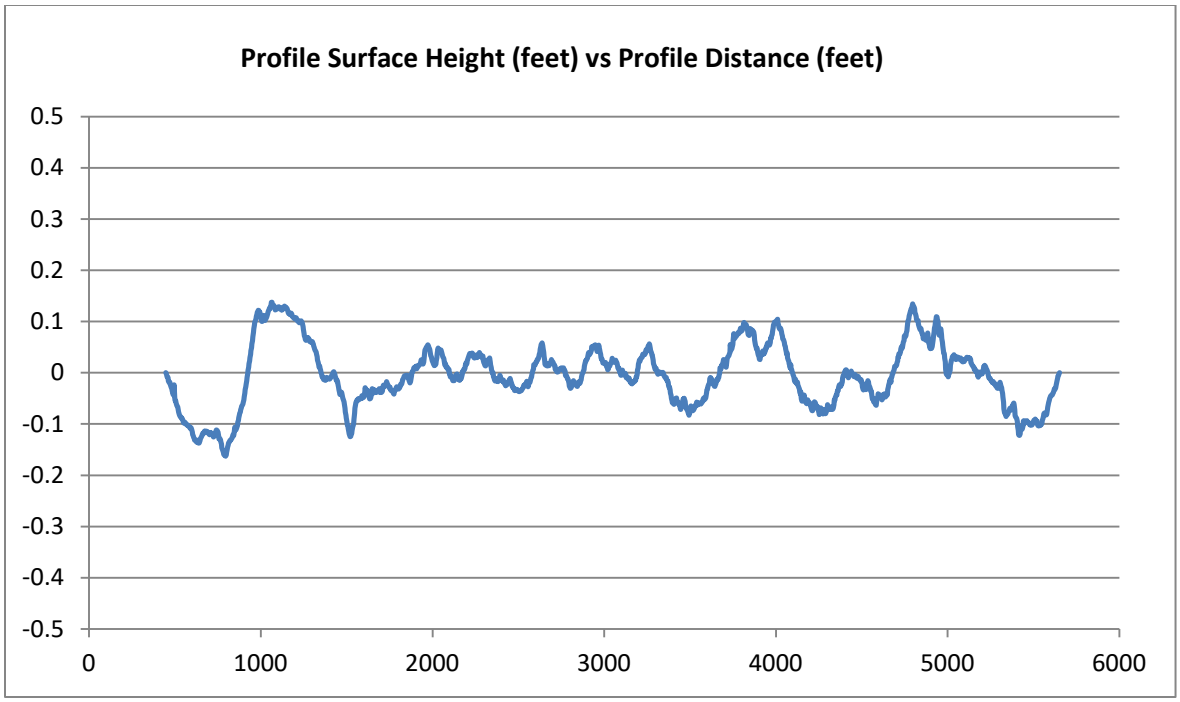

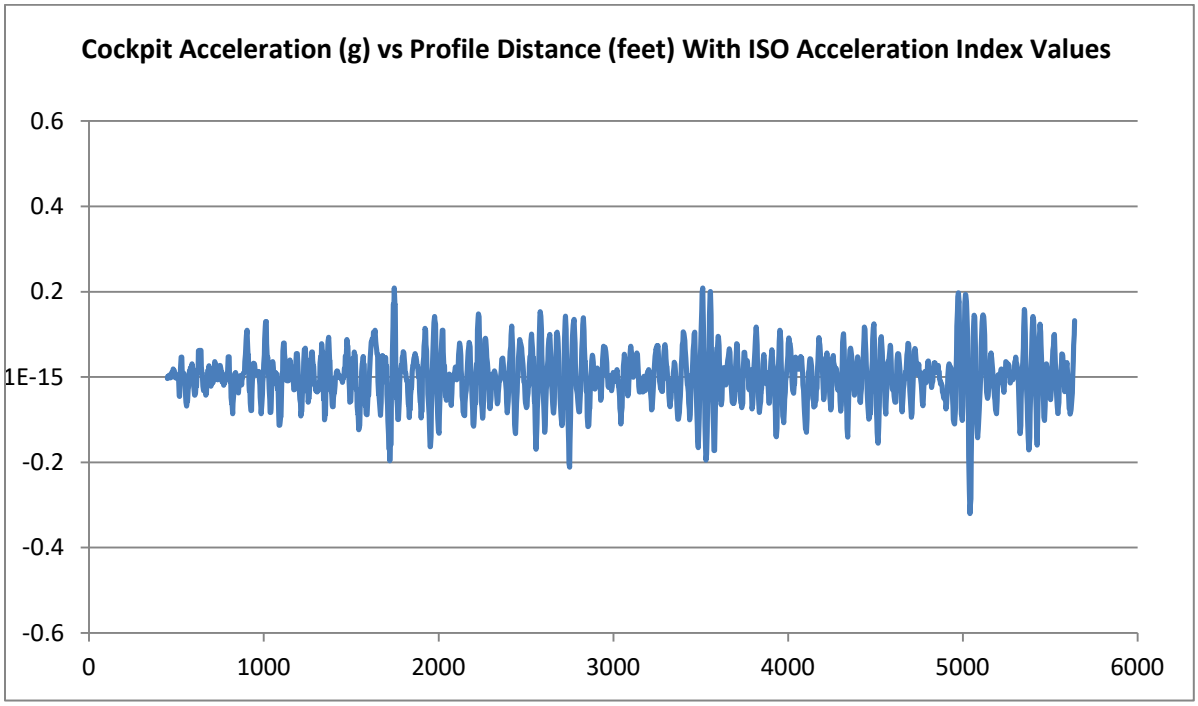

Figure D-44. Runway Profile 44—Profile Height, Cockpit Acceleration, and Acceleration ISO Indices

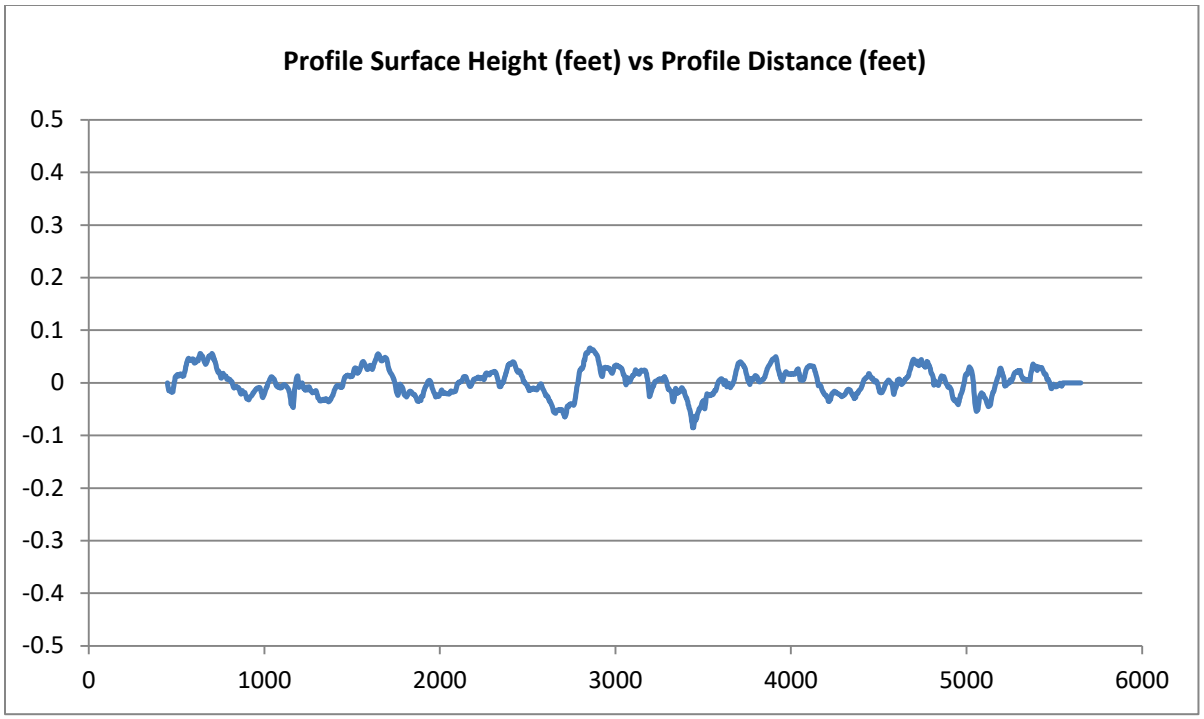

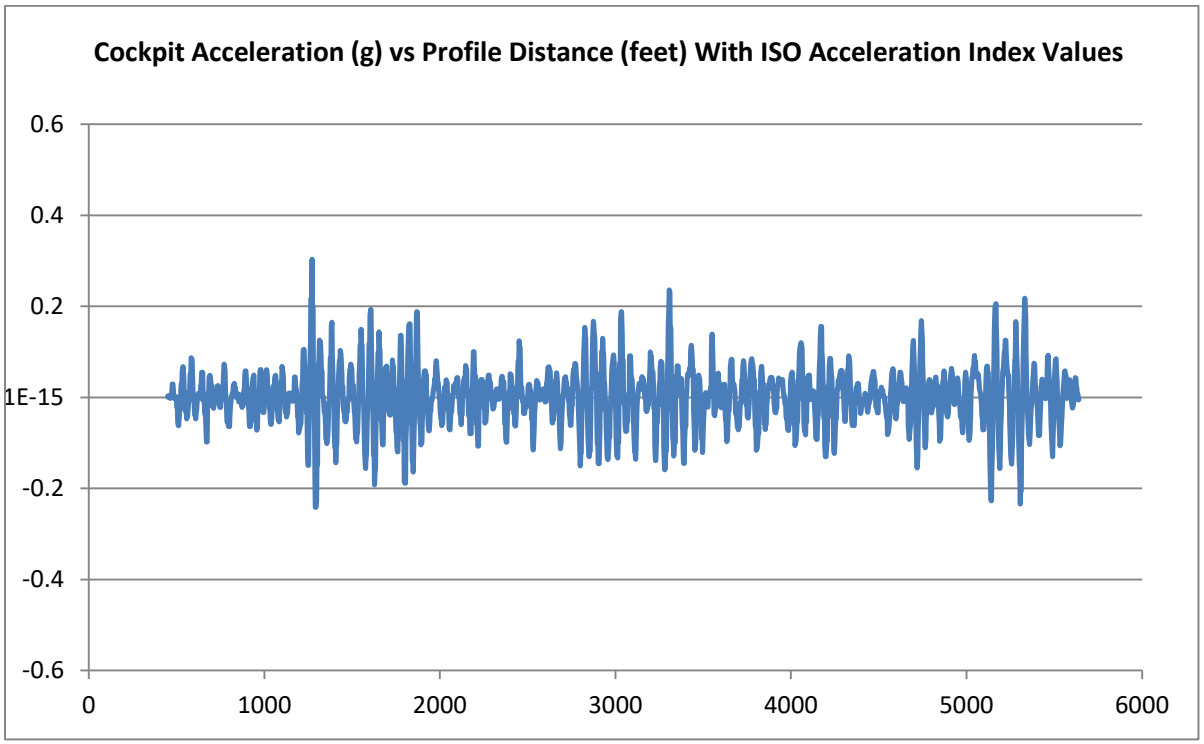

Figure D-45. Runway Profile 45—Profile Height, Cockpit Acceleration, and Acceleration ISO Indices

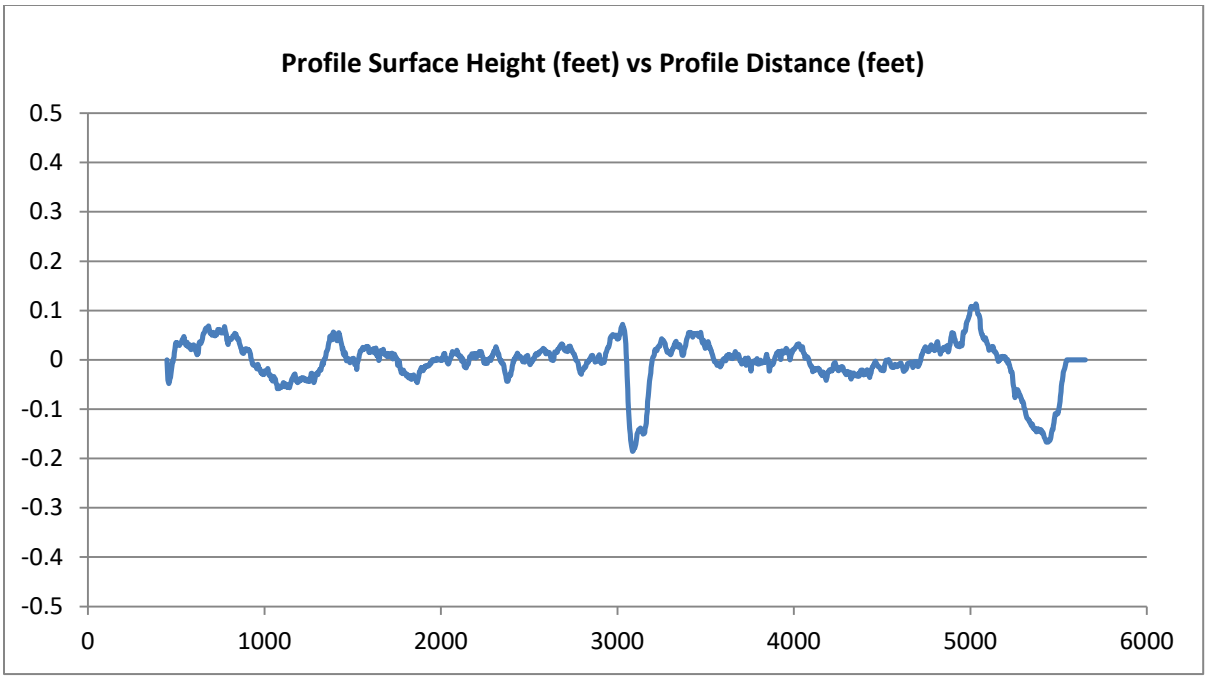

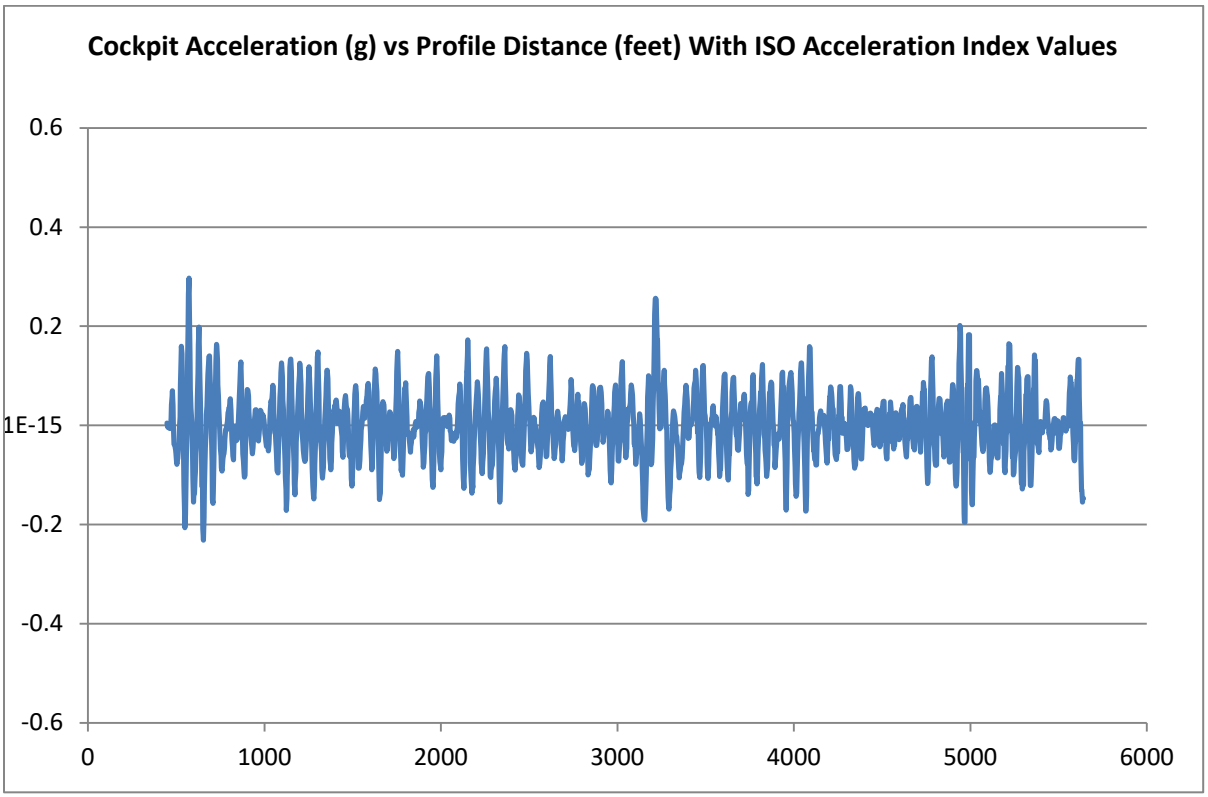

Figure D-46. Runway Profile 46—Profile Height, Cockpit Acceleration, and Acceleration ISO Indices

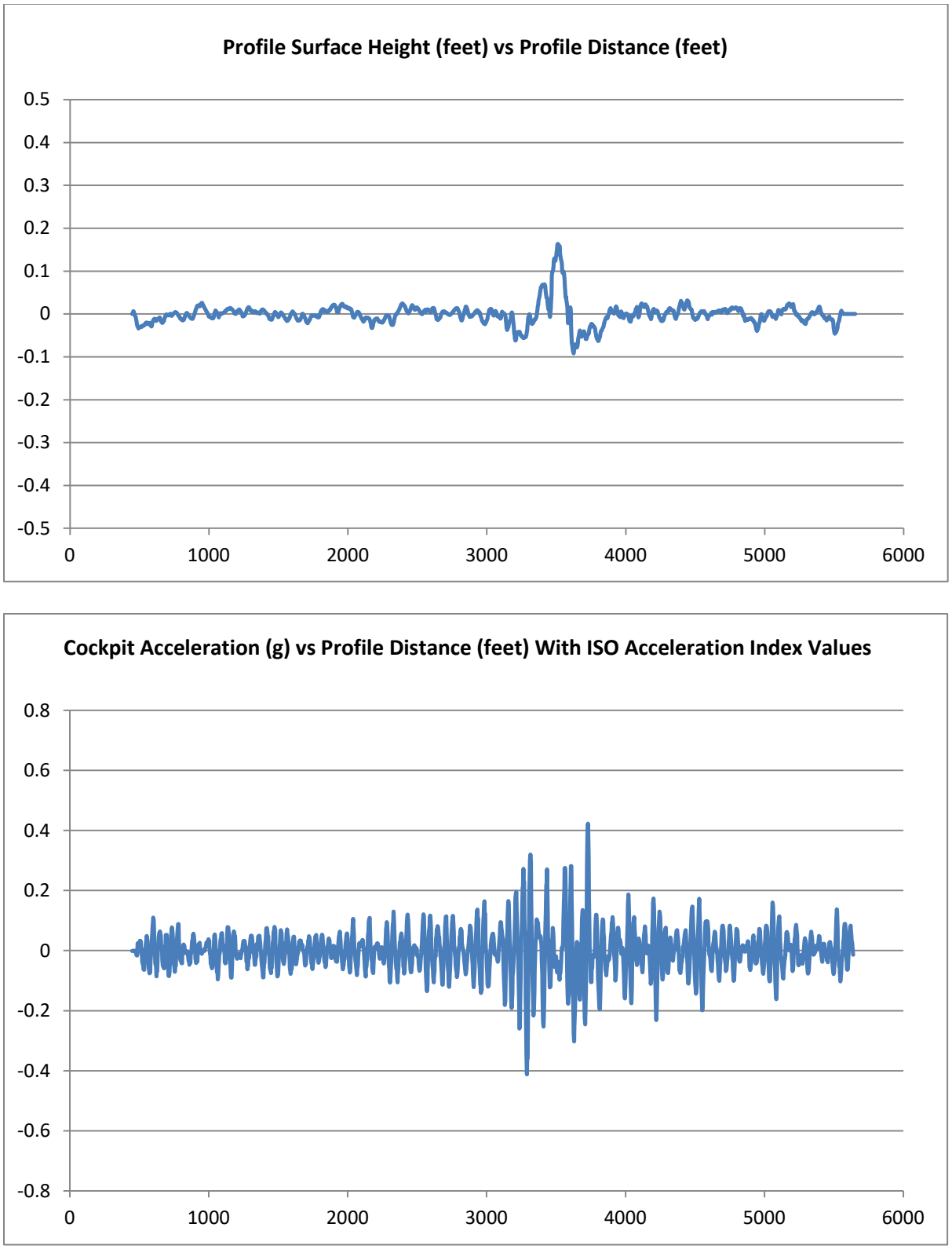

Figure D-47. Runway Profile 47—Profile Height, Cockpit Acceleration, and Acceleration ISO Indices

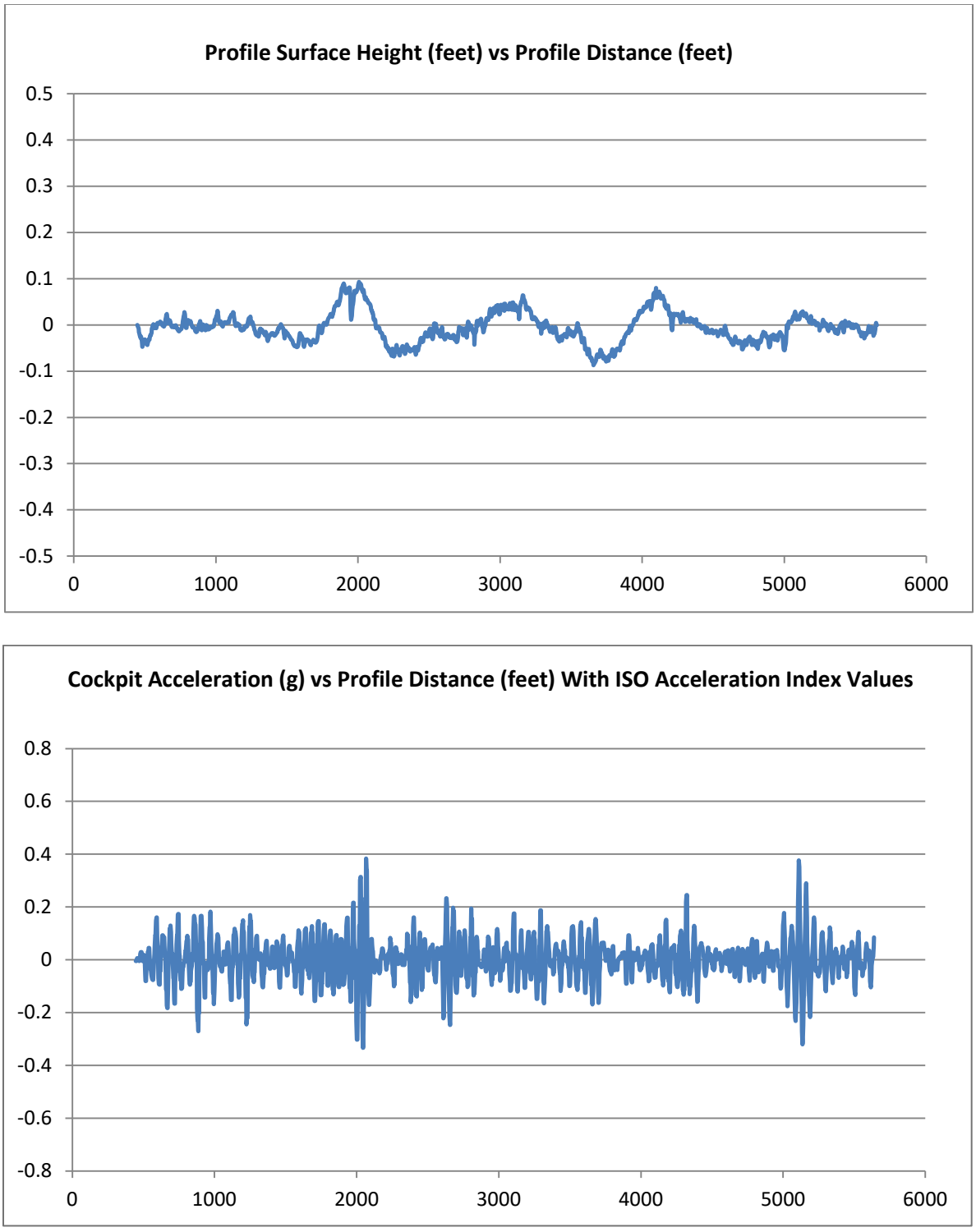

Figure D-48. Runway Profile 48—Profile Height, Cockpit Acceleration, and Acceleration ISO Indices

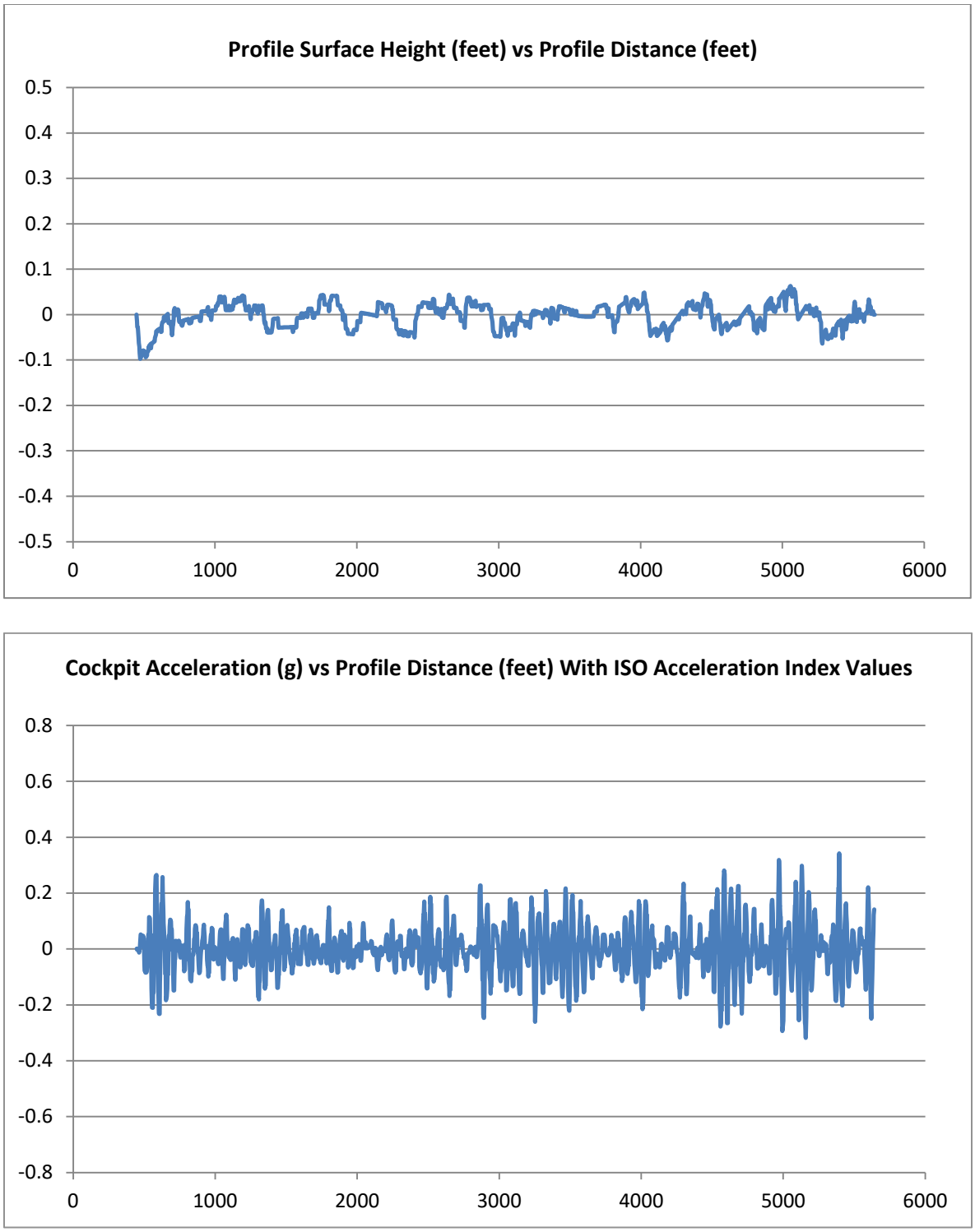

Figure D-49. Runway Profile 49—Profile Height, Cockpit Acceleration, and Acceleration ISO Indices

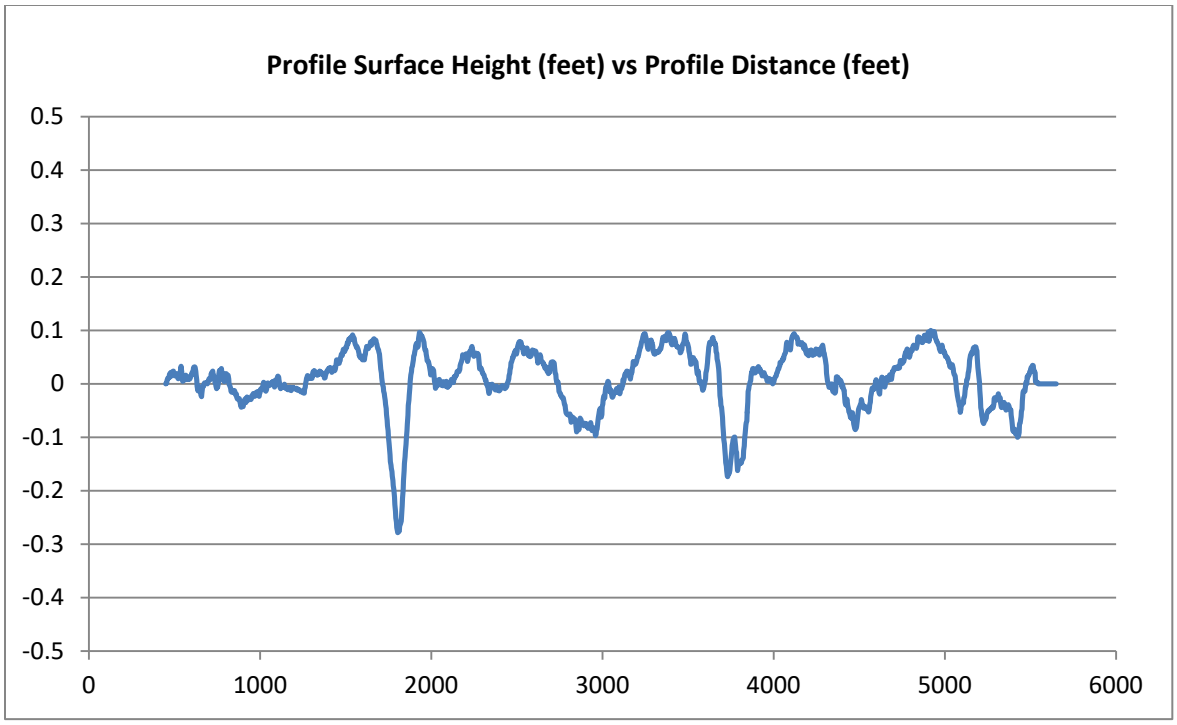

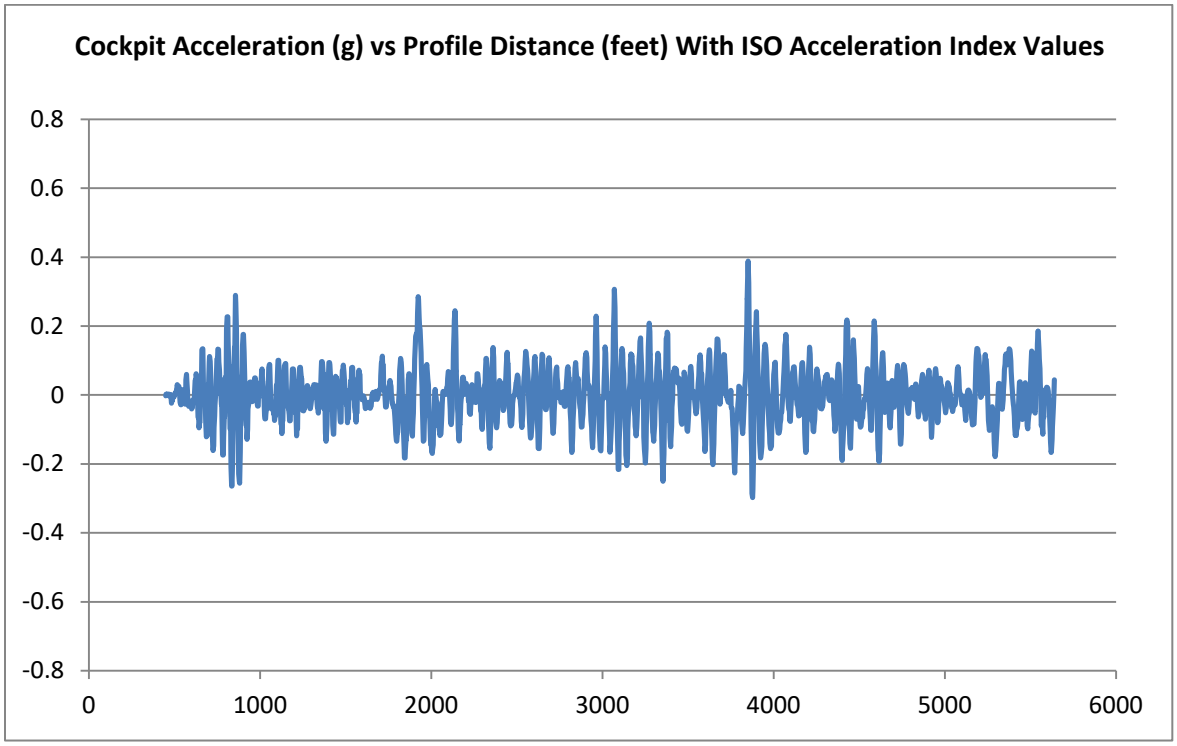

Figure D-50. Runway Profile 50—Profile Height, Cockpit Acceleration, and Acceleration ISO Indices

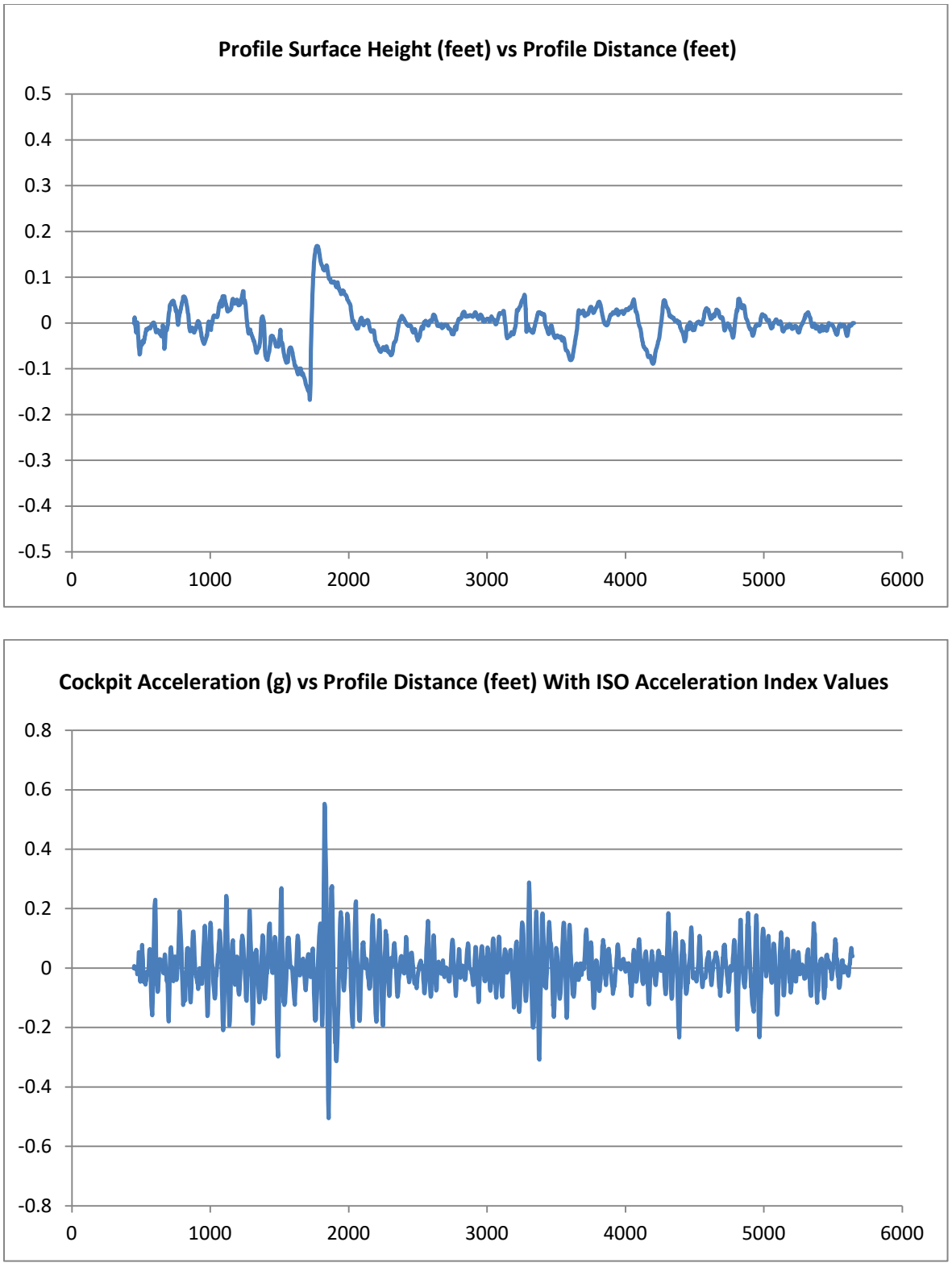

Figure D-51. Runway Profile 51—Profile Height, Cockpit Acceleration, and Acceleration ISO Indices

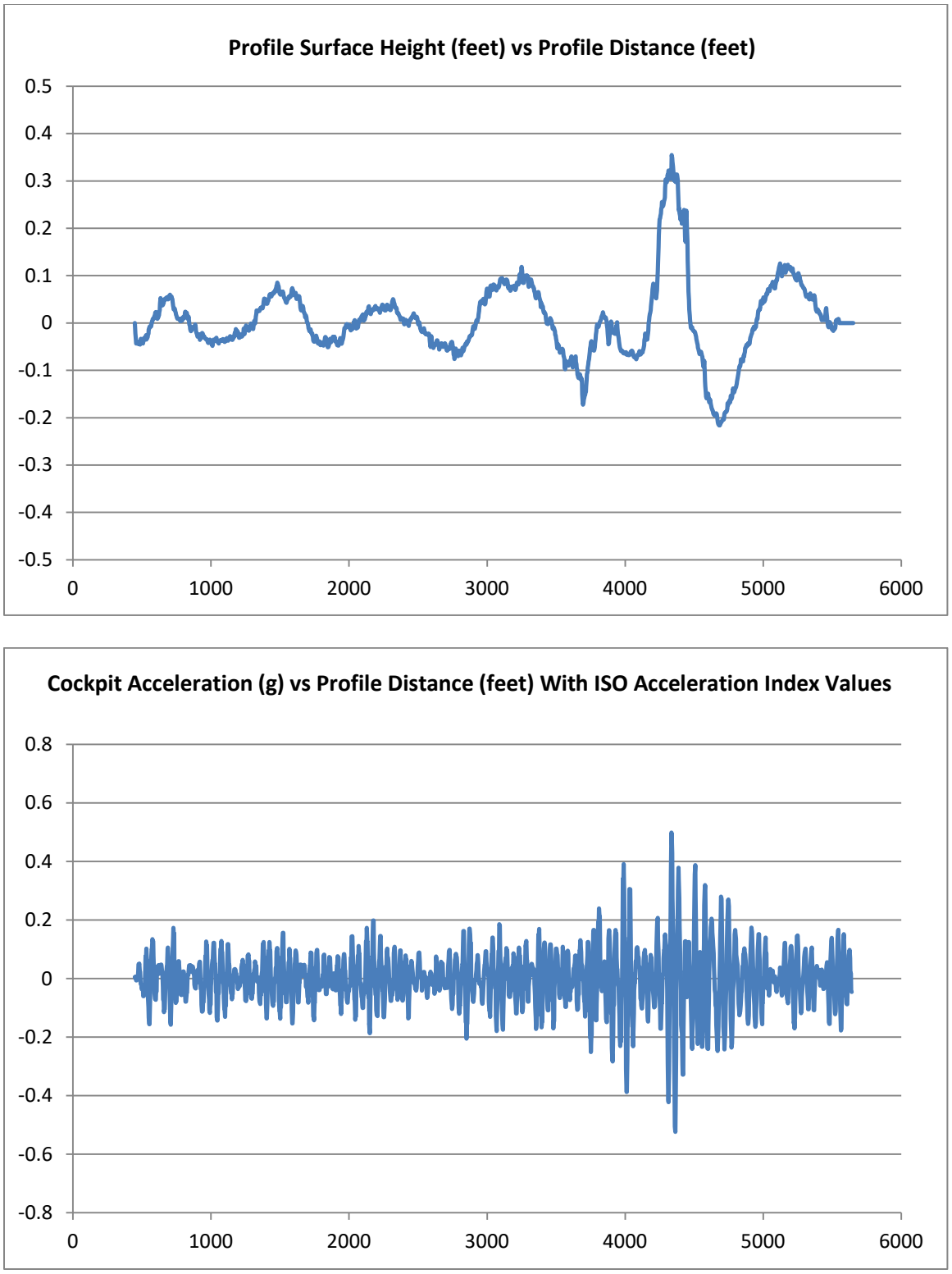

Figure D-52. Runway Profile 52—Profile Height, Cockpit Acceleration, and Acceleration ISO Indices

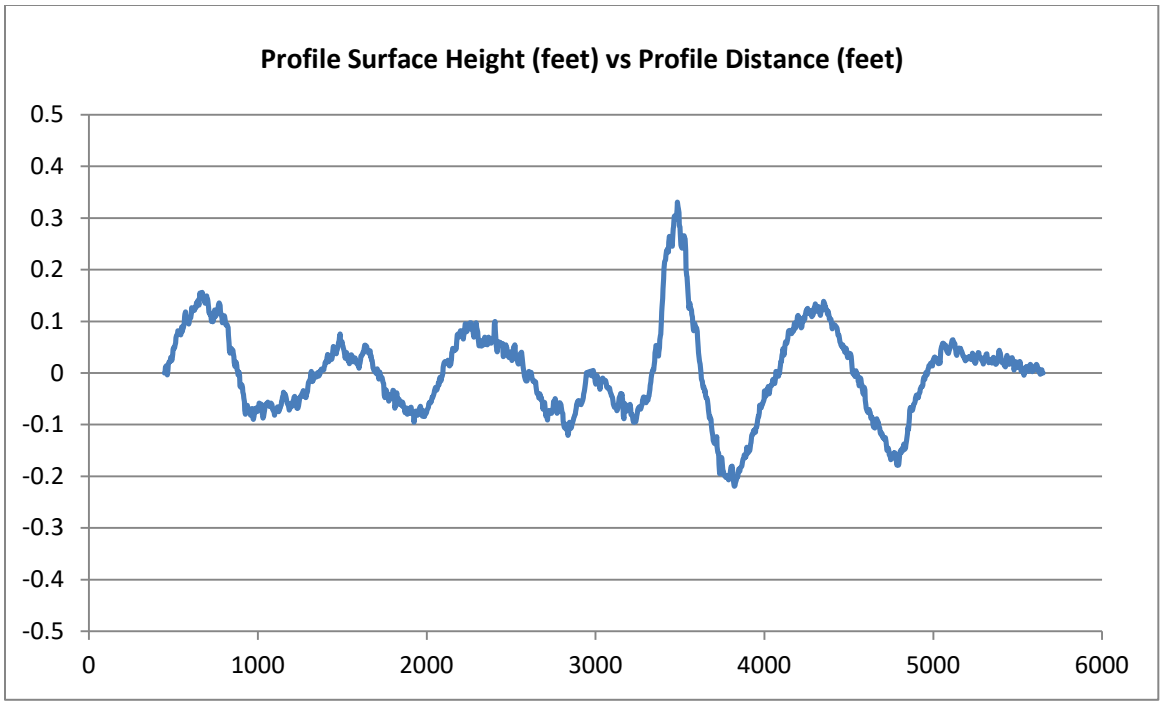

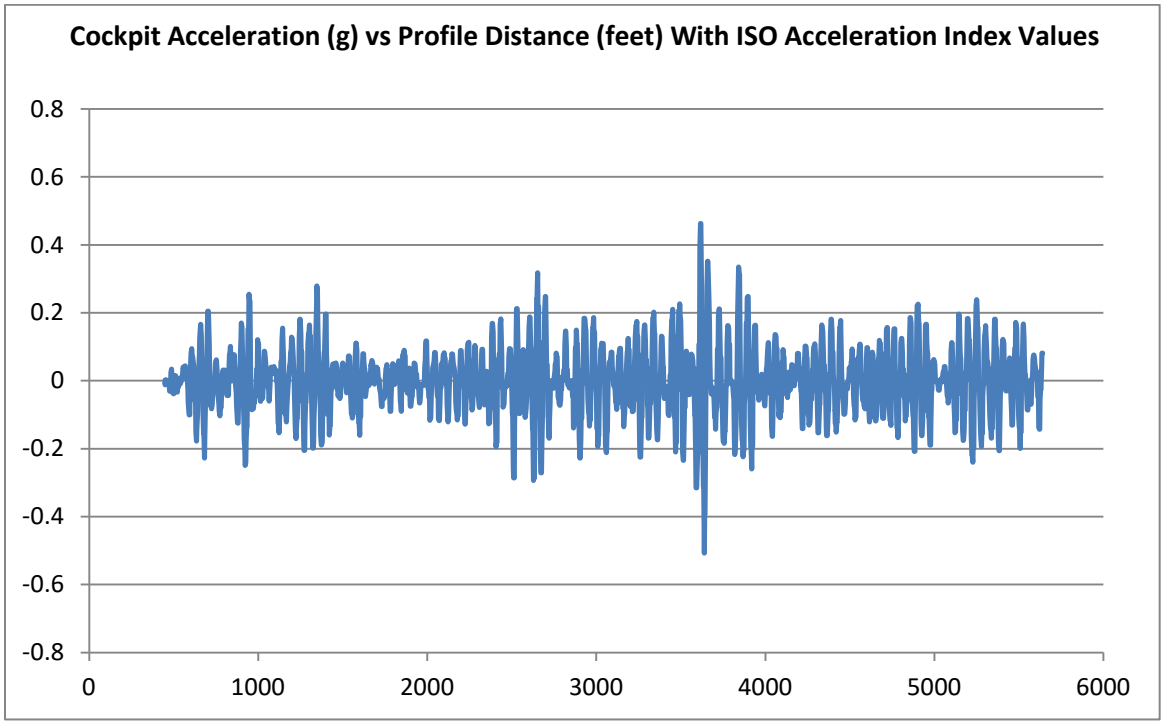

Figure D-53. Runway Profile 53—Profile Height, Cockpit Acceleration, and Acceleration ISO Indices

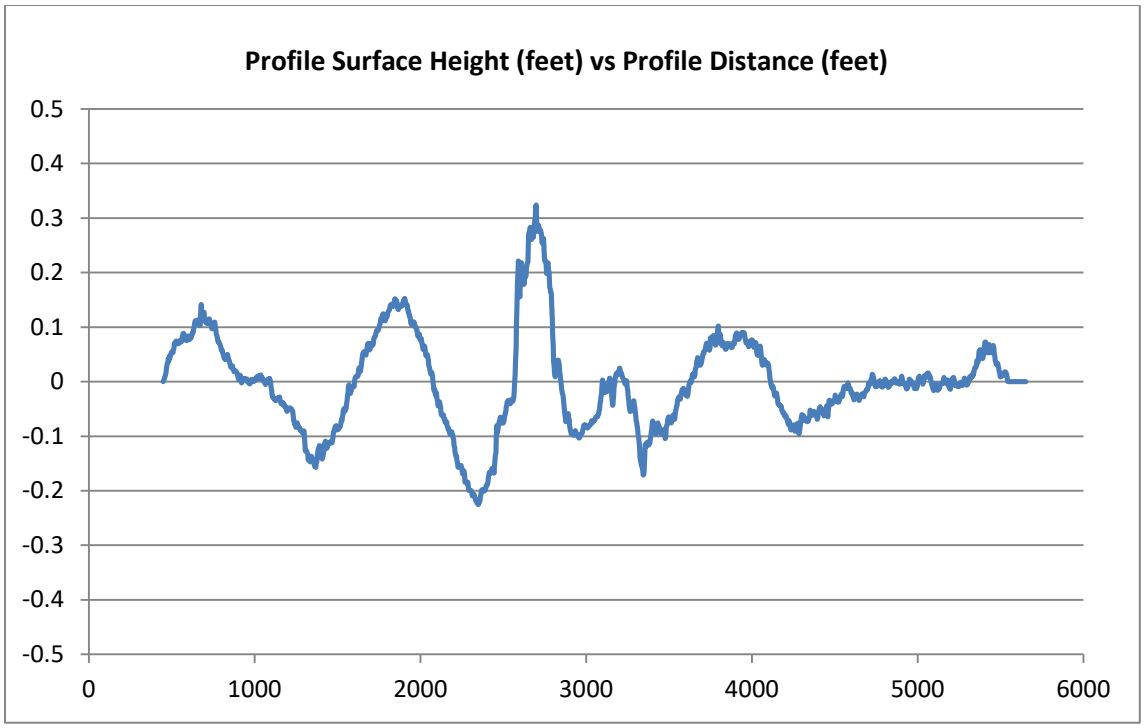

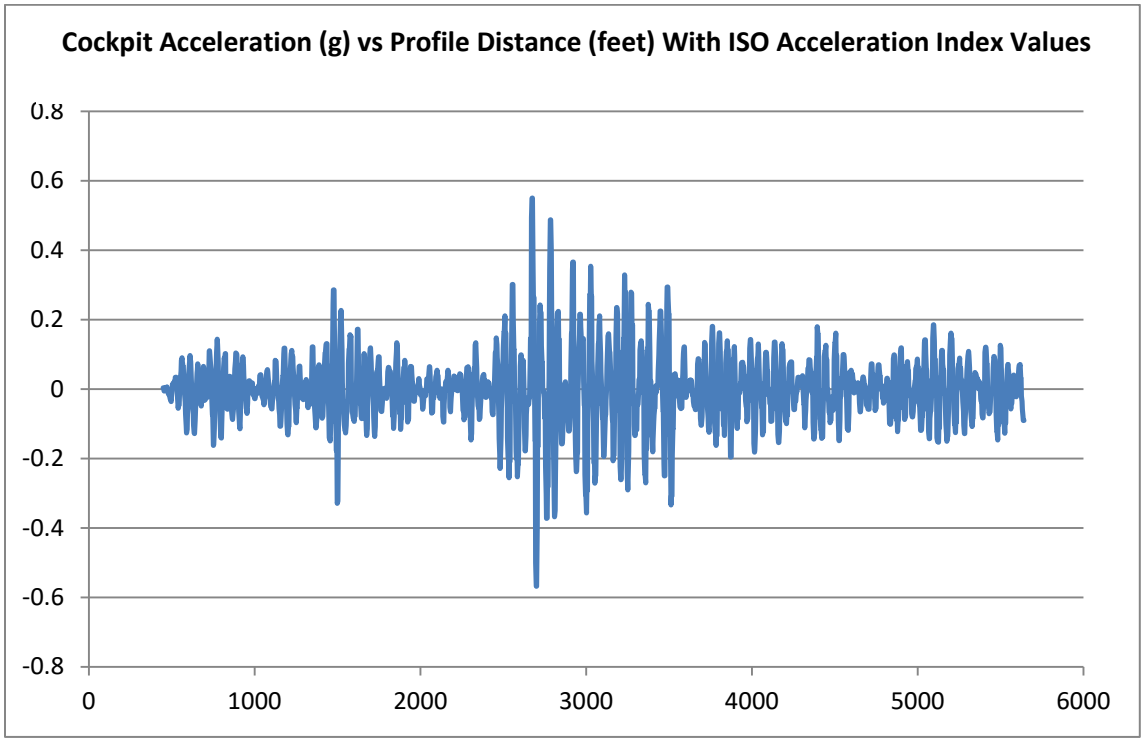

Figure D-54. Runway Profile 54—Profile Height, Cockpit Acceleration, and Acceleration ISO Indices

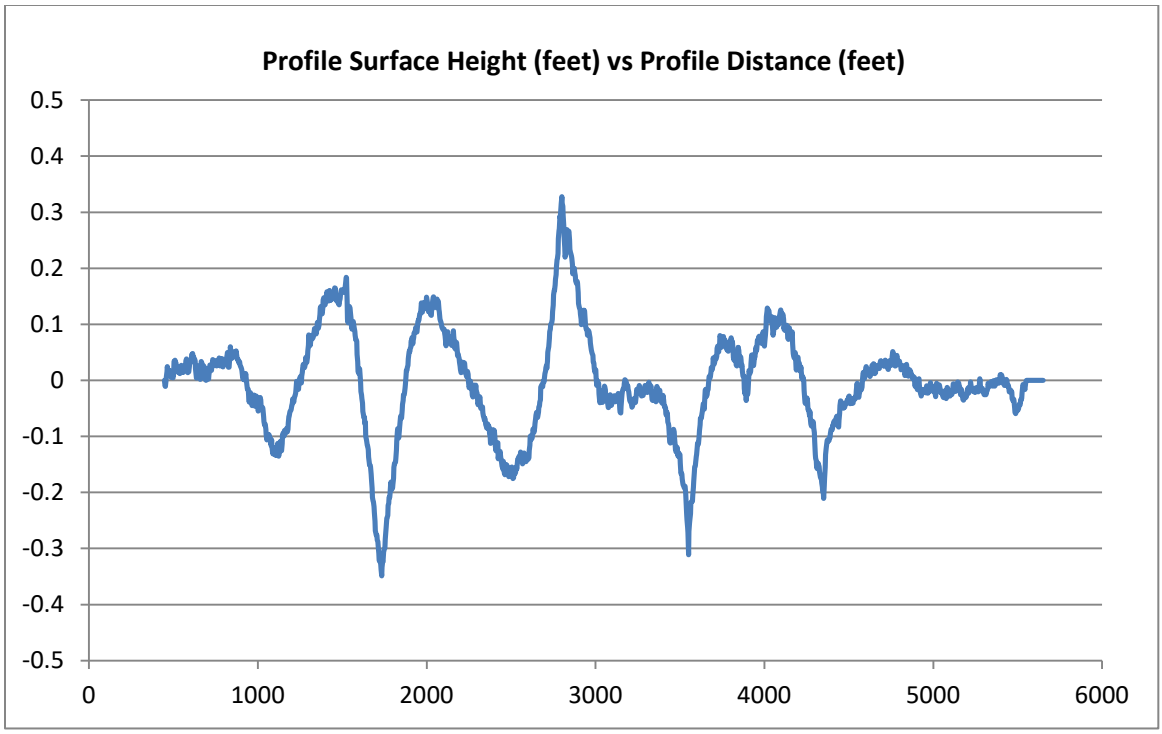

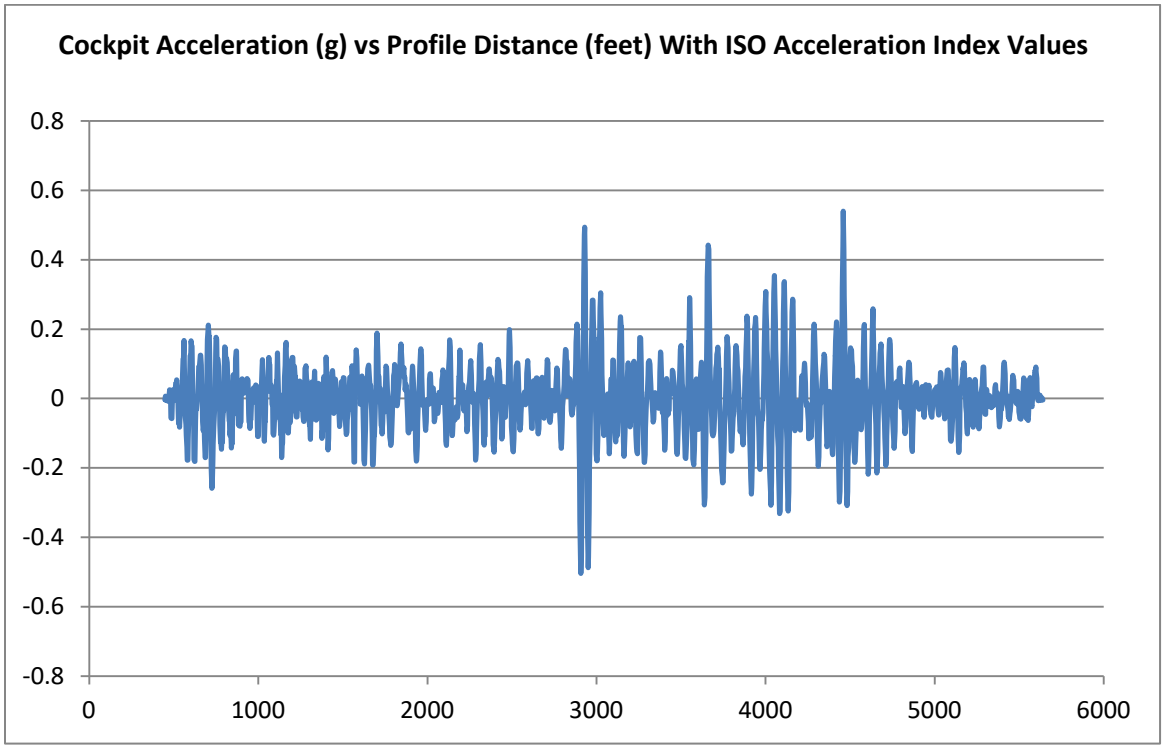

Figure D-55. Runway Profile 55—Profile Height, Cockpit Acceleration, and Acceleration ISO Indices

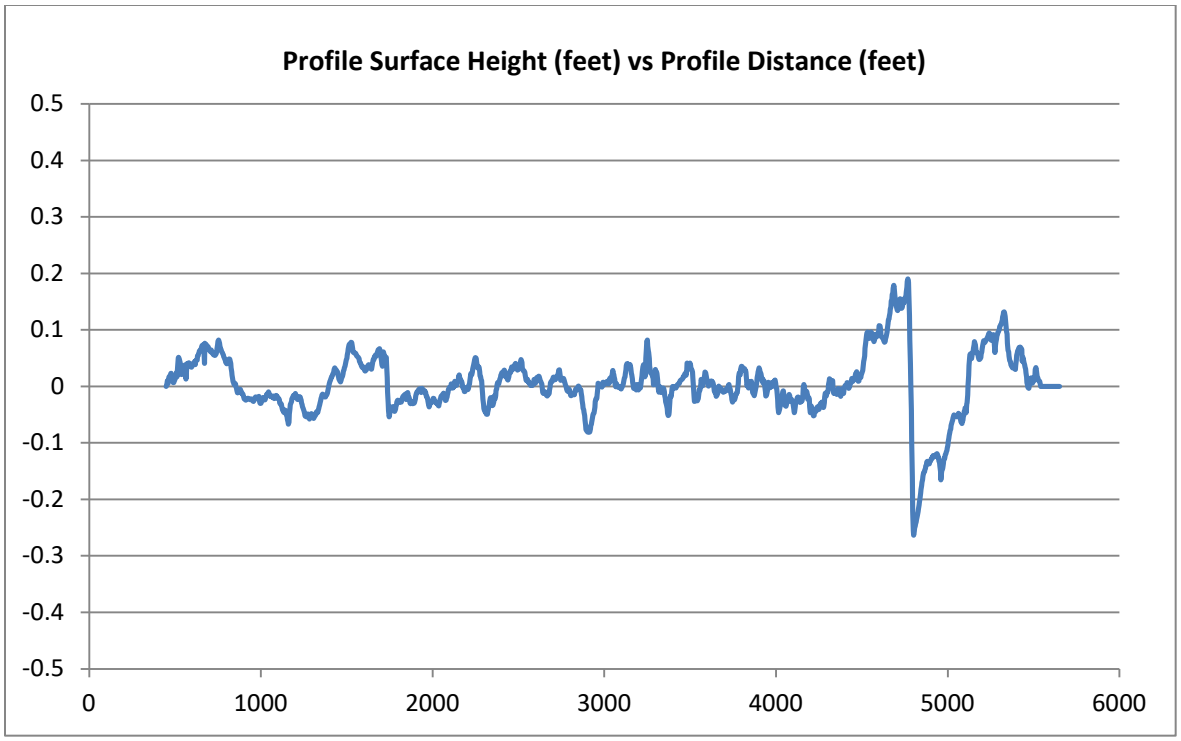

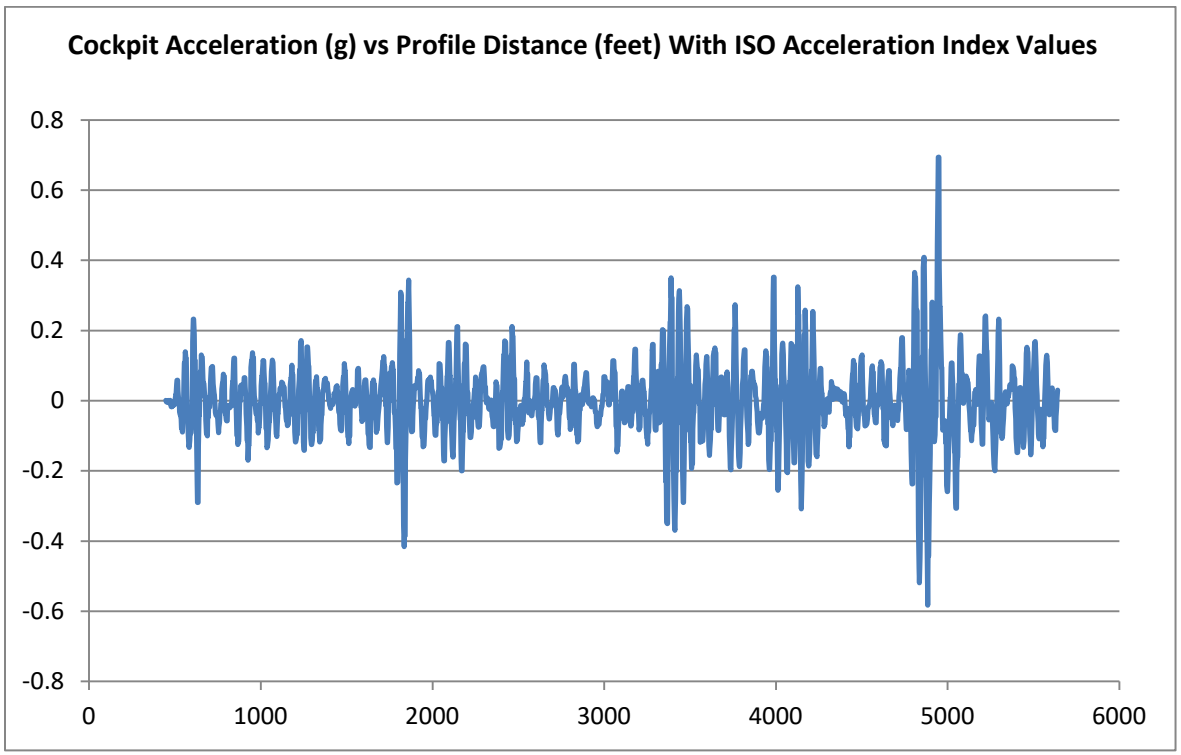

Figure D-56. Runway Profile 56—Profile Height, Cockpit Acceleration, and Acceleration ISO Indices

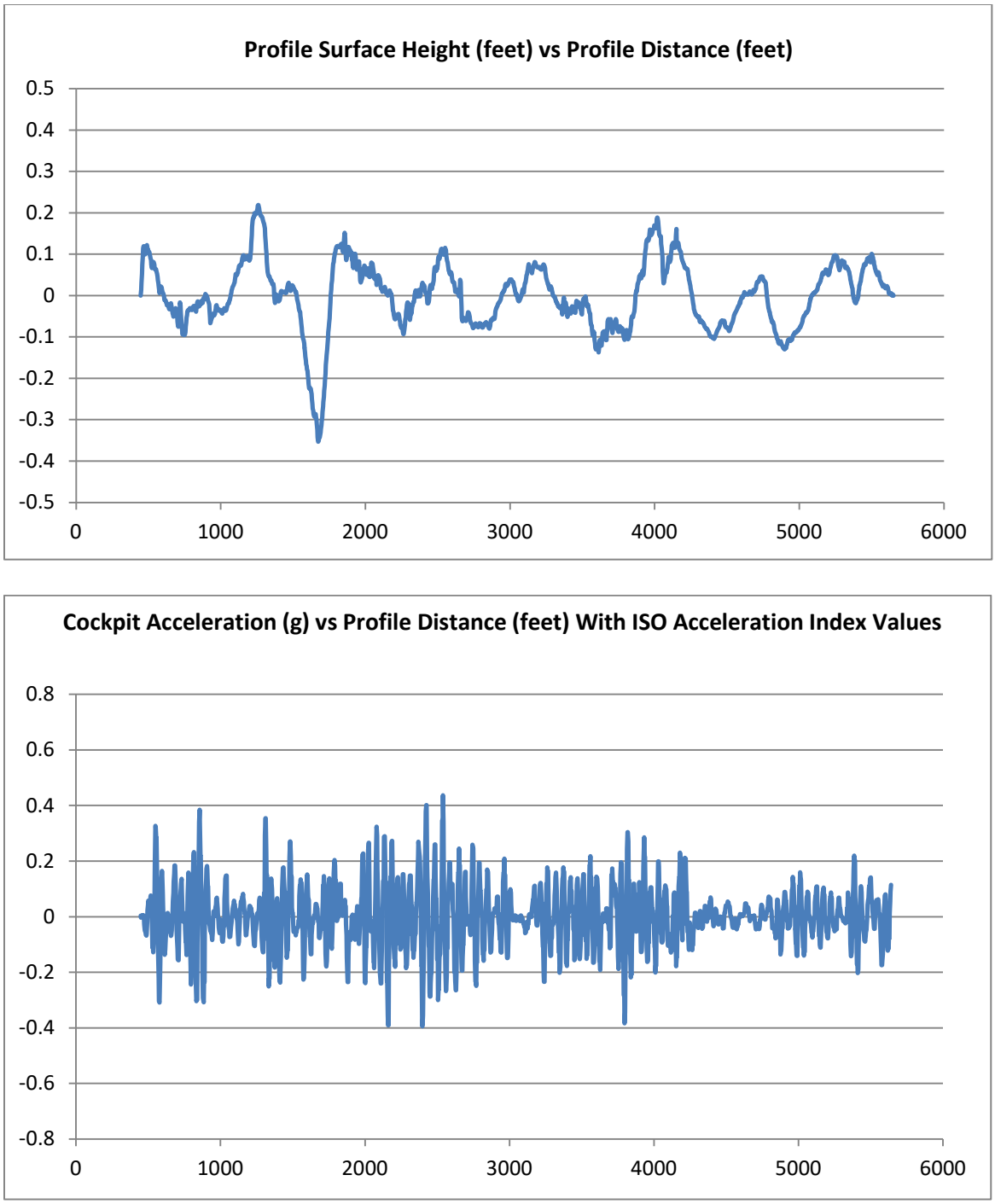

Figure D-57. Runway Profile 57—Profile Height, Cockpit Acceleration, and Acceleration ISO Indices

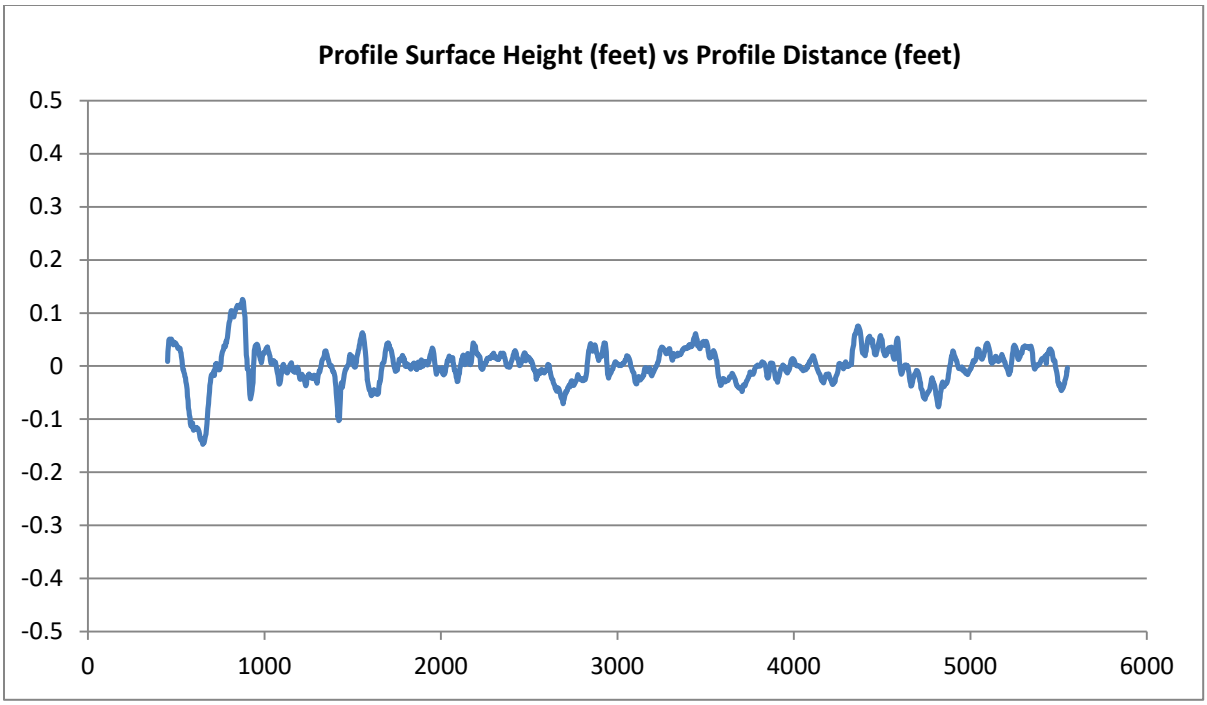

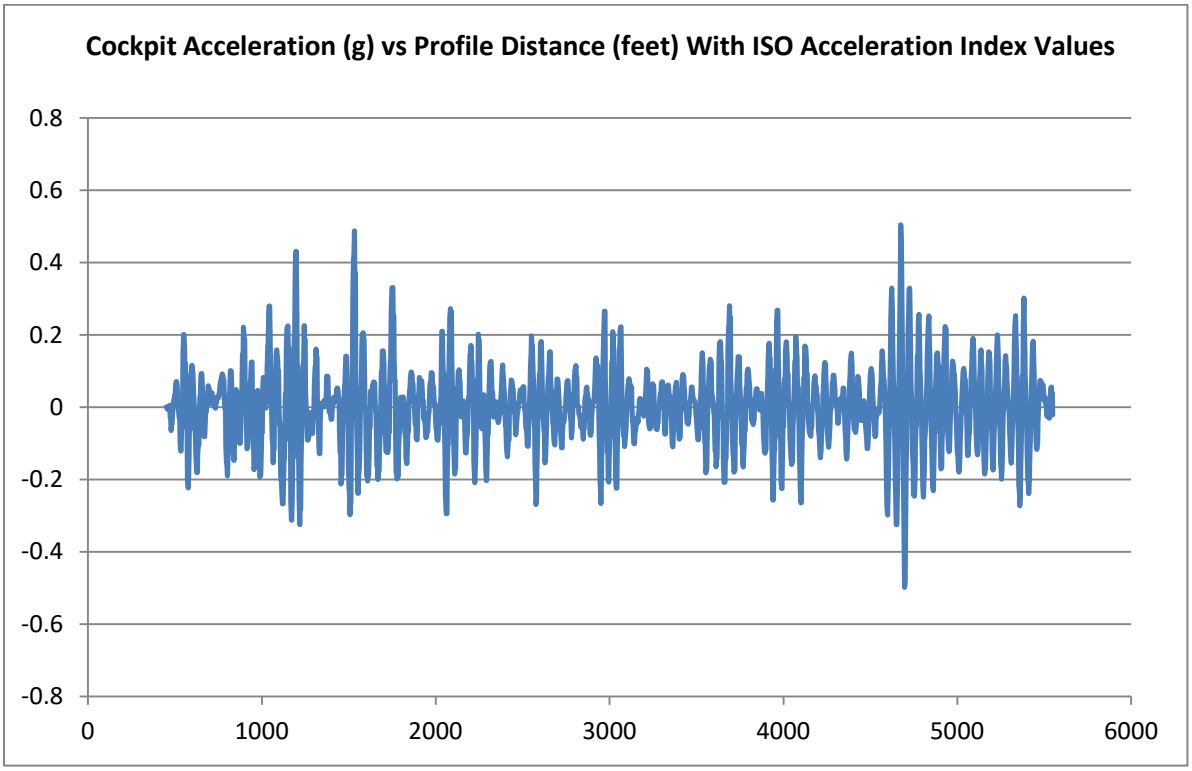

Figure D-58. Runway Profile 58—Profile Height, Cockpit Acceleration, and Acceleration ISO Indices

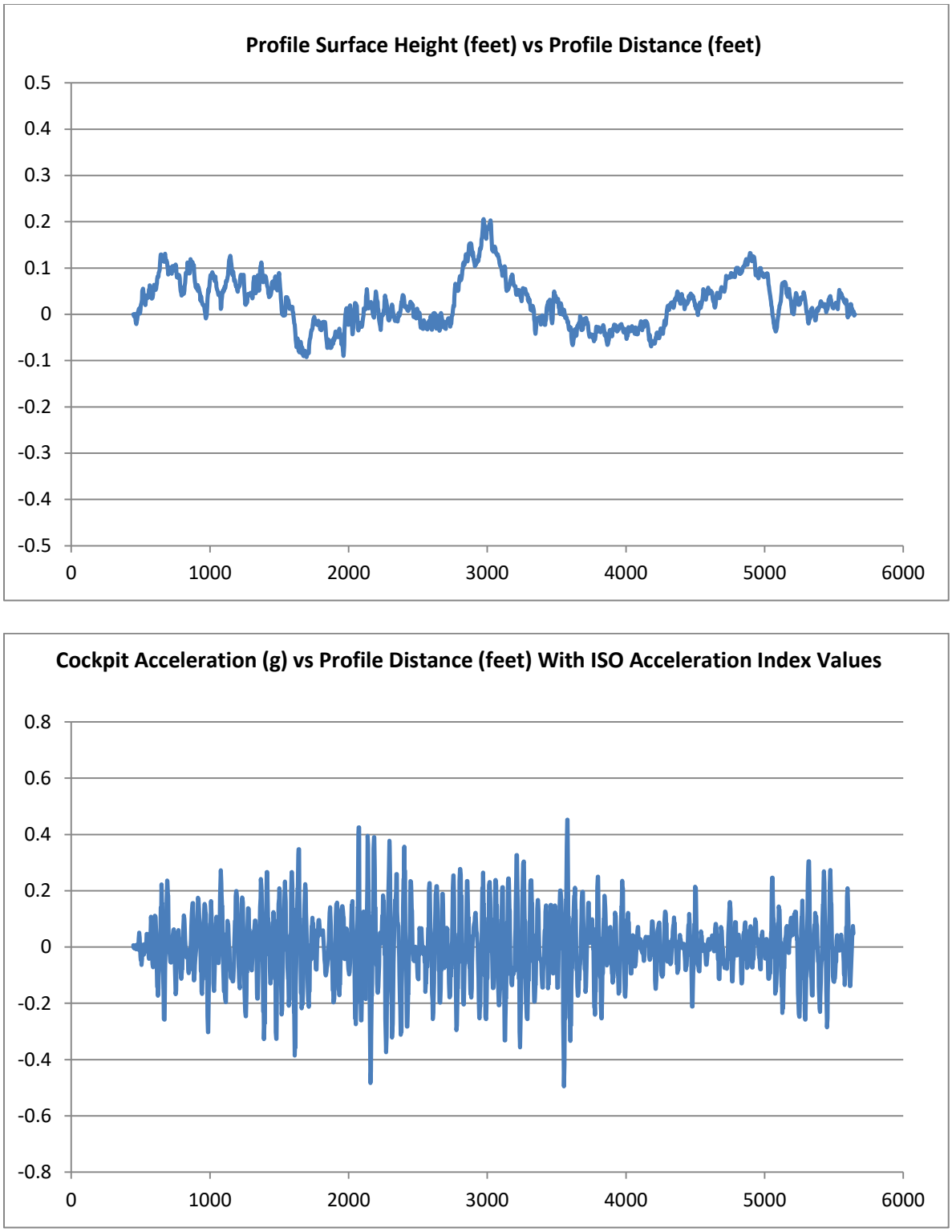

Figure D-59. Runway Profile 59—Profile Height, Cockpit Acceleration, and Acceleration ISO Indices

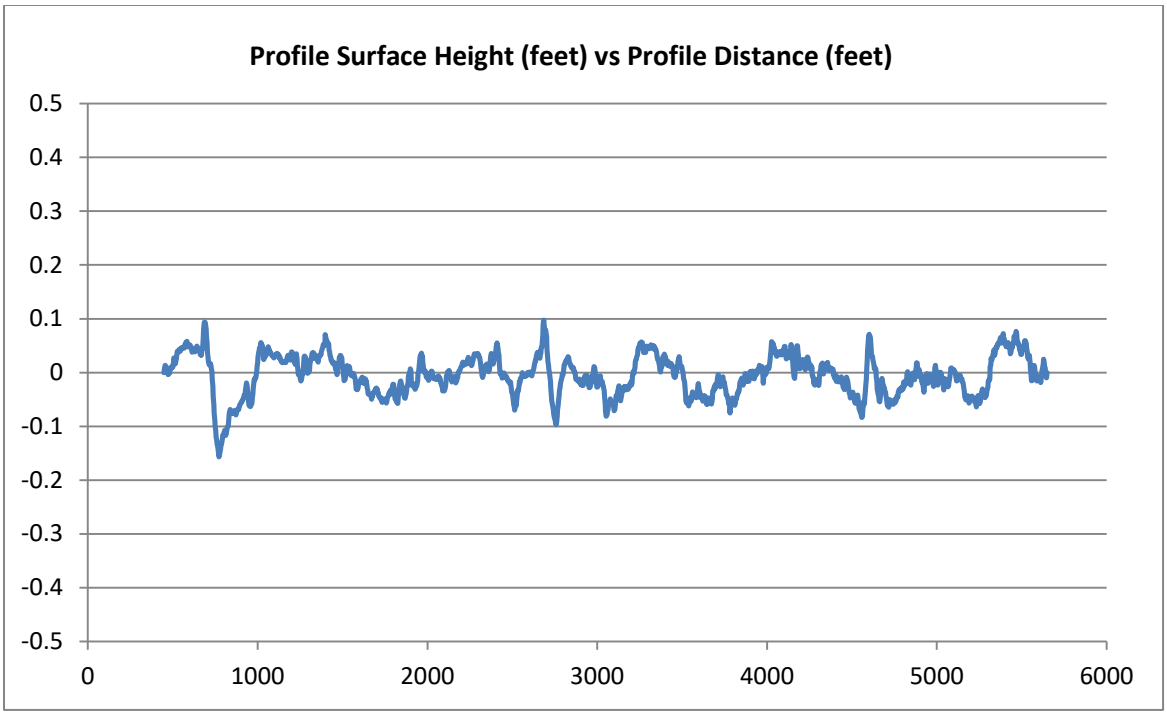

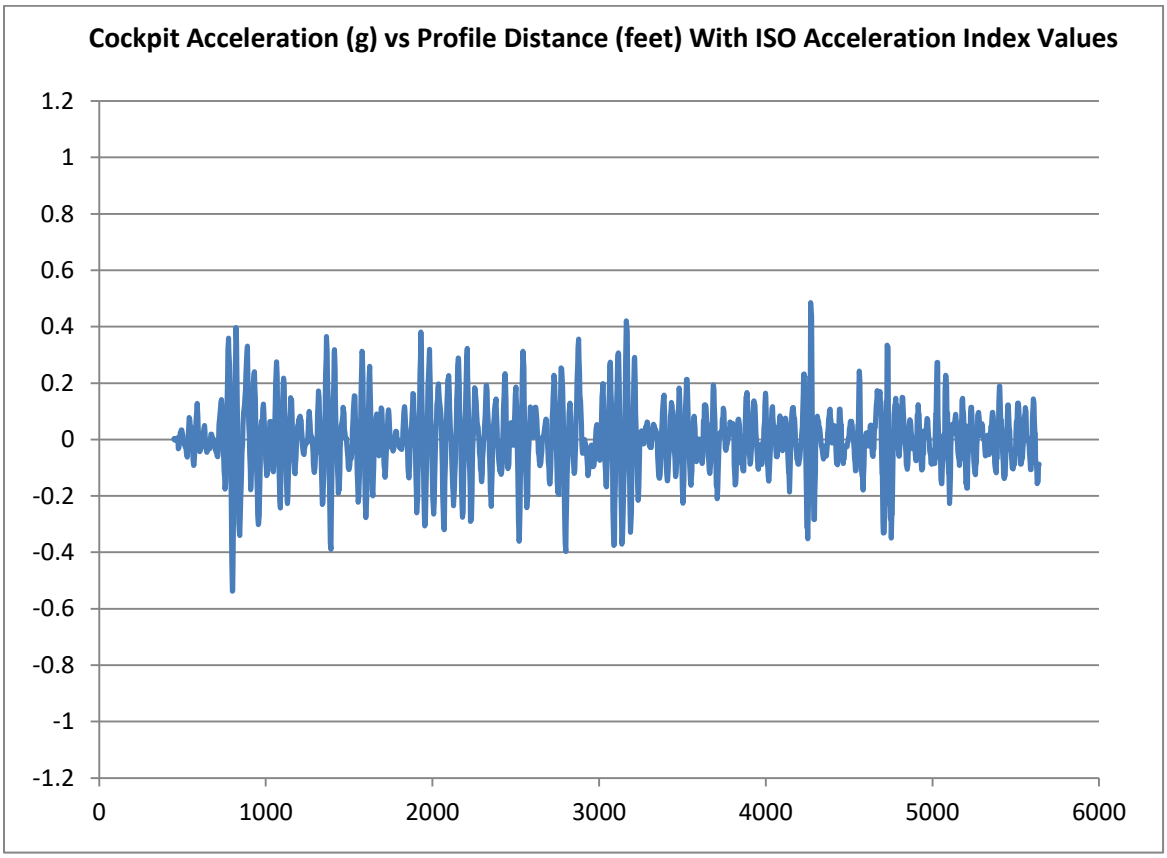

Figure D-60. Runway Profile 60—Profile Height, Cockpit Acceleration, and Acceleration ISO Indices

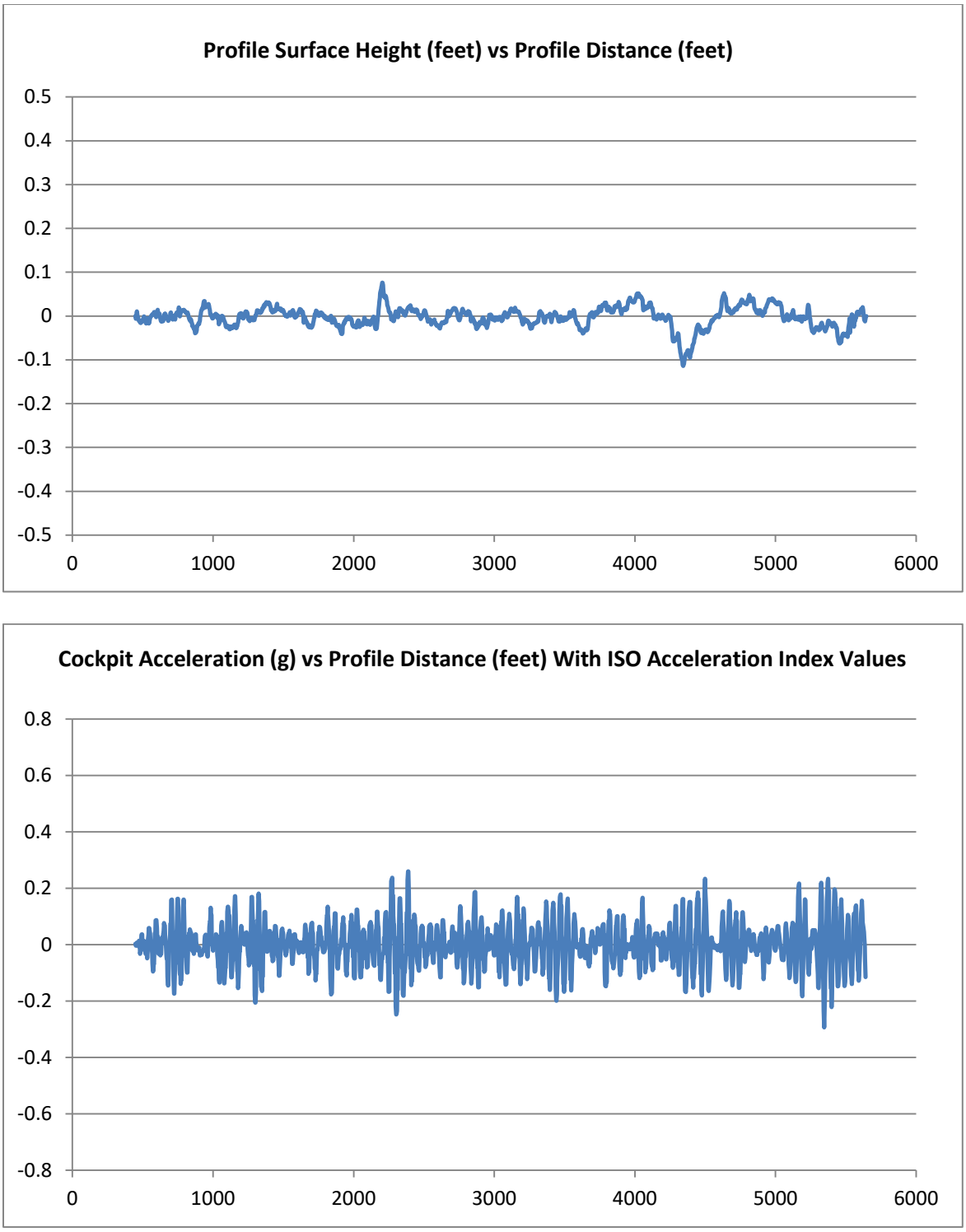

Figure D-61. Runway Profile 61—Profile Height, Cockpit Acceleration, and Acceleration ISO Indices

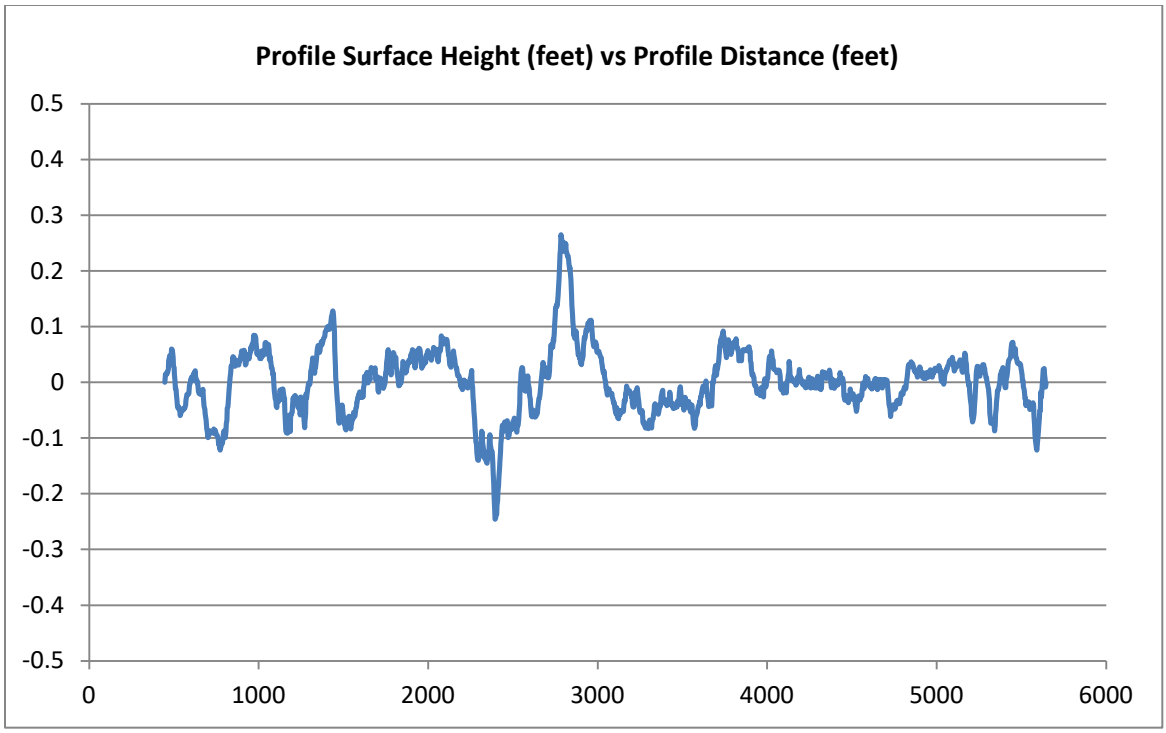

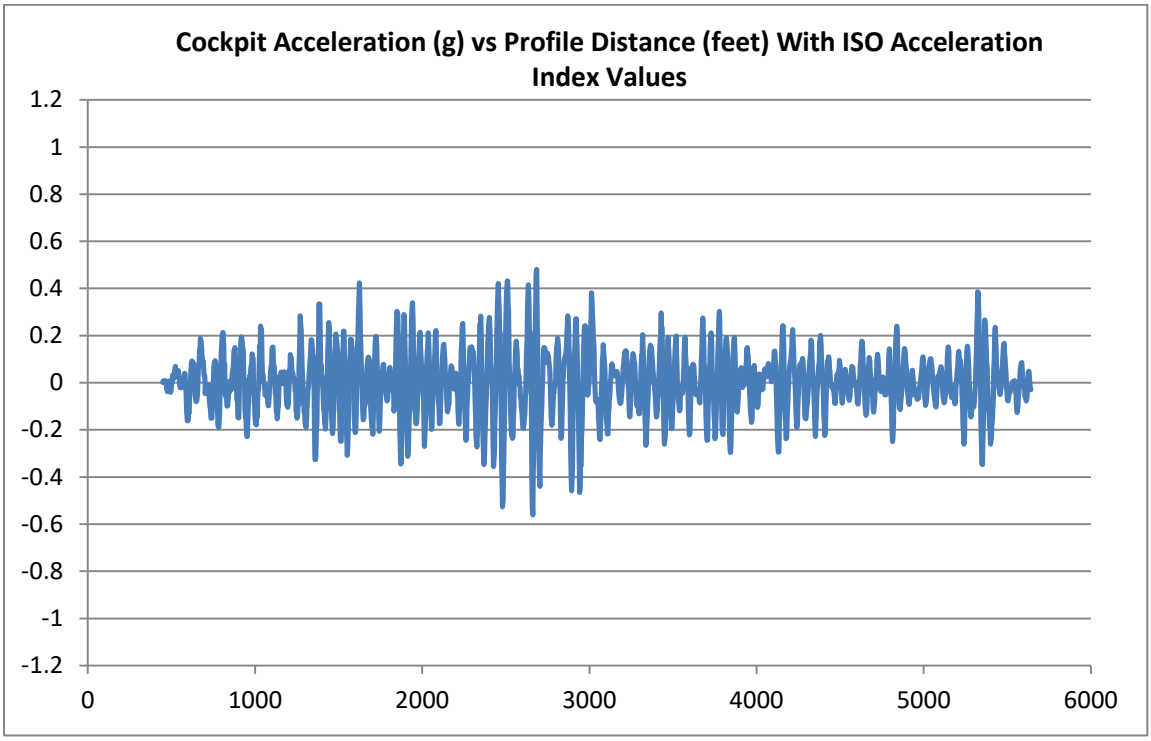

Figure D-62. Runway Profile 62—Profile Height, Cockpit Acceleration, and Acceleration ISO Indices

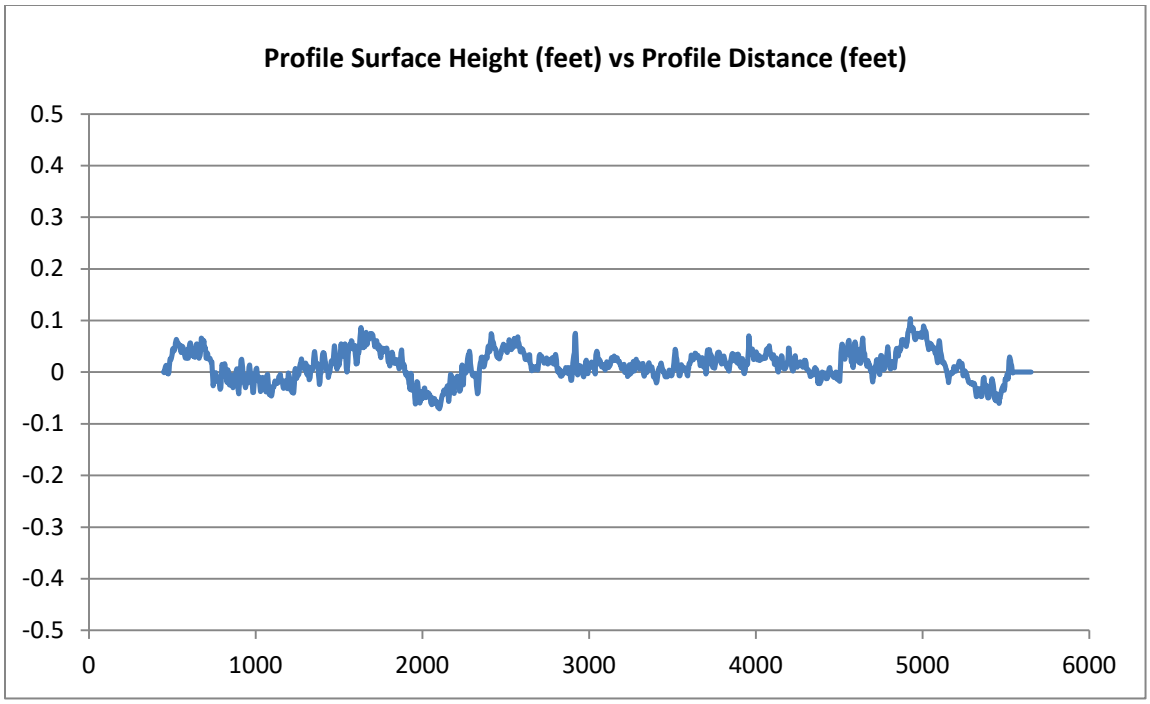

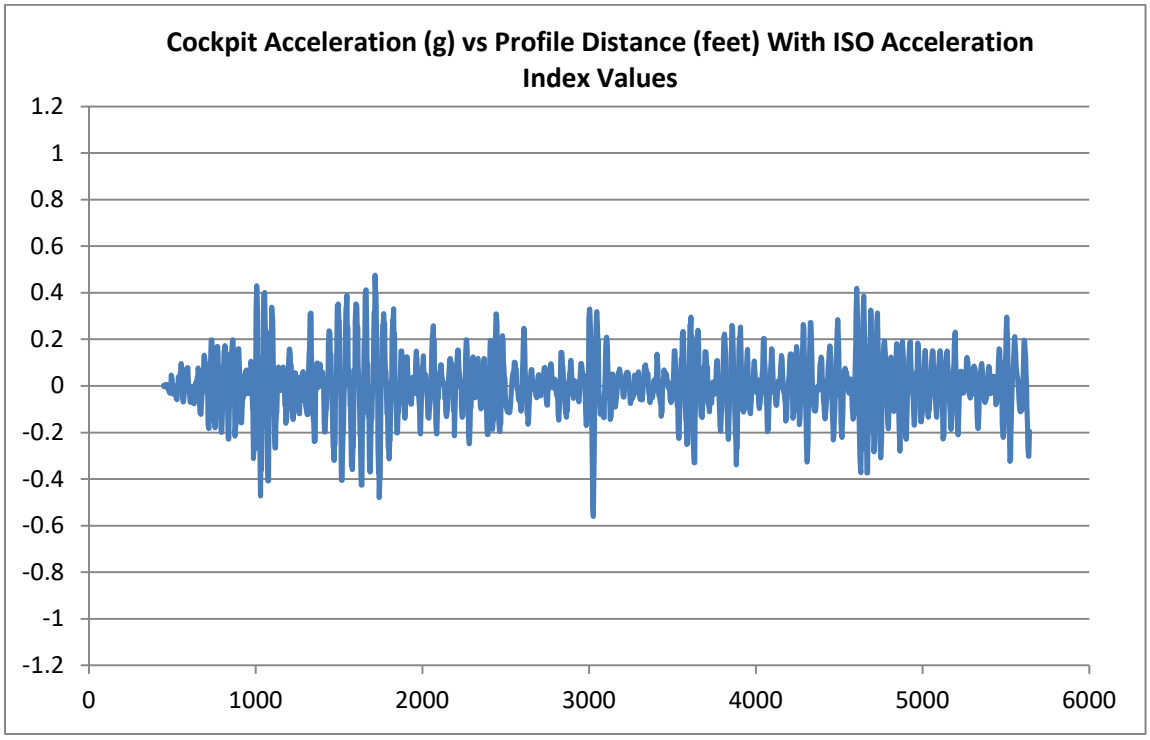

Figure D-63. Runway Profile 63—Profile Height, Cockpit Acceleration, and Acceleration ISO Indices

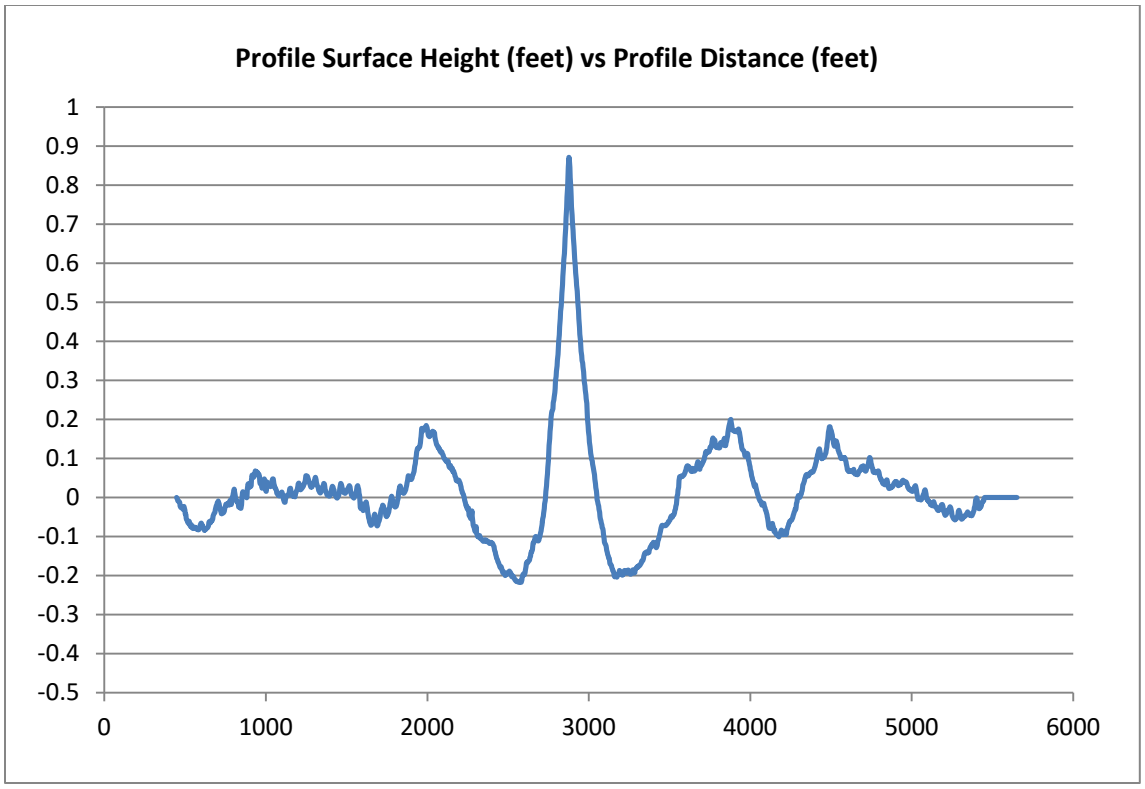

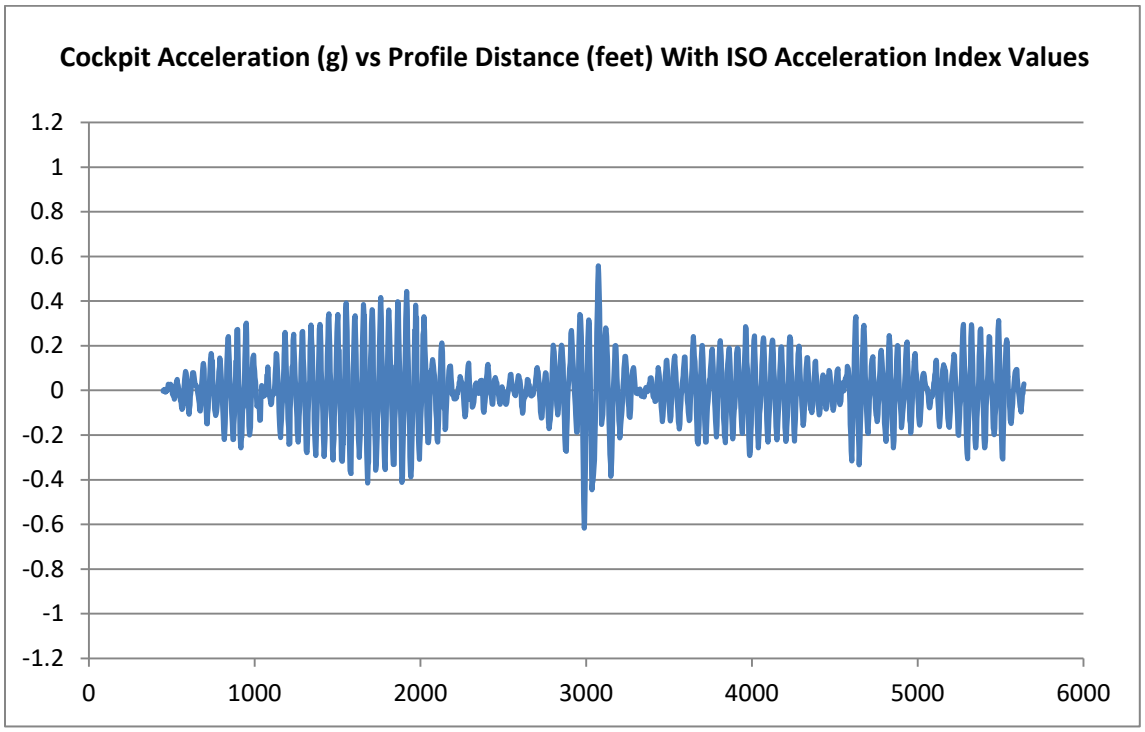

Figure D-64. Runway Profile 64—Profile Height, Cockpit Acceleration, and Acceleration ISO Indices

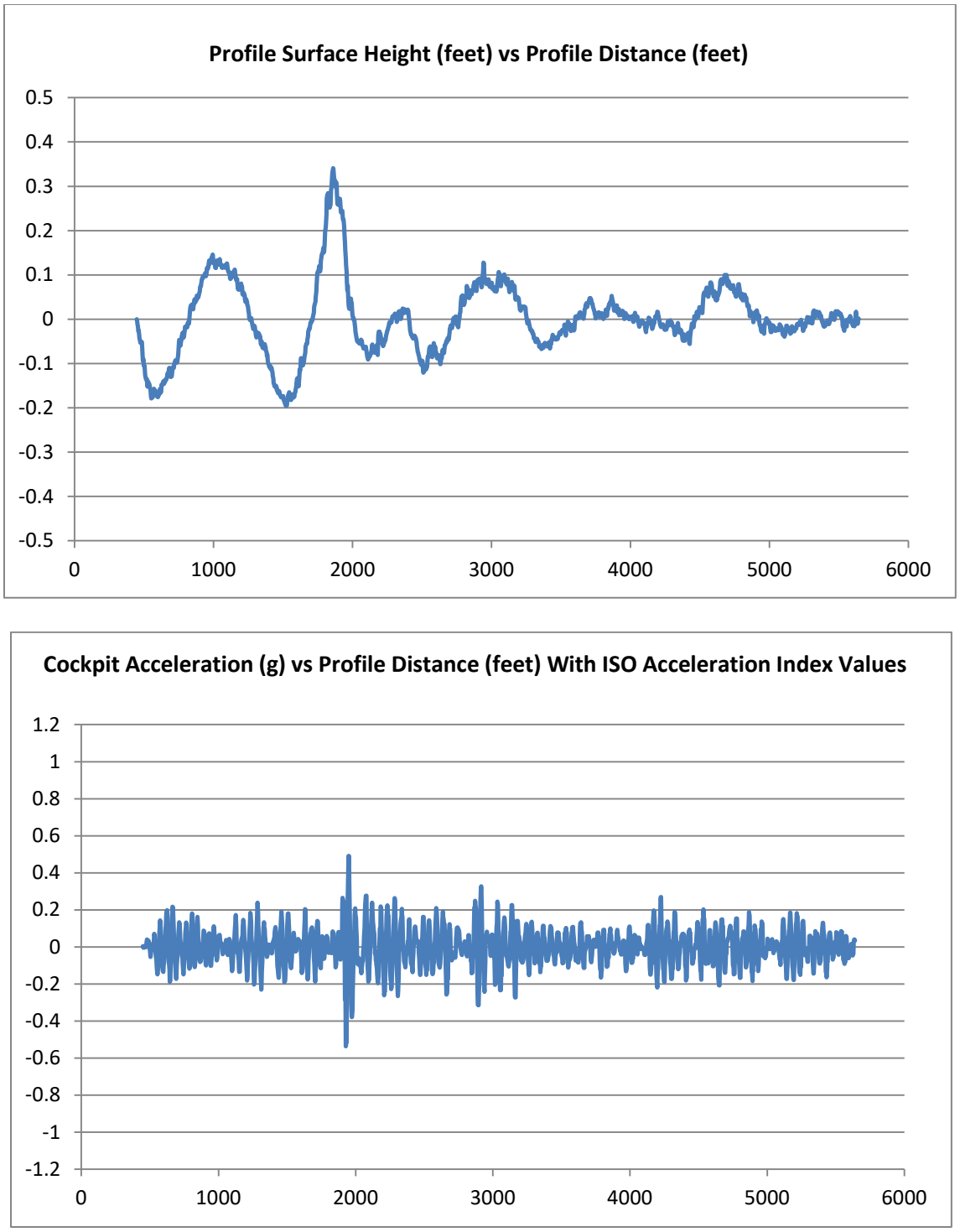

Figure D-65. Runway Profile 65—Profile Height, Cockpit Acceleration, and Acceleration ISO Indices

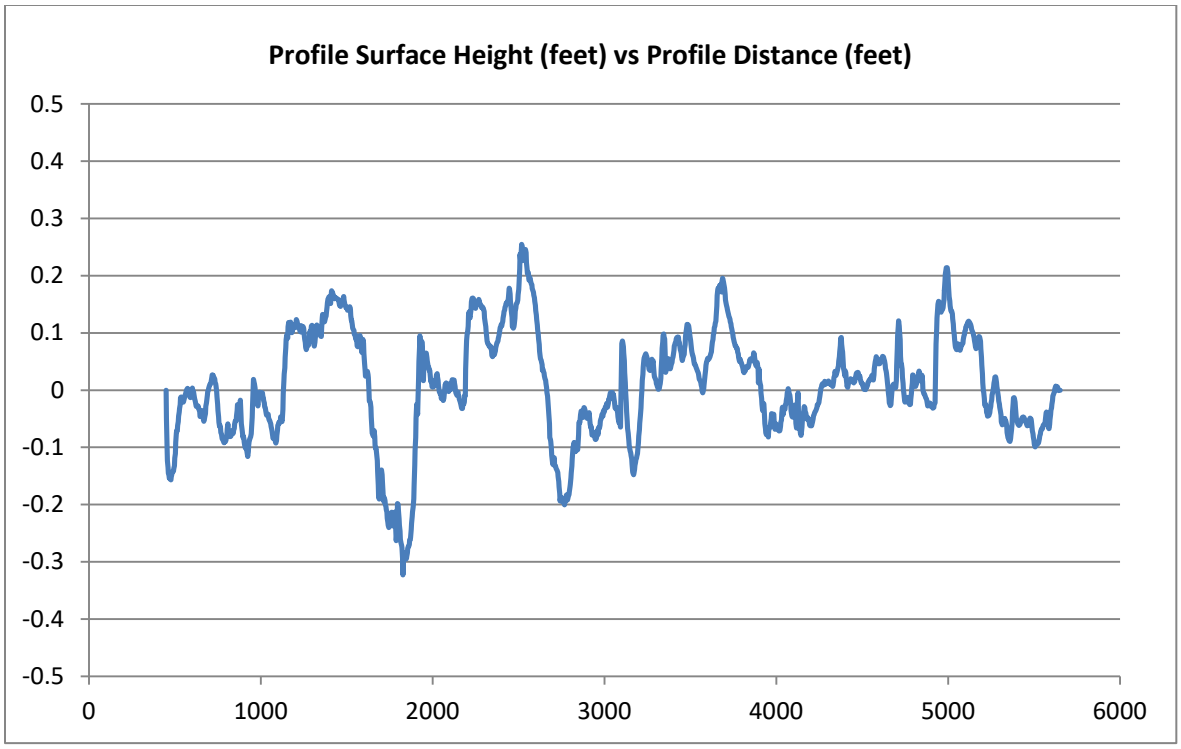

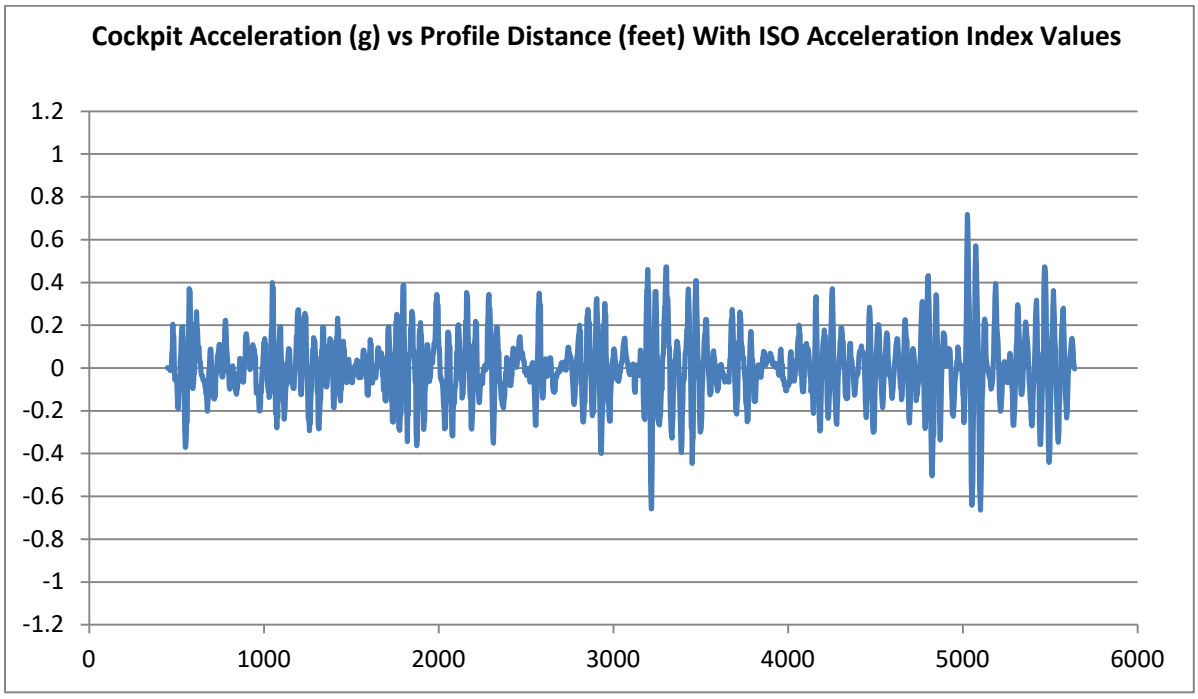

Figure D-66. Runway Profile 66—Profile Height, Cockpit Acceleration, and Acceleration ISO Indices

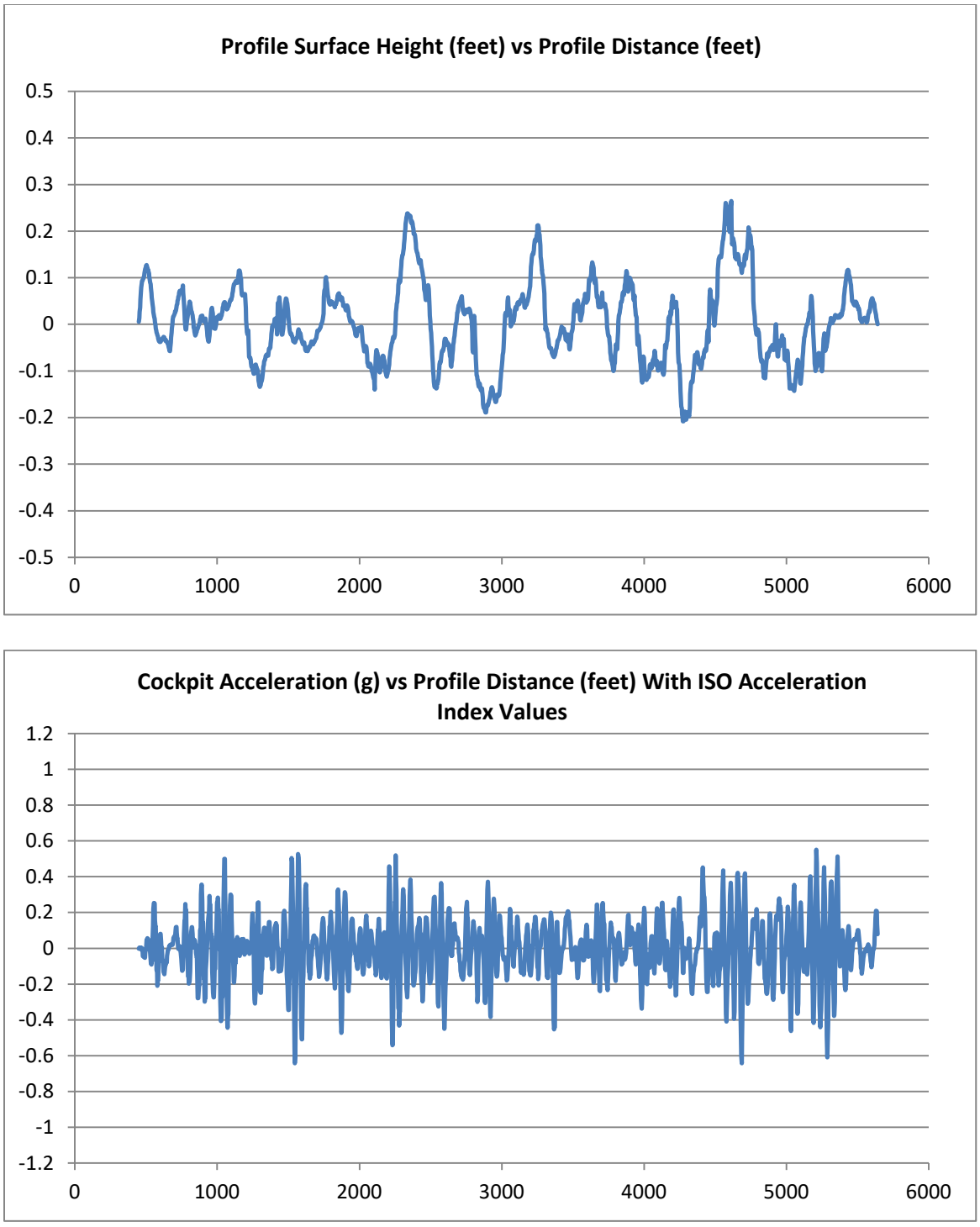

Figure D-67. Runway Profile 67—Profile Height, Cockpit Acceleration, and Acceleration ISO Indices

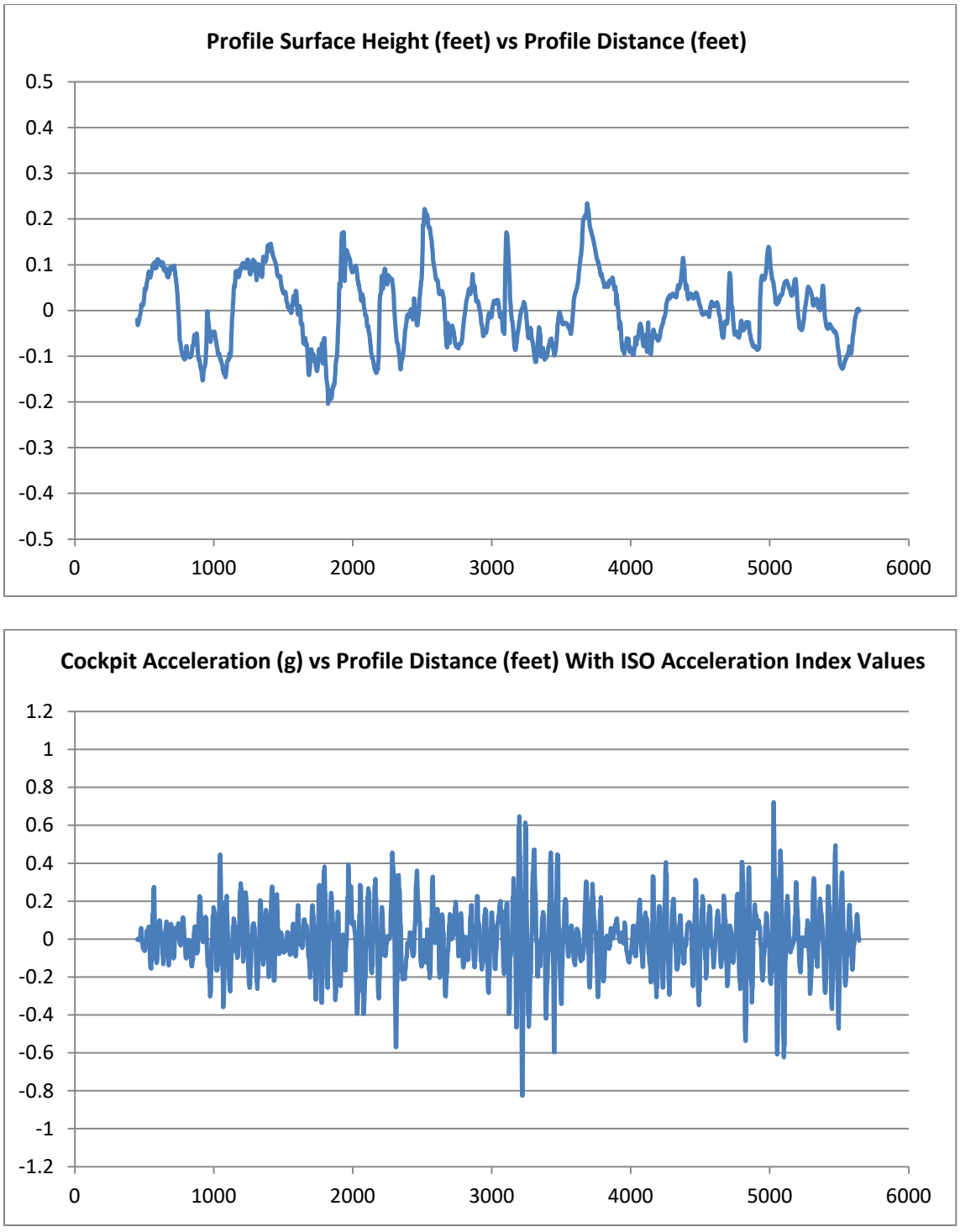

Figure D-68. Runway Profile 68—Profile Height, Cockpit Acceleration, and Acceleration ISO Indices

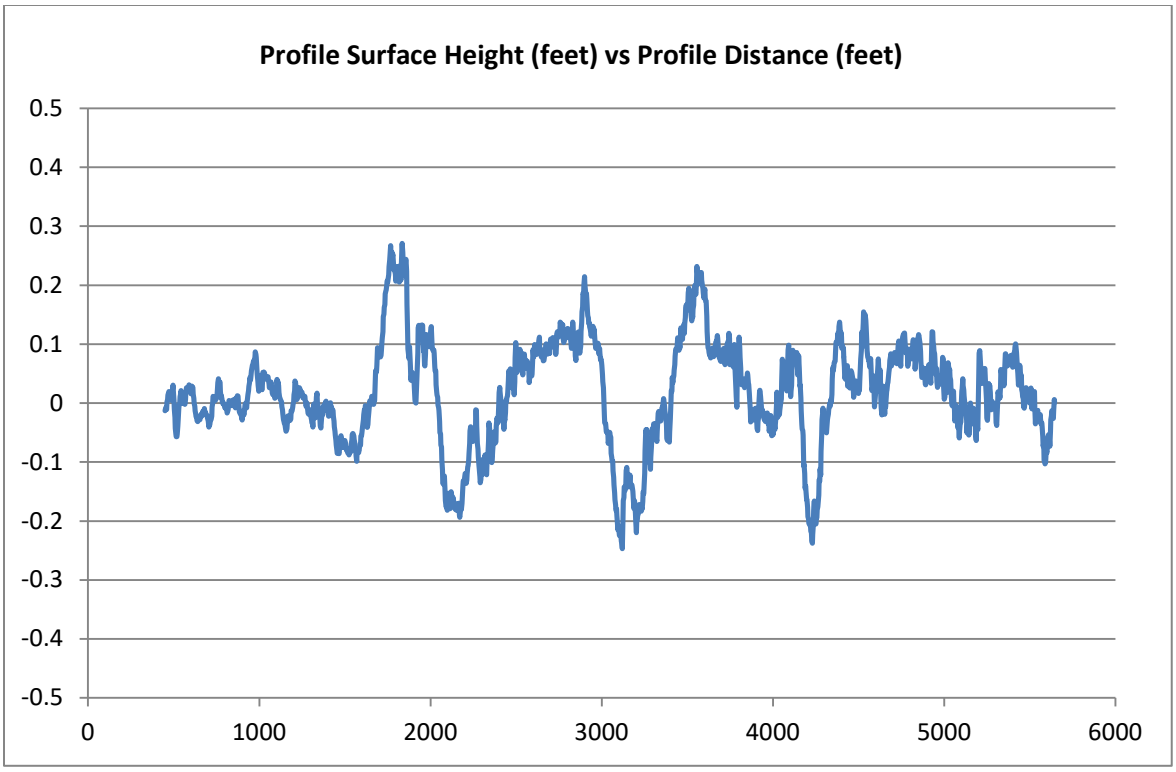

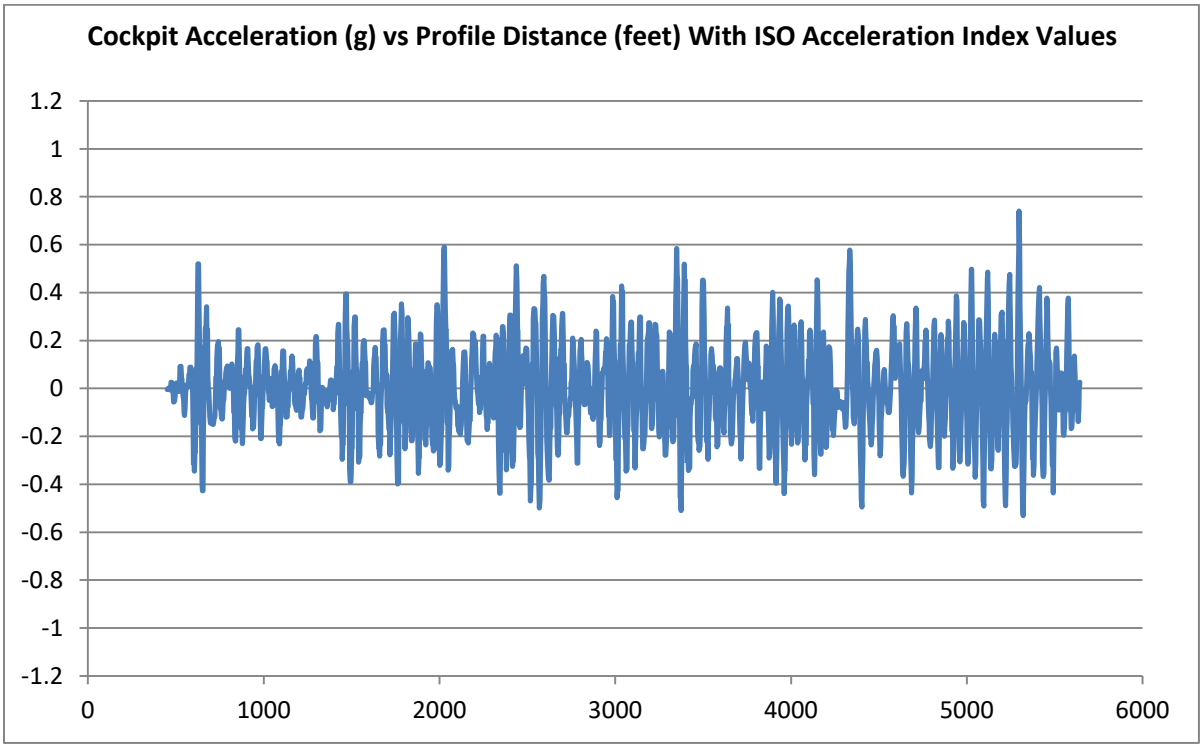

Figure D-69. Runway Profile 69—Profile Height, Cockpit Acceleration, and Acceleration ISO Indices

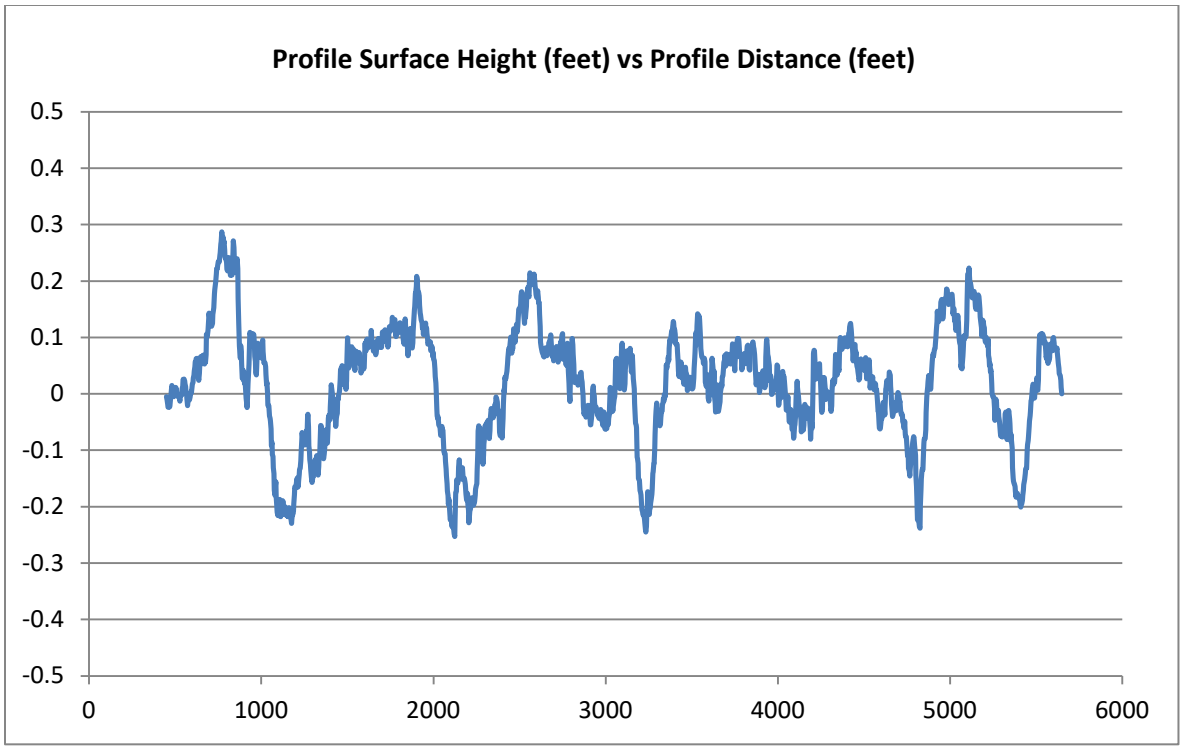

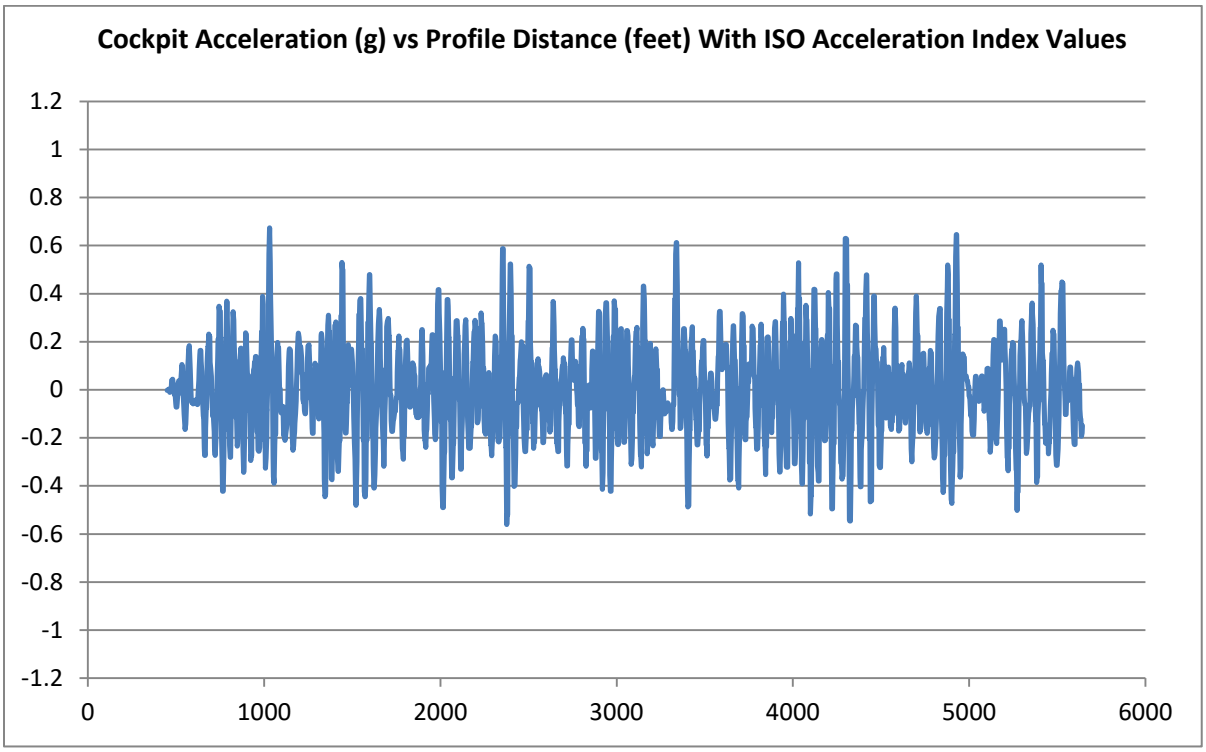

Figure D-70. Runway Profile 70—Profile Height, Cockpit Acceleration, and Acceleration ISO Indices

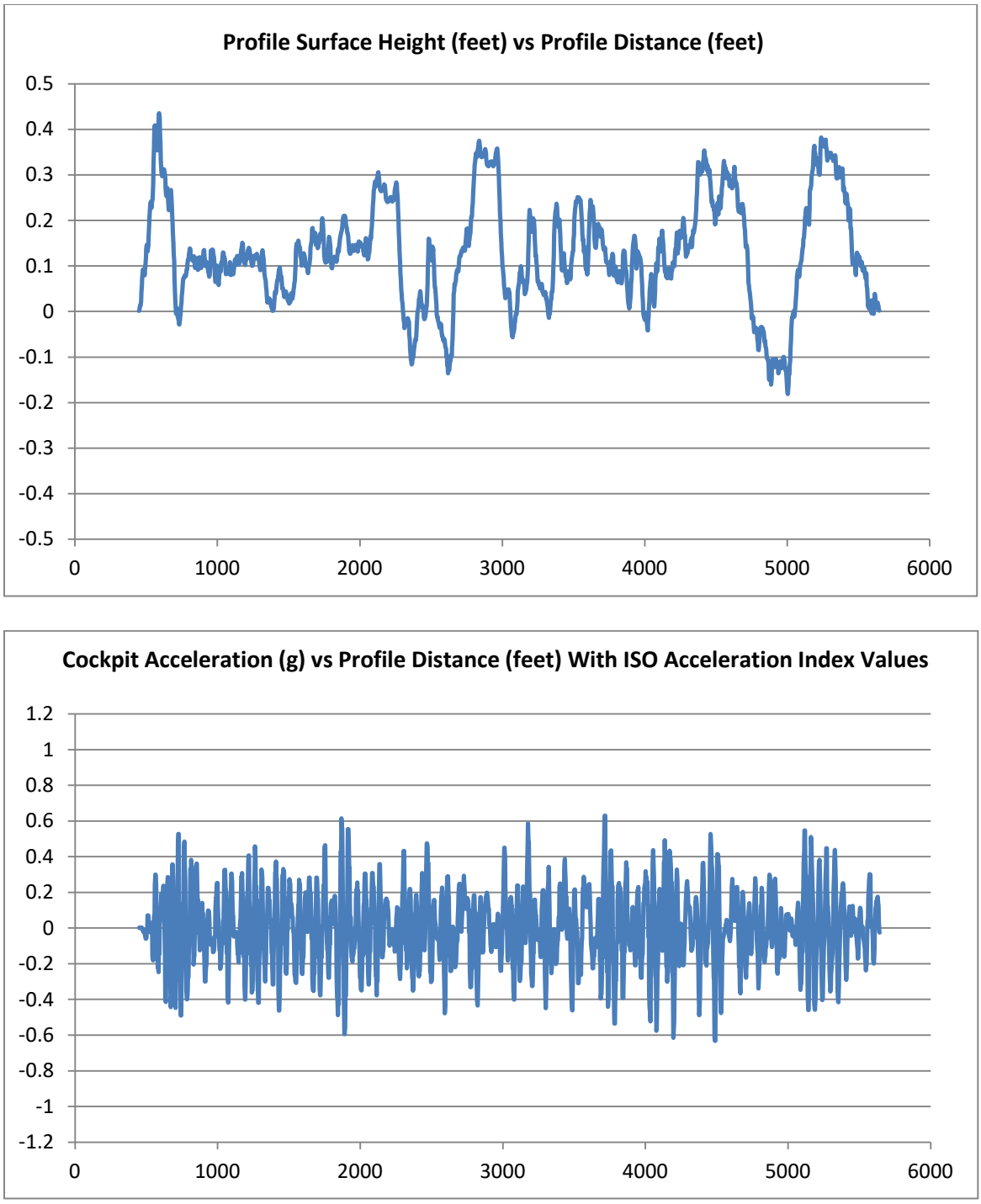

Figure D-71. Runway Profile 71—Profile Height, Cockpit Acceleration, and Acceleration ISO Indices

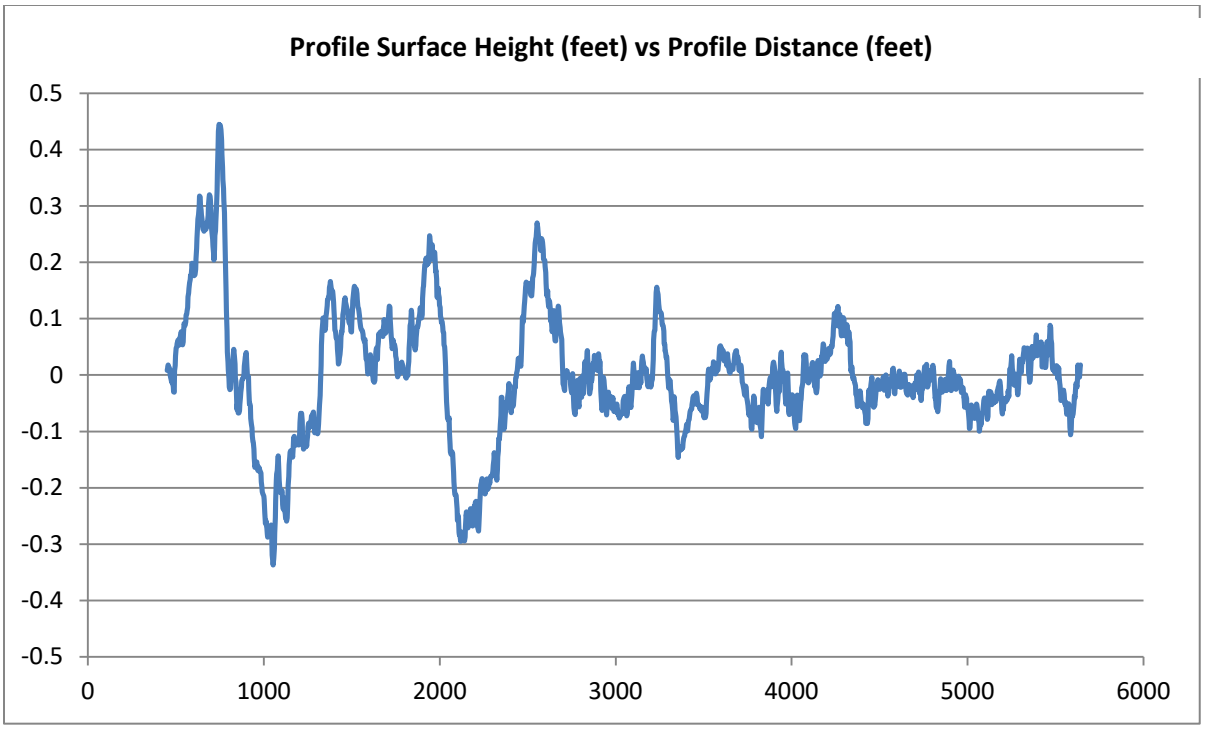

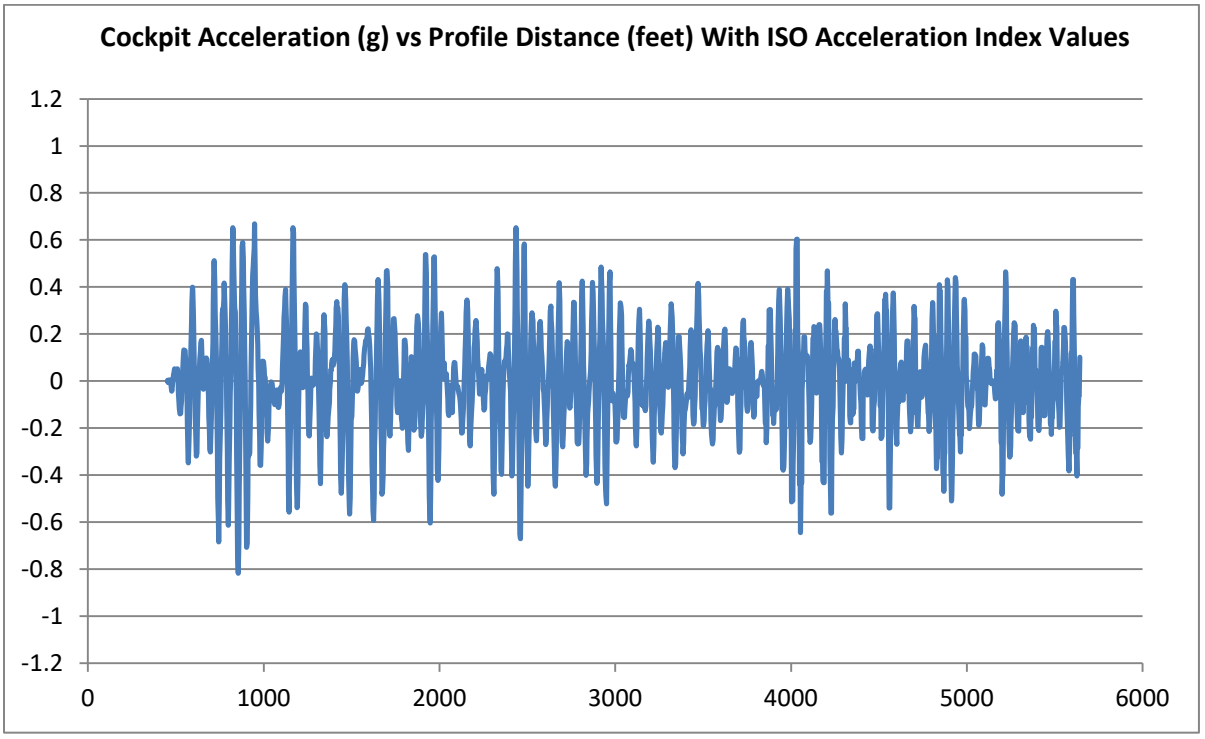

Figure D-72. Runway Profile 72—Profile Height, Cockpit Acceleration, and Acceleration ISO Indices

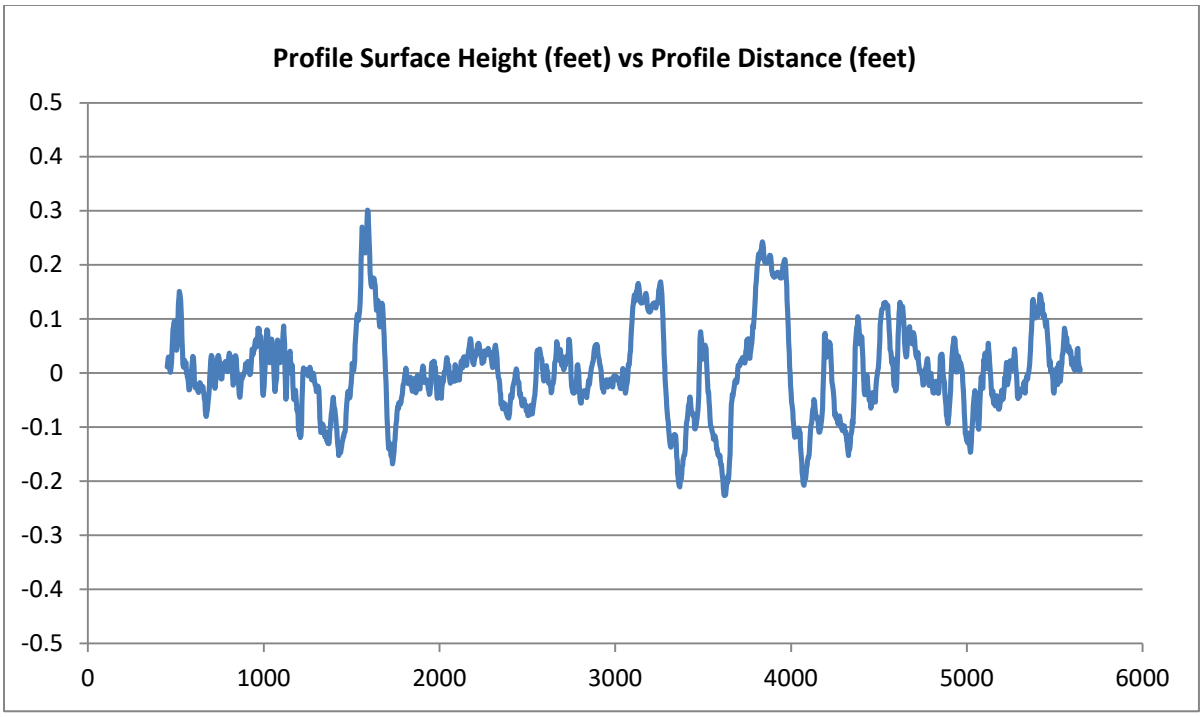

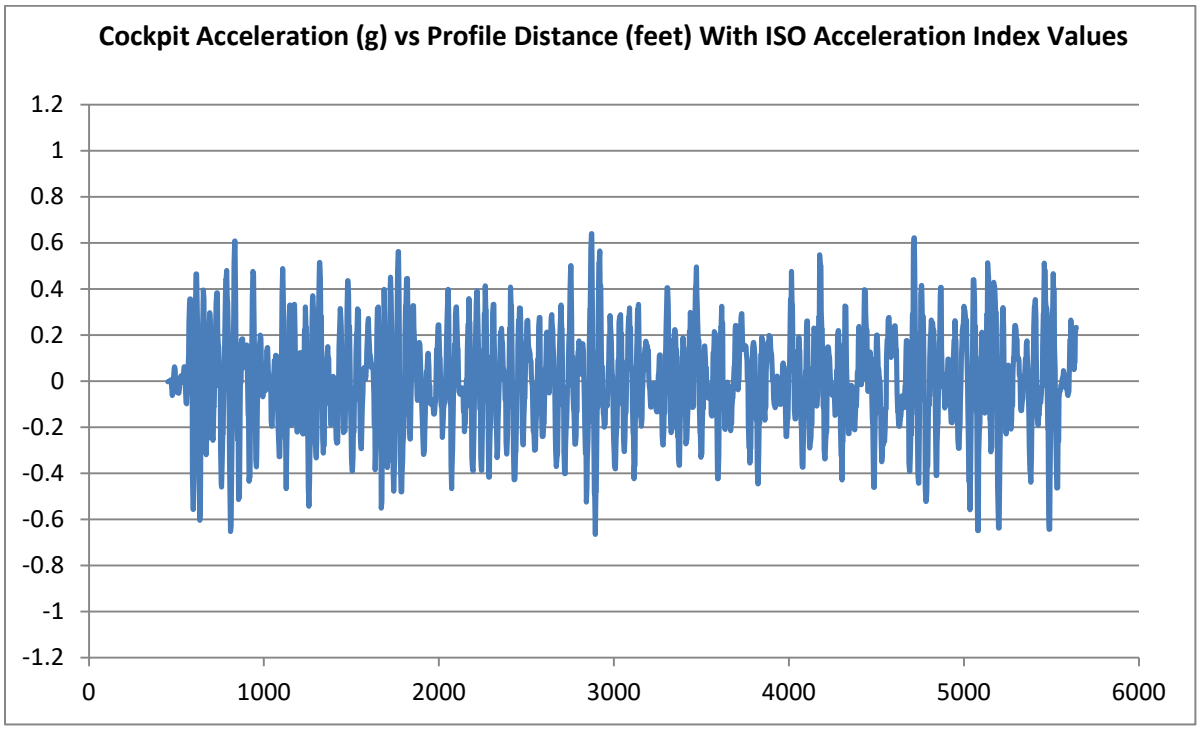

Figure D-73. Runway Profile 73—Profile Height, Cockpit Acceleration, and Acceleration ISO Indices

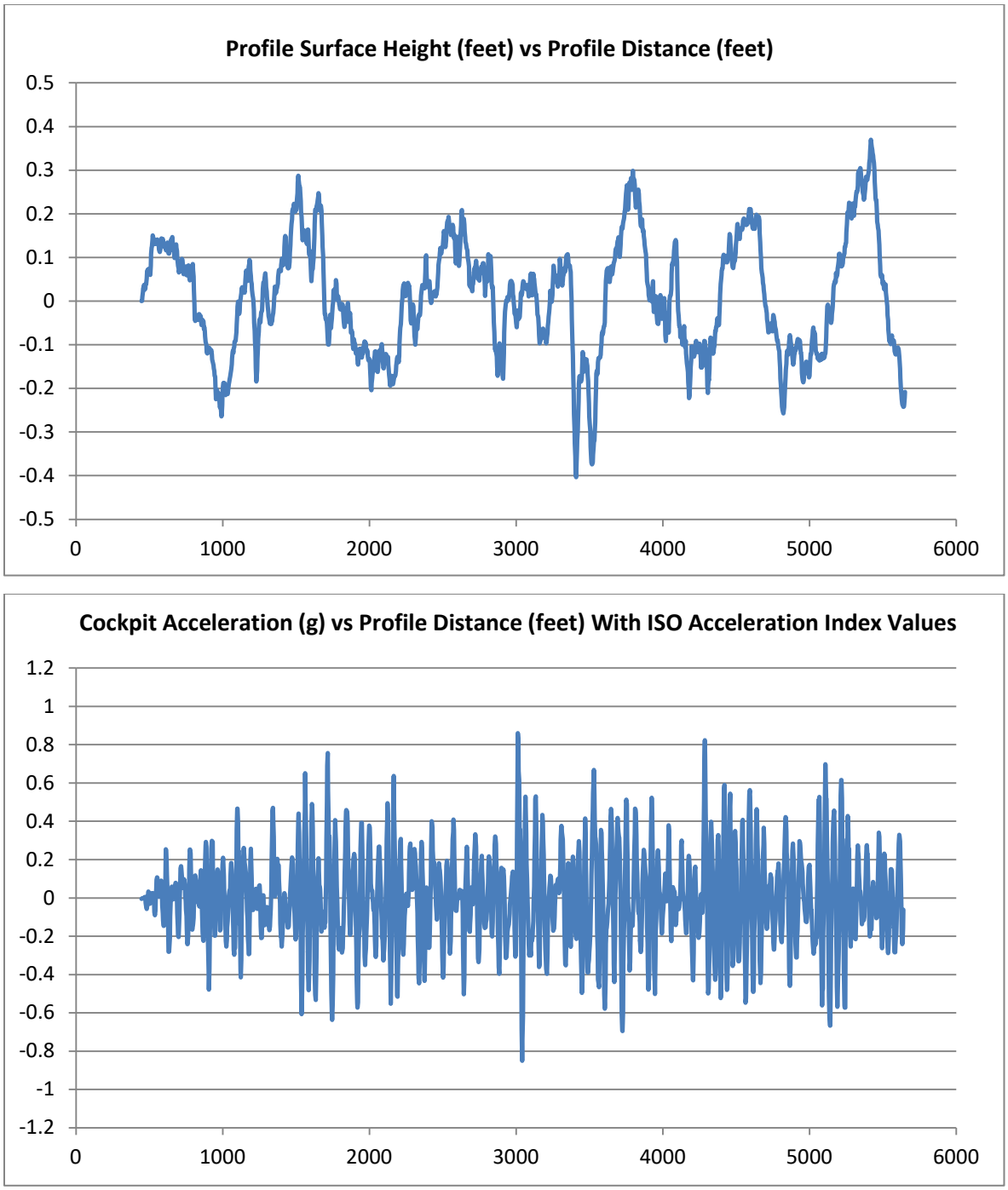

Figure D-74. Runway Profile 74—Profile Height, Cockpit Acceleration, and Acceleration ISO Indices

APPENDIX E—THE B737-800 SIMULATOR DATA COLLECTION PARAMETER LIST

Collected Data Parameter	Units	Software Label	Description
Time	seconds		Elapsed time
Roughness Active	true/false	zactive	Roughness model active flag
Buffet Disable Flag	true/false	mdisbuf	Generic roughness buffet disable flag
Profile Number	integer	zprofnum	Roughness profile number
Runway Roughness Level	integer	ci99_env_rwyroughness_i2	Generic roughness intensity level
Profile Gain	percent	zprofgain	Profile height gain for real-world profiles
Profile Distance	feet	rwdist[1]	Aircraft nose gear distance along profile
Profile Distance	feet	rwdist[2]	Aircraft main gear distance along profile
R/W Height at Nose Gear	feet	rwheight[0]	Profile height at nose gear
R/W Height at Main Gear	feet	rwheight[1]	Profile height at main gear
Actual Cockpit Vert Acc	G	mizacc	Cockpit accelerometer vertical acceleration
Demanded Cockpit Vert Acc	G	mitrzacc	Motion system demanded cockpit vertical acceleration
Flight Rotational Acc	rad/s^2	movqd	Flight model calculated pitch acceleration
Demanded cabin heave	inches	miacc_heav	Demanded motion platform heave
Gross Weight	pounds	l99_acset_gw_f4	Aircraft gross weight
Calculated Cockpit Vert Acc	G	gcp	Roughness model calculated cockpit vertical acceleration
Airspeed	knots	vve	Aircraft airspeed
Nose Gear Force	pounds	vfzg[0]	Nose gear vertical force
Left Gear Force	pounds	vfzg[1]	Left main gear vertical force
Right Gear Force	pounds	vfzg[2]	Right main gear vertical force
Pitch Angle	degrees	vthetadg	Aircraft pitch angle
Roll Angle	degrees	vphidg	Aircraft roll angle
Heading Angle	degrees	vpsidg	Aircraft heading angle
Iyy	$slug - ft^2$	viyy	Aircraft moment of inertia around Y axis
Bending Mode Z Accel	G	modeposzaccel[4]	Cockpit vertical acceleration due to flexible modes
Nose Gear Compression	inches	vee[0]	Nose gear strut compression
LM Gear Compression	inches	vee[1]	Left main gear strut compression
RM Gear Compression	inches	vee[2]	Right main gear strut compression

APPENDIX F—ACCELEROMETER SIGNAL PROCESSING AND ISO INDEX COMPUTATIONS

F.1 INTRODUCTION.

International Organization for Standardization (ISO) International Standard 2631, Part 1: "General Requirements" and Part 5: "Method for evaluation of vibration containing multiple shocks," [F-1] contains procedures for computing indices that can be used to evaluate the effect of human whole-body vibration on human health, comfort, and safety. Part 1 of ISO 2631 specifies three indices applicable to vibration in six degrees of freedom acting on, with applicable weighting factors, standing, seated, and recumbent bodies. Vertical vibration acting on a seated person is the only case of interest in the current work and this description of the application of the ISO procedures is for that case only. Part 5 of ISO 2631 provides a single index for vertical acceleration acting on a seated person. The four indices are as follows, with the first three from Part 1 and the fourth from Part 5.

- Basic evaluation method using weighted root-mean-square (RMS) acceleration.
- Running RMS method.
- Fourth-power vibration dose method.
- Spinal response acceleration dose method.

A frequency weighting (filter) function must be applied to the raw acceleration signal before calculation of the first three indices. The fourth index does not require the application of a frequency weighting function. In addition, a weighted acceleration signal crest factor is defined for determining when the second through fourth indices may be applicable as a supplement to the basic RMS method. The applicable section of ISO 2631 is reproduced below in sufficient detail to define the procedure required to calculate each of the indices, followed by a detailed description of the procedure developed to weight the acceleration records measured in the cockpit of the simulator.

F.2 INDEX DEFINITIONS [F-1].

1. Weighted RMS, reproduced from ISO 2631 Part 1, units = m/s^2

$$a_{\mathrm{W}} = \left[\frac{1}{T} \int_0^T a_{\mathrm{W}}^2(t)\, \mathrm{d}t \right]^{\frac{1}{2}}$$

Where

$a_{\mathrm{W}}(t)$ is the weighted acceleration (translational or rotational) as a function of time (time history), in meters per second squared (m/s^2) or radians per second squared (rad/s^2), respectively;

T is the duration of the measurement, in seconds.

2. From running RMS , reproduced from ISO 2631 Part 1, units = m/s^2

$$a_W(t_0) = \left\{ \frac{1}{\tau} \int_{t_0-\tau}^{t_0} [a_W(t)]^2 \, dt \right\}^{\frac{1}{2}}$$

the maximum transient vibration value, MTVV, is defined as

MTVV = max[$a_W(t_0)$]

i.e. the highest magnitude of $a_W(t_0)$ read during the measurement period (T).

3. Fourth Power Vibration Dose (reproduced from ISO 2631 Part 1, units = $m/s^{1.75}$) is

$$\text{VDV} = \left\{ \int_0^T [a_W(t)]^4 \, dt \right\}^{\frac{1}{4}}$$

Where

$a_W(t)$ is the weighted acceleration (translational or rotational) as a function of time (time history), in meters per second squared (m/s^2) or radians per second squared (rad/s^2), respectively;

T is the duration of the measurement, in seconds.

4. Spinal Response Acceleration Dose (reproduced from ISO 2631 Part 5, units = m/s^2)

5.2.3 Spinal response in vertical direction (z-axis)

In the z-direction, the spinal response is non-linear and is represented by a recurrent neural network model.

The basis for this modeling technique is discussed in Annex C. Lumbar spine z-axis acceleration , a_{lz}, in meters per second squared is predicted using the following equations:

$$a_{lz}(t) = \sum_{j=1}^{7} W_j u_j(t) + W_8 \tag{2}$$

$$u_j(t) = \tanh\left[\sum_{i=1}^{4} w_{ji} a_{lz}(t-i) + \sum_{i=5}^{12} w_{ji} a_{sz}(t-i+4) + w_{j13} \right] \tag{3}$$

The model coefficients in Equations (2) and (3) are specific to a sampling rate of 160 per second. Therefore, data collected at a different sampling rate shall be resampled to 160 samples per second.

5.3 Calculation of acceleration dose

The acceleration dose, D_k, in meters per second squared, in the k-direction is defined as

$$D_k = \left[\sum_i A_{ik}^6\right]^{1/6}$$

Where

A_{ik} is the i^{th} peak of the response acceleration $a_{lk}(t)$;
$k = x$, y, or z.

A MATLAB computer program is provided in the standard for solving equations (2) and (3) above. The MATLAB program was translated into Visual Basic for computation of the acceleration dose. A sample time history is also provided in the standard with the corresponding spinal response dose output results for checking independent implementations of the model. See the description of the Visual Basic implementation given below.

F.3 FREQUENCY WEIGHTING [F-1].

The filter for weighting the acceleration signals is implemented as a set of four differential equations defined by their frequency response functions. The frequency response functions are defined in the standard as four separate sections and these have to be transformed into the base differential equations for solution in the time domain. The response functions, as defined in the standard, and the base differential equations are shown below with the following nomenclature.

p = Laplace operator
$H(p)$ = Laplace transform
$|H(p)|$ = frequency response function
ω = frequency in rad/s
f = frequency in Hz
= $\omega / 2\pi$
ω_i, f_i, Q_i = response shaping parameters
x = input to the filter, acceleration in m/s^2
y = weighted output from the filter, acceleration in m/s^2

1. Band limiting - high pass section

Frequency response function:

$$|H_h(p)| = \left|\frac{1}{1 + \sqrt{2}\,\omega_1/p + (\omega_1/p)^2}\right| = \sqrt{\frac{f^4}{f^4 + f_1^4}}$$

Differential equations for numerical solution in terms of y and z:

$$\ddot{y} = \ddot{x} - \sqrt{2}\omega_1\dot{y} - \omega_1^2 y$$
$$\dot{y} = z$$
$$\dot{z} = \ddot{y} = \ddot{x} - \omega_1\left(\sqrt{2}z + \omega_1 y\right)$$

2. Band limiting - low pass section

Frequency response function:

$$|H_{\mathrm{l}}(p)| = \left|\frac{1}{1 + \sqrt{2}\,p/\omega_2 + (p/\omega_2)^2}\right| = \sqrt{\frac{f_2^4}{f^4 + f_2^4}}$$

Differential equations for numerical solution in terms of y and z:

$$\ddot{y} = \omega_2^2 x - \sqrt{2}\omega_2\dot{y} - \omega_2^2 y$$
$$\dot{y} = z$$
$$\dot{z} = \ddot{y} = \omega_2\left(\omega_2 x - \sqrt{2}z - \omega_2 y\right)$$

3. Acceleration-velocity transition (proportionality to acceleration at lower frequencies and proportionality to velocity at higher frequencies)

Frequency response function:

$$|H_{\mathrm{t}}(p)| = \left|\frac{1 + p/\omega_3}{1 + p/(Q_4\omega_4) + (p/\omega_4)^2}\right| = \sqrt{\frac{f^2 + f_3^2}{f_3^2}} \cdot \sqrt{\frac{f_4^4 \cdot Q_4^2}{f^4 \cdot Q_4^2 + f^2 \cdot f_4^2(1 - 2Q_4^2) + f_4^4 \cdot Q_4^2}}$$

Differential equations for numerical solution in terms of y and z:

$$\ddot{y} = \frac{\omega_4^2}{\omega_3}\dot{x} - \omega_4^2 x - \frac{\omega_4}{Q_4}\dot{y} - \omega_4^2 y$$
$$\dot{y} = z$$
$$\dot{z} = \ddot{y} = \omega_4\left(\frac{\omega_4}{\omega_3}\dot{x} + \omega_4 x - \frac{1}{Q_4}z - \omega_4 y\right)$$

4. Upward step (steepness approximately 6 dB per octave, proportionality to jerk)

Frequency response function:

$$|H_{\mathrm{s}}(p)| = \left|\frac{1 + p/Q_5\omega_5 + (p/\omega_5)^2}{1 + p/(Q_6\omega_6) + (p/\omega_6)^2} \cdot \left(\frac{\omega_5}{\omega_6}\right)^2\right| = \frac{Q_6}{Q_5} \cdot \sqrt{\frac{f^4 \cdot Q_5^2 + f^2 \cdot f_5^2(1 - 2Q_5^2) + f_5^4 \cdot Q_5^2}{f^4 \cdot Q_6^2 + f^2 \cdot f_6^2(1 - 2Q_6^2) + f_6^4 \cdot Q_6^2}}$$

Differential equations for numerical solution in terms of y and z:

$$\ddot{y} = \ddot{x} + \frac{\omega_5}{Q_5}\dot{x} + \omega_5^2 x - \frac{\omega_6}{Q_6}\dot{y} - \omega_6^2 y$$
$$\dot{y} = z$$
$$\dot{z} = \ddot{y} = \ddot{x} + \frac{\omega_5}{Q_5}\dot{x} + \omega_5^2 x - \frac{\omega_6}{Q_6} z - \omega_6^2 y$$

All of the frequency response functions except one require differentiation of the input signal. The following difference equations are used to differentiate numerically:

$$\dot{x} \approx \frac{\Delta x}{\Delta t} = \frac{x(t+h) - x(t-h)}{2h}$$
$$\ddot{x} \approx \frac{\Delta^2 x}{\Delta t^2} = \frac{x(t+h) - 2x(t) + x(t-h)}{h^2}$$

Where h = sample spacing = 1 / (sample rate)

F.4 COMPUTER IMPLEMENTATION OF THE WEIGHTING FUNCTIONS [F-1].

Each of the four weighting functions is implemented in a separate subroutine in a Visual Basic computer program. The subroutines are called in series with the measured cockpit acceleration used as input to the first subroutine and the output from the first subroutine fed into the input of the second subroutine, and so on through all four subroutines. The subroutines are called in the following order:

1. Low-pass section.
2. Acceleration-velocity transition.
3. High-pass section.
4. Upward step.

The order was selected primarily to reduce inaccuracies at high frequency during differentiation of the input. The low pass section does not require differentiation and attenuates the high frequencies before differentiation in the following sections. The acceleration-velocity transition filter requires only first order differentiation so that section follows the low pass. The other two filters require second order differentiation so they are executed last.

The overall transfer function is calculated from the frequency response functions as:

$$|H_{Overall}(p)| = |H_l(p)| \cdot |H_t(p)| \cdot |H_h(p)| \cdot |H_s(p)|$$

The frequency response shaping parameters are specified in the ISO standard as shown in the following table:

Table A.1 — Parameters of the transfer functions of the principal frequency weightings

Weighting	Band-limiting		Acceleration-velocity transition (a-v transition)			Upward step			
	f_1 Hz	f_2 Hz	f_3 Hz	f_4 Hz	Q_4	f_5 Hz	Q_5	f_6 Hz	Q_6
W_k	0,4	100	12,5	12,5	0,63	2,37	0,91	3,35	0,91
W_d	0,4	100	2,0	2,0	0,63	∞	—	∞	—
W_f	0,08	0,63	∞	0,25	0,86	0,062 5	0,80	0,1	0,80

Weighting W_k is applicable to the present study and is for vertical motion of a seated subject.

Also, $\omega_i = 2\pi.f_i$

The principal steps in the weighting procedure are:

1. Read the accelerometer signal from an external data file. The 737-800 simulator sample rate is 60 Hz.
2. Fit cubic splines through the accelerometer data points and interpolate to a sample rate of 1,280 Hz.
3. Smooth the first one-second of the data record to suppress start-up transients during filtering.
4. Apply the weighting functions in series as explained above.
5. Fit cubic splines through the weighted data record and decimate down to a sample rate of 160 Hz.

The weighting function equations are solved using Runge-Kutta integration. The sample rate is increased from 60 Hz to 1,280 Hz to minimize numerically induced distortions over the frequency range of interest (about 0.02 to 100 Hz). The final sample rate of 160 Hz was selected because the Spinal Response Acceleration Dose index must be computed at a sample rate of 160 Hz and the same rate was used to compute the weighted indices for compatibility. Initially increasing the sample rate is particularly important in differentiating the input signals, as illustrated in the following figures.

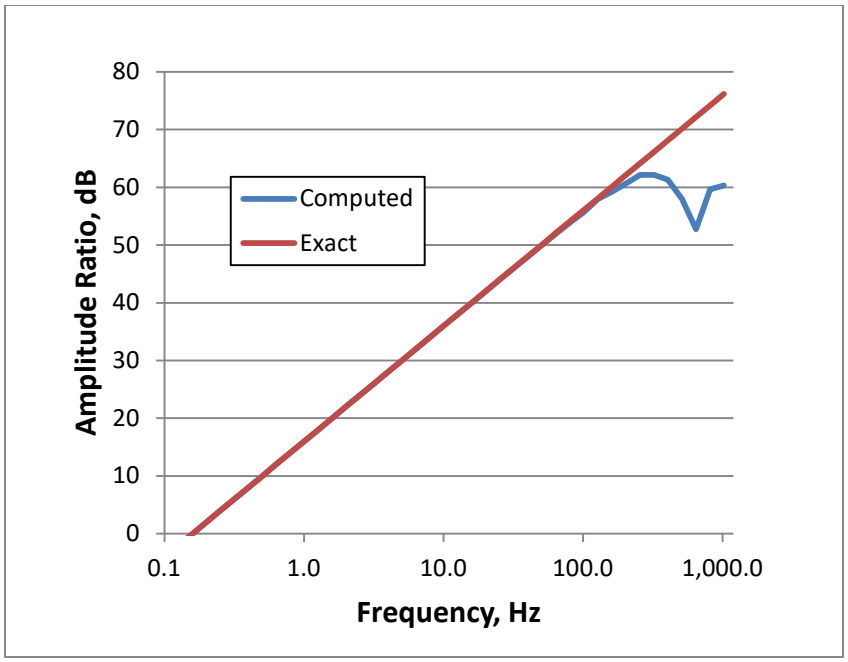

Computed and Exact Amplitude Ratios for First Order Differentiation

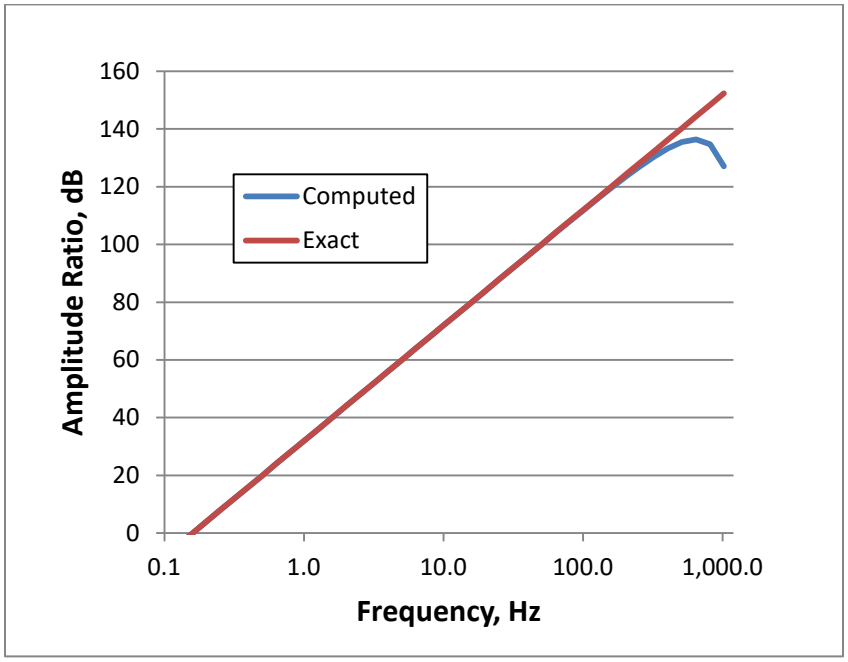

Computed and Exact Amplitude Ratios For Second Order Differentiation

The frequency response of the weighting procedure is shown in the figure below. The curve marked "ISO" was produced by direct computation from the frequency transfer functions given above. The curve marked "FAA implementation" was produced by running unit amplitude sine waves through the weighting function computer program and plotting the amplitudes of the output sine waves.

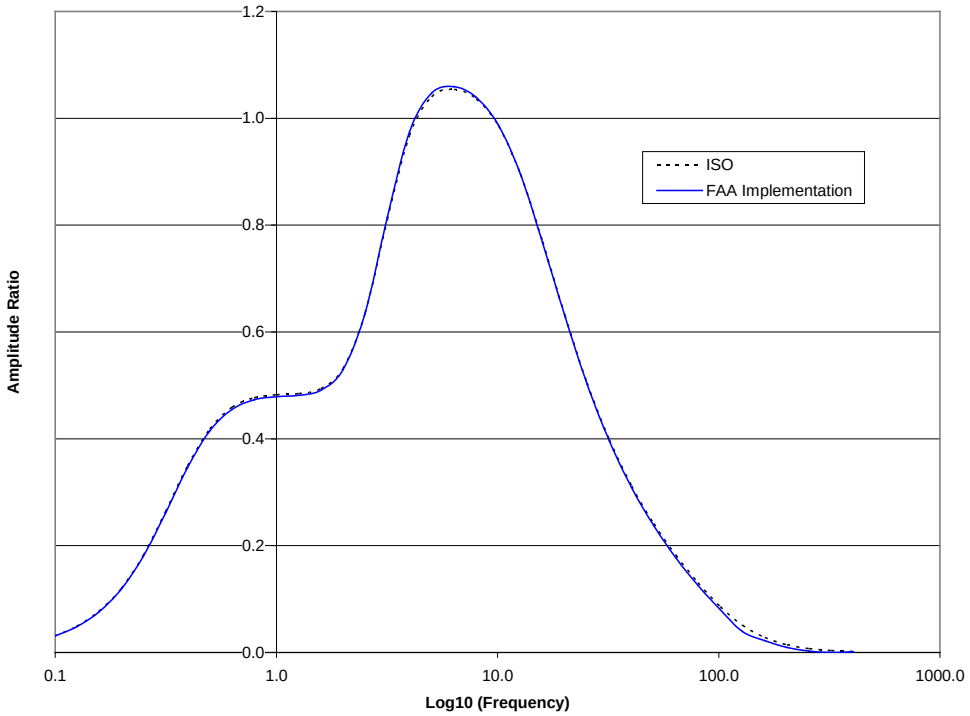

Frequency Response of the Weighting Procedure Compared With the ISO Specified Frequency Transfer Function. Amplitude ratio plotted on a linear scale.

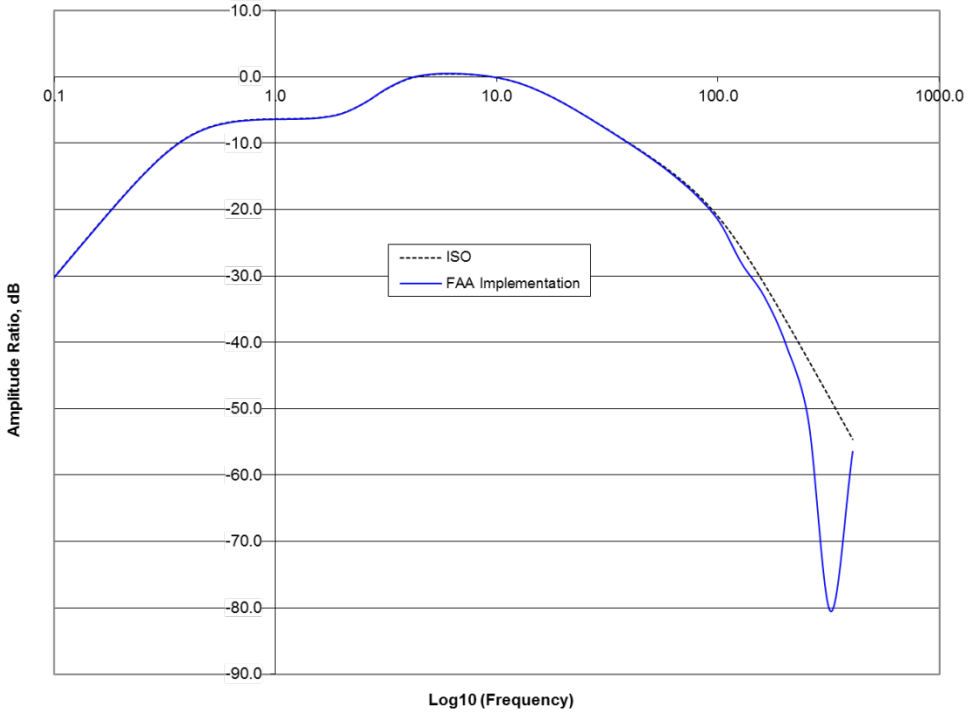

Frequency Response of the Weighting Procedure Compared With the ISO Specified Frequency Transfer Function. Amplitude ratio plotted on a logarithmic scale.

The next figure is a screen shot of the VB computer program showing a raw acceleration data record and the final weighted data record. Computed index values are also shown in the right pane.

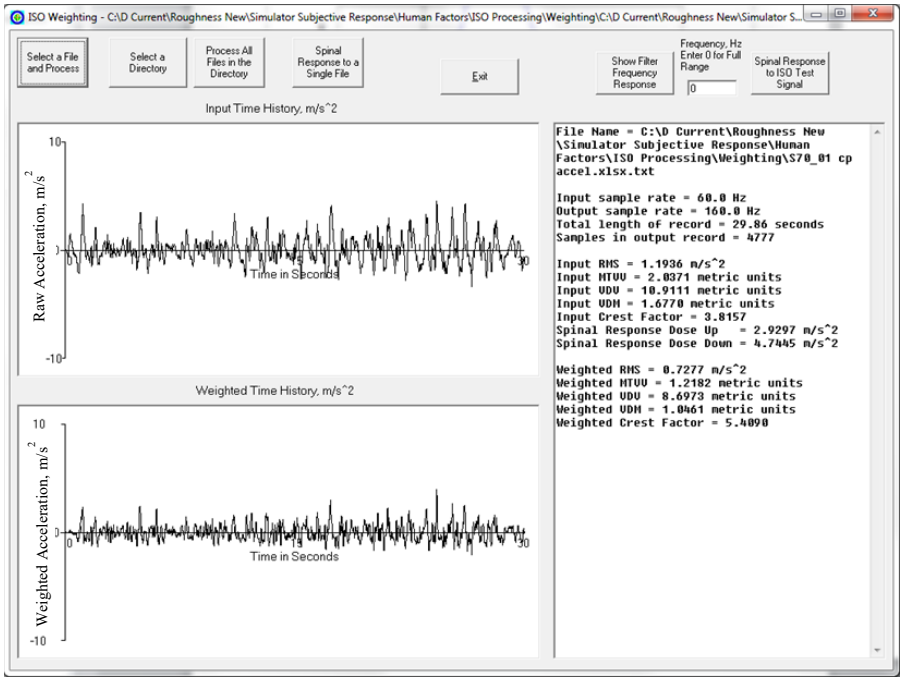

The final figure is a screen shot showing the input and output for the check example of the Spinal Response Acceleration Dose procedure given in the ISO standard. The output shown in the lower left pane was calculated with the VB implementation of the ISO MATLAB program. The peak values and the dose values are shown in the right pane.

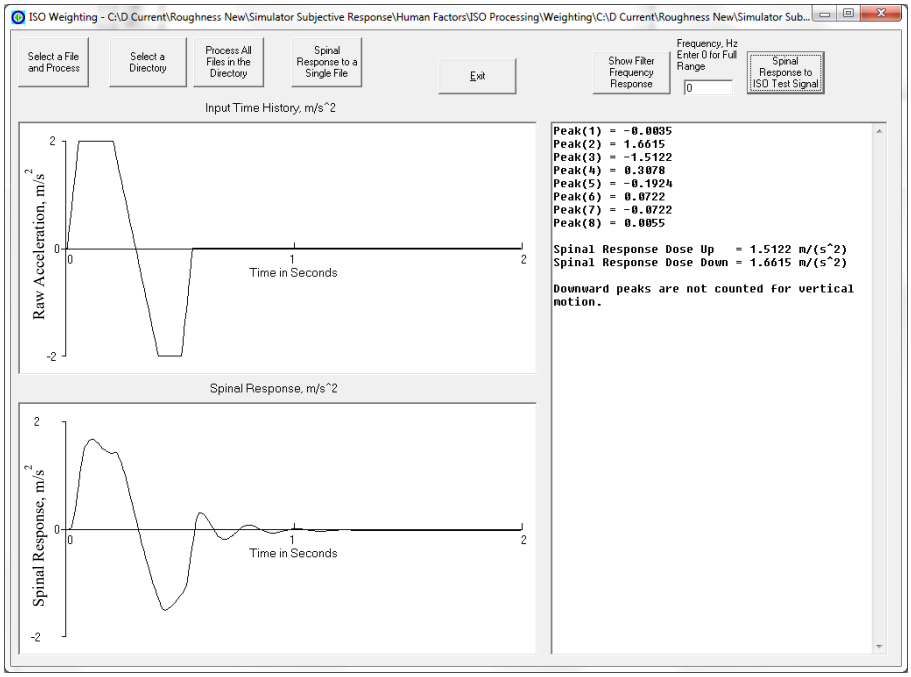

A copy of the computer program's source code for weighting acceleration signals and computing the index values is available on request from the FAA Airport Technology R&D Branch, ANG-E260. A version of the program implemented in Microsoft® Excel® is also available.

F.5 REFERENCE.

F-1. International Organization for Standardization (ISO) 2631, May 1, 1997,"Mechanical Vibration and Shock—Evaluation of Human Exposure to Whole-Body Vibration," 2631-1:1997 "Part 1: General Requirements," "Part 5: Method for Evaluation Containing Multiple Shocks.".

Honeywell

Q-Flex® QA-700 Accelerometer

Economical temperature-compensated sensor

For Q-Flex technology in an economical temperature-compensated package, Honeywell produces the QA700 for a broad array of moderate performance applications, including: flight and flight simulator control systems, radar platform leveling, high-speed train ride control, and seismic sensing.

As with the entire Q-Flex family of accelerometers, the QA700 features a patented Q-Flex etched-quartz-flexure seismic system. An amorphous quartz proof-mass structure provides excellent bias, scale factor, and axis alignment stability.

The integral electronics develops an acceleration-proportional output current providing both static and dynamic acceleration measurements. By use of a customer supplied output load resistor, appropriately scaled for the acceleration range of the application, the output current can be converted into a voltage.

As an option, the QA700 can be provided with a temperature-compensating algorithm where bias, scale factor, and axis misalignment performance are dramatically improved.

Features

- Tactical navigation grade performance
- High value
- Environmentally rugged
- Analog output
- Compact design
- Field-adjustable range
- Dual built-in test
- Optional thermal compensation

Configuration Drawings

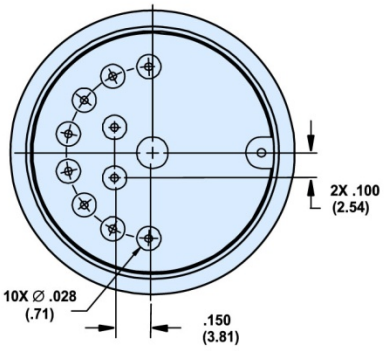

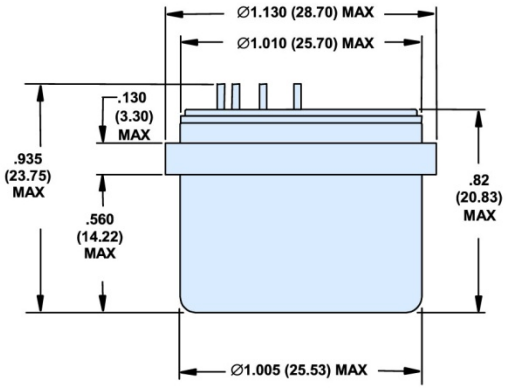

Performance Characteristics

Additional product specifications, outline drawings and block diagrams, and test data are available on request.

Performance	
Input Range [g]	±30
Bias [mg]	<8
One-year Composite Repeatability [µg]	<1200
Temperature Sensitivity [µg/ºC]	<70
Scale Factor [mA/g]	1.23 to 1.43
One-year Composite Repeatability [ppm]	<1200
Temperature Sensitivity [ppm/ºC]	<200
Axis Misalignment [µrad]	<2000
Vibration Rectification [µg/g^2rms]	<50 (50-200 Hz) <100 (200-750 Hz) <150 (750-2000 Hz)
Intrinsic Noise [µg-rms]	<7 (0-10 Hz) <70 (10-500 Hz) <1500 (500-10,000 Hz)
Environment	
Operating Temperature Range [ºC]	-55 to +96
Shock [g]	250
Vibration Peak Sine [g]	25 @ 20-2000 Hz
Resolution/Threshold [µg]	<1
Bandwidth [Hz]	>300
Thermal Modeling	
	-010 NO -020 YES
Electrical	
Quiescent Current per Supply [mA]	<16
Quiescent Power [mW] @ ±15 VDC	<480
Electrical Interface	Temp Sensor
	Voltage Self Test
	Current Self Test
	Power / Signal Ground
	-10 VDC Output +10 VDC Output
Input Voltage	±13 to±18
Physical	
Weight [grams]	46 Nominal, 50 Max.
Diameter below mounting surface [inches]	Ø1.07 ±0.01
Height - bottom to mounting surface [inches]	.600 Max
Case Material	300 Series Stainless Steel

Find out more:
www.inertialsensor.com

Defense & Space Redmond

Honeywell International, Inc.

MAIL ADDRESS: P.O. Box 97001

15001 N.E. 36th Street

Redmond, Washington 98073-9701

PHONE: 888 206 1667

FAX: 425 883 2104

www.honeywell.com

EXP025, August 2005

ISO-9001 Certification Since 1995

Honeywell

APPENDIX H—MATLAB® CODE TO GENERATE SHIFTED LOGARITHMIC FITS

```
% Program logshift computes a shifted logarithmic fit y = a ln(x + s) + b of
% y = pilot rating of runway vs. x = ISO roughness parameters:
%   i.  Weighted RMS
%   ii. Weighted VDV, iii. DKup, iv. MTVV

% Display header:
fprintf(1,'\n\n----------------\n');
fprintf(1,'Program logshift\n');
fprintf(1,'----------------\n\n');
plot_type=input('Plot avg. ratings & conf. (1), indiv. ratings (2), or avg. ratings w/o conf. (3)?','s');
if size(plot_type)==[0 0];plot_type='2';disp('Individual ratings selected');end

% Specify roughness data location, min & max allowed shift, max number of iterations:
t35_95 = 2.03011;t1570_95=1.96148;t1570_90=1.64582;t1570_50 = .67465;
file_in='h:\RoughnessFinalAnalysis_08_15_2013.xls';sheet_in='Averages';data_range='c5:m84';
sheet_in2='CombinedRatings';data_range2a='a1:e1572';data_range2b='h1:l1572';
s_min=[0 0 0 0]';s_max=[2 5 35 15]';eps_stop=.000005;
x_max=[1.5 3.5 25 10;2.2 3.5 25 10];% Max parameter value to plot (row1:taxiway,row2:runway)

% Read data points
xls_data=xlsread(file_in,sheet_in,data_range);col=[2 3 4 6 8]';max_iter=100;
xls_data2a=xlsread(file_in,sheet_in2,data_range2a);
xls_data2b=xlsread(file_in,sheet_in2,data_range2b);
appr=['Taxiway ';'Runway   '];ISO=['Weighted RMS (m/s^2)         ';'Weighted MTVV (m/s^2)        ';'Weighted VDV (m/s^1^.^7^5)
';'DKup (m/s^2)              '];
unit = ones(37,1);unit2=ones(1572,1);%Column vector of ones

% Loop over taxiways and runways(kk = row 1 to begin taxiway data or row 38 to begin runway data)
for kk=1:37:38%kk=row where taxiway or runway data begins (1 or 38)
   b=xls_data(kk:kk+36,11);% b = 37 pilot ratings
   crest = xls_data(kk:kk+36,9);
   if kk==1
```

```
   b2=xls_data2a(1:1572,1);
else
   b2=xls_data2b(1:1572,1);
end
varb=var(b);
varb2=var(b2);
kk1=(kk-1)/37+1;%kk1=1 for taxiways, 2 for runways
% Loop over ISO parameters p=1:4
for p=1:4%p=1:Wt. RMS, p=2:Wt. MTVV, p=3: Wt. VDV, p=4: DKup
   fprintf(1,['Fit y = a*ln(x+s) + b for %8s With y=Pilot Rating Vs. x= %13s\n'],appr(kk1,1:8),ISO(p,1:27))
   fprintf(1,'-------------------------------------------------------------------------\n')
   xx=[0:.1:x_max(kk1,p)];unit1=ones(size(xx));
   xi = xls_data(kk:kk+36,col(p));
   xc=xi(find(crest==1));

   % Find sqrt(r-squared) for min, max, and middle values of shift s to start the iteration
   s0 = s_min(p)*unit;
   A = [log(xi+s0),unit];% A = [ln(pth ISO parameter + s0) , 1]
   x0 = linsolve(A,b);% x0 = least squares solution of Ax = b using shift s0 by the QR method
   r = (b - A*x0);% r = residual vector (difference between data and fit)
   rsq0 = r'*r;% sum of squares of residuals

   s1 = s_max(p)*unit;
   A = [log(xi+s1),unit];% A = [ln(pth ISO parameter + s1) , 1]
   x1 = linsolve(A,b);% x1 = least squares solution of Ax = b using shift s1 by the QR method
   r = (b - A*x1);% r = r,esidual vector (difference between data and fit)
   rsq1 = r'*r;%sum of squares of residuals

   s = (s_min(p)+s_max(p))/2*unit;
   A = [log(xi+s),unit];% A = [ln(pth ISO parameter + s) , 1]
   x = linsolve(A,b);% x1 = least squares solution of Ax = b using shift s by the QR method
   r = (b - A*x);% r = residual vector (difference between data and fit)
   rsq = r'*r;% sum of squares of residuals
```

```
max_y=max([rsq0,rsq,rsq1]);
s_save = [s0(1) s1(1) s(1)];rsq_save = [rsq0 rsq1 rsq];

% Iteration to find the shift s that minimizes r-squared
disp(' Iteration          s          a          b              r^2              R^2   Max Error');
disp(' ---------  ----------  ----------  ----------  ----------------  ----------------   ---------');
for k=1:max_iter
   if abs(s1(1)-s0(1))>=eps_stop;
      if          rsq1<=rsq0;if          rsq<=rsq1;s0=s;rsq0=rsq;x0=x;else          s0=s;rsq0=rsq;x0=x;s=s1;rsq=rsq1;x=x1;s1=2*s1-
s0;A=[log(xi+s1),unit];x1=linsolve(A,b);r = b-A*x1;rsq1=r'*r;end
      elseif rsq<=rsq0;s1=s;rsq1=rsq;x1=x;
      else s1=s;rsq1=rsq;x1=x;s=s0;rsq=rsq0;x=x0;s0=2*s0-s1;A=[log(xi+s0),unit];x0=linsolve(A,b);r=b-A*x0;rsq0=r'*r;
      end
      s = (s0+s1)/2;
      A = [log(xi+s),unit];
      x = linsolve(A,b);
      r = (b - A*x);
      rsq = r'*r;
      R2=1-rsq/varb/36;
      s_save = [s_save s(1)];rsq_save=[rsq_save rsq];
      fprintf(1,'%10i  %10f  %10f  %10f  %16.12f  %16.12f %10f\n',k,s(1),x(1),x(2),rsq,R2,s1(1)-s0(1));
   else
      break
   end
end

% Show the best fit
if k==max_iter;
   disp('*** Error - Failed to converge.\n\n');
else
   if rsq<=rsq1 && rsq<=rsq0
      R2=1-rsq/varb/36;
      fprintf(1,'Solution:   %10f  %10f  %10f  %16.12f  %16.12f %10f\n',s(1),x(1),x(2),rsq,R2,(s1(1)-s0(1))/2);
```

```
    a0=x(1);b0=x(2);shift=s(1);r2=rsq;
  elseif rsq1<=rsq0
    R2=1-rsq1/varb/36;
    fprintf(1,'Solution:  %10f %10f %10f %16.12f %16.12f %10f\n',s1(1),x1(1),x1(2),rsq1,R2,s1(1)-s0(1));
    a0=x1(1);b0=x1(2);shift=s1(1);r2=rsq1;
  else
    R2=1-rsq0/varb/36;
    fprintf(1,'Solution:  %10f %10f %10f %16.12f %16.12f %10f\n',s0(1),x0(1),x0(2),rsq0,R2,s1(1)-s0(1));
    a0=x0(1);b0=x0(2);shift=s0(1);r2=rsq0;
  end

  % Fill in the left side of the shift vs. r^2 plot
  for ks=.1:.1:.7
    s = ks*shift*unit;
    A = [log(xi+s),unit];% A = [ln(pth ISO parameter + s) , 1]
    x = linsolve(A,b);% x1 = least squares solution of Ax = b using shift s by the QR method
    r = (b - A*x);% r = residual vector (difference between data and fit)
    rsq = r'*r;% sum of squares of residuals
    s_save = [s_save s(1)];rsq_save=[rsq_save rsq];
  end

  %Plot the best fit and show the shift yielding min. r^2
  if plot_type(1)=='1' | plot_type(1)=='3'
   [s_save ind] = sort(s_save);% Sort shift iterates into ascending order
   rsq_save = rsq_save(ind);% Sort corresponding values of r^2
   R2=1-r2/varb/36;
   figure('Position',[11 11 900 600]);
   title({['Shifted Log Fit for ' appr(kk1,1:8) 'Avg. Rating Vs. ' ISO(p,1:13)],['y = ' num2str(a0) '*ln(x+' num2str(shift) ')+ '
num2str(b0)]},'FontSize',16,'Color','b');
   text(x_max(kk1,p)/8,9,['R^2=' num2str(R2)],'Color','b','FontSize',14)
   hold on
   yy=a0*log(xx+shift*unit1) + b0*unit1;%y-values on fitted curve at xx x-values
   y_bar=mean(b)*unit;%Average y-value of input data
```

```
xis=log(xi+shift*unit);%Log of shifted x-values of input data
x_bar=mean(xis)*unit;%Mean of log of shifted x-values of input data
steyx=sqrt(((b-y_bar)'*(b-y_bar)-((xis-x_bar)'*(b-y_bar))^2/((xis-x_bar)'*(xis-x_bar)))/35);%Standard error
temp=1/37*unit1 + (log(xx+shift*unit1)-x_bar(1)*unit1).^2/((xis-x_bar)'*(xis-x_bar));%
yy_conf95=t35_95*steyx*sqrt(temp);
yy_pred95=t35_95*steyx*sqrt((unit1+temp));
if plot_type(1)=='1'
   grid on;
   plot(xi,b,'bd',xx,yy,'m-',xx,yy-yy_conf95,'r--',xx,yy-yy_pred95,'r:',xx,yy+yy_conf95,'r--
',xx,yy+yy_pred95,'r:','LineWidth',3,'MarkerFaceColor','b');
   legend('37 Pilot Avg. Ratings','Fitted Curve','95% Confidence Interval','95% Prediction Interval');
   axis([0 x_max(kk1,p) 0 10]);
   xlabel(ISO(p,1:27));ylabel('Avg. Pilot Rating');
   figure('Position',[11 11 900 600]);grid on
   title(['Inverse of Shifted Log Fit: ' appr(kk1,1:8) ISO(p,1:13) ' Vs. Avg. Pilot Rating'],'FontSize',16,'Color','b');
   hold on
   plot(b,xi,'bd',yy,xx,'r--','MarkerFaceColor','b');
   axis([0 10 0 x_max(kk1,p)]);
   ylabel(ISO(p,1:27));xlabel('Avg. Pilot Rating');
   legend('37 Pilot Avg. Ratings','Fitted Curve');
   figure('Position',[11 11 900 600]);grid on
   title({['Residual (r^2) Vs. Shift (s)'],['For ' appr(kk1,1:8) ISO(p,1:13)]},'FontSize',16,'Color','b');
   hold on
   plot(s_save,rsq_save,'r.:',shift,r2,'r*');text(shift,r2-.25,[' (' num2str(shift) ',' num2str(r2) ')']);
   legend('r^2 of Least Squares Fit','Optimum Shift & Min. r^2');
   axis([min(s_save) max(s_save) min(rsq_save)-1 max(rsq_save)]);
   xlabel('s');ylabel('r^2');
else
   yc=b(find(crest==1));
   if p==1 %Extra plot vs. quadratic best fit predicted by Excel
      if                          kk==1;yq=2.9977*xx.*xx-11.089*xx+10.083*ones(size(xx));rr2=.9499;else;yq=1.7558*xx.*xx-
8.3822*xx+10.403*ones(size(xx));rr2=.9848;end%Quadratic fits from Excel
      plot(xi,b,'bd',xc,yc,'mo',xx,yy,'r-',xx,yq,'g-','LineWidth',2,'MarkerFaceColor','b');
```

```
                text(x_max(kk1,p)/8,9,['R^2=' num2str(R2)],'Color','r','FontSize',14)
                text(x_max(kk1,p)/8-.1,9.5,['R^2=' num2str(rr2)],'Color','g','FontSize',14)
                legend('37 Pilot Avg. Ratings','High crest factor case','Shifted Log. Fit','Quadratic Fit');
                axis([0 x_max(kk1,p) 0 10]);
                xlabel(ISO(p,1:27));ylabel('Avg. Pilot Rating');
                figure('Position',[11 11 900 600]);
                title({['Shifted Log Fit for ' appr(kk1,1:8) 'Avg. Rating Vs. ' ISO(p,1:13)],['y = ' num2str(a0) '*ln(x+' num2str(shift) ')+ '
num2str(b0)]},'FontSize',16,'Color','b');
                text(x_max(kk1,p)/8,9,['R^2=' num2str(R2)],'Color','b','FontSize',14)
              end
              % Plot high crest factor cases
              plot(xi,b,'bd',xc,yc,'mo',xx,yy,'r-','LineWidth',3,'MarkerFaceColor','b');
              legend('37 Pilot Avg. Ratings','High crest factor case','Fitted Curve');
              title({['Shifted Log Fit for ' appr(kk1,1:8) 'Avg. Rating Vs. ' ISO(p,1:13)],['y = ' num2str(a0) '*ln(x+' num2str(shift) ')+ '
num2str(b0)]},'FontSize',16,'Color','b');
              axis([0 x_max(kk1,p) 0 10]);
              xlabel(ISO(p,1:27));ylabel('Avg. Pilot Rating');
            end
          end

          % Fixed point iteration to find the shift that puts the best fit thru (0,10)
          fprintf(1,['\nFit y = a*ln(x+s) + b Through (0,10) for %8s With y=Pilot Rating Vs. x= %13s\n'],appr(kk1,1:8),ISO(p,1:27))
          disp(' Iteration          s          a          b              r^2              R^2');
          disp(' ---------  ----------  ----------  ----------  ----------------  ----------------');
          for kfp=1:1000
             s = exp((10-b0)/a0)*unit;
             if abs(s(1)-shift)<eps_stop;break;end
             A = [log(xi+s),unit];% A = [ln(pth ISO parameter + s) , 1]
             x = linsolve(A,b);% x1 = least squares solution of Ax = b using shift s by the QR method
             r = (b - A*x);% r = residual vector (difference between data and fit)
             rsq = r'*r;% sum of squares of residuals
             R2=1-rsq/varb/36;
             a0 = x(1);b0 = x(2);
```

```
            shift = s(1);
            %1if 10*floor(kfp/10)==kfp;fprintf(1,'%10i  %10f  %10f  %10f  %16.12f  %16.12f\n',kfp,shift,a0,b0,rsq,R2);end
          end
          fprintf(1,'%10i  %10f  %10f  %10f  %16.12f  %16.12f\n\n',kfp,shift,a0,b0,rsq,R2);
          disp(' ')
          if plot_type(1)=='1'
            figure('Position',[11 11 900 600]);grid on % Plot the fit through (0,10)
            title({['Shifted Log Fit Through (0,10) for ' appr(kk1,1:8) 'Avg. Rating Vs. ' ISO(p,1:13)],['y = ' num2str(a0) '*ln(x+' num2str(shift) ')+ ' num2str(b0)]},'FontSize',16,'Color','b');
            text(x_max(kk1,p)/8,9,['R^2=' num2str(R2)],'Color','b','FontSize',14)
            hold on
            yy=a0*log(xx+shift*unit1) + b0*unit1;
            plot(xi,b,'bd',xx,yy,'r-','LineWidth',2,'MarkerFaceColor','b');
            axis([0 x_max(kk1,p) 0 10]);
            xlabel(ISO(p,1:27));ylabel('Avg. Pilot Rating');
            legend('37 Pilot Avg. Ratings','Fitted Curve');
          end

      end

      %Find the best fit to 1572 individual pilot responses
      fprintf(1,['Fit y = a*ln(x+s) + b to individual pilot responses for %8s With y=Pilot Rating Vs. x= %13s\n'],appr(kk1,1:8),ISO(p,1:27))
      fprintf(1,'-----------------------------------------------------------------------------------------------------\n')
      if kk==1
         xii = xls_data2a(1:1572,p+1);
      else
         xii = xls_data2b(1:1572,p+1);
      end

      % Find sqrt(r-squared) for min, max, and middle values of shift s to start the iteration
      s0 = s_min(p)*unit2;
      A = [log(xii+s0),unit2];% A = [ln(pth ISO parameter + s0) , 1]
```

```
x0 = linsolve(A,b2);% x0 = least squares solution of Ax = b using shift s0 by the QR method
r = (b2 - A*x0);% r = residual vector (difference between data and fit)
rsq0 = r'*r;% sum of squares of residuals

s1 = s_max(p)*unit2;
A = [log(xii+s1),unit2];% A = [ln(pth ISO parameter + s1) , 1]
x1 = linsolve(A,b2);% x1 = least squares solution of Ax = b using shift s1 by the QR method
r = (b2 - A*x1);% r = r,esidual vector (difference between data and fit)
rsq1 = r'*r;%sum of squares of residuals

s = (s_min(p)+s_max(p))/2*unit2;
A = [log(xii+s),unit2];% A = [ln(pth ISO parameter + s) , 1]
x = linsolve(A,b2);% x1 = least squares solution of Ax = b using shift s by the QR method
r = (b2 - A*x);% r = residual vector (difference between data and fit)
rsq = r'*r;% sum of squares of residuals
max_y=max([rsq0,rsq,rsq1]);
s_save = [s0(1) s1(1) s(1)];rsq_save = [rsq0 rsq1 rsq];

% Iteration to find the shift s that minimizes r-squared
disp(' Iteration          s          a          b              r^2              R^2   Max Error');
disp(' ---------  ----------  ----------  ----------  ----------------  ----------------   ---------');
for k=1:max_iter
   if abs(s1(1)-s0(1))>=eps_stop;
      if          rsq1<=rsq0;if          rsq<=rsq1;s0=s;rsq0=rsq;x0=x;else          s0=s;rsq0=rsq;x0=x;s=s1;rsq=rsq1;x=x1;s1=2*s1-
s0;A=[log(xii+s1),unit2];x1=linsolve(A,b2);r = b2-A*x1;rsq1=r'*r;end
      elseif rsq<=rsq0;s1=s;rsq1=rsq;x1=x;
      else s1=s;rsq1=rsq;x1=x;s=s0;rsq=rsq0;x=x0;s0=2*s0-s1;A=[log(xii+s0),unit2];x0=linsolve(A,b2);r=b2-A*x0;rsq0=r'*r;
      end
      s = (s0+s1)/2;
      A = [log(xii+s),unit2];
      x = linsolve(A,b2);
      r = (b2 - A*x);
      rsq = r'*r;
```

```
      R2=1-rsq/varb2/1051;
      s_save = [s_save s(1)];rsq_save=[rsq_save rsq];
      fprintf(1,'%10i  %10f  %10f  %10f  %16.12f  %16.12f %10f\n',k,s(1),x(1),x(2),rsq,R2,s1(1)-s0(1));
   else
      break
   end
end

% Show the best fit
if k==max_iter;
   disp('*** Error - Failed to converge.\n\n');
else
   if rsq<=rsq1 && rsq<=rsq0
      R2=1-rsq/varb2/1051;
      fprintf(1,'Solution:   %10f  %10f  %10f  %16.12f  %16.12f %10f\n',s(1),x(1),x(2),rsq,R2,(s1(1)-s0(1))/2);
      a0=x(1);b0=x(2);shift=s(1);r2=rsq;
   elseif rsq1<=rsq0
      R2=1-rsq1/varb2/1051;
      fprintf(1,'Solution:   %10f  %10f  %10f  %16.12f  %16.12f %10f\n',s1(1),x1(1),x1(2),rsq1,R2,s1(1)-s0(1));
      a0=x1(1);b0=x1(2);shift=s1(1);r2=rsq1;
   else
      R2=1-rsq0/varb2/1051;
      fprintf(1,'Solution:   %10f  %10f  %10f  %16.12f  %16.12f %10f\n',s0(1),x0(1),x0(2),rsq0,R2,s1(1)-s0(1));
      a0=x0(1);b0=x0(2);shift=s0(1);r2=rsq0;
   end

   % Fill in the left side of the shift vs. r^2 plot
   for ks=.1:.1:.7
      s = ks*shift*unit2;
      A = [log(xii+s),unit2];% A = [ln(pth ISO parameter + s) , 1]
      x = linsolve(A,b2);% x1 = least squares solution of Ax = b using shift s by the QR method
      r = (b2 - A*x);% r = residual vector (difference between data and fit)
      rsq = r'*r;% sum of squares of residuals
```

```
    s_save = [s_save s(1)];rsq_save=[rsq_save rsq];
  end

  %Plot the best fit and show the shift yielding min. r^2
  if plot_type(1)=='2'
    [s_save ind] = sort(s_save);% Sort shift iterates into ascending order
    rsq_save = rsq_save(ind);% Sort corresponding values of r^2
    R2=1-r2/varb2/1051;
    % 95% Plot shifted log fit with confidence and prediction intervals
    figure('Position',[11 11 900 600]);grid on
    title({['Shifted Log Fit for ' appr(kk1,1:8) 'Individual Rating Vs. ' ISO(p,1:13)],['y = ' num2str(a0) '*ln(x+' num2str(shift) ')+ '
num2str(b0)]},'FontSize',16,'Color','b');
    text(x_max(kk1,p)/8,9,['R^2=' num2str(R2)],'Color','b','FontSize',14)
    hold on
    yy=a0*log(xx+shift*unit1) + b0*unit1;%y-values on fitted curve at xx x-values
    y_bar=mean(b2)*unit2;%Average y-value of input data
    xis=log(xii+shift*unit2);%Log of shifted x-values of input data
    x_bar=mean(xis)*unit2;%Mean of log of shifted x-values of input data
    steyx=sqrt(((b2-y_bar)'*(b2-y_bar)-((xis-x_bar)'*(b2-y_bar))^2/((xis-x_bar)'*(xis-x_bar)))/1570);%Standard error
    temp=1/1572*unit1 + (log(xx+shift*unit1)-x_bar(1)*unit1).^2/((xis-x_bar)'*(xis-x_bar));%
    yy_conf95=t1570_95*steyx*sqrt(temp);
    yy_pred95=t1570_95*steyx*sqrt((unit1+temp));
    plot(xii,b2,'b.',xx,yy,'m-',xx,yy-yy_conf95,'r--',xx,yy-yy_pred95,'r:',xx,yy+yy_conf95,'r--
',xx,yy+yy_pred95,'r:','LineWidth',3,'MarkerFaceColor','b');
    axis([0 x_max(kk1,p) 0 10]);
    legend('1572 Pilot Ratings','Fitted Curve','95% Confidence Interval','95% Prediction Interval');
    xlabel(ISO(p,1:27));ylabel('Avg. Pilot Rating');
    % Plot shifted log fit with 95%,90%,50% prediction intervals
    figure('Position',[11 11 900 600]);grid on
    title({['Shifted Log Fit & Prediction Intervals for ' appr(kk1,1:8) 'Individual Rating Vs. ' ISO(p,1:13)],['y = ' num2str(a0)
'*ln(x+' num2str(shift) ')+ ' num2str(b0)]},'FontSize',16,'Color','b');
    text(x_max(kk1,p)/3,9,['R^2=' num2str(R2)],'Color','k','FontSize',14)
    hold on
```

```
            yy_pred90=t1570_90*steyx*sqrt((unit1+temp));
            yy_pred50=t1570_50*steyx*sqrt((unit1+temp));
            plot(xii,b2,'b.',xx,yy,'k-','LineWidth',2)
            plot(xx,yy-yy_pred95,':','Color',[1 0 0],'LineWidth',3,'MarkerFaceColor','b')
            plot(xx,yy-yy_pred90,'-.','Color',[.95 .05 0],'LineWidth',3,'MarkerFaceColor','b')
            plot(xx,yy-yy_pred50,'--','Color',[.6 .25 .05],'LineWidth',3,'MarkerFaceColor','b')
            plot(xx,yy+yy_pred95,':','Color',[1 0 0],'LineWidth',3,'MarkerFaceColor','b')
            plot(xx,yy+yy_pred90,'-.','Color',[.95 .05 0],'LineWidth',3,'MarkerFaceColor','b')
            plot(xx,yy+yy_pred50,'--','Color',[.6 .25 .05],'LineWidth',3,'MarkerFaceColor','b')
            axis([0 x_max(kk1,p) 0 10]);
            legend('1572 Pilot Ratings','Fitted Curve','95% Prediction Interval','90% Prediction Interval','50% Prediction Interval');
            xlabel(ISO(p,1:27));ylabel('Avg. Pilot Rating');
            % Plot sqrt(r^2) as a function of shift & show minimizing shift
            figure('Position',[11 11 900 600]);grid on
            title({['Residual (r^2) Vs. Shift (s)'],['For ' appr(kk1,1:8) ISO(p,1:13)]},'FontSize',16,'Color','b');
            hold on
            plot(s_save,rsq_save,'r.:',shift,r2,'r*');text(shift,r2-.25,[' (' num2str(shift) ',' num2str(r2) ')']);
            legend('r^2 of Least Sq. Fit to Indiv. Resp.','Optimum Shift & Min. r^2');
            axis([min(s_save) max(s_save) min(rsq_save)-1 max(rsq_save)]);
            xlabel('s');ylabel('r^2');
          end
        end
    end
end
```

AIRPORT PAVEMENT ROUGHNESS

Test Demonstration
Pre-Brief

Introductions

- Gordon Hayhoe
  - FAA, Airport Technical R&D Branch, AJP-6312, William J. Hughes Technical Center
- Al Larkin
  - FAA, Airport Technical R&D Branch, AJP-6312, William J. Hughes Technical Center
- Cynthia Murray
  - Statistical Analyst, Cherokee-CRC
- George Lyddane
  - Human Factors Analyst, Cherokee-CRC
- Skip Hudspeth
  - Simulator/Flight Operations Engineer, Cherokee-CRC
- Jeard Ballew
  - Project Operations Management, Cherokee-CRC

Background

- New Construction:
  - Current runway roughness standards are in place for the construction of new taxiways and runways.
- Post-Construction:
  - However, there is no system in place today to determine when in service pavement becomes "too rough"
  - Repairs are often based on pilot complaints alone.

Study Objectives

- Develop Subjective Ratings for correlation to roughness indexes.
  - Develop a subjective rating scale
    - Scaled from "0=Impassable" to "10=Perfect"
- Develop Roughness limits to determine when pavement maintenance is necessary.

Test Description

- 80 Test scenarios (40 taxiways and 40 runways)
- 2 Warm up scenarios for familiarization
- Scenarios are automated with aircraft moving at constant speed for 30 seconds
  - Taxiways – 20 knots
  - Runways – 100 knots
- Same airport visual scene used for every run
- Many levels of roughness along the spectrum from smooth to very rough
- Assume role of non-flying pilot or observer
- Focus on rating the " Ride Quality"

Pilot Rating Form

- Scale: 0-10
  - 0 = Impassable: A surface which is so bad that you doubt the aircraft will make it to the end at the speed you are traveling.
  - 10 = Perfect: A surface which is so smooth that at the speed you are traveling you would hardly know the surface was there.
- Consider ratings as you move along the surface.
- Indicate rating with a small mark across the vertical line anywhere on the scale.
  - e.g., 5.2 or 6.8
- Check appropriate Ride Quality Box at the bottom.
  - Acceptable: Ride Quality Does Not Need Improvement
  - Uncomfortable: Ride Quality Improvement is recommended
  - Unacceptable: Ride Quality Must Be Improved

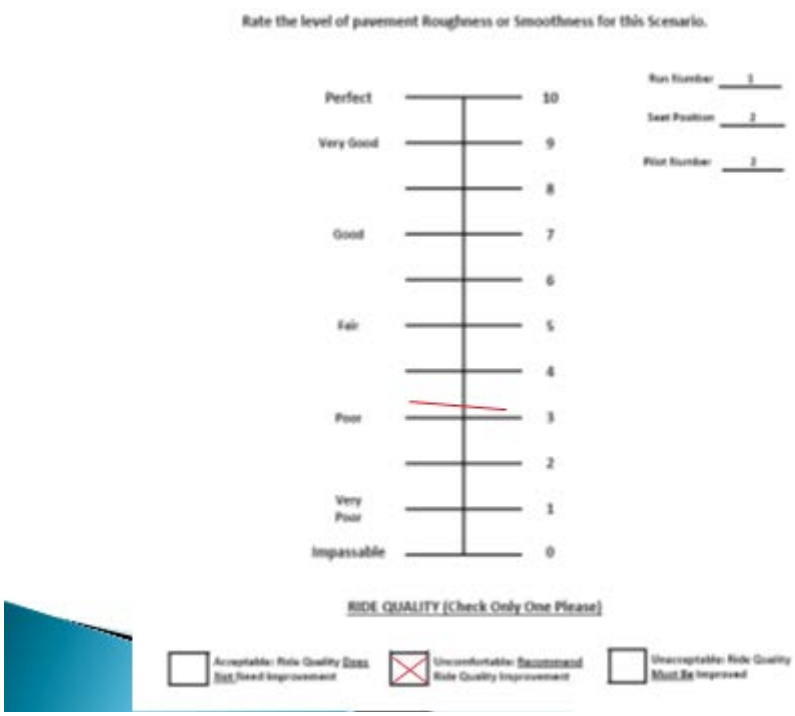

Pilot Rating Form

- Please keep conversations to a minimum.
- Do not discuss individual ratings or opinions.
- Pilot Notes: If you have special comments for a particular scenario for debrief please feel free to make a note on the applicable rating form.

Post – Brief Discussion

Session Debrief

- Realism
- General Impressions
- Criteria for ratings
- Suggestions for study improvements
- Opinions of system to gather this info

POST-FLIGHT QUESTIONNAIRE
Pilot Number= Seat Pos=

- Scale: 5= Excellent, 4= Good, 3= Fair, 2= Poor, 1= Very Poor
- Roughness Fidelity for Amplitude=
- Roughness Fidelity for Frequency=
- Visual Fidelity for Amplitude=
- Visual Fidelity for Frequency=
- Aural Fidelity for Loudness=
- Aural Fidelity for Realism=

General Impressions: Beneficial/Pretty good/So So/Waste of time

Criteria for ratings

- Influence of sharp jolts: High, Medium, Low
- Influence of no slope in visual scene: High, Medium, Low

Suggestions for study improvements:

THANK YOU!

APPENDIX J—POST-FLIGHT QUESTIONNAIRE

Roughness Simulation Post-Flight Rating Form

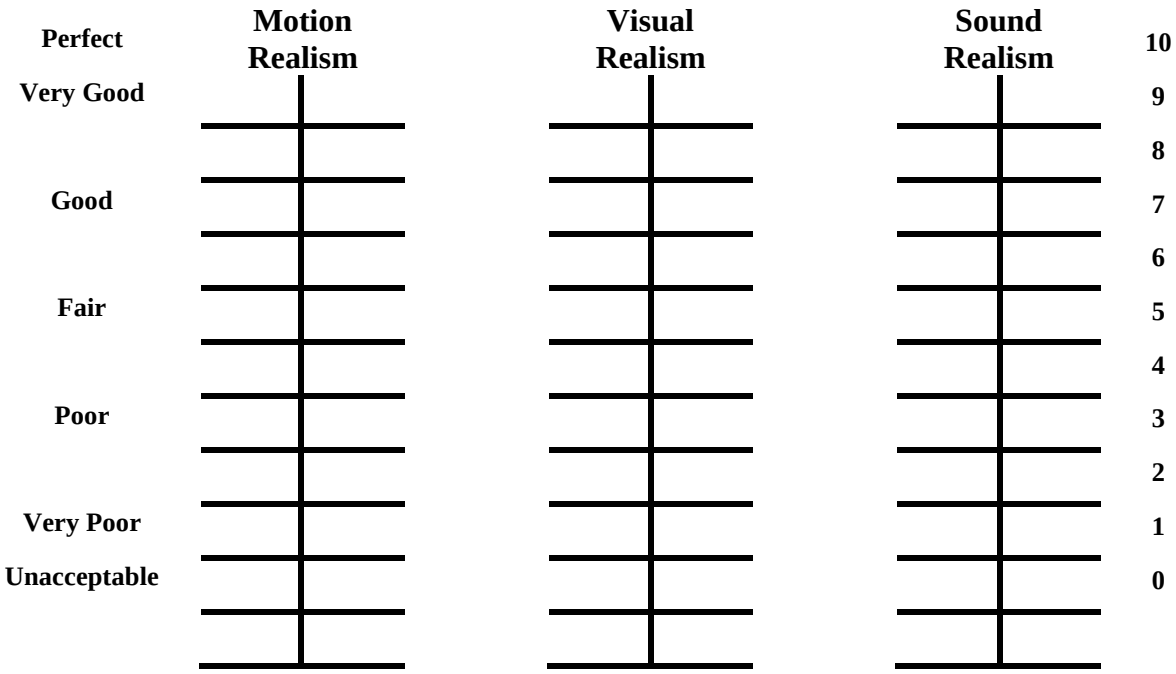

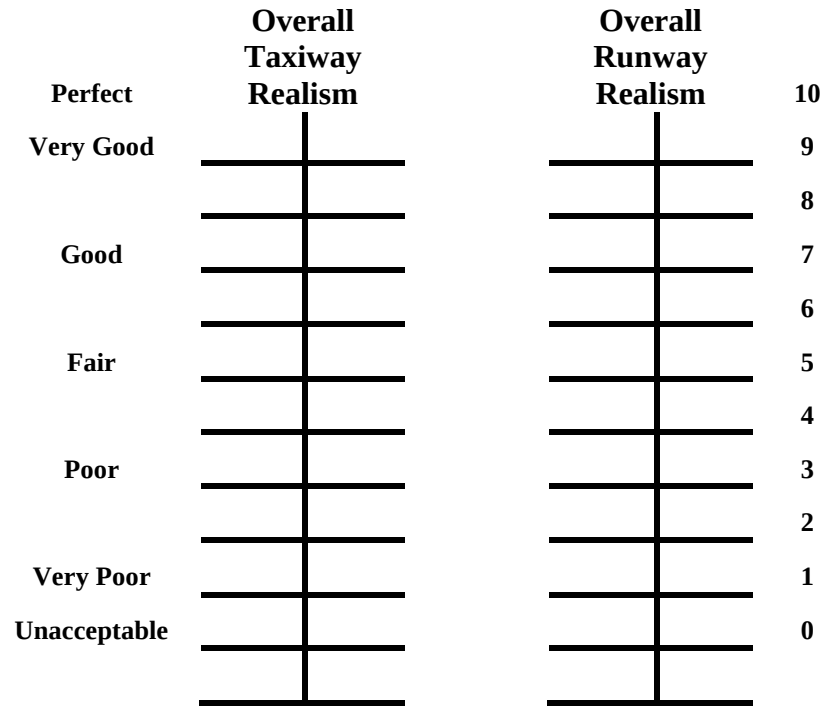

Pilot Number _____ **Seat Position** _____

APPENDIX K—PILOT RATING FORM

Rate the Level of Pavement Roughness or Smoothness for this Scenario

Run Number _____

Seat Position _____

Pilot Number _____

NEED FOR IMPROVEMENT (Check Only One Box)

☐ Acceptable: Ride Quality Does Not Need Improvement

☐ Unacceptable: Ride Quality Needs Improvement

APPENDIX L—PILOT BACKGROUND DATA

Pilot #	Employer at Time of Study	Type Rated in Which Aircraft	Man Hours per Aircraft	First Officer/Captain	Military/Branch	Non-Military
1	SWA	B-707, B-720, B-737, BE-400, MU-300,	707/720 - 1100, 737 - 3530, BE400/MU300 - 2800	FO	Yes, Navy & AF Reserves	X
2	SWA	B-737, B-707, B-720	B707 - 2,500, B737 - 2,000 hrs	FO	Yes, USAF	X
3	AA	737-800	B737 - 5000, MD-80 - 1500, Fokker F-100 - 3000, Cessna 402 - 500, Military: T-37 - 3500, T-38 - 120, F-15 - 1700.	FO	USAF - 20 yrs	X
4	SWA	B737, 757, 767, 707 and 720	B737 - 7000, 757/767 - 1500, 720 - 1000.	FO	USAF	X
5	AA	737	B737 - 4287	Captain	Yes, Navy	X
6	USAF, OK Air Nat Guard	B707/B720; L382; BE400/MU200	B707/720 -700+, L382 - 3,500+, BE400/MU200 - 200+	Capt equivalent	AF, Air Nat Guard	
7	AA	DC-3, DC-9, B737, B767, B777	DC-3 - 2000, DC9 - 10000, B737 - 4000, B767 - 1500, B777 - 1200	Captain	Yes, Army	X
8	AA	737-800	4500	Captain	Yes, US AF	X
9	AA	737-800, S-80, B757/767, and the MD-11	737 - 2500; S-80 - 6000; B757/767 - 1000; MD-11 - 950	Captain on the 737 & S-80, F/O on the B757/767 & MD-11 and F-16	Yes, USAF	X
10	USAF Reserves	B400, 707, 717, MU36	B400 - 150; 707 - 2500	Captain	Yes,	
11	Delta	737	737 - 5000, MD-88 - 1125, 727 - 1430, DA20 - 1350	FO	Coast Guard - Retired	X
12	SWA	737, 727, DC3, DC3S	B737 - 14500, B727 - 1500, DC3/DC3S - 500	Captain	USMC - Retired	X
13	US Airways	B737, 767, A320	B737 - 7000, 757/767 - 1500, 720 - 1000.	Captain	Yes, AF	X
14	Midland Financial (part 91 corporate) and OK Air Nat Guard	Civilian: BE-400/MU-300; CE-750; CL-601; CL-604 Military: C-130; KC-135	Civilian: 2100; Military: 2500	Captain/Aircraft Commander	USAF-Guard	

Pilot No.	Employer at Time of Study	Type Rated in Which Aircraft	Man Hours per Aircraft	First Officer/Captain	Military/Branch	Non-Military
15	Delta & OK Air Nat Guard	Boeing 777 and KC-135	B777 - 2000, KC-135 - 1500	FO on 777. Instructor on KC-135	23 yrs of Military in USAFR and ANG.	X
16	Retired from Delta	A330, B747		Captain	No	X
17	US Airways	A330	A330 - 340	FO	USAFR - retired	X
18	US Airways	CE500/550/525, LR JET, B737, Airbus 319/320/321, E190	CE500/550/525 - 2500, LR Jet - B737 - 3000, A319/320/321 - 1500, E190 - 5000	currently F/O, although I've flown captain everywhere except US Airways	Yes, USAF	X
19	Sun Country	A320, B737, BE400, CL600, DHC 8, L382	A320 - 109, B737 - 162, BE400 - 200, CL600 - 1000, DHC8 - 275, L382 - 3115	Both	Yes, USAF	X
20	Delta	B707/B720; B737; B757/767; DC9; A320/319	707/720 - 5000+, B737 – 235, B757/767 – 380, M88 – 719, A320 - 895	FO	US Navy - Retired	X
21	AA	737-800	B737 - 5000+	FO	No	X
22	SWA	B737 -200, 300, 500, 700, 800	B737 - 10,555	Captain	Yes, Air Force - T-37, T-38, KC-135	X
23	United	707/737	B707 - 2500, B737 - 6500	FO	Retired Navy pilot	X
24	OK Air Nat Guard	Boeing B-707 & 720	C130 - 1750, KC135R - 1200	Currently a check airman/evaluator	Yes	
25	SW - SIM Instructor	KC-135	Flew the KC-135s primarily, approx. 9000 hours in the KC-135s	N/A	Yes, 20 yr, AF	X
26	World Airways - on furlough	B-707, B-720, B-727, B-737, B-757, B-767, MD-11.	14,000 +	MD-11 FO. Captain or Check Airman on all the other aircraft.	USAF retired. Primary aircraft KC-135 and E-3A.	X
27	SWA	737, 757, 767, BE-40, MU-30, B-707, B-720	737 - 7800 hours	FO	Yes, AF	X
28	Delta	1. B737, B757, B767, EMB170, EMB190, DC9 (SIC)	B737- 1650, B757/767- 1160, DC9 (MD88)- 475 hrs, EMB170/190- 1000	Capt EBM 170, FO in all other aircraft	No	X

Pilot No.	Employer at Time of Study	Type Rated in which Aircraft	Man Hours per Aircraft	First Officer/Captain	Military/Branch	Non-Military
29	United	707,720,727,737,777,A320,L382	B707 - 1000+, B720 - 1000+, B727 - 1000+, B737 - 1000+, B777 - 100, A320 - 1000+, L382 - 1000+	time was before SIC types existed.	Yes, Air Force	X
30	OK Air National Guard	BE-400 / MU-400, L-382, B-737, B-707/720	C130 - ~2200, KC135 - 1200	Commander (Captain) in C-130 and KC-135	Yes, USAF	
31	SWA	(B737-SWA) DC-9, B767,B757, G100	14,000	Captain	Yes, USAF	X
32	OK Air National Guard	Boeing 707 (KC-135R), Beech B300	KC-135 - 2400; King Airs - 1100	Captain (AC)	AF	
33	United	EMB-145, B737	EMB145 - 2000, B737 - 5500	FO	No	X
34	AA	Lear 60	F/A-18 - 1350, LR60 - 350, MD-80 - 4850, 737 - 3680	FO	Yes, USMC (former Marine fighter pilot	X
35	Delta	737ng	B737 - 3000	Captain	Yes, AF	X
36	OK Air National Guard	B-707, B-720, BE-400, MU-300	B-707/B-720 - 2184, BE-400/MU-300 - 120 hrs	Instructor Pilot	Yes, AF	